FUNCTIONALIZATIONS OF CYCLIC ENAMINONES AND APPLICATIONS TO THE SYNTHESIS OF BIOACTIVE COMPOUNDS

A DISSERTATION
SUBMITTED TO THE FACULTY OF THE GRADUATE SCHOOL
OF THE UNIVERSITY OF MINNESOTA
BY

YONG WOOK KIM

IN PARTIAL FULFILLMENT OF THE REQUIREMENTS
FOR THE DEGREE OF
DOCTOR OF CHEMISTRY

GUNDA I. GEORG

APRIL 2014

Acknowledgements

First and foremost, I would like to thank my advisor, Professor Gunda Georg, for her guidance and support throughout my graduate studies at the University of Minnesota. I appreciate the scientific freedom and encouragement in my research. I also would like to thank Professor Thomas Hoye, Professor Chris Douglas and Rodney Johnson for serving my committee for this thesis.

I thank all of the past and current members of the Georg group. Dr. Micah Niphakis helped me to start the research when I first joined the group. Dr. Yiyun Yu provided meaningful discussions to make my research better. I especially thank to Dr. Kwon Ho Hong, who helped me inside the lab as well as outside of the lab. I also thank Korean friends in Chemistry Department for sharing fun activities beyond chemistry.

I thank to my parents, who endlessly love and support me. I also thank my sister and brother for support. Most importantly, I thank my wife Min Ae for her love, support and patience during my graduate study.

Abstract

Six-membered cyclic enaminones (2,3-dihydropyridin-4(1*H*)-ones) are versatile synthetic intermediates for the preparation of piperidine-containing biologically active compounds such as indolizidines and quinolizidines alkaloids. In this thesis, the functionalizations of cyclic enaminones have been described. In addition, novel IKKβ inhibitors have been discovered from the cyclic enaminone derivatives.

A palladium-catalyzed C5 arylation of cyclic enaminones using arylboronic acids has been developed. A unique mixture of $Cu(OAc)_2$ and $CuCl_2$ oxidants is essential for efficient cross-coupling of electronically diverse boronic acids. In addition to serving as palladium reoxidants, these reagents are believed to assist aryl delivery through a putative arylcopper intermediate.

Another direct C5 arylation reaction has been developed using diaryliodonium tosylates under metal-free and copper-catalyzed reactions. Metal-free conditions offer a green alternative, where the use of heavy transition metals has been excluded. On the other hand, copper-catalyzed conditions provide highly efficient C5 arylation method under mild conditions within a short period of time.

We have developed direct C6 arylation using the oxidative boron-Heck reaction that proceeds with excellent selectivity over C5 arylation and conjugate addition reactions. C6 arylated cyclic enaminone can serve as an intermediate in total synthesis of lasubine II. Furthermore, an acid-controlled reactivity switch to a conjugate addition reaction is viable when the reaction is carried out with *N*-carbamylated substrates.

Novel scaffolds that incorporate cyclic enaminone motifs were designed and synthesized using copper-catalyzed amidation and reductive amination. Biological assays showed that some analogues possess IKKβ inhibitory activity.

Table of Contents

List of Tables

Chapter 1

Chapter 2

Chapter 3

List of Figures

Chapter 1

Chapter 2

Chapter 3

Chapter 4

Chapter 5

List of Schemes

Chapter 1

Chapter 2

List of Compounds

Chapter 2

Chapter 1

Introduction to cyclic enaminones

1.1 Introduction

Scheme 1-1. **Utility of cyclic enaminones**

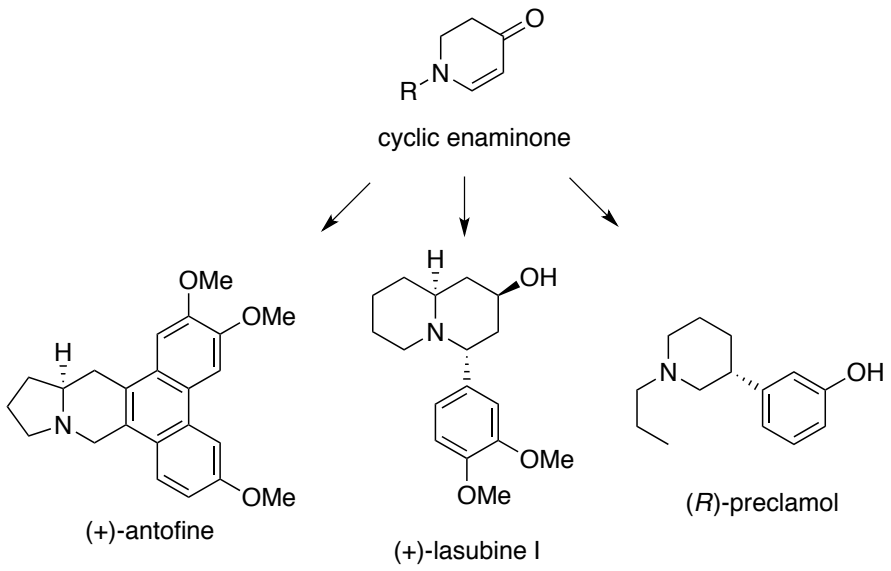

Piperidine-containing compounds such as indolizidines and quinolizidines alkaloids are known to possess biological activities and regarded as pharmacophore in drug discovery.[1] Six-membered cyclic enaminones (2,3-dihydropyridin-4(1*H*)-ones) are versatile intermediates for the preparation of these structures.[2] Representative examples of compounds that can be prepared from cyclic emaninone intermediates are shown in scheme 1-1. Especially, (–)-antofine exhibits very potent antiproliferative activity and preclamol is known to be a dopamine autorecepter

agonist.

Scheme 1-2. Synthetic transformations of cyclic enaminones

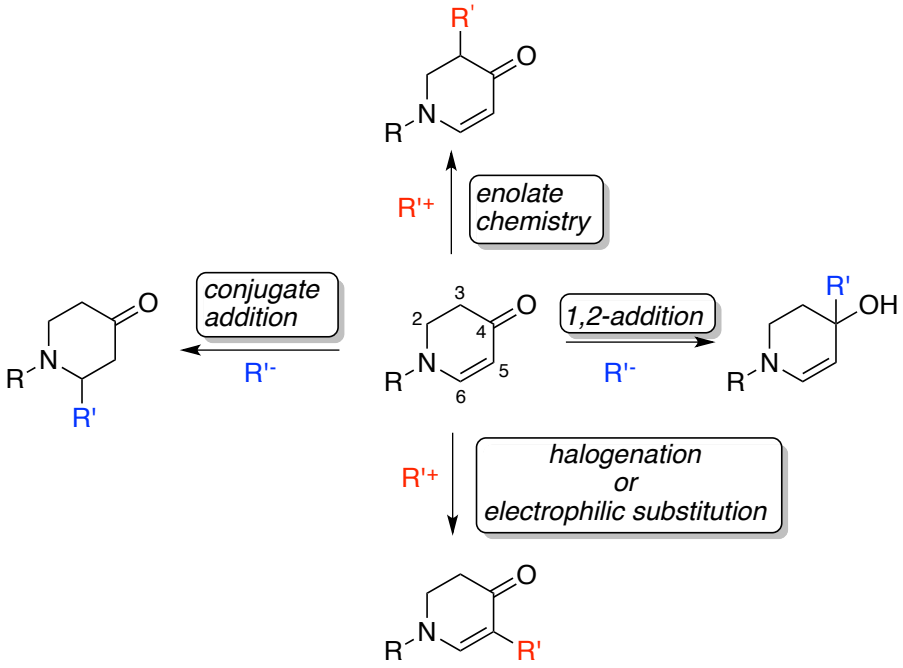

Enaminones are described as vinylogous amide or acyl enamine, and their chemical properties are different from amides and enamines. Generally, enaminones are more stable than enamines and more reactive than amides. In particular, cyclic enaminones are ideal substrates for the synthesis of nitrogenous heterocyclic derivatives under various reaction conditions. There are two electrophilic carbons (C4 and C6) and two nucleophilic carbons (C3 and C5) in six membered cyclic enaminones. Various transformations from six membered cyclic enaminones are shown in scheme 1-2. Enolate chemistry can be used to functionalize at the C3 position. The C4 keto group of the α,β-unsaturated ketone can be subjected to 1,2-

addition. For example, Luche reduction will give an alcohol, which can be used to append other functional groups at the C4 position. Halogenation or electrophilic substitution reactions are viable because of the nucleophilic nature of C5. Conjugate addition to the enone functionalizes the C6 position.

1.2 Functionalizations of cyclic enaminones

1.2.1 Total synthesis of (+)-elaeokanine A and (+)-elaeokanine C

Scheme 1-3. Total synthesis of (+)-elaeokanine A and (+)-elaeokanine C

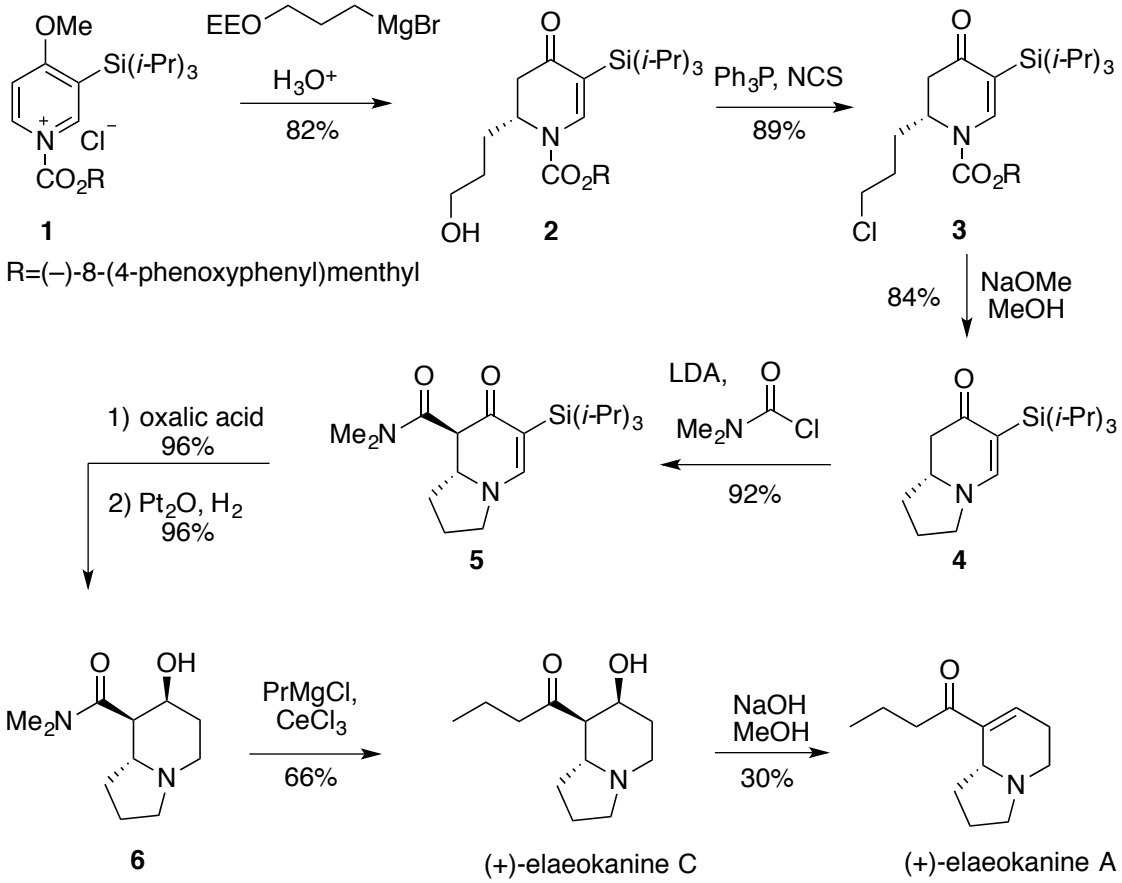

Cyclic enaminones have been used as versatile intermediates in the total syntheses of various natural products with a number of chemical transformations.

As shown scheme 1-3, a cyclic enaminone was used in the total synthesis of (+)-elaeokanine A and (+)-elaeokanine C.[3] Reaction of chiral 1-acylpyridinium salt **1** with a Grignard reagent afforded a C2 and C5 disubstituted cyclic enaminone **2**. Chlorination with *N*-chlorosuccinimide followed by the removal of the chiral auxiliary established the indolizidine scaffold **4**. The functionalization α to the carbonyl group (C3 position) was accomplished using LDA and dimethylcarbamyl chloride. After the desilylation and hydrogenation, (+)-elaeokanine C was obtained using an organocerium reagent to convert the amide to a ketone. This synthesis shows the functionalizations of cyclic enaminones at C2, C3, C4 and C5 positions as well as a cyclization at the nitrogen.

1.2.2 Total synthesis of tricyclic alkaloid (–)-porantheridine

The total synthesis of the tricyclic alkaloid porantheridine was reported using cyclic enaminone chemistry (scheme 1-4).[4] Addition of the zinc enolate of 2-pentanone to the pyridinium salt **7** produced a C2 and C5 functionalized cyclic enaminone intermediate **8**, which was converted to a hydroxyl cyclic enaminone **9** by stereoselective reduction and the removal of the chiral auxiliary. Formation of the bicyclic carbamate, desilylation and copper-mediated 1,4-addition of a Grignard reagent provided a C6 functionalized *trans*-piperidone **11**. The 2,6-disubstituted piperidine **13** was synthesized by reductive deoxygenation of the ketone and

subsequent hydrolysis. Final cyclization afforded the desired natural product. This synthesis demonstrates the C2 and C6 alkylation reactions of cyclic enaminones in natural product synthesis.

Scheme 1-4. Total synthesis of (–)-porantheridine

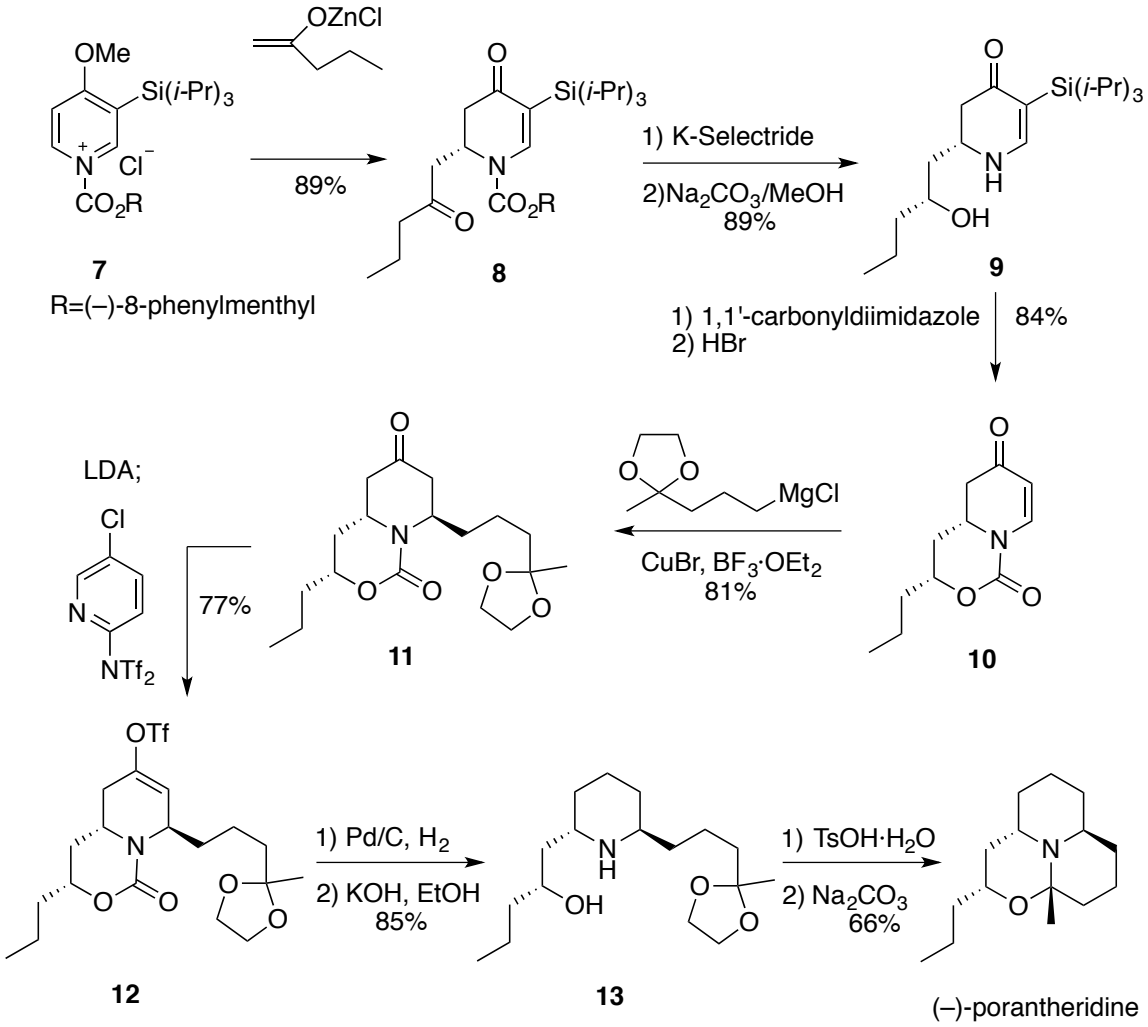

1.2.3 Enantioselective Lewis acid catalyzed [2+2] photocycloaddition of cyclic enaminones

Scheme 1-5. **Enantioselective [2+2] photocycloaddition of cyclic enaminones**

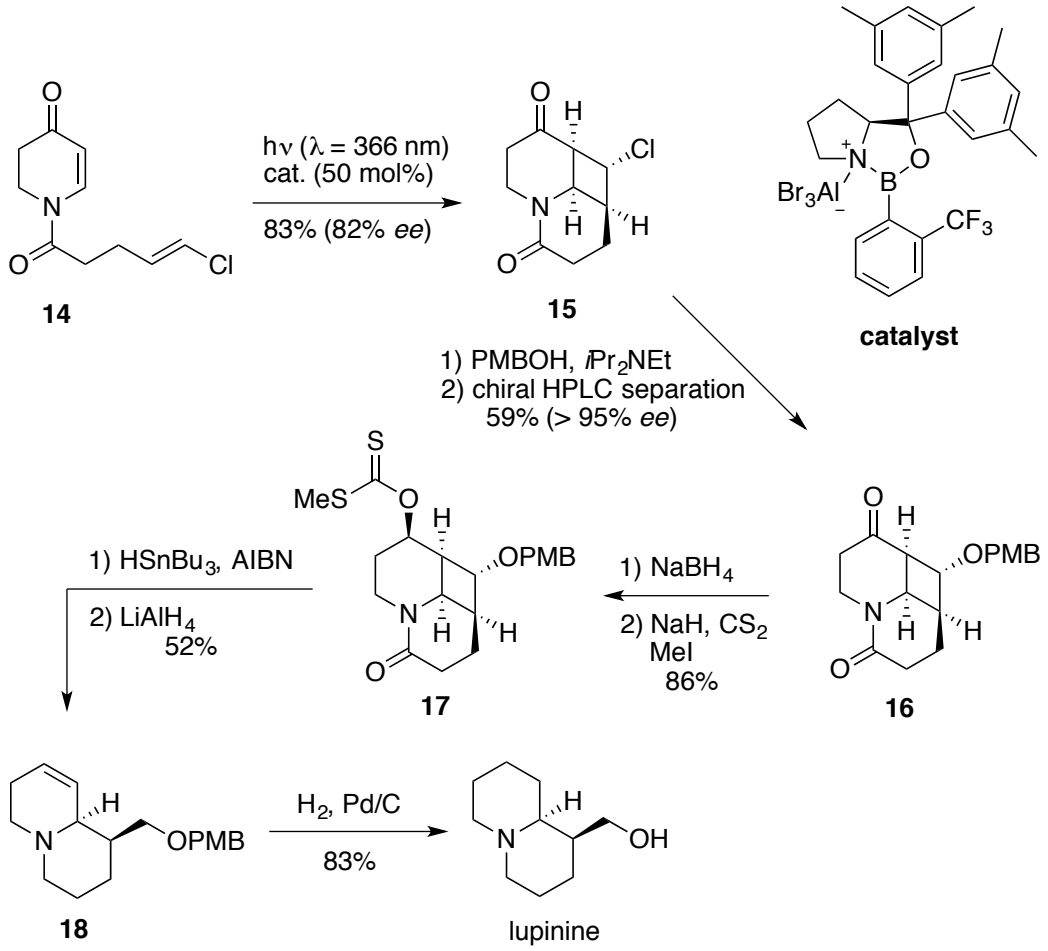

Most recently, an enantioselective Lewis acid catalyzed [2+2] photocycloaddition of cyclic enaminones was reported.[5] Because an extensive bathochromic absorption shift of cyclic enaminones was observed upon Lewis acid coordination (> 50 nm), reaction of the uncomplexed cyclic enaminone could be avoided at a specific wavelength. Therefore, an enantioselective photocycloaddition was viable using a

chiral Lewis acid catalyst with a wavelength that dose not affect the uncomplexed cyclic enaminones. This method was used to synthesize the quinolizidine alkaloid lupinine. Enantioselective photocycloaddition of the cyclic enaminone **14** furnished the product **15** in high yield and enantioselectivity (83% and 82% *ee*). Displacing the chlorine substituent by *para*-methoxybenzyloxy group (elimination then readdition) and chiral HPLC purification provided a single enantiomer **16**. A xanthate moiety was introduced to the secondary alcohol after diastereoselective reduction of the ketone for a reductive ring opening reaction. A radical mediated fragmentation and lactam reduction by $LiAlH_4$ provided the hexahydroquinolizine derivative **18**, which was converted to lupinine by concomitant hydrogenation and hydrogenolysis.

1.2.4 Synthesis of an acyclic amino alcohol from a cyclic enaminone

Scheme 1-6. **Synthesis of an acyclic amino alcohol from a cyclic enaminone**

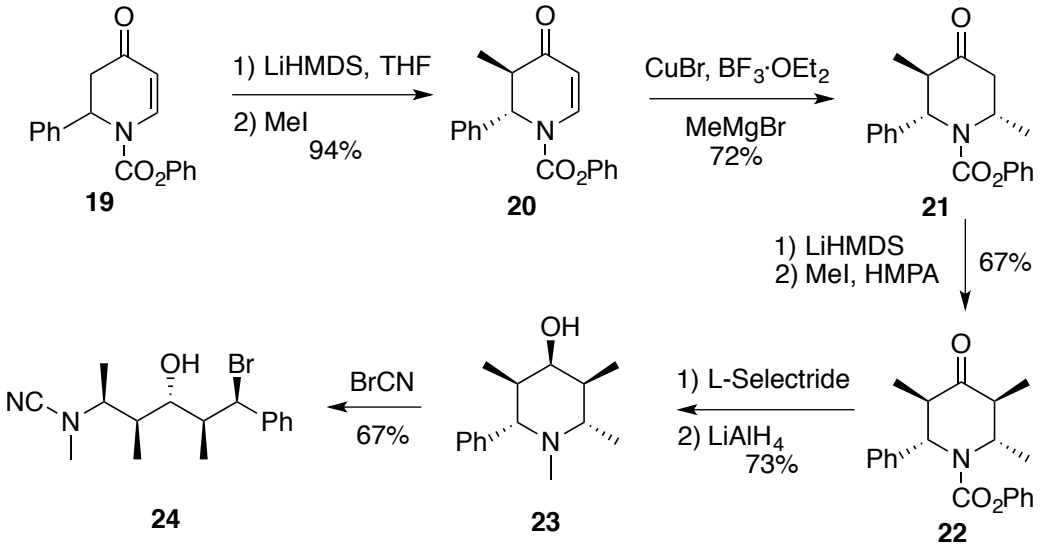

In cyclic system, it is easier to introduce stereocenters in a stereocontrolled fashion compared to an acyclic system. Considering the ability to functionalize cyclic enaminones, they can be great intermediates for the preparation of acyclic compounds with multiple chiral centers (scheme 1-6).[6] Starting from the C2 functionalized cyclic enaminone **19**, C3 and C6 methylation can be easily achieved in a stereoselective manner. C5 methylation and stereospecific reduction with L-Selectride gave the alcohol **23** as a single diastereomer. Reduction with $LiAlH_4$ and the von Braun ring-opening reaction with cyanogen bromide were performed to afford the acyclic amino alcohol **24** with five stereocenters. This method provides the synthesis of acyclic amine derivatives with multiple chiral centers and functionalities from cyclic enaminones.

1.2.5 Diels-Alder reactions of 5-vinyl cyclic enaminones

5-Vinyl cyclic enaminones undergo facile Diels-Alder reaction with dienophiles (scheme 1-7).[7] 5-Vinyl cyclic enaminones are readily available from cyclic enaminones by iodination with NIS and catalytic [hydroxyl(tosyloxy)iodo]benzene (HTIB) and subsequent Stille coupling reaction with vinyltributyltin. Depending on the dienophiles, this cycloadduct proceeded to a ring-opening event to form a functionalized aromatic ring. For example, a 5-vinyl cyclic enaminone **25** was reacted with 1,4-naphthoquinone to form the expected Diels-Alder product. Upon exposure to air, the adduct was oxidized and aromatized to form an anthraquinone derivative **29**. This transformation could be achieved in a one-pot procedure by adding silica gel to

the Diels-Alder product. When di-*tert*-butylacetylene dicarboxlate or benzyne were used as dienophiles, both cycloadducts aromatized and converted to the respective benzene derivatives (**30** and **31**). As shown by these examples, cyclic enaminones are also suitable substrates for the preparation of functionalized benzene derivatives.

Scheme 1-7. **Diels-Alder reactions of a 5-vinyl cyclic enaminone**

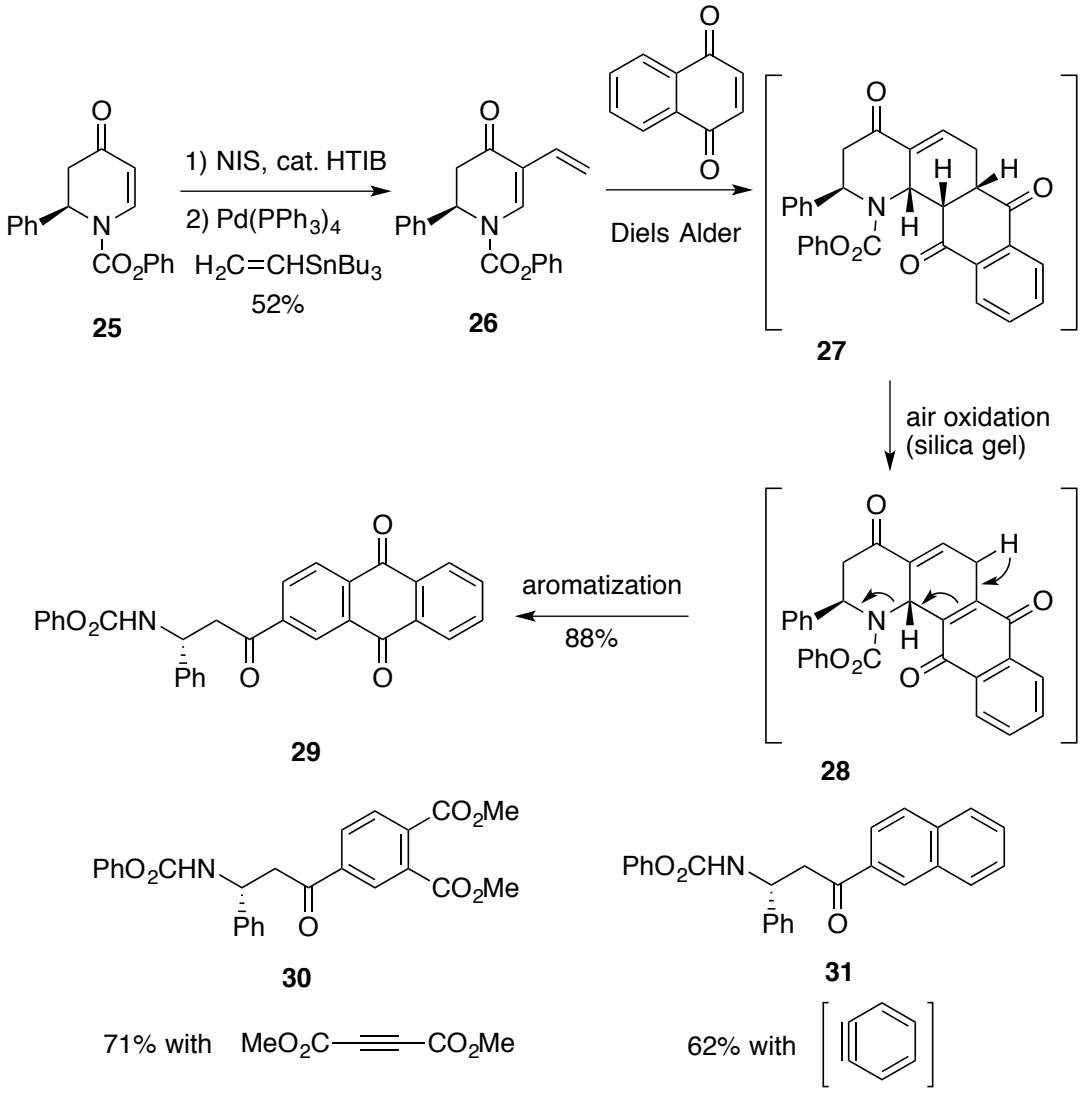

1.3 C5-functionalization of cyclic enaminones

1.3.1 C5-functionalizations developed by the Comins' group

Scheme 1-8. **Regiospecific functionalizations at the C5 position**

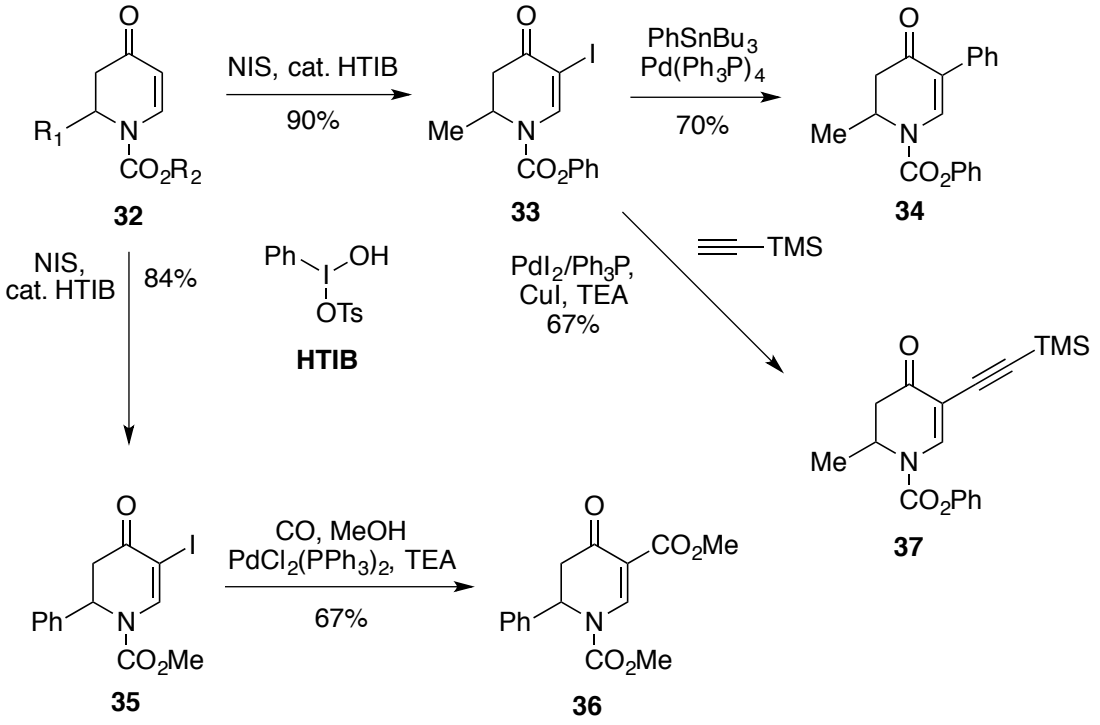

Comins' *et al* reported a regiospecific C5 functionalization using halogenation followed by a palladium-catalyzed cross-coupling reaction.[8] After the failure of using C5-brominated cyclic enaminones in the palladium-catalyzed cross-coupling reactions, iodo derivatives were successfully employed. As shown in scheme 1-7, the vinyl group was installed by a Stille cross-coupling. In addition, it was shown that C5-iodinated cyclic enaminons could serve as coupling partners for other Stille

coupling reactions (arylation), for Sonogashira coupling and for carboalkoxylation (scheme 1-8).

This strategy was used for the total synthesis of (–)-septicine,[9a] which has cytotoxic activities against human cancer cell lines (scheme 1-9).[9b] Unlike the cross-coupling shown above (scheme 1-8), a brominated cyclic enaminone was used as a coupling partner in a Negishi coupling. Bromodesilylation of the indolizidinone **38** provided the bromide **39**, which was converted to a bromovinyl triflate **40** by conjugate reduction followed by addition of Comins' reagent. Negishi cross-coupling between this bromovinyl triflate **40** and in situ generated 3,4-dimethoxyphenylzinc bromide provided (–)-septicine.

Scheme 1-9. **Total synthesis of (–)-septine**

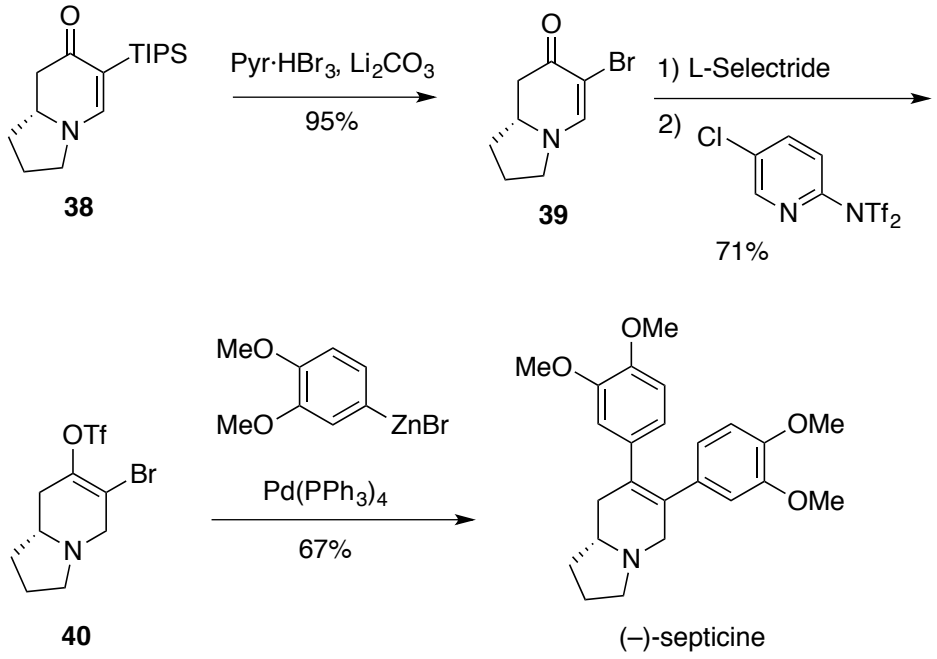

Scheme 1-10. **Synthesis of C5 alkylidene derivative**

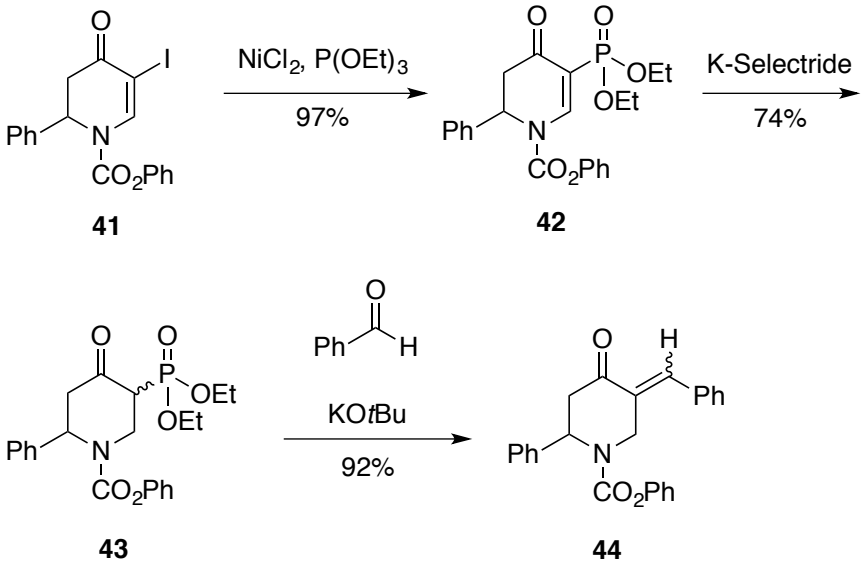

C5-alkylidene derivatives of cyclic enaminones can be accessed from C5-iodinated cyclic enaminones using a Horner-Wadsworth-Emmons reaction (scheme 1-10).[10] The phosphorus derivative **42** was synthesized from iodide **41** using nickel catalysis. The resulting vinyl phosphonate **42** was reacted with K-Selectride to provide the double bond reduced phosphonate **43**. Anion formation of the phosphonate **43** followed by addition of benzaldehyde provided the cyclic enaminone **44** with an alkylidene group installed at the C5 position.

5-(1-Hydroxyalkyl) cyclic enaminone **46** can be prepared by hydroxyalkylation of C5-iodinated cyclic enaminone **45** using the Nozaki-Hiyama-Kishi (NHK) reaction (scheme 1-11).[11] The resulting secondary alcohol **46** provides ways for further functionalization. Because the hydroxyl group is γ to the nitrogen, the NHK product forms an *N*-acyliminium ion in the presence of a Lewis acid. γ–Attack of nucleophiles can install new functional groups. In this way, the hydroxyl group can be converted to

allyl, hydrogen, alkoxy and furanyl groups. For example, addition of allyltrimethylsilane with $BF_3 \cdot OEt_2$ to the NHK product **46** gave γ–allylated cyclic enaminone **48**.

Scheme 1-11. **The Nozaki-Hiyama-Kishi reaction of iodinated cyclic enaminones**

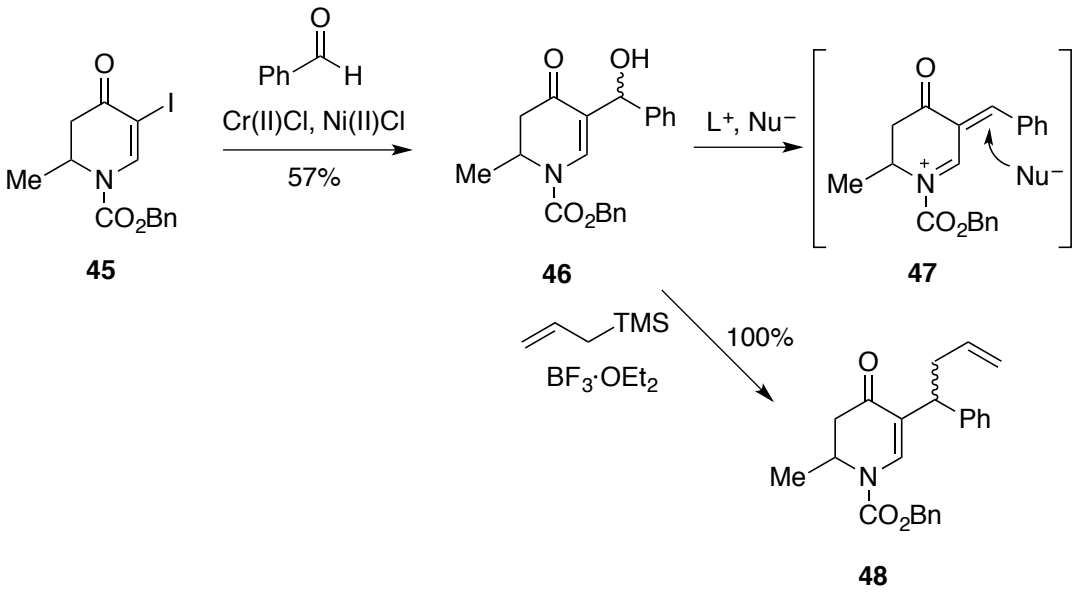

1.3.2 Suzuki coupling of 5-iodoenaminones

Although several methods to functionalize at C5 position using palladium catalysis were reported by the Comins' group, arylation reactions are scarce and the use of organozinc or organotin reagents make it difficult to use in practical way due to the limited availibility. The Georg group developed an efficient and convenient method to afford C5-arylated cyclic enaminones.[12] An iodination and subsequent Suzuki coupling of cyclic enaminones using a wide range of arylboronic acids provided

various C5-arylated cyclic enaminones. The use of microwave irridation enabled the reaction to proceed in a very short time (15 min).

Scheme 1-12. **Microwave-assisted Suzuki coupling of α-iodoenaminones**

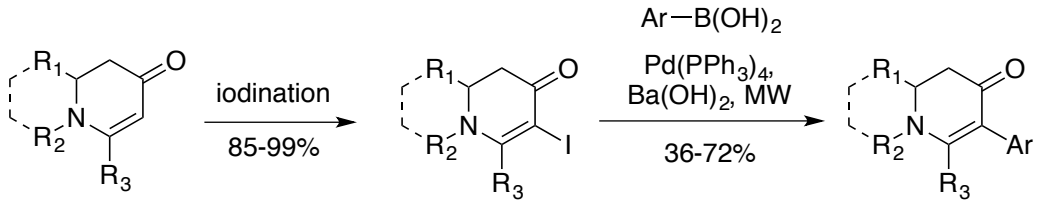

1.3.3 Direct functionalizations of cyclic enaminones

C5 arylation of cyclic enaminones has been accomplished using a two-step synthesis involving halogenation and a palladium-catalyzed cross-coupling reaction. Taking advantage of the innate nucleophilicity of cyclic enaminones, a direct functionalization could be realized using an electrophilic palladium(II) catalyst.

1.3.3.1 Direct arylation using trifluoroborate

As shown in the proposed mechanism (figure 1-1), electrophilic attack of palladium on the cyclic enaminone generates a palladium complex, which undergoes transmetallation with an organometallic aryl donor. A reductive elimination would provide the coupled product. The palladium(0) species can be oxidized to palladium(II) catalyst by a copper oxidant.

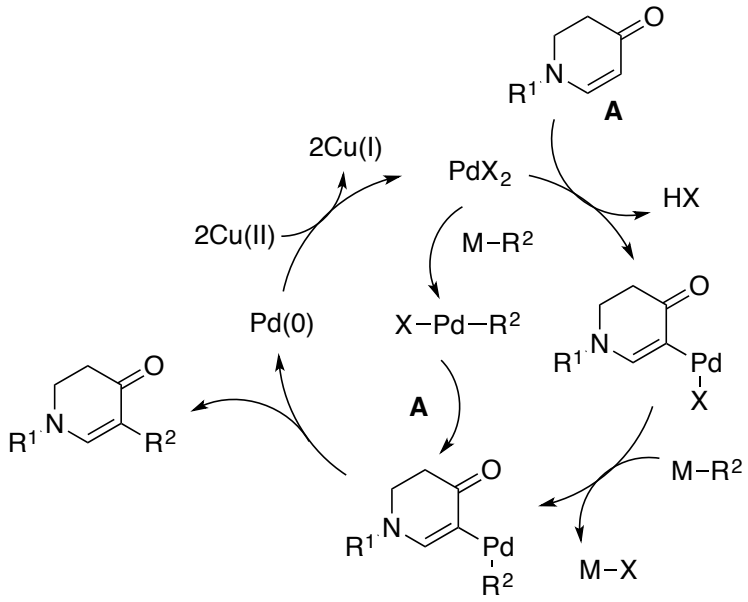

Figure 1-1. **Proposed mechanism for direct arylation of cyclic enaminone.**

Aryltrifluoroborates were used as robust equivalents of arylboronic acids in the direct C5 arylation of cyclic enaminones.[13] The slow addition of the trifluoroborates was necessary to achieve a high yield in the reaction by suppression of homocoupling. The reaction with electron-rich reagents showed rapid and high yielding results while electron-deficient and sterically encumbered counterparts required longer time and proceeded in lower yields. Various types of cyclic enaminones were compatible with the reaction condition. A substrate with the decreased nucleophilicity did not produce any product, which is consistent with the proposed hypothesis.

Table 1-1. **Scope of direct arylation using trifluoroborates**

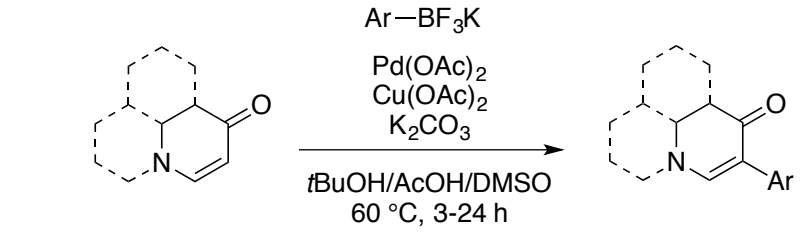

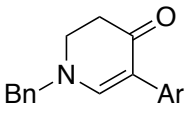

Ar = Ph (72%)
= 4-Me-C_6H_4 (86%)
= 2-Me-C_6H_4 (40%)
= 2-MeO-C_6H_4 (27%)
= 4-CF_3-C_6H_4 (44%)
= 4-Ac-C_6H_4 (42%)
= 4-Br-C_6H_4 (73%)
= 4-Cl-C_6H_4 (71%)
= 2-Naphthyl (96%)
= 3,4,5-$(MeO)_3$-C_6H_4 (83%)
= 3-OH-C_6H_4 (97%)
= 4-CbzNH-C_6H_4 (80%)

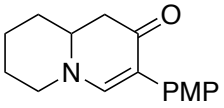

98%

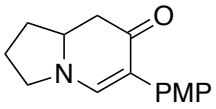

70%

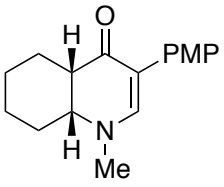

86%

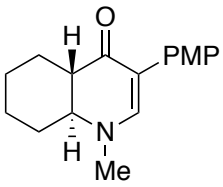

77%

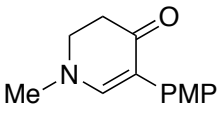

80%

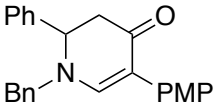

79%

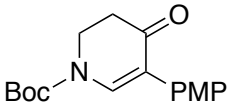

not observed

Table 1-2. **Scope of direct arylation using organosilanes**

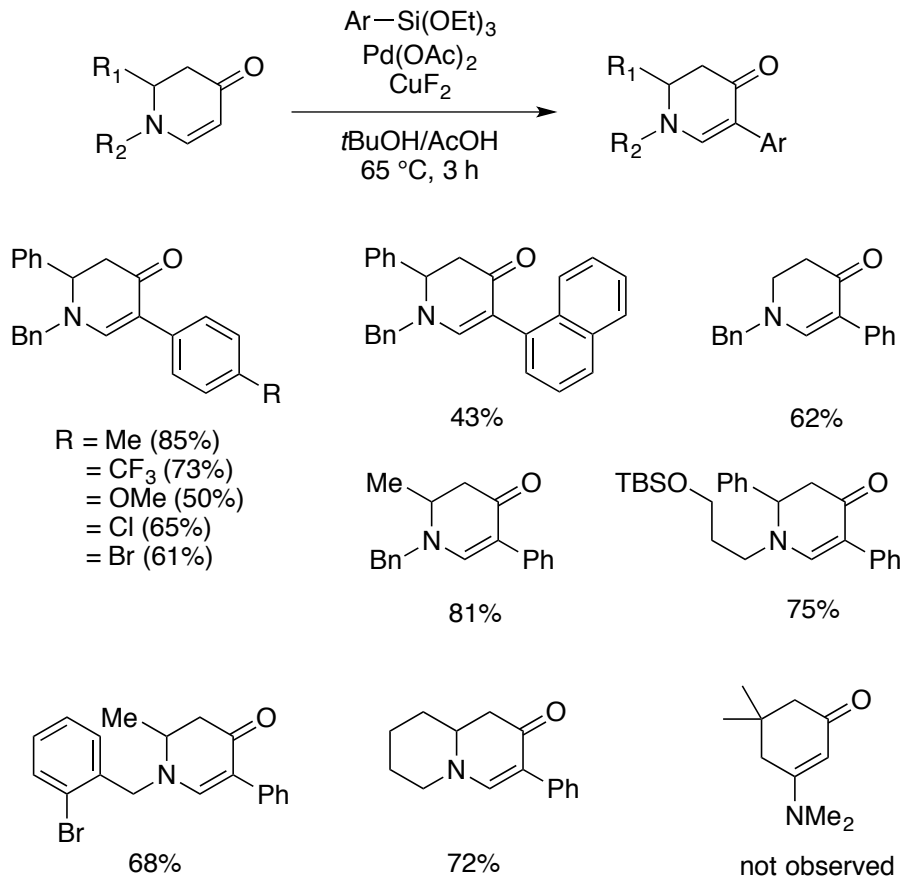

1.3.3.2 Direct arylation using organosilanes

A similar method for a C5 arylation of cyclic enaminones was developed using a Hiyama-type cross-coupling reaction (table 1-2).[14] Triethoxy(aryl)silanes were successfully employed as aryl donors with various cyclic enaminones under palladium(II) catalysis. It was found that the fluoride additives were necessary for the activation of the silanes. It is worth noting that CuF_2 was used for the first time as bifunctional activator/reoxidant.

1.3.3.3 Direct alkenylation

Table 1-3. **Scope of alkenes**

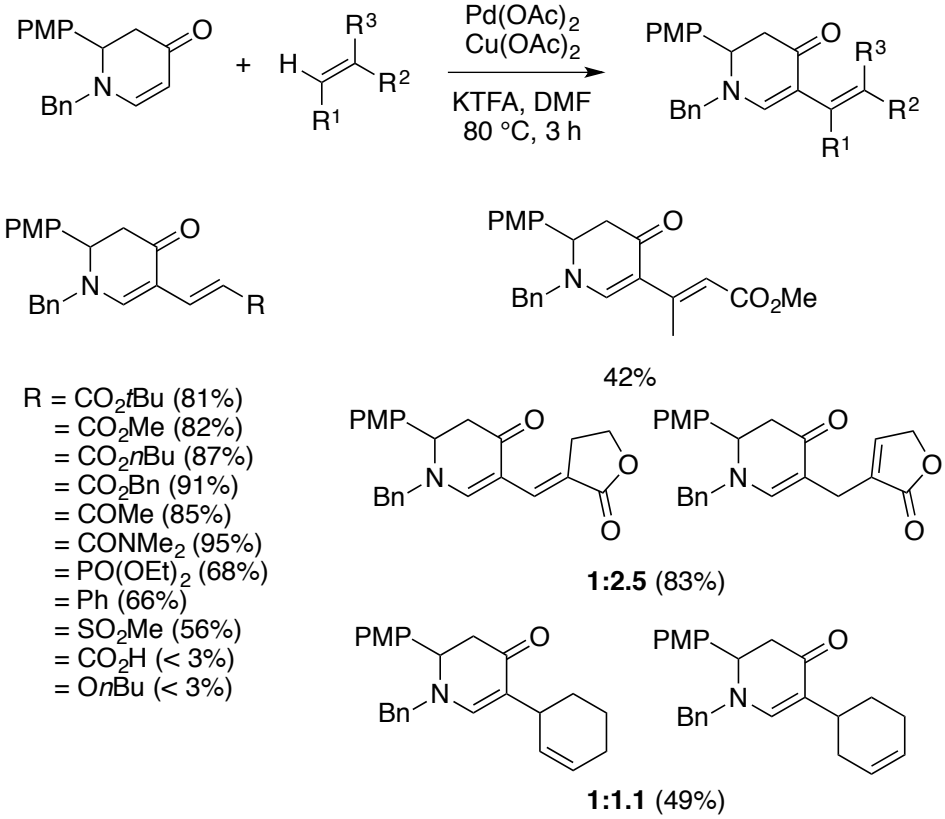

The dehydrogenative Heck reaction (Fujiwara-Moritani reaction) has often been used in aromatic substrates while the reactions between two alkenes are rare. Cyclic enaminones could serve as a suitable substrate for this type of transformations.[15a] After a series of optimization processes, KTFA (potassium trifluoroacetate) was chosen as an optimal reagent with $Pd(OAc)_2$ and $Cu(OAc)_2$. Acrylic esters, vinyl ketone, vinylphosphonates, styrene, and vinylsulfones were viable coupling partners. However, acrylic acid and vinyl ethers did not afford the diene products.

Unconjugated dienes were preferentially formed when α-methylene-γ-lactone or cyclohexene were used as olefin donors.

Table 1-4. **Scope of cyclic enaminones**

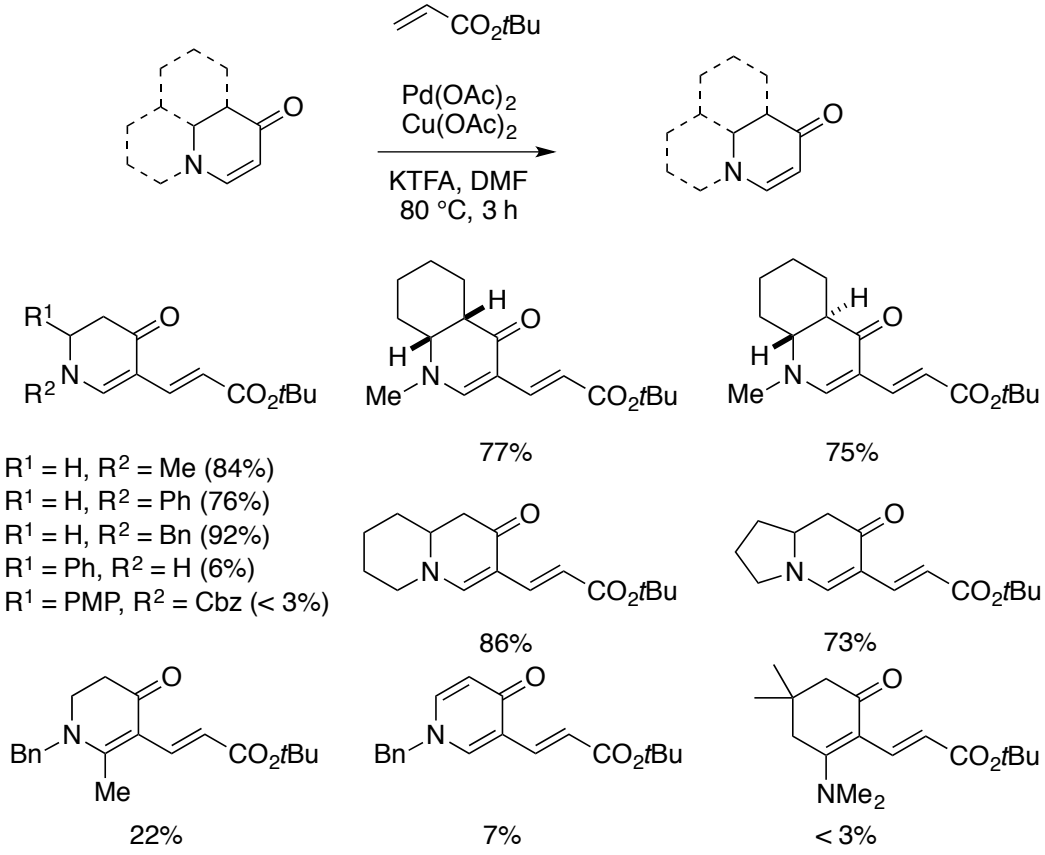

Similar to previous findings, electronically unattenuated cyclic enaminones provided excellent yields (table 1-4). The lack of reactivity of trisubstituted or *N*-H and *N*-Cbz cyclic enaminones is attributable to steric or electronic factors. 4-Pyridone was found to be a poor substrate for this reaction and an *E*-enaminone afforded only a trace amount of product.

These alkenylated cyclic enaminones are suitable substrates for Diels-Alder reaction as dienophiles (scheme 1-13).[15b] The reaction between diene **49** and the dienophile yielded 1,3,5-trisubstituted benzene instead of Diels-Alder adduct **50**. Electron-withdrawing groups and the amino leaving group are believed to facilitate the aromatization in the presence of O_2. Finally, retro-Michael reaction releasing methyl amine affords 1,3,5-trisubstituted benzene. This reaction provides an alternative synthesis for asymmetric arenes.

Scheme 1-13. **Synthesis of 1,3,5-trisubstituted benzene**

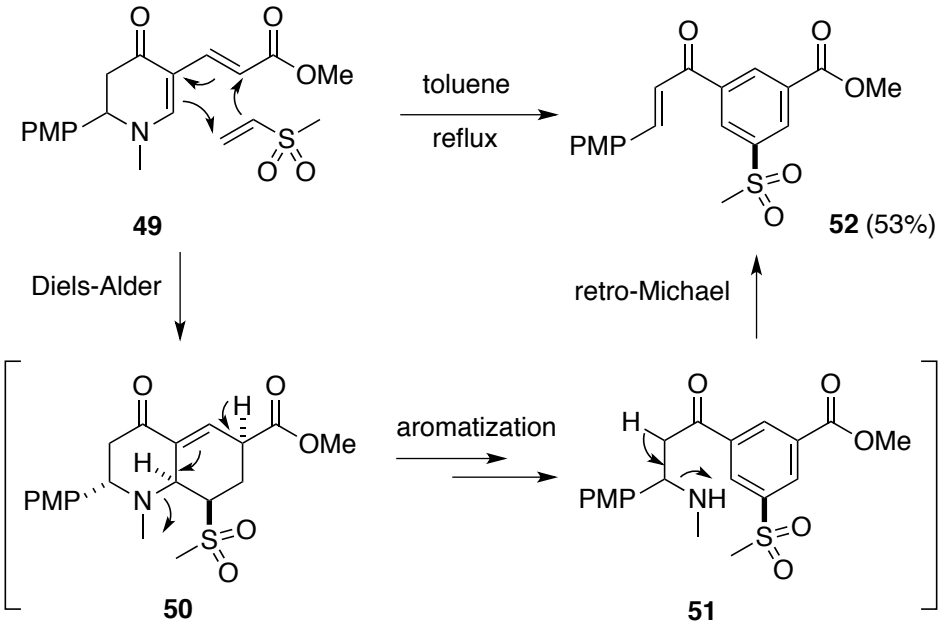

1.3.4 Applications of direct C5 arylation in total synthesis

1.3.4.1 Total syntheses of (+)-ipalbidine and (+)-antofine

Scheme 1-14. Syntheses of (+)-ipalbidine and (+)-antofine

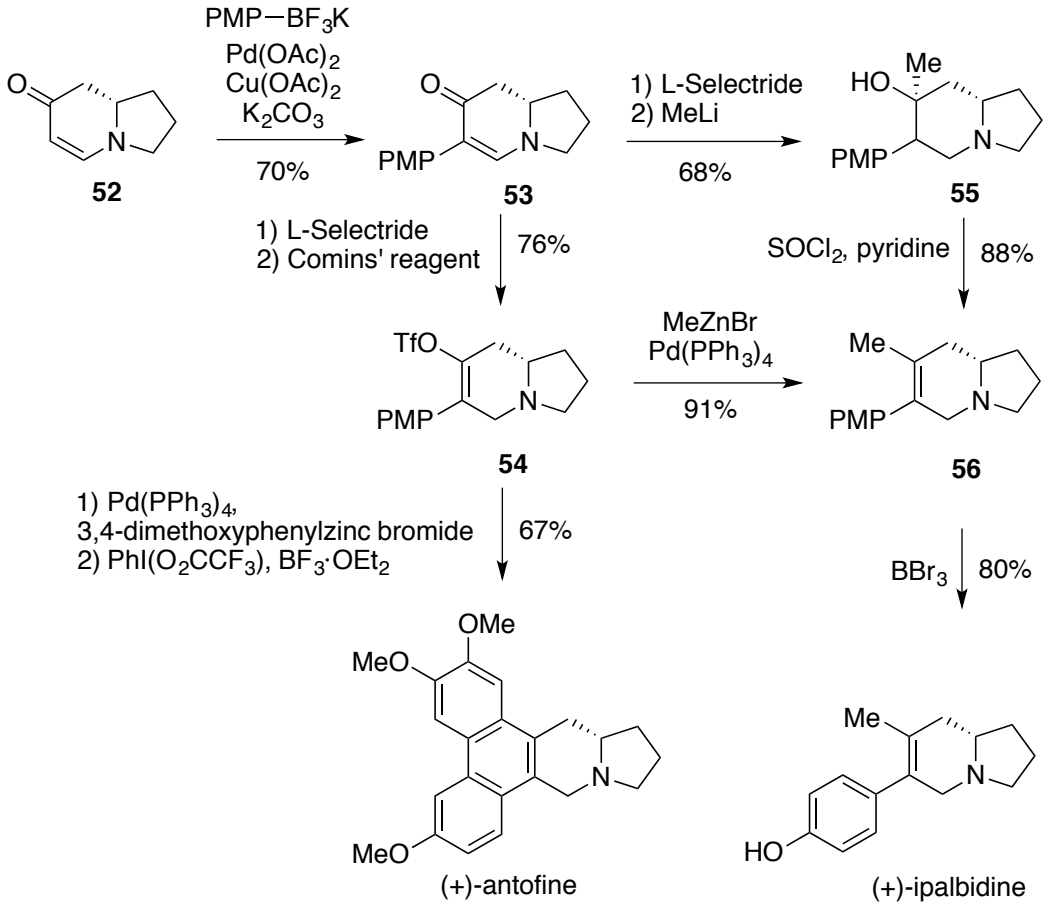

A direct C5 arylation developed previously using organotrifluoroborates was used to prepare arylindolizidine derivatives.[16a] (+)-Ipalbidine is known to have non-addictive analgesic activity and inhibitory effects on respiratory burst of leukocytes.[16b-d] (-)-Antofine exhibits high potency of cancer cell growth inhibition by

inducing arrest in the G2/M phase of the cell cycle.[16e] The total syntheses of (+)-ipalbidine and (+)-antofine were accomplished from a cyclic enaminone intermediate **53** (scheme 1-14). 1,4-Reduction by L-Selectride followed addition of MeLi to the resulting ketone furnished the tertiary alcohol **55**. Dehydration by using $SOCl_2$ and pyridine and BBr_3 deprotection provided (+)-ipalbidine. Alternatively, the compound **53** was reduced by L-Selectride and the resulting enolate was trapped by Comins' reagent to prepare the vinyl triflate **54**, from which the (+)-ipalbidine precursor could be synthesized by Negishi coupling using methylzinc bromide. (+)-Antofine was synthesized in two steps from the vinyl triflate **54**. The 3,4-dimethoxyphenyl group was installed using a Negishi coupling and a biaryl coupling reaction using PIFA completed the synthesis of (+)-antofine.

1.3.4.2 Total syntheses of (*R*)- and (*S*)-boehmeriasin A

The same synthetic pathway was employed in the synthesis of both enantiomers of boehmeriasin A (scheme 1-15).[17a] Boehmeriasin A was found to be more potent than paclitaxel in various cancer cell lines including lung, colon, breast, prostate and kidney.[17b] This natural product has a quinolizidine scaffold that can be made from a bicyclic enaminone derivative **58**. The arylquinolizidines **59** were synthesized following the direct C5 arylation protocol developed previously using 3,4-dimethoxyphenyltrifluoroborate. L-Selectride reduction and a subsequent trapping of the resulting enolate using Comins' reagent provided the vinyl triflate **60**. Palladium catalyzed coupling of the vinyl triflate with 4-methoxyphenylzinc bromide provided

the biarylated intermediate **61**. An oxidative ring closure of the biarylquinolizidine derivatives mediated by VOF_3 furnished both enantiomers of boehmeriasin A in good yields.

Scheme 1-15. Syntheses of (*R*)- and (*S*)-boehmeriasin A

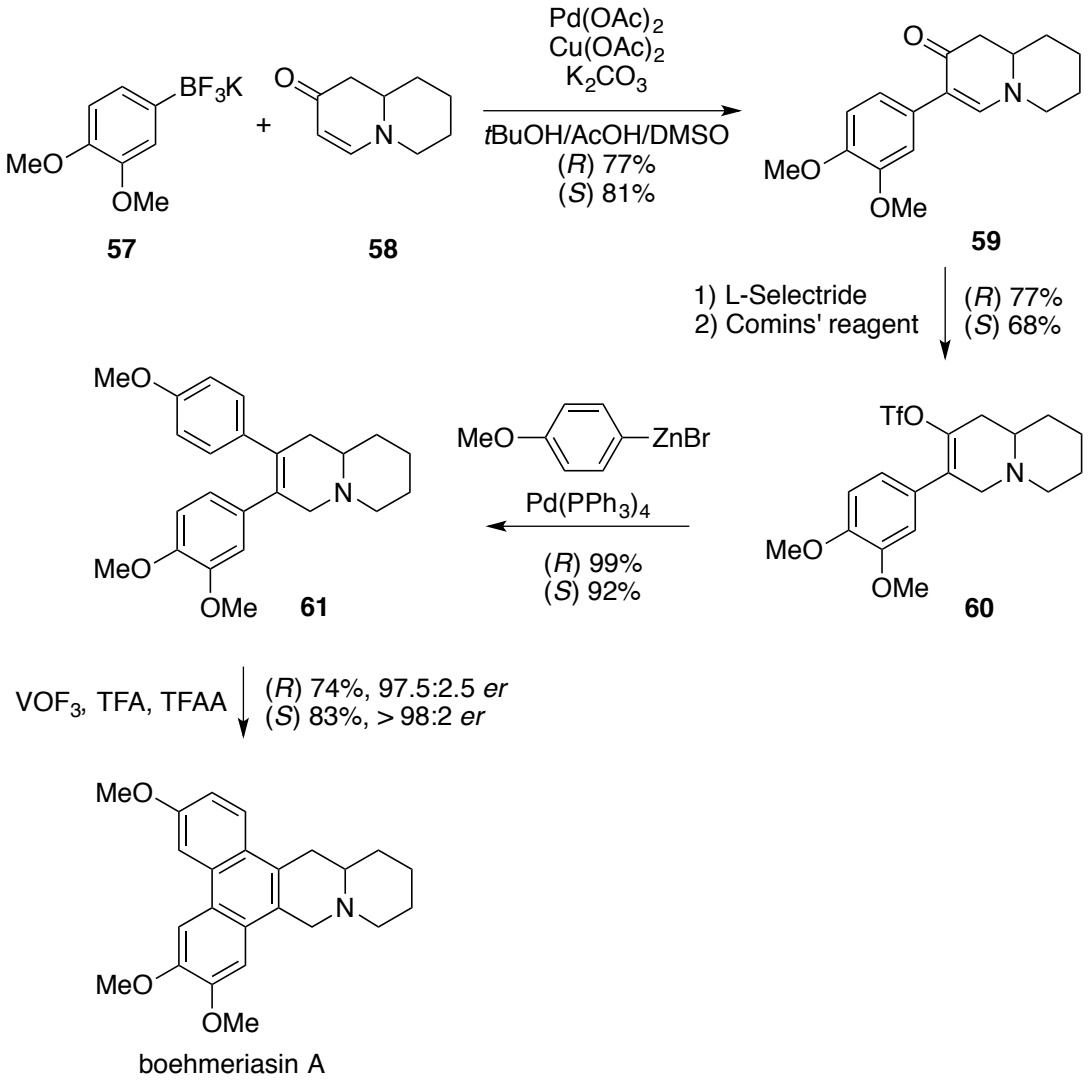

1.3.4.3 Synthesis of phenanthroindolizidines by oxidative aryl-alkene coupling

Scheme 1-16. Oxidative biaryl coupling

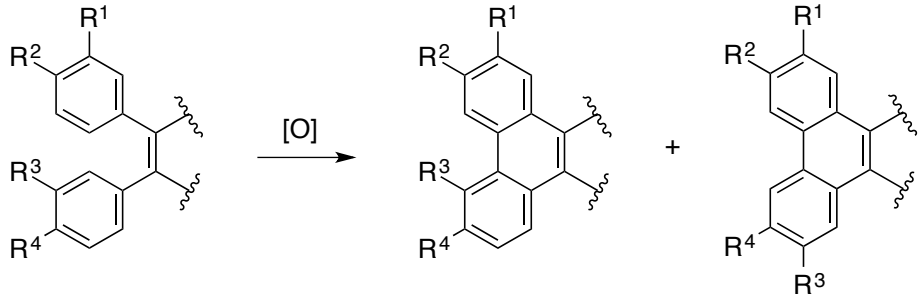

Oxidative biaryl coupling reactions have been used frequently to construct the phenanthrene systems in natural product synthesis (scheme 1-16). However, substrates with sterically disfavored substituents such as a methoxy group at the R^3 position often produce undesired regioisomer. To address this issue, a novel approach was designed involving an aryl-alkene coupling.[18] A cyclic enaminone with an indolizidine scaffold was directly converted to the corresponding vinyl triflate by L-Selectride reduction and enolate trapping. A Negishi cross-coupling between the vinyl triflate and a various biarylzinc bromides provided a series of arylated indolizidines (scheme 1-17).

Scheme 1-17. Coupling of indolizidine and biaryl fragments

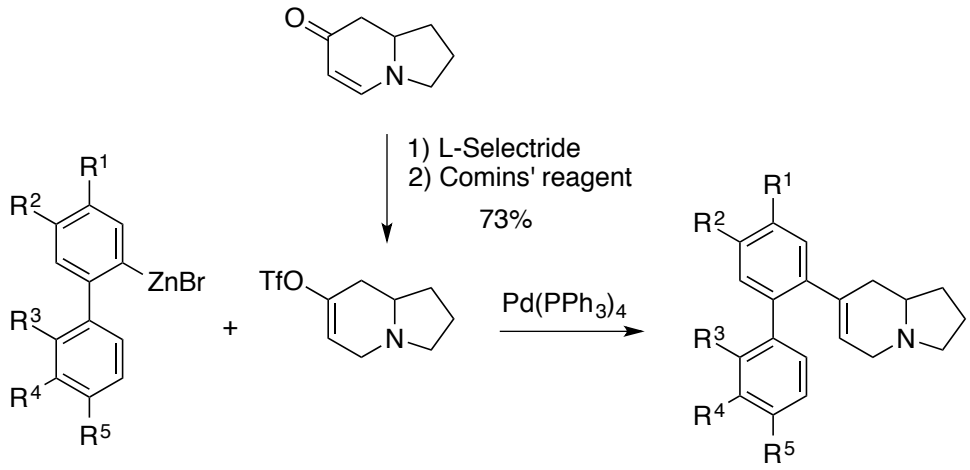

VOF_3 mediated oxidative aryl-alkene coupling was successfully applied to the preparation of eight phenanthroindolizidines including tylocrebrine, tylophorine and antofine (table 1-5). This protocol provides regioselective preparation of phenanthroindolizidines, although R^3-containing substrates showed low reactivity compared to others.

Table 1-5. Aryl-alkene biaryl coupling

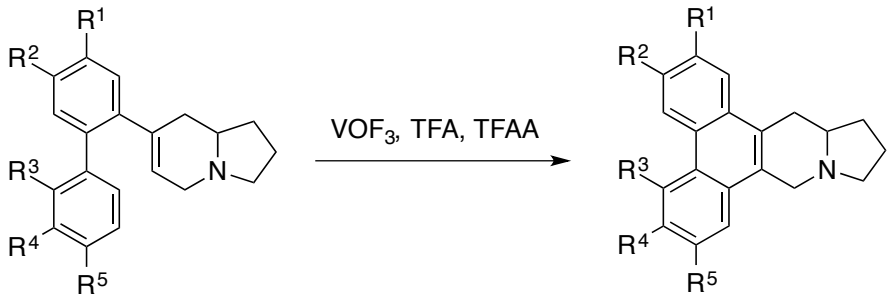

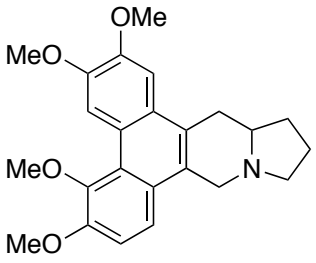

tylocrebrine (62%)

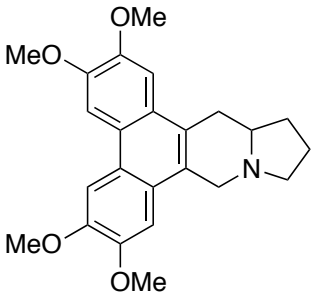

tylophorine (89%)

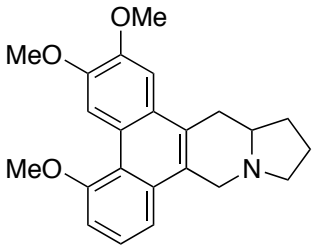

28%

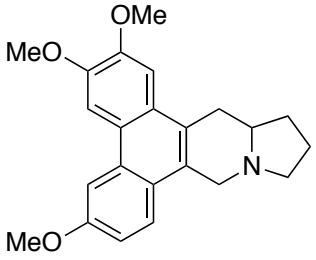

antofine (85%)

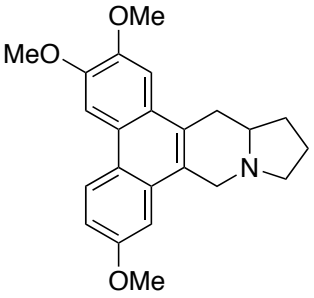

70%

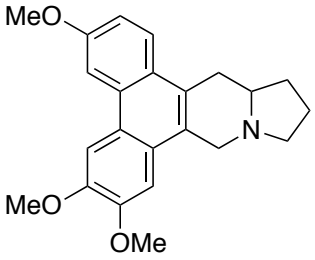

68%

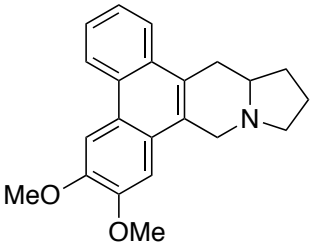

85%

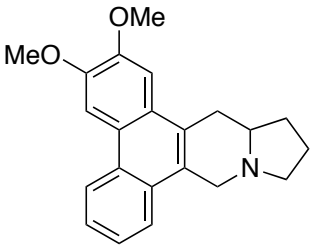

65%

Chapter 2

C5 arylation of cyclic enaminone using boronic acids

2.1 Introduction

As discussed in Chapter 1, a few ways for C5 arylation of cyclic enaminones have been developed. Comins' group achieved C5 arylation by Negishi coupling or Stille coupling in two-step sequence. Georg's group also developed a C5 arylation method for cyclic enaminones in two steps using a Suzuki coupling assisted by microwave. Direct C5 arylations were also developed using aryltrifluoroborates or arylsilanes under oxidative Pd(II)-catalysis. Although these methods provide a short and convenient route to arylated enaminones, several shortcomings limit their utility and inspired us to expand the scope and efficiency of this reaction. In this chapter, the development of a new arylation protocol that accommodates arylboronic acids, which are more readily available than either aryltrifluoroborates or arylsilanes will be described.

2.2 Copper effect in cross-coupling reactions

Copper additives have been shown to improve Stille[19] and Suzuki[20] reactions and are used in Sonogashira[21] reactions. It has been postulated that copper transmetallates with organometals to generate a more reactive organocopper intermediate, which

assists the delivery of the aryl group to the palladium center.[22]

2.2.1 Copper effect in the Stille coupling

Liebeskind *et al.* reported the effect of CuI on the kinetics of a typical Stille coupling.[19a] Cocatalytic Cu(I) salts yielded an over 100-fold rate increase when triphenylphosphine was used as the Pd ligand (table 2-1). In ethereal solvents such as THF or dioxane, CuI works as a scavenger for any free ligand, which is known to prevent the rate-limiting transmetallation step. In highly polar aprotic solvents such as NMP and DMF, it has been suggested that CuI forms a more reactive organocopper species when organostannanes are unsaturated or without strong ligands.

Table 2-1. Effect of added CuI on the rate of the Stille coupling

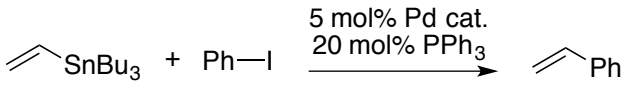

CuI (mol%)	k_{obs}	yield (%)
0	2.66	85
5	13.5	91
10	303	> 95
15	590	78

More recently, a significant enhancement of the Stille reaction by the combination of CuI and CsF was reported.[19b] It was suggested that the transmetallation between the organostanne and CuI is in an equilibrium (figure 2-1). Therefore, the removal of

Bu_3SnI into insoluble Bu_3SnF drives the equilibrium into the formation of the more reactive organocopper intermediate.

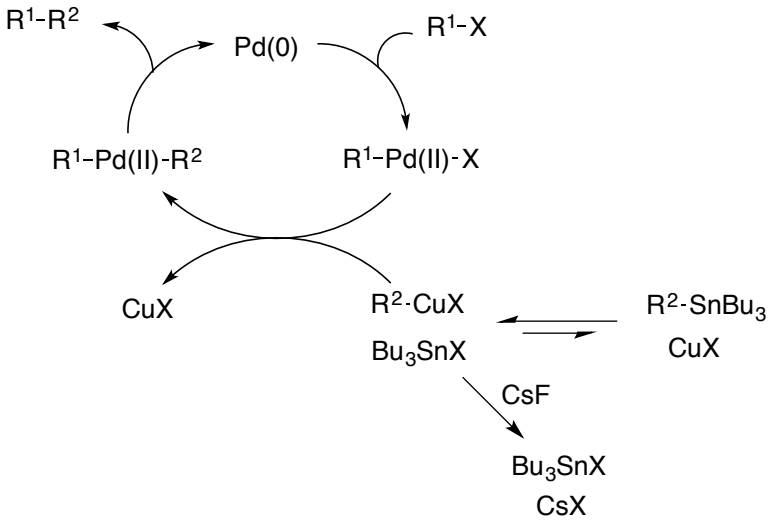

Figure 2-1. Proposed mechanism of the Stille coupling.

Table 2-2. Effects of CuI and CsF in the Stille coupling

reagents	yield (%)
$Pd(PPh_3)_4$	2
$Pd(PPh_3)_4$, CsF	8
$Pd(PPh_3)_4$, CuI	46
$Pd(PPh_3)_4$, CsF and CuI	98
CsF and CuI	0

The series of reactions described in table 2-2 demonstrates the effects of CuI and

CsF. The addition of CsF did not improve noticeably the reaction efficiency.[19b] On the other hand, the addition of CuI showed a significant improvement of the yield. In addition, the combination of these two additives proceeded in quantitative yield, which implies the formation of the reactive organocopper species as described in the proposed mechanism.

2.2.2 Copper effect in the Suzuki coupling

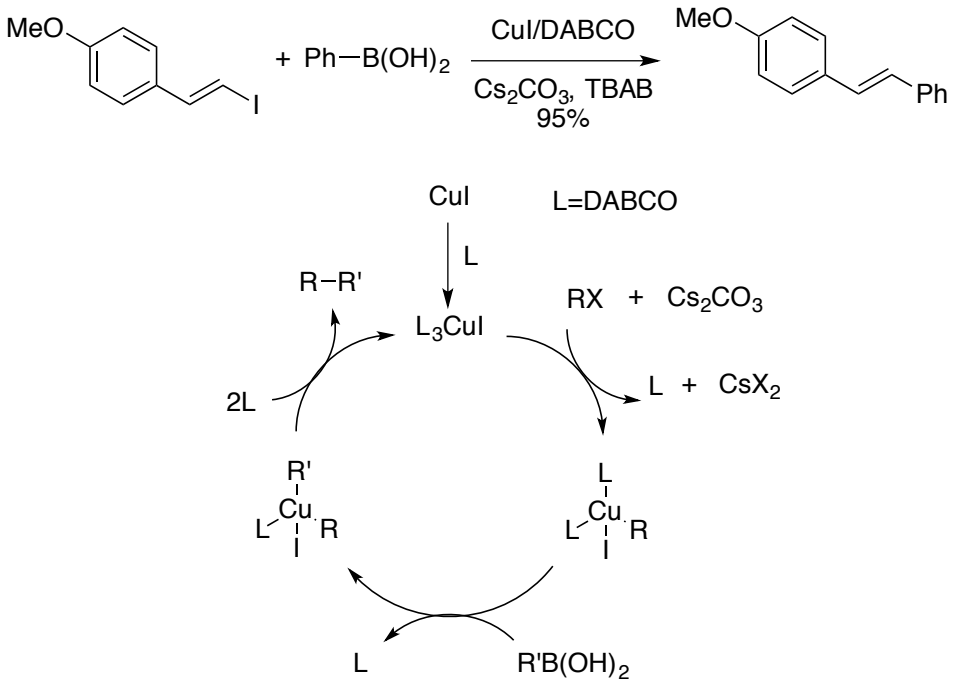

Figure 2-2. Copper catalyzed Suzuki coupling reaction.

Copper salts have also been employed in Suzuki coupling reactions. For example, the CuI/DABCO catalytic system in place of a palladium catalyst has been reported in the Suzuki coupling reaction (figure 2-2).[20a] The reaction between the vinyl halide

and phenylboronic acid afforded the corresponding product under Cu(I) catalysis. In the proposed mechanism, the authors suggested a four-centered organocopper intermediate. After a subsequent transmetallation with the vinyl halide and the arylboronic acid, the resulting intermediate undergoes a reductive elimination to afford the coupled product.

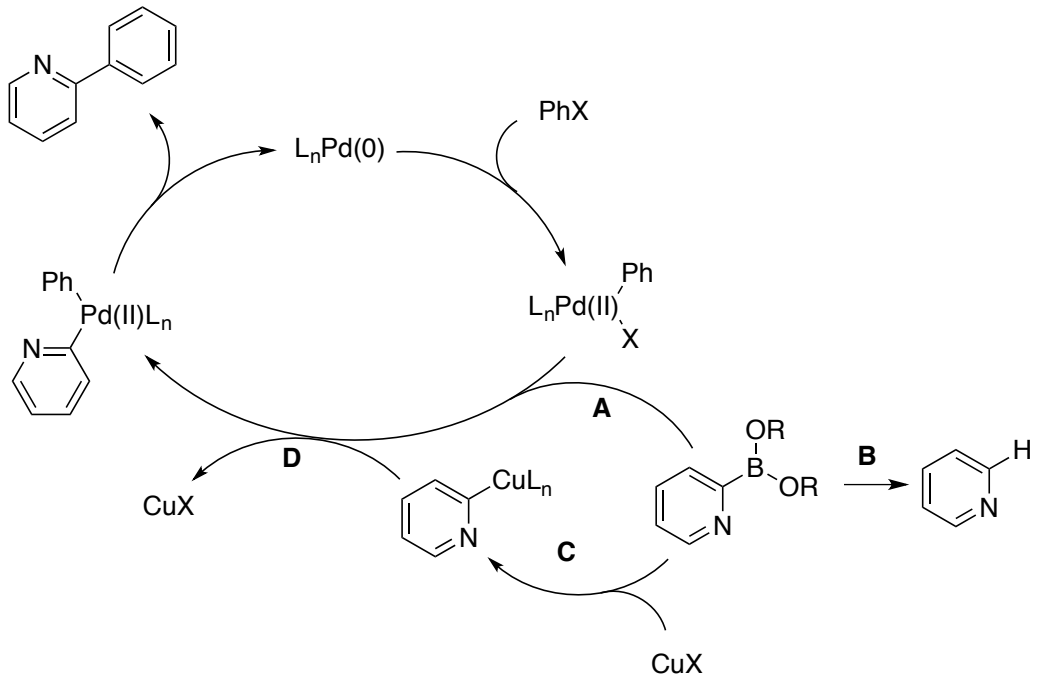

Figure 2-3. Proposed mechanism of copper facilitated Suzuki reaction.

On the other hand, 2-pyridyl boronates, which are notoriously poor coupling partners, undergo high-yielding Suzuki reactions in the presence of copper but not without (figure 2-3).[22a] Because the direct transmetallation (path A) is slower than the deboronation (path B), the authors suggested that the formation of an organocopper species (path C) and a second transmetallation to the palladium complex (path D)

could explain this efficient process. The reaction indeed proceeded in high yield with a copper additive while standard conditions without copper additive displayed low conversion to product (scheme 2-1, eq 1). When homocoupling experiments were conducted to support the transmetallation from boron to copper, the product was not observed in the absence of a copper additive, which provides indirect evidence for step C (scheme 2-1, eq 2). The second transmetallation from copper to palladium (step D) was verified by the coupling reaction between independently prepared arylcopper and a preformed palladium complex (scheme 2-1, eq 3). In this study, the role of copper was suggested to facilitate the transmetallation of an organoboron to a palladium complex via an organocopper intermediate.

Scheme 2-1. Copper facilitated Suzuki reaction

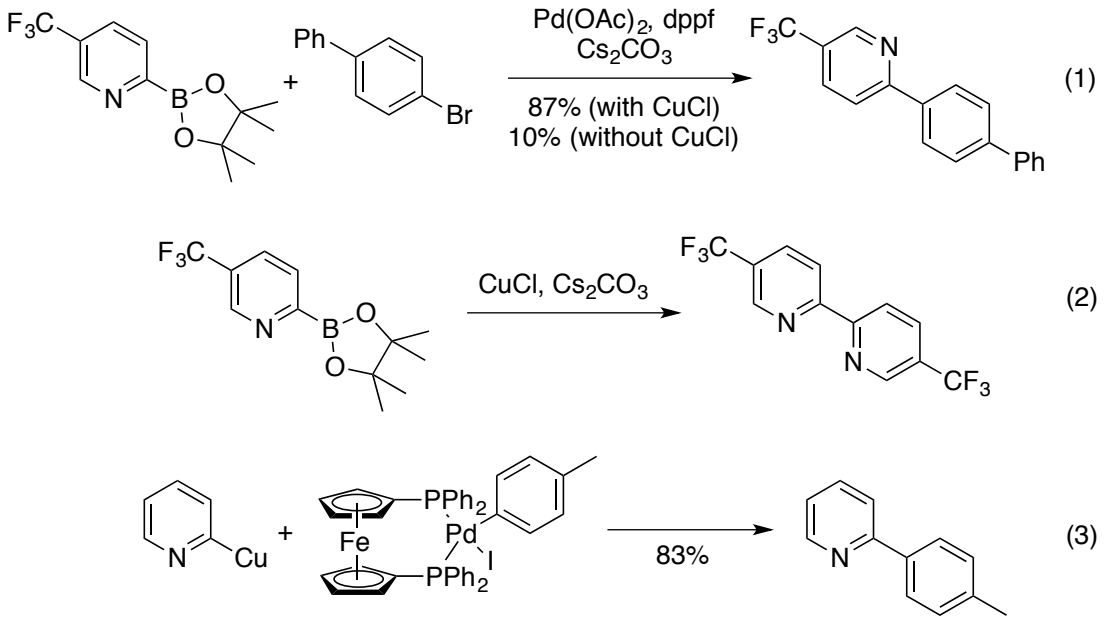

2.3 Formation of arylcopper species using arylboronic acids

The formation of an arylcopper species from an arylboronic acid with copper(I) additives was shown in the above discussed Suzuki coupling reactions. Prior to these discoveries, Chan,[23a] Evans[23b] and Lam[23c] independently reported carbon-heteroatom cross-coupling reactions using arylboronic acids mediated by copper(II) (scheme 2-2).[23] The reaction mechanism implicates the arylcopper species as a reactive intermediate, which was made from the transmetallation of the arylboronic acid with cupric acetate.

Scheme 2-2. Copper mediated carbon-heteroatom coupling reaction.

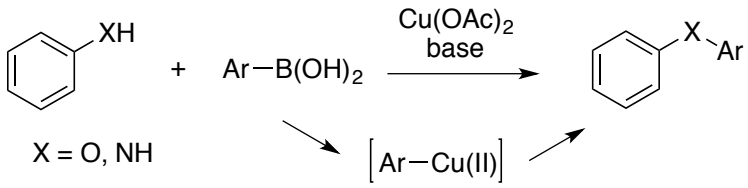

To develop a more efficient method to functionalize the C5 position in the cyclic enaminone system, we took advantage of the idea that the formation of a reactive arylcopper species would facilitate the direct C5 arylation of cyclic enaminones. By analogy with the previous reports described above, we chose an arylboronic acid and cupric acetate for the palladium(II) catalyzed reaction to generate an intermediate arylcopper species (figure 2-4).

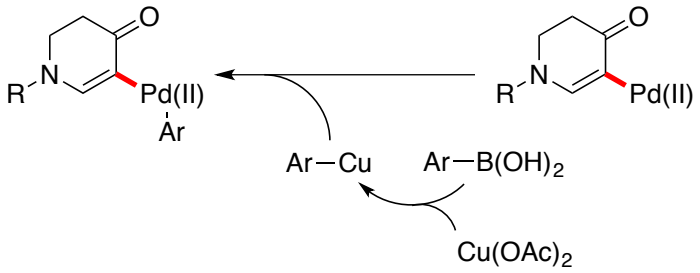

Figure 2-4. Formation of an arylcopper species in the direct C5 arylation.

2.4 Reaction Optimization

2.4.1 Screening of solvents

Table 2-3. Screening of solvents[a]

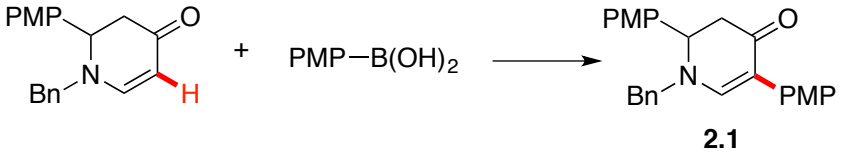

2.1

entry	solvent	yield (%)	entry	solvent	yield (%)
1	*t*-BuOH	6	8	NMP	14
2	*t*-AmOH	< 3	9	Dioxane	< 3
3	Toluene	< 3	10	MeCN	9
4	DMSO	11	11	DMF/DMSO = 20/1	9
5	AcOH	4	12	DMF/AcOH/DMSO = 20/5/1	< 3
6	**DMF**	**18**	13	DMF/AcOH = 4/1	15
7	DMA	18	14	DMF/H_2O = 9/1	15

[a] Reaction conditions: cyclic enaminone (1 equiv), arylboronic acid (2 equiv), $Pd(OAc)_2$ (10 mol%), $Cu(OAc)_2$ (2 equiv), solvent (0.2 M) under N_2 for 20 h at 60 °C, the yield was determined by ^1H NMR analysis of the crude product using Ph_3SiMe (1 equiv) as the internal standard.

We undertook an intensive screening process (table 2-3) using *N*-benzyl-2-(*p*-methoxyphenyl)-2,3-dihydropyridin-4(1*H*)-one and *p*-methoxyphenylboronic acid as model substrates. Since the reaction conditions require an oxidant to regenerate the Pd(II) catalyst, we hypothesized that our copper source could serve a dual role as an oxidant and to assist transmetallation. As such, $Pd(OAc)_2$ (10 mol%) and $Cu(OAc)_2$ (2 equiv) were initially chosen based on previously optimized conditions for enaminone coupling reactions.[13] Amide solvents (DMF, NMP and DMA) were superior to other solvents; however, the yields were quite low. It is worth noting that the use of a cosolvent to promote the oxidation of Pd(0)[24] or to increase the electrophilicity of the Pd(II) center[25] did not improve the yields (table 2-3, entries 11 and 12).

2.4.2 Screening of oxidants

We next screened various oxidants, finding no improvement in yield over $Cu(OAc)_2$ (table 2-4). Interestingly, the use of $CuCl_2$ was comparable to $Cu(OAc)_2$ (table 2-4, entry 10). We noted that in most reactions the majority of cyclic enaminone remained unreacted and the major product was 4,4'-dimethoxy-1,1'-biphenyl, suggesting that the low yields resulted from consumption of the boronic acid and the reoxidant through a competing homodimerization pathway.

Table 2-4. Screening of oxidants[a]

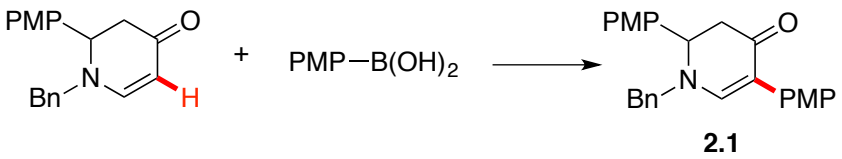

2.1

entry	oxidant (equiv)	yield (%)	entry	oxidant (equiv)	yield (%)
1	$Cu(OTf)_2$ (2)	11	6	$Cu(OAc)_2$ (1) + Ag_2O (1)	16
2	Duroquinone (2)	< 3	7	$Cu(OAc)_2$ (1) + air	8
3	$PhCO_3t$-Bu (1)	< 3	8	$Cu(OAc)_2$ (1) + O_2	8
4	Ag_2O (2)	< 3	9	O_2	0 (0[b])
5	AgOAc (2)	15	10	$CuCl_2$ (2)	18

[a] Reaction conditions: cyclic enaminone (1 equiv), arylboronic acid (2 equiv), $Pd(OAc)_2$ (10 mol%), DMF (0.2 M) under N_2 for 20 h at 60 °C, the yield was determined by ^1H NMR analysis of the crude product using Ph_3SiMe (1 equiv) as the internal standard. [b] DMSO was used as a solvent.

2.4.3 Screening of additives

Next we turned to screening various additives to improve our low reaction yields (table 2-5). We were pleased to find that many organic and inorganic additives improved yields. Most notably, the addition of potassium salts (table 2-5, entries 3 and 9), acetate salts (table 2-5, entries 8–10) or chloride salts (table 2-5, entries 16–24) seemed to have beneficial effects. Particularly, the conditions with LiCl (table 2-5, entry 17), Mg_2Cl (table 2-5, entry 21), $BiCl_3$ (table 2-5, entry 23), and $CuCl_2$ (table 2-5, entry 24) showed higher yields in comparison with other additives. Among chloride salts, $CuCl_2$ was the best additive and yielded 73% of the reaction product (table 2-5, entry 24). We were curious whether these additive effects would persist if

oxygen was used instead of $Cu(OAc)_2$. It turned out that chloride salts combined with molecular oxygen showed very low yields (table 2-5, entries 25 and 26). The unique mixture of $Cu(OAc)_2$ and a chloride source was essential for the efficiency of the reaction.

Table 2-5. Screening of additives[a]

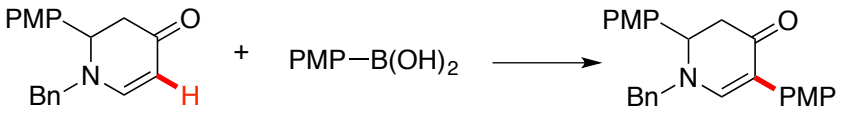

2.1

entry	additive (equiv)	yield (%)	entry	additive (equiv)	yield (%)
1	none	18	14	Me_3CCO_2H (1)	16
2	NaF (2)	16	15	TFA (0.1)	31
3	KF (2)	41	16	HCl[c] (1)	22
4	CsF (2)	28	17	LiCl (1)	55
5	TBAF[b] (2)	11	18	NaCl (1)	18
6	KTFA (1)	33	19	KCl (1)	16
7	$LiBF_4$ (1)	17	20	CsCl (1)	34
8	NaOAc (1)	29	21	$MgCl_2$ (1)	51
9	KOAc (1)	47	22	$CaCl_2$ (1)	25
10	CsOAc (1)	28	23	$BiCl_3$ (1)	61
11	K_2CO_3 (1)	34	**24**	**$CuCl_2$ (1)**	**73**
12	Cs_2CO_3 (1)	17	25[d]	$CuCl_2$ (1)	15
13	K_3PO_4 (1)	31	26[d]	LiCl (1)	0

[a] Reaction conditions: cyclic enaminone (1 equiv), arylboronic acid (2 equiv), $Pd(OAc)_2$ (10 mol%), $Cu(OAc)_2$ (2 equiv), solvent (0.2 M) under N_2 for 20 h at 60 °C, the yield was determined by ^1H NMR analysis of the crude product using Ph_3SiMe (1 equiv) as the internal standard. [b] 1.0 M in THF. [c] 12.1 M. [d] O_2 was used as a reoxidant.

2.4.4 Screening of copper additives

The advantageous effects of $CuCl_2$ led us to examine alternative sources of copper and optimal quantities of these additives (table 2-6). As seen in entries 5 and 6, the highest yields (81%) were obtained when using at least two equivalents of $CuCl_2$. Interestingly, CuCl only moderately improved yields and CuI completely suppressed product formation.

Table 2-6. Screening of copper additives[a]

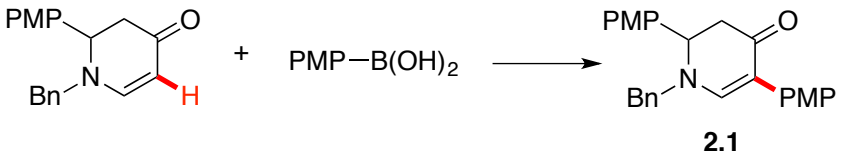

2.1

entry	additive (equiv)	yield (%)
1	CuCl (2)	31
2	CuI (2)	0
3	$CuCl_2$ (0.5)	60
4	$CuCl_2$ (1)	73
5	**$CuCl_2$ (2)**	**81**
6	$CuCl_2$ (3)	81

[a] Reaction conditions: cyclic enaminone (1 equiv), arylboronic acid (2 equiv), $Pd(OAc)_2$ (10 mol%), $Cu(OAc)_2$ (2 equiv), solvent (0.2 M) under N_2 for 20 h at 60 °C, the yield was determined by ^1H NMR analysis of the crude product using Ph_3SiMe (1 equiv) as the internal standard.

2.4.5 Screening of reaction temperature and time

Table 2-7. Screening of reaction temperature and time[a]

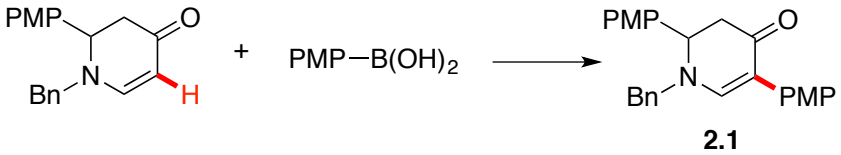

2.1

entry	time	temperature (°C)	yield (%)
1	20 hr	25	71
2	2 hr	40	78
3	2 hr	50	79
4	2 hr	60	81
5	2 hr	80	74
6	10 min	60	78
7	20 min	60	80
8	30 min	60	81
9	40 min	60	80
10	50 min	60	80
11	**1 hr**	**60**	**81**

[a] Reaction conditions: cyclic enaminone (1 equiv), arylboronic acid (2 equiv), $Pd(OAc)_2$ (10 mol%), $Cu(OAc)_2$ (2 equiv), solvent (0.2 M) under N_2, the yield was determined by ^1H NMR analysis of the crude product using Ph_3SiMe (1 equiv) as the internal standard.

We also investigated the optimal reaction temperature and time that it takes to complete the reaction (table 2-7). We found that the reaction is completed in less than 2 hours and at temperatures over 40 °C (table 2-7, entries 2–5), although the highest yield was observed at 60 °C. High temperature seems to decompose the compounds, leading to decreased yields (table 2-7, entry 5). On the other hand, room temperature conditions provided a slightly lower conversion due to the slow rate of the reaction (table 2-7, entry 1). We found that the rate of the reaction is extremely

fast and reaction for 1 hour at 60 °C provided the same yield of **2.1** (81%) as obtained from a 20 hours reaction time.

2.5 Scope of arylboronic acids

Having established a high-yielding protocol for cross-coupling, we applied our optimized conditions to a collection of electronically diverse arylboronic acids (table 2-8). In contrast to our previously reported method using trifluoroborates,[13] both electron-rich and electron-poor arylboronic acids coupled smoothly and in high yields. As exemplified by the lower yields of *o*-methoxy substituted arenes (table 2-8, entry 3) compared with those of *p*- and *m*-methoxy substituted arenes (table 2-8, entries 1 and 2), steric factors clearly reduced cross-coupling efficiency, albeit to a lesser extent than we had previously noted in reactions with trifluoroborates.[3a] In general, this method was found to have excellent functional group compatibility. A phenol (table 2-8, entry 6), an aryl bromide (table 2-8, entry 9), a 1º amide (table 2-8, entry 11), a ketone (table 2-8, entry 12) and an aldehyde (table 2-8, entry 15) were all well tolerated. However, thienylboronic acid coupled in low yield (table 2-8, entry 17) and furanylboronic acid did not afford any product (table 2-8, entry 18).

Table 2-8. Scope of arylboronic acids[a]

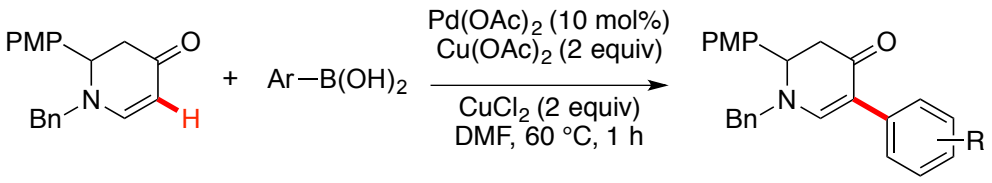

entry	R	yield (%)	entry	R	yield (%)
1	4-OMe (**2.1**)	81	10	4-CF_3 (**2.10**)	80
2	3- OMe (**2.2**)	80	11	4-$CONH_2$ (**2.11**)	74
3	2- OMe (**2.3**)	51	12	4-Ac (**2.12**)	82
4	H (**2.4**)	80	13	4-NO_2 (**2.13**)	90
5	4-Me (**2.5**)	75	14	4-CN (**2.14**)	78
6	4-OH (**2.6**)	62	15	4-formyl (**2.15**)	83
7	4-F (**2.7**)	85	16	2-naphthyl (**2.16**)	83
8	4-Cl (**2.8**)	78	17	3-thienyl (**2.17**)	24
9	4-Br (**2.9**)	86	18	3-furanyl (**2.18**)	0

[a] Reaction conditions: cyclic enaminone (1 equiv), arylboronic acid (2 equiv), $Pd(OAc)_2$ (10 mol%), $Cu(OAc)_2$ (2 equiv), solvent (0.2 M) under N_2.

2.6 Scope of cyclic enaminones

Next we varied the enaminone component, and used *p*-methoxyphenylboronic acid as a model boronic acid (table 2-9). As we observed previously,[13] mono- and bicyclic enaminones with *N*-alkyl substituents were all suitable substrates in this transformation (table 2-9, **2.19**–**2.23**). Notably, *N*-phenyl enaminone **2.20** was also formed in comparable yields to the *N*-benzyl (table 2-9, **2.19**) or the *N*-methyl (Table 4, **2.21**) analogs despite its tempered nucleophilicity. In contrast, the arylation of *N*-carbamylated enaminone **2.26** was not observed. A methyl group in the C6 position was surprisingly well-tolerated, furnishing tetrasubstituted olefinic compound **2.28**.

However, substrates with more sterically demanding groups at C6, such as *tert*-butyl or phenyl, did not react.

Table 2-9. Scope of cyclic enaminones[a]

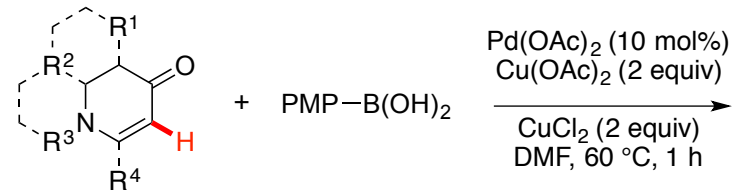

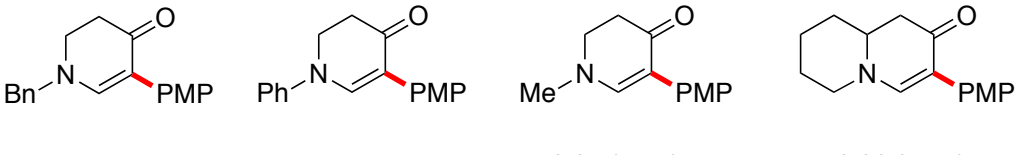

2.19 (70%) **2.20** (60%) **2.21** (65%) **2.22** (82%)

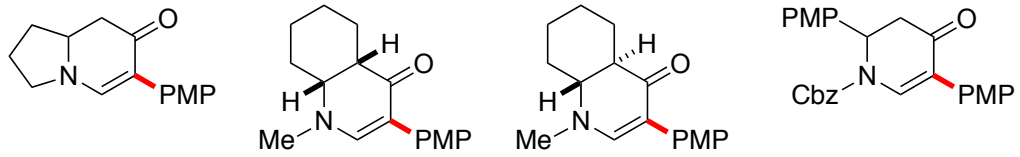

2.23 (56%) **2.24** (76%) **2.25** (83%) **2.26** (Not observed)

2.27 (Not observed)

2.28 (61%, R = Me)
(Not observed, R = *t*-Bu or Ph)

[a] Reaction conditions: cyclic enaminone (1 equiv), arylboronic acid (2 equiv), $Pd(OAc)_2$ (10 mol%), $Cu(OAc)_2$ (2 equiv), solvent (0.2 M) under N_2.

2.7 Mechanistic considerations

Table 2-10. Arylboronic acid homocoupling[a]

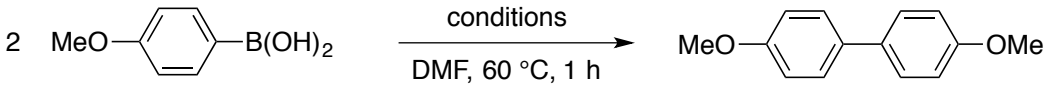

entry	$Pd(OAc)_2$	$Cu(OAc)_2$	$CuCl_2$	yield (%)
1	10 mol%	2 equiv	2 equiv	70
2	10 mol%	2 equiv	none	82
3	10 mol%	none	2 equiv	9
4	none	2 equiv	2 equiv	14
5	none	2 equiv	none	25
6	none	none	2 equiv	6

[a]Reaction conditions: 2a (0.4 M) in DMF under N_2 at 60 °C for 1 h.

The expanded substrate scope and lack of dependency on the electronic nature of the boronic acids led us to speculate that this reaction was proceeding through a mechanism which was distinct from our previously reported method using trifluoroborates.[13] To shed light on the mechanism and respective roles of each reagent, we investigated the optimized reaction conditions in further detail (tables 2-10 and 2-11).

We first noted that subjecting *p*-methoxyphenylboronic acid to the cross-coupling conditions in the absence of an enaminone coupling partner resulted in high yields of the homocoupled by-product (table 2-10, entry 1).[26] Similar results were obtained in the absence of $CuCl_2$ (table 2-10, entry 2), but yields were considerably lower in the absence of $Cu(OAc)_2$ or $Pd(OAc)_2$ (table 2-10, entries 3–6). Notably, under

palladium-free condition (table 2-10, entry 4), we observed rapid and near complete (> 95%) consumption of the boronic acid in under 15 min.

Table 2-11. Cross-coupling of cyclic enaminone and arylboronic acid[a]

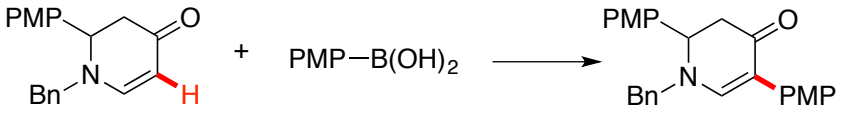

2.1

entry	$Pd(OAc)_2$	$Cu(OAc)_2$	$CuCl_2$	yield (%)
1	none	2 equiv	2 equiv	0
2	none	2 equiv	none	0
3	none	none	2 equiv	0
4	10 mol%	none	none	< 5
5	10 mol%	2 equiv	2 equiv	81
6	10 mol%	2 equiv	none	18
7	10 mol%	none	2 equiv	18
8	10 mol%	4 equiv	none	25
9	100 mol%	none	none	30
10	100 mol%	2 equiv	2 equiv	66
11	100 mol%	2 equiv	none	49
12	100 mol%	none	2 equiv	60

[a]Reaction conditions: **2a** (0.4 M) in DMF under N_2 at 60 °C for 1 h, the yield was determined by ^1H NMR analysis of the crude product using Ph_3SiMe (1 equiv) as the internal standard.

In the presence of the cyclic enaminone coupling partner, cross-coupling was only observed in the presence of palladium (table 2-11). Thus, in contrast to arylboronic acid homocoupling, cyclic enaminone cross-coupling is an exclusively Pd-mediated process. Indeed, the reaction proceeds, albeit in modest yield, in the absence of any copper source when using 100 mol% of $Pd(OAc)_2$ (table 2-11, entry 9). Nevertheless, under these stoichiometric conditions, which presumably minimizes the necessity of a

reoxidant, product formation was improved upon the addition of $Cu(OAc)_2$, $CuCl_2$ or both (table 2-11, entries 10–12). Interestingly, the beneficial effects of the mixed $Cu(OAc)_2/CuCl_2$ system was enhanced when $Pd(OAc)_2$ was employed catalytically (table 2-11, entry 5). Neither $Cu(OAc)_2$ or $CuCl_2$ alone provided high yields of arylated enaminone **2.1**. Additionally, doubling the quantity of $Cu(OAc)_2$ (table 2-11, entry 8) did not significantly improve the coupling reaction, thereby indicating that the effects of the $Cu(OAc)_2$ and $CuCl_2$ system are cooperative and not merely additive.

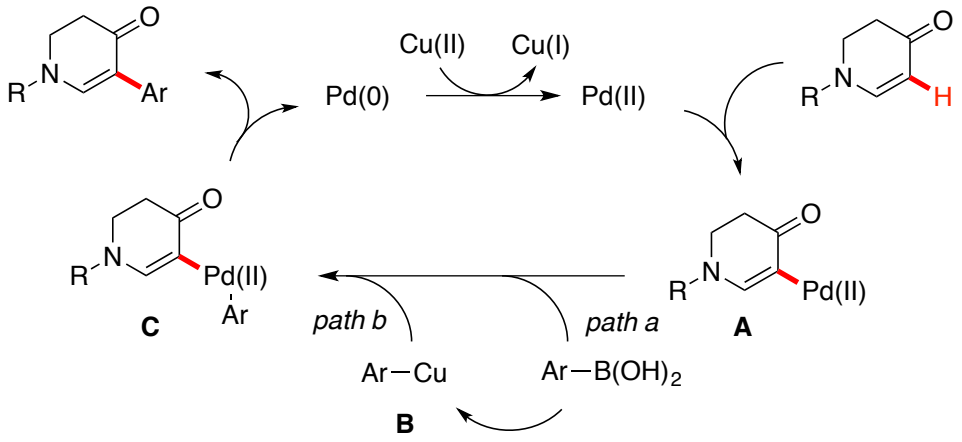

Figure 2-5. Proposed mechanism.

We propose a mechanism that could explain these observations (figure 2-5). We envision that electrophilic palladation initially furnishes an enaminone-palladium complex **A**, which has previously been shown to occur within minutes at room temperature.[15] Once this palladium-enaminone complex has formed, the aryl group is delivered to the palladium center via transmetallation, which could come either

directly from the arylboronic acid (path a) or from a putative arylcopper intermediate (path b). Although the former cannot be completely ruled out, we believe that the latter mechanism is plausible considering the following: (1) arylboronic acids are known to readily transmetallate with $Cu(OAc)_2$ to form organocopper species;[23] (2) the arylboronic acid is rapidly consumed upon exposure to the $Cu(OAc)_2/CuCl_2$ mixture in the absence of palladium; (3) in contrast to our previously developed trifluoroborate cross-coupling method,[13] the rate of reaction is extremely fast; and (4) the reaction efficiency is seemingly independent of the electronic nature of the arylboronic acid. Collectively, these data suggest that $Cu(OAc)_2$ and $CuCl_2$ have mutual roles on improving the efficiency of cross-coupling, presumably through facilitating the delivery of the aryl moiety to the Pd-center via an arylcopper intermediate. However, the precise roles of each reagent in this process remain elusive.

2.8 Conclusion

In summary, we have developed a new method for the C–H arylation of cyclic enaminones using boronic acids as aryl donors. In large part, the success of this reaction is due to a mixture of $Cu(OAc)_2$ and $CuCl_2$ that appear to be cooperative and allows for efficient cross-coupling with a diverse set of arylboronic acids without the previously observed preference for electron-rich coupling partners.[3a] Although the exact role of each copper additive is not clear, we believe that these reagents not only serve as Pd-reoxidants, but also assist aryl delivery to the palladated enaminone

through a putative arylcopper intermediate. As such, this reaction represents a significant advancement over previously developed methods for enaminone arylation and leads us to speculate that this copper additive mixture could be of more general utility in boronic acid cross-coupling reactions where transmetallation is disfavored.

Chapter 3

C5 arylation of cyclic enaminone using diaryliodonium salts

3.1 Introduction

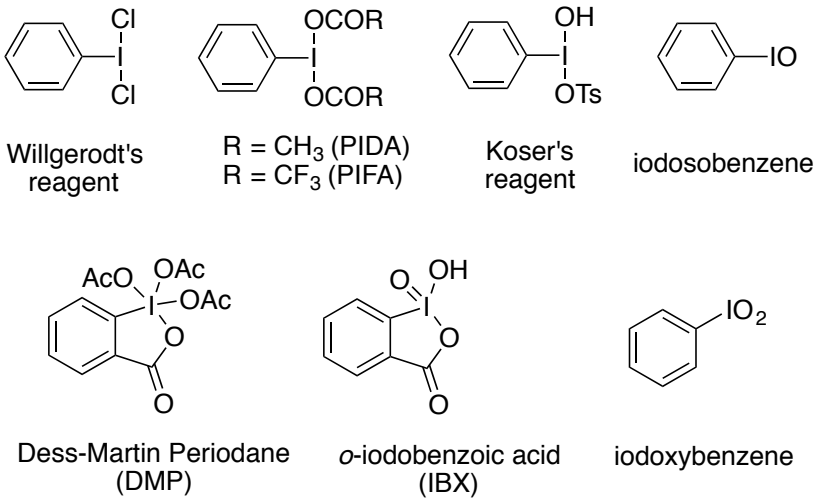

Figure 3-1. **Representative hypervalent iodine reagents.**

Hypervalent iodine reagents were first observed in 1886 and their oxidizing properties have been known over a century.[27] In addition to their oxidizing properties, these reagents have drawn considerable attention due to low toxicity, mild reactivity and easy preparation. Representative examples of hypervalent iodine reagents are shown in fig 3-1. In particular, the reactivities of iodine(III) compounds are similar to those of transition metals, such as participating in reductive elimination reactions and ligand exchange.[28] In this regard, this class of molecular entities can serve as an

alternative to transition metal mediated reactions. In this chapter, the development of a metal-free and copper-catalyzed direct C5 arylation of cyclic enaminones using diaryliodonium salts will be discussed.

3.1.1 The characteristics of diaryliodonium salts

Diaryliodonium salts belong to a class of the most common $ArIL_2$ (L: heteroatom ligand), aryl-λ^3-iodanes. Aryl-λ^3-iodanes have a pseudotrigonal bipyramid geometry with 10 electrons (figure 3-2).[28] The aryl group and two lone pairs of electrons reside in the equatorial position while the two heteroatom ligands are in the apical positions. The aryl-iodine bond is a normal covalent bond but the linear L–I–L bond is a hypervalent three-center four-electron bond. A partial positive charge develops in the central iodine atom since the filled nonbonding orbital has a node at the iodine atom, which makes this compound highly electrophilic.

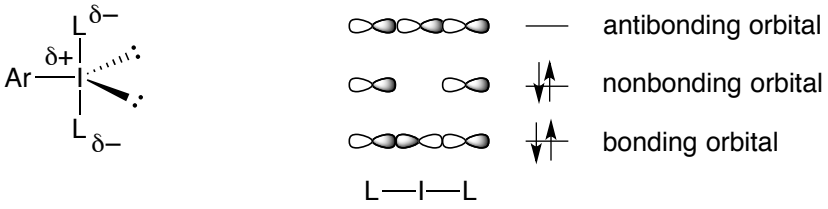

Figure 3-2. **Structure and molecular orbitals of an aryl-λ^3-iodane.**

$ArIL_2$ is usually used in oxidation reactions (scheme 3-1, eq 1). The first ligand is removed in the ligand exchange step (the formation of Nu–I bond) and the second

ligand is consumed for the reductive elimination step, serving as leaving group. Diaryliodonium salts (Ar_2IL) are not good oxidants, however, one carbon ligand (Ar) can be transferred to a nucleophile (the formation of Ar–Nu bond) with reductive elimination of ArI (scheme 3-1, eq 2).

Scheme 3-1. **Reactivity of hypervalent iodine reagents**

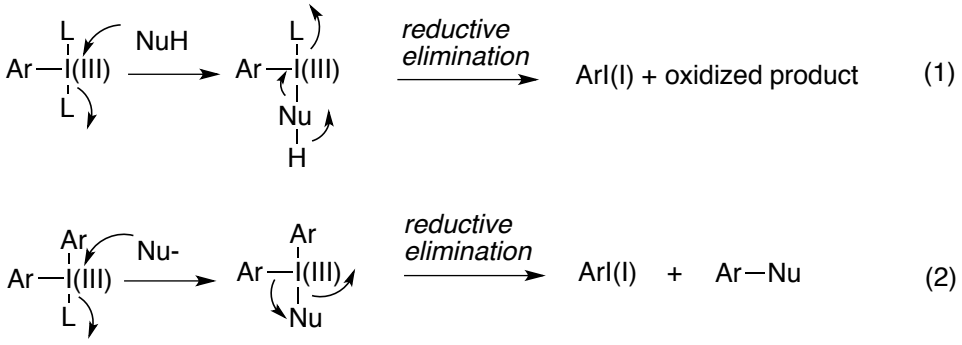

3.1.2 Synthetic applications of diaryliodonium salts

As stated above, diaryliodonium salts belong to the class of aryl-λ^3-iodanes, Ar_2IL. This class of reagents is mostly used in arylation reactions of various substrates. The scope of the reactions spans from the traditional α-arylation of carbonyl compounds to metal catalyzed cross-coupling reactions and C–H bond activation.

3.1.2.1 General α-arylation of carbonyl compounds

Scheme 3-2. α-Arylation of carbonyl compounds

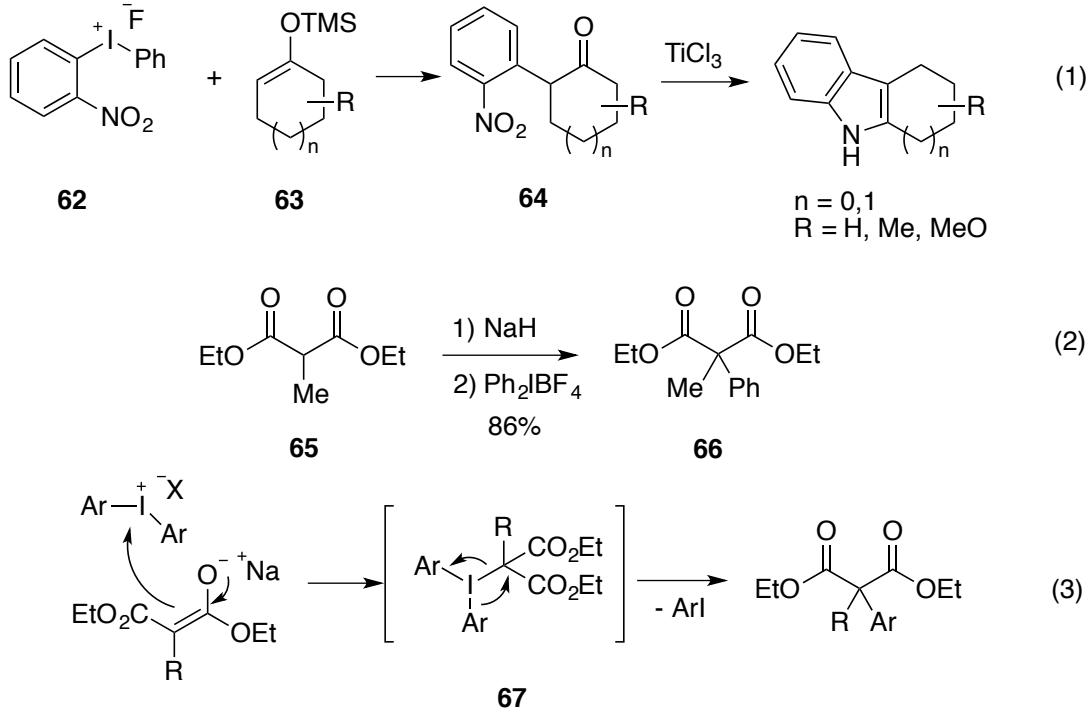

In the arylation reaction between diaryliodonium salts and carbonyl compounds, strong bases such as *tert*-butoxide or LDA were used to generate the corresponding enolates.[29] In some cases, silyl enol ethers were also successfully used instead of enolates (scheme 3-2, eq 1).[30] An arylation of a TMS-enol ether **63** could be accomplished using (2-nitrophenyl)phenyliodonium fluoride **62**. The more electron deficient nitrophenyl group rather than phenyl group was transferred to the substrate.[31] This intermediate **64** was converted to carbocycle fused indoles via the reduction of the nitro group by $TiCl_3$ and spontaneous cyclization.

A highly efficient arylation of malonates was also reported using diaryliodonium salts (scheme 3-2, eq 2).[32] In this study, the use of palladium catalyst with aryl iodide did not furnish any arylated product. Instead, efficient arylation was observed with or

without the palladium catalyst when iodonium salts were employed. An addition elimination mechanism was proposed involving a tricoordinated iodine intermediate **67** (scheme 3-2, eq 3).

3.1.2.2 Asymmetric α-arylation of carbonyl compounds

Scheme 3-3. **Enantioselective α-arylation of aldehyde**

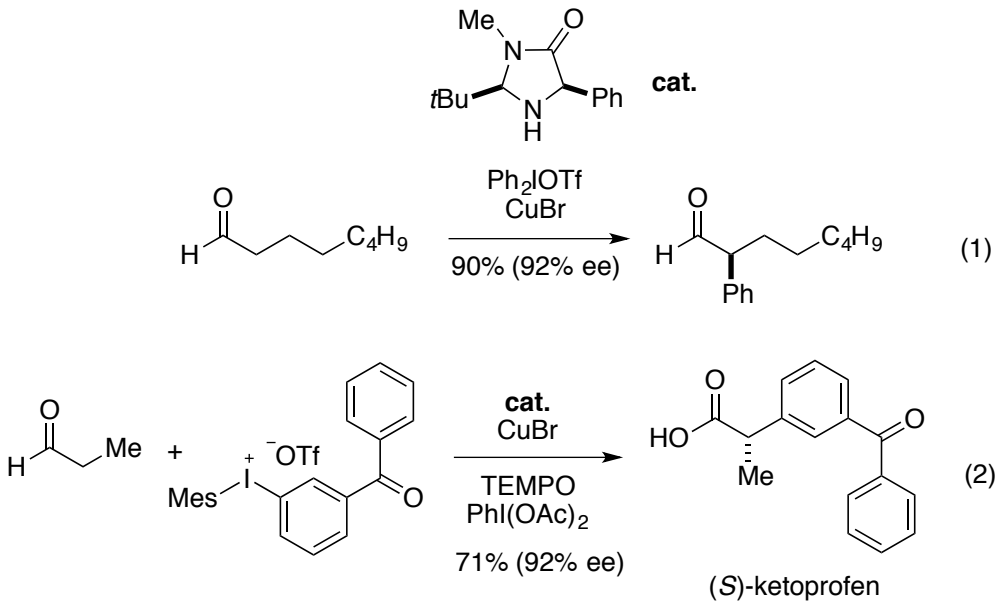

Conventional strategies for asymmetric α-arylations of carbonyl compounds include using binap-based chiral iodonium salts[33] or a chiral base to desymmetrize the substrate.[34] These methods, however, lack practicality because of low ee and limited reagent availability. Recently, new strategies have been designed for α-arylations using diaryliodonium salts. The MacMillan[35] and Gaunt[36] groups independently reported the copper catalyzed enantioselective α-arylation of carbonyl compounds.

MacMillan and co-workers developed the enantioselective α-arylation of aldehydes using a combination of copper and amine catalyst (scheme 3-3, eq 1). This protocol provides access towards α-formyl benzylic stereocenters. For example, a commercial medicinal agent, (*S*)-ketoprofen was prepared by one-pot procedure, involving arylation and in situ aldehyde oxidation (scheme 3-3, eq 2).

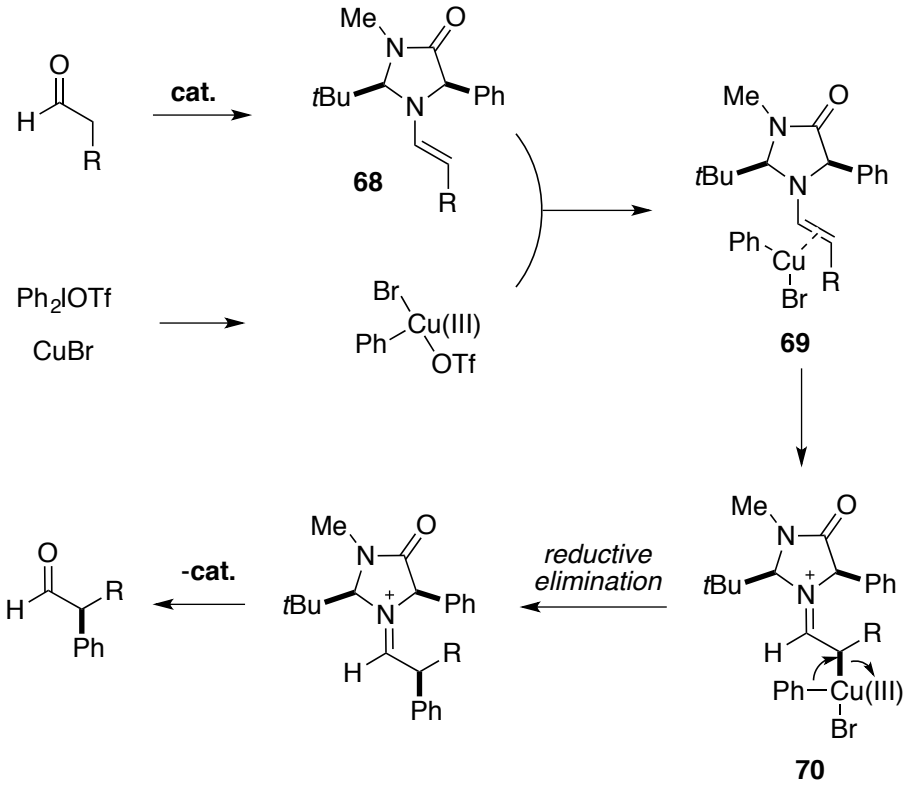

Figure 3-3. **Mechanism for aldehyde α-arylation.**

The tandem catalysis pathway for α-arylation is described in figure 3-3. The activated chiral enamine **68** obtained after condensation of the aldehyde and amine catalyst forms a π-Cu complex **69** with the highly electrophilic aryl–Cu(III) species.

Bond isomerization leads to the η^1-iminium intermediate **70**, which undergoes reductive elimination and iminium hydrolysis to generate the enantioenriched product, CuBr(I) and regenerates the organocatalyst.

Scheme 3-4. **Enantioselective α-arylation of *N*-acyloxazolidinone**

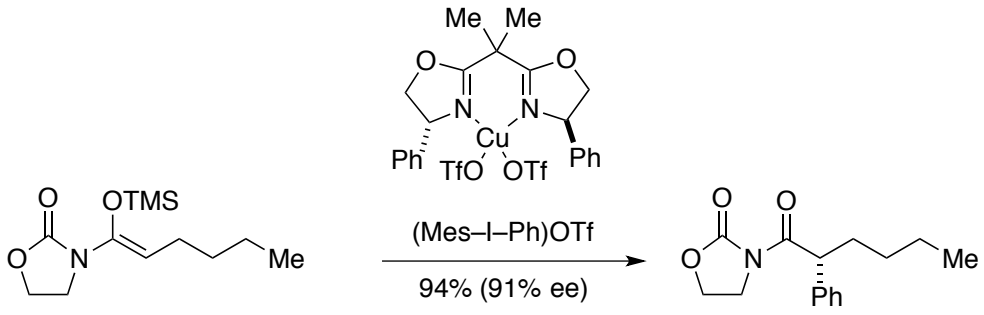

Whereas MacMillan and co-workers chose organocatalyst to desymmetrize the substrate, Gaunt and co-workers exploited a chiral copper catalyst that forms a chiral aryl electrophile. The enantioselective α-arylation of *N*-acyloxazolidinone was developed using a chiral copper(II)-bisoxazoline complex and diaryliodonium salts (scheme 3-4).[37] Silylketenimides derived from *N*-acyloxazolidinones were used as substrates for this transformation as the products can be converted to various functional groups, including carboxylic acids, esters, ketones, aldehydes and alcohols in one step.

3.1.2.3 Metal catalyzed cross coupling reactions

Diaryliodonium salts have been used as an aryl source in palladium catalyzed

arylation of arenes with *ortho*-directing groups via C–H activation. Daugulis and Zaitsev reported only one example of an *ortho*-arylation of an anilide with diphenyliodonium hexafluorophosphate, while all other reactions proceeded with aryl iodides (scheme 3-5, eq 1).[37] On the other hand, Sanford *et al*. reported more a general method for *ortho* C–H arylation of arenes using tetrafluoroborate salts (scheme 3-5, eq 2).[38] In contrast to the conventional Pd(0)/Pd(II) catalysis, a Pd(II)/Pd(IV) catalytic cycle facilitated by highly oxidizing iodonium reagent was suggested (scheme 3-5, eq 3). After the formation of the cyclometalated Pd(II) complex, oxidation of the Pd(II) complex by an aryliodonium salt generates the putative Pd(IV) intermediate. Subsequent C–C bond formation by reductive elimination affords the product as well as the regenerated Pd(II) catalyst.

Scheme 3-5. **Metal–catalyzed C–H arylation of arenes**

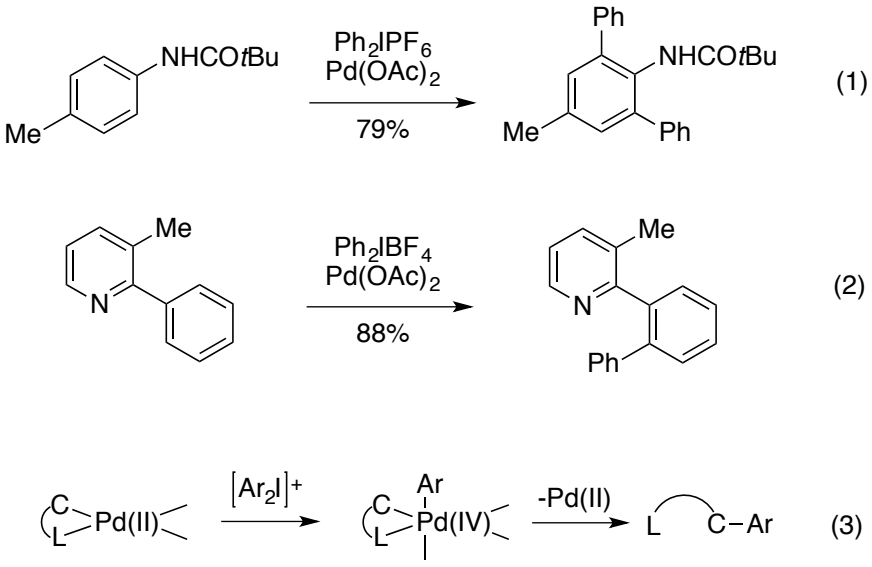

L = pyridine, quinoline, oxazolidinone, etc

The use of diaryliodonium salts with copper catalyst in C–H activation of arenes showed very interesting results (scheme 3-6).[39] Phenyl electrophiles were selectively installed at the C–H bond *meta* to an amido substituent. The highly electrophilic Cu(III)-aryl species activates the aromatic ring to afford anti-oxy-cupration of the carbonyl group of the amide substituent, placing the Cu(III)-aryl species at the *meta* position. Subsequent aromatization by deprotonation and reductive elimination provides the *meta* product.

Scheme 3-6. ***meta*-Selective C–H arylation**

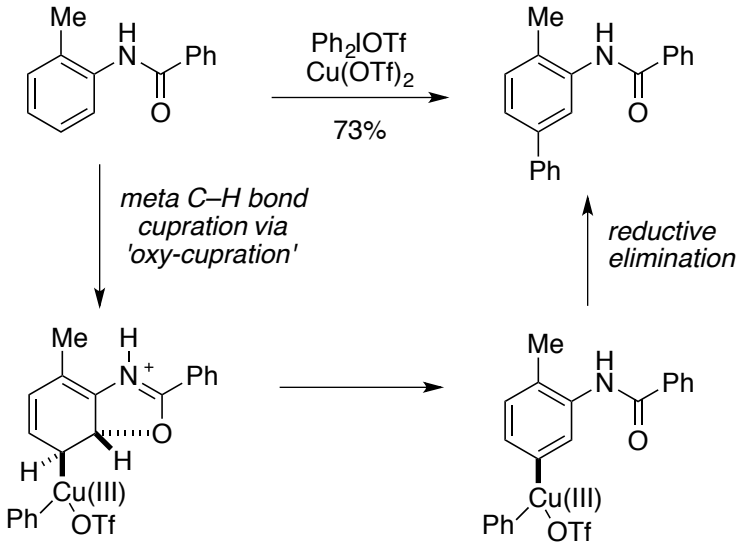

Diaryliodonium salts were also used in C–H arylation of indoles with palladium or copper catalyst. Sanford and co-workers reported a palladium catalyzed C2-arylation (scheme 3-7, eq 1).[40] The C2-arylation resulted from initial C3 palladation and a fast migration of palladium to the C2 position. Similar to the arylation of arenes (scheme 3-5), a Pd(II)/Pd(IV) pathway was suggested for the formation of C2 arylated indoles.

Scheme 3-7. **C–H arylation of indoles**

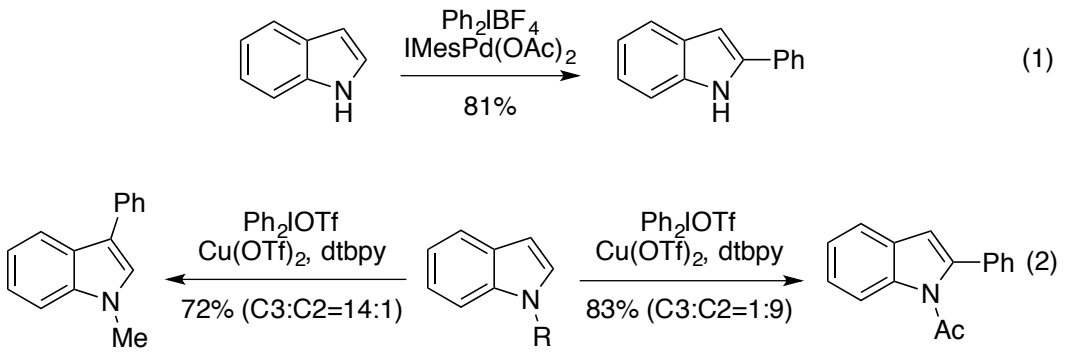

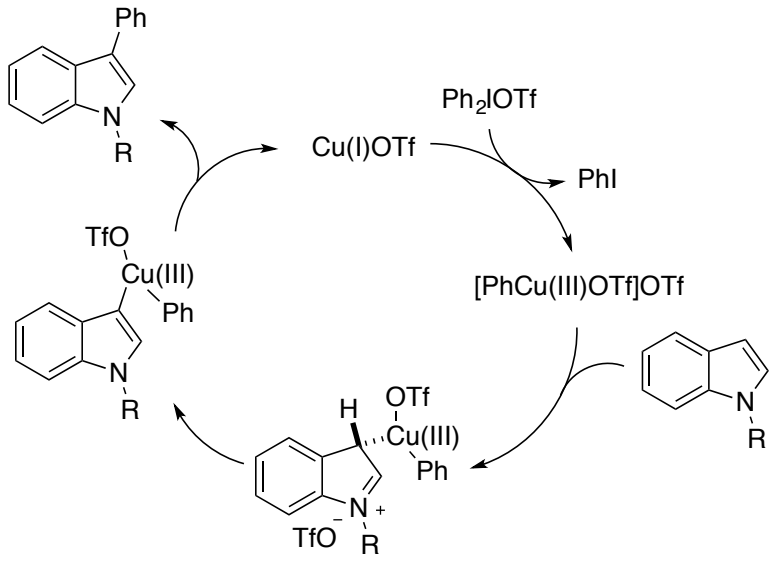

Figure 3-4. **Proposed catalytic cycle for arylation of indole.**

Gaunt and co-workers published a site-selective arylation of indoles (scheme 3-7, eq 2).[41] When *N*-H or *N*-Me indoles were used, C3 arylated indoles were obtained preferentially. Electrophilic substitution with Cu(III)-aryl species occurs at the more electrophilic C3 position, forming the C–Cu(III) bond (figure 3-4). Without the migration to the C2 position, reductive elimination of the Cu(III) complex occurs to provide the C3 isomer. On the other hand, a migration of copper from C3 to C2 was

suggested to account for the formation of the C2 isomer when a *N*-acetyl group is present (figure 3-5).

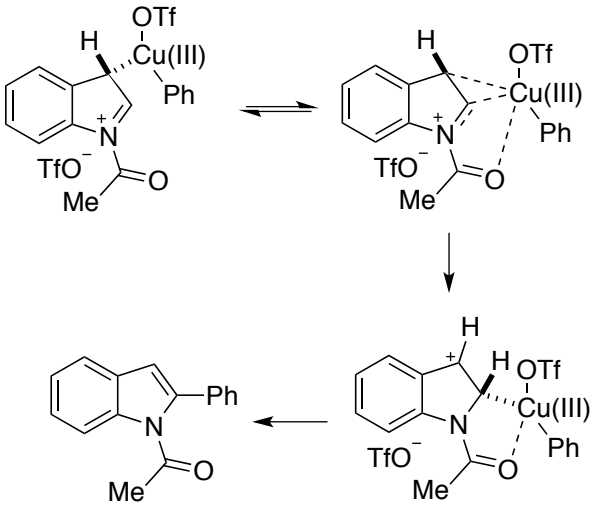

Figure 3-5. **Proposed C3–C2 migration.**

3.1.2.4 Metal-free arylation

A metal-free cross-coupling reaction of two unfunctionalized arenes was reported using Koser's reagent and TMSBr, mediated by an in situ generated diaryliodonium salt (scheme 3-8).[42] Reaction with thiophene **71** and Koser's reagent produces a diaryliodonium tosylate **72**. This stable iodonium salt can be activated by the addition of TMSBr to react with the electron-rich arene, providing the biaryl product **73** by hydroarylation and elimination of iodobenzene.

Scheme 3-8. **Metal-free arylation of thiophenes**

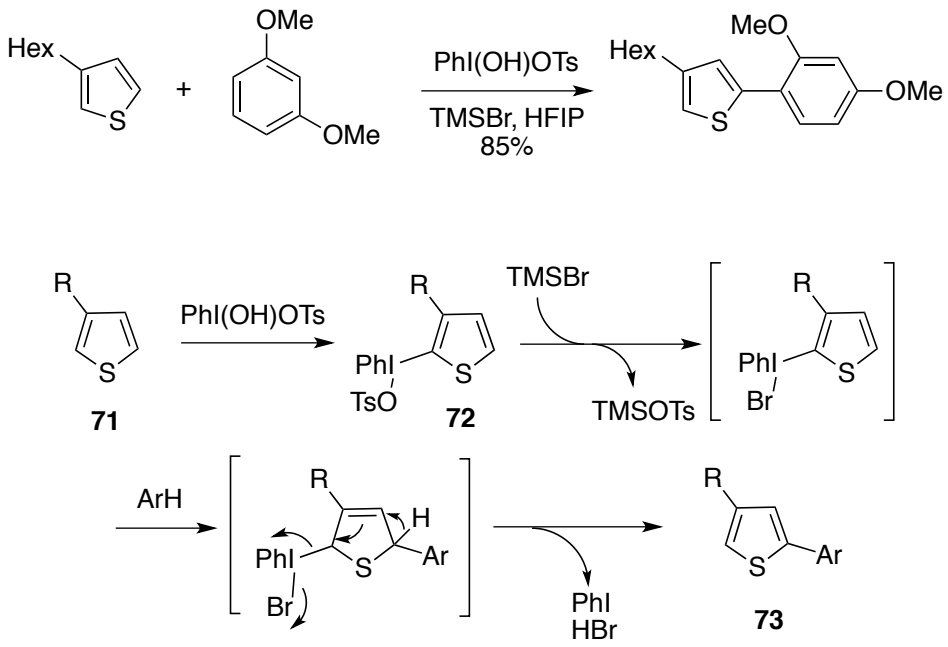

Efficient direct arylations of indoles and pyrroles have been reported in the absence of metal catalysts (scheme 3-9).[43] Eelectron-deficient aromatic moiety of diaryliodonium salt was transferred to C3 position of indoles, however, the selectivity is not as good as seen in the metal-catalyzed reactions described above. A reaction with a symmetric diaryliodonium salt provided the C3 arylated indole in good yield (scheme 3-9, eq 1). A pyrrole was also successfully employed in the metal-free arylation reaction (scheme 3-9, eq 2).

Scheme 3-9. **Metal-free arylation of indole and a pyrrole**

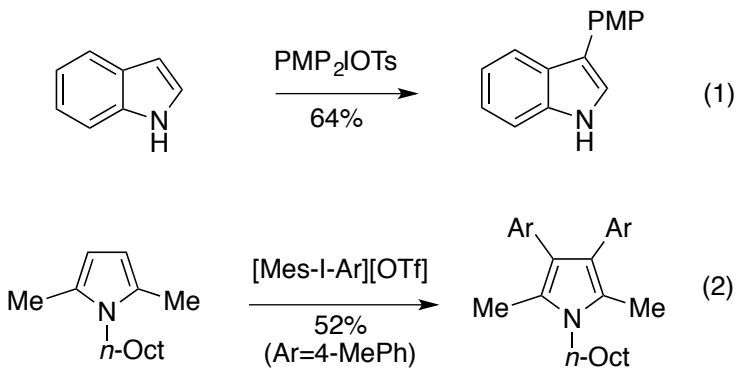

The metal-free direct arylation of skatole was also reported using a diaryliodonium salt and organic base (scheme 3-10).[44] As direct arylation of skatole provides a relatively unstable indolenine (**74**), it was reduced to the more stable indoline derivative (**75**) for the purpose of characterization. In this manner, direct C3 quaternizations of indoles have been achieved, however, this protocol shows some limitations in terms of delivering electron rich arenes.

Scheme 3-10. **Metal-free arylation of skatole**

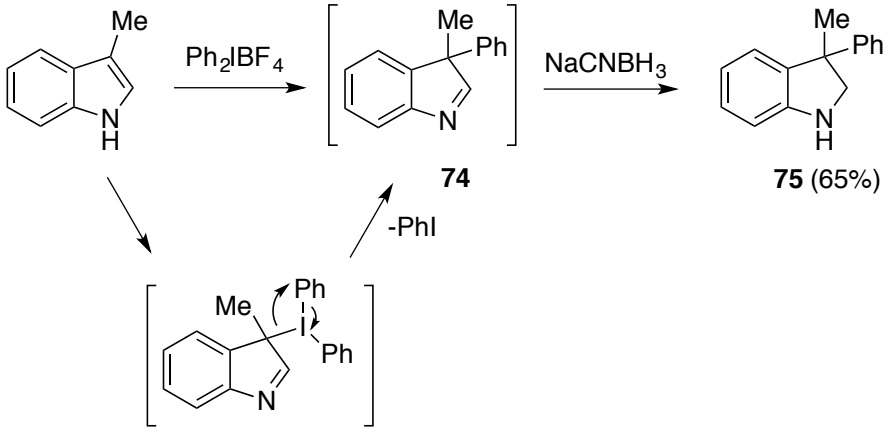

3.1.2.5 Other arylation chemistry using diaryliodonium salts

Recently, organocatalytic C–H bond arylations of aldehydes have been reported using diaryliodonium salts (scheme 3-11).[45] An *N*-heterocyclic carbene (NHC) catalyst was introduced for a reactivity Umpolung of aldehydes, affording nucleophilic species for reaction with electrophilic iodonium salts. The aldehyde **76** undergoes nucleophilic attack by the NHC catalyst to form a transient nucleophilie **79**, which readily reacts with the iodonium salt **77**. The tertiary carbinol **81** formed through aryl transfer by reductive elimination would release the NHC catalyst to afford a bis-heteroaryl ketone **78**.

Scheme 3-11. **C–H bond arylation of an aldehyde to form a bis-heteroaryl ketone**

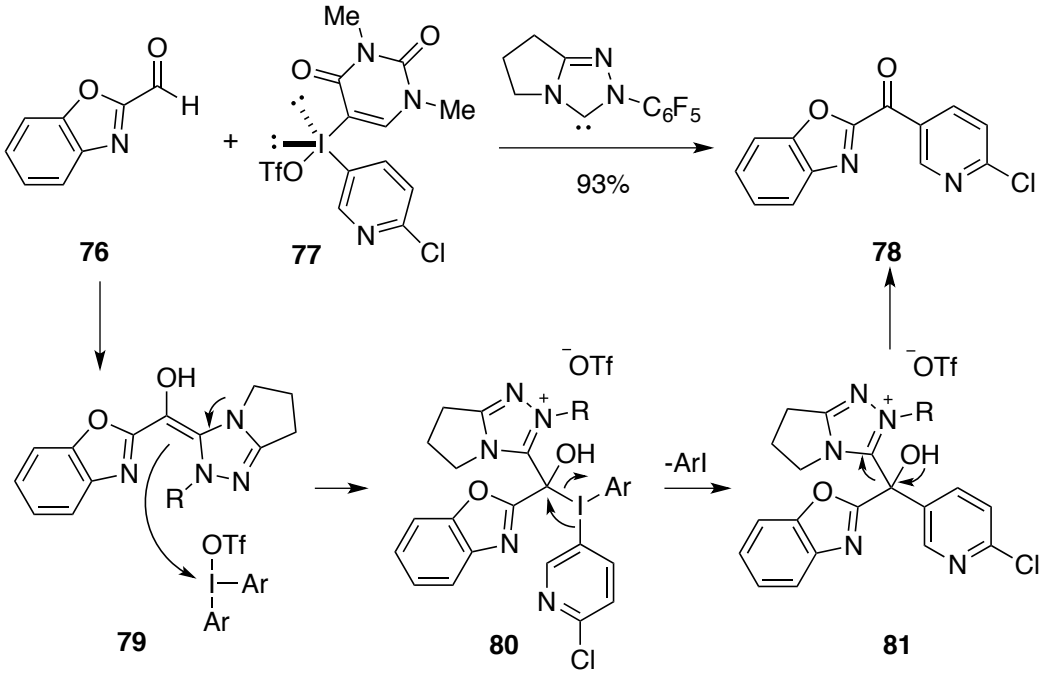

Scheme 3-12. **Carbofunctionalization of alkynes**

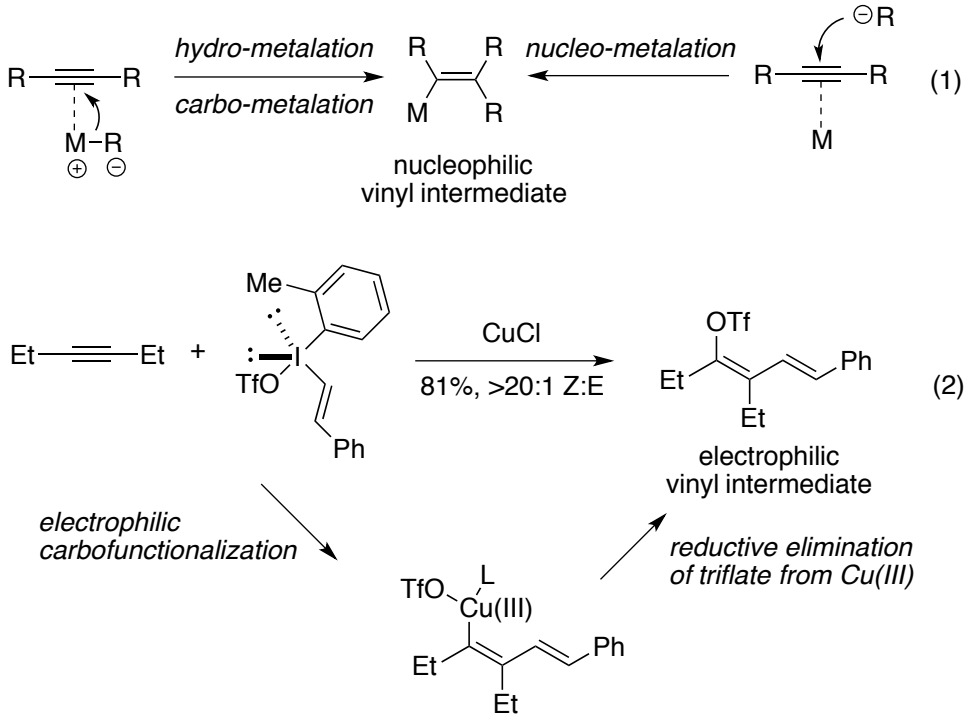

Gaunt and co-workers reported that alkynes can be used to prepare highly functionalized tetrasubstituted alkenyl triflates (scheme 3-12).[46] A novel copper catalysis with diaryliodonium salts proceeds via an electrophilic carbofunctionalization pathway, which is opposite to a classical carbometalation. Metal-catalyzed activation of alkynes often generates nucleophilic vinyl metal species through binding of the metal to the π-orbital of the alkyne (scheme 3-12, eq 1). Unlike the metal-catalyzed reaction of alkynes, a reaction of an alkyne with the Cu(III)–aryl species forms the polarity-reversed, electrophilic vinyl intermediate (vinyl triflate) whose reactivity would be utilized for the synthesis of useful tetrasubstituted alkenes using cross-coupling reactions.

Scheme 3-13. **Carboarylation of alkyne via vinyl cation**

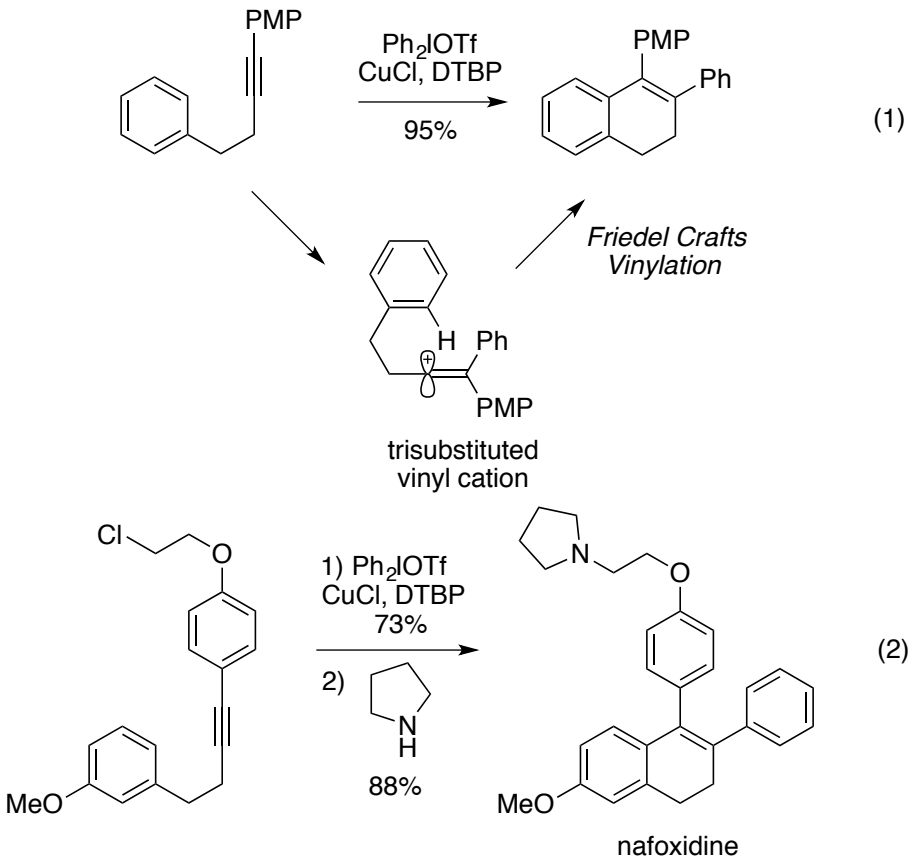

A similar strategy was applied for a copper-catayzed carboarylation of alkynes, producing an all carbon tetrasubstituted alkene (scheme 3-13).[47] A putative stabilized trisubstituted vinyl cation-type intermediate was proposed, which could be generated from a reaction between a electron-rich alkyne and an electrophilic aryl–Cu(III) species. This intermediate could be intercepted by a tethered arene nucleophile via a Friedel-Crafts-type process. This protocol was successfully employed in the synthesis of complex unsaturated systems, exemplified by the synthesis of the anticancer agent nafoxidine (scheme 3-13, eq 2).

3.1.3 Design plan: C5 arylation of cyclic enaminone

Scheme 3-14. **Design plan for the C5 arylation of cyclic enaminones**

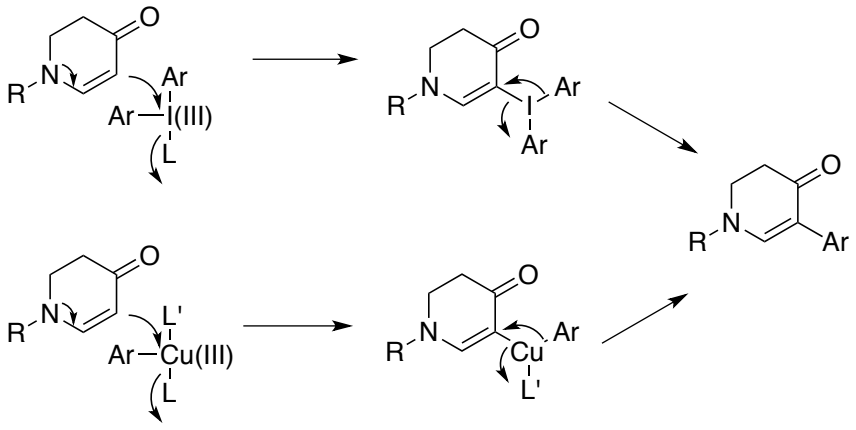

Our group has described C5 arylation of cyclic enaminones using arylboron or arylsilicon coupling partners under oxidative Pd(II) catalysis (chapter 1 and 2). As shown above, diaryliodonium salts have been utilized for C–Ar bond formation via electrophilic addition and reductive elimination with or without a metal catalyst. Based on the reactions developed using diaryliodonium salts, it was envisioned that these electrophilic reagents can be analogously introduced to the nucleophilic cyclic enaminone system for a C5 arylation reaction, thereby providing metal-free or copper catalyzed arylation methods (scheme 3-14).

3.2 Metal free C5 arylation of cyclic enaminones

When diphenyliodium bromide was used as aryl source in the palladium(II)-catalyzed C5 arylation of cyclic enaminone, the reaction proceeded smoothly in 61%

yield (scheme 3-15, eq 1). We further tested if the reaction would proceed under metal-free conditions. Two substrates, a *N*-benzyl and a *N*-carbamylated cyclic enaminones were reacted with diphenyliodonium tosylate and triflate. The electron-rich *N*-benzyl substrate yielded the arylated product in low yields. The conditions employing a tosylate salt gave a little higher yield than the conditions using the triflate salt (scheme 3-15, eq 2). The electron-deficient *N*-carbamylated cyclic enaminone did not furnish any arylated product (scheme 3-15, eq 3), which was consistent with our hypothesis (scheme 3-14). Therefore, we initiated the development of the arylation method using diaryliodonium salts.

Scheme 3-15. **Preliminary results**

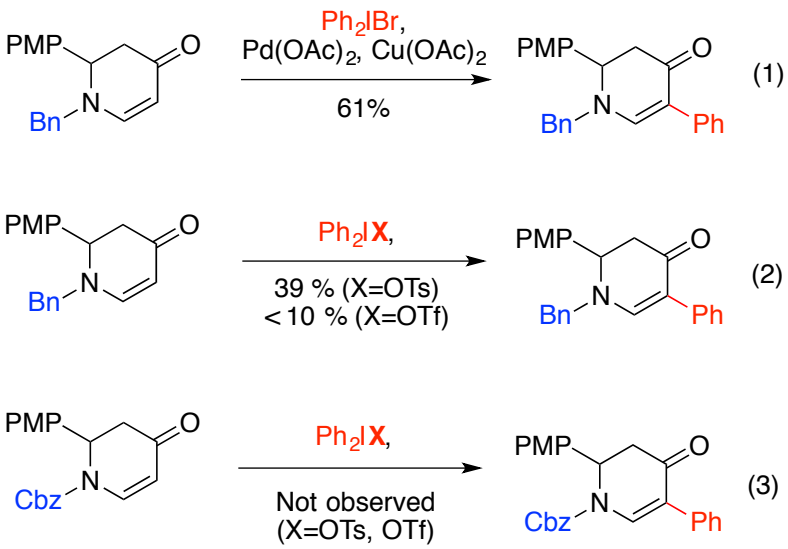

3.2.1 Reaction optimization

3.2.1.1 Screening of diaryliodonium salts

Table 3-1. Screening of diaryliodonium salts[a]

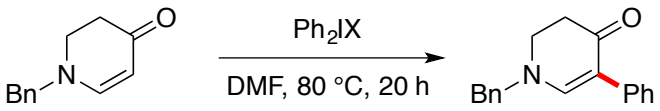

3.1

entry	X	yield (%)
1	Cl	0
2	Br	0
3	OTf	35
4	BF_4	15
5	PF_6	24
6	NO_3	12
7	**OTs**	**44**

[a] Reaction conditions: cyclic enaminone (1 equiv), diaryliodonium salt (1.2 equiv), solvent (0.2 M) under N_2 for 20 h at 80 °C, the yield was determined by ^1H NMR analysis of the crude product using Ph_3SiMe (1 equiv) as the internal standard.

First we screened various diphenyliodonium salts as aryl source for a metal-free C5 arylation reaction of cyclic emaninones. We found that the results vary significantly depending on the counter anion of the dipenyliodonium salts. Chloride and bromide salts did not furnish any products (table 3-1, entries 1 and 2). Tetrafluoroborate, hexafluorophosphate and nitrate salts (table 3-1, entrie 4-6) afforded product but in very low yield. The triflate and tosylate salts were better than the others, however, the yields were 35% and 44% respectively.

3.2.1.2 Screening of solvents

Table 3-2. Screening of solvents[a]

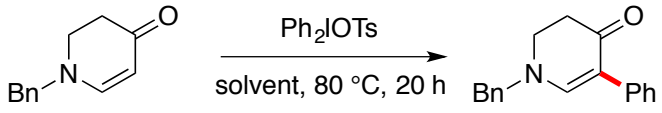

3.1

entry	solvent	yield (%)	entry	solvent	yield (%)
1	DMF	44	8	DCE	55
2	DMA	45	9	toluene	56
3	NMP	41	10	AcOH	0
4	HFIP[b]	< 3	11	MeCN	0
5	isopropanol	46	12[c]	DCE	38
6	THF[b]	< 3	13[c]	toluene	< 3
7	1,4-dioxane	44			

[a] Reaction conditions: cyclic enaminone (1 equiv), diphenyiodonium tosylate (1.2 equiv), solvent (0.2 M) under N_2 for 20 h at 80 °C, the yield was determined by ^{1}H NMR analysis of the crude product using Ph_3SiMe (1 equiv) as the internal standard. [b] At 60 °C. [c] Diphenyliodonium triflate was used.

We next screened various solvents. To some degree, the solubility of the reagent affects the efficiency but not entirely. Amide solvents such as DMF, DMA and NMP provided comparably higher yield (table 3-2, entries 1-3), however, no significant difference in yield was observed between those solvents. Although iodonium salt are soluble in alcoholic solvents such as 1,1,1,3,3,3-hexafluoro-2-propanol (HFIP) and isopropanol, arylation proceeded only in isopropanol in 46% yield (table 3-2, entries 4 and 5). In ethereal solvents, the non-polar 1,4-dioxane solvent provided a noticeable yield while polar THF afforded only trace amounts of product (table 3-2, entries 6 and 7). DCE and toluene were better solvent systems that showed a slight

improvement in yields (table 3-2, entries 8 and 9). We also conducted experiments with diphenyliodonium triflate in DCE and toluene (table 3-2, entries 12 and 13). It was interesting to find that the conditions in DCE provided 38% yield, while the reaction was suppressed in toluene.

3.2.1.3 Screening of temperature

Table 3-3. Screening of temperature[a]

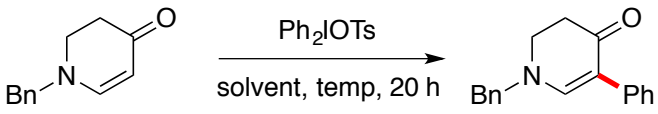

3.1

entry	solvent	temp	yield (%)
1	DCE	80 °C	55
2	toluene	80 °C	56
3	DCE	60 °C	57
4	toluene	60 °C	< 3
5	DCE	40 °C	0
6	DCM	40 °C	0
7	DCE	23 °C	0
8	DCM	23 °C	0

[a] Reaction conditions: cyclic enaminone (1 equiv), diphenyliodonium tosyalte (1.2 equiv), solvent (0.2 M) under N_2 for 20 h, the yield was determined by ^{1}H NMR analysis of the crude product using Ph_3SiMe (1 equiv) as the internal standard.

With DCE and toluene as our optimal solvents, we explored the temperature of the reaction in each solvent. The yields at 80 °C are quite similar in both DCE and toluene (table 3-3, entries 1 and 2). When we decreased the reaction temperature to 60 °C, the reaction in DCE still showed comparable yield but the reaction in toluene lost

reactivity, affording only a trace amount of product (table 3-3, entries 3 and 4). However, with DCE as well as DCM as the solvent, the reaction suffered from reduced reactivity when the reaction was cool to either 40 °C or room temperature (table 3-3, entries 5-8).

3.2.1.4 Screening of reagent concentration

Table 3-4. Screening of concentration and reagent[a]

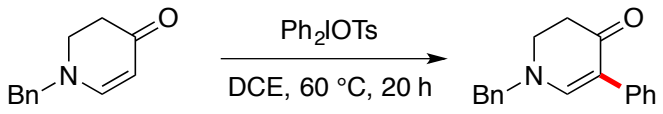

3.1

entry	concentration	reagent	yield (%)
1	0.1	1.2 equiv	62
2	0.2	1.2 equiv	57
3	0.5	1.2 equiv	59
4	0.1	2.0 equiv	58
5	0.1	3.0 equiv	58
6	0.05	2.0 equiv	56

[a] Reaction conditions: cyclic enaminone (1 equiv), diphenyliodonium tosylate (1.2-3.0 equiv), solvent (0.05-0.5 M) under N_2 at 60 °C for 20 h, the yield was determined by ^{1}H NMR analysis of the crude product using Ph_3SiMe (1 equiv) as the internal standard.

We turned our attention to screening for the optimal reaction concentration and for the amount of reagents. In general, the concentration or the amount of reagent did not affect the reaction efficiency substantially (table 3-4). Increasing or decreasing the solvent concentration/the amount of diphenyliodonium tosylate virtually afforded the same yields, providing no tendency on those parameters. The best yield was obtained

when the concentration was 0.1 M with the use of 1.2 equivalents of the diaryliodonium reagent (table 3-4, entry 1).

3.2.1.5 Screening of additives

Table 3-5. Screening of additives[a]

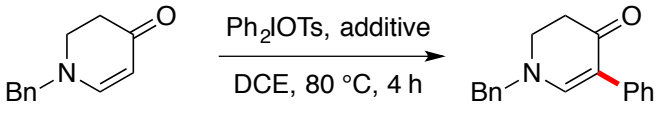

3.1

entry	additive	yield (%)
1	$TsOH \cdot H_2O$	0
2	K_2CO_3	0
3	pyridine	0
4	TEA	0
5	DABCO	0
6	DTBP	46
7[b]	DTBP	69

[a] Reaction conditions: cyclic enaminone (1 equiv), diaryliodonium salt (1.2 equiv), additive (1.2 equiv), DCE (0.1 M) under N_2, the yield was determined by ^1H NMR analysis of the crude product using Ph_3SiMe (1 equiv) as the internal standard. [b] At 60 °C for 20 h. DABCO = 1,4-Diazabicyclo[2.2.2]octane, DTBP = 2,6-di-tert-butylpyridine.

While the reaction proceeds in moderate yields, we were curious whether various additives would facilitate the reaction at 80 °C for 4 hours. Surprisingly, the reactions were completely suppressed with the addition of organic/inorganic acids or bases (table 3-5, entries 1-5). However, we found that the addition of DTBP afforded the product in 46% yield. Thus, the reaction was re-tested under the optimized condition

(at 60 °C for 20 h), affording a slightly improved yield (table 3-5, entry 7).

3.2.2 Scope of cyclic enaminones

Table 3-6. Scope of cyclic enaminones[a]

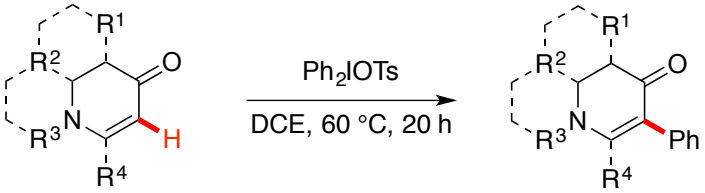

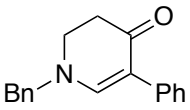

3.1 (62%)

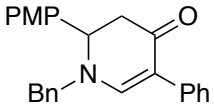

3.2 (54%)

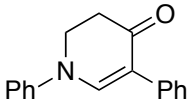

3.3 (53%)

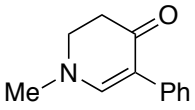

3.4 (51%)

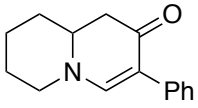

3.5 (53%)

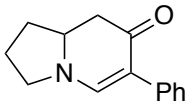

3.6 (45%)

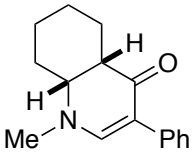

3.7 (41%)
(from *cis*)

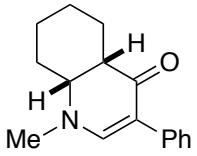

3.7 (47%)
(from *trans*)

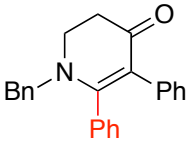

3.8 (22%)

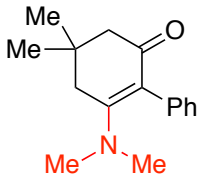

3.9 (20%)

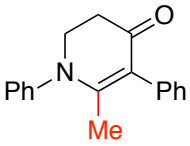

3.10 (49%)

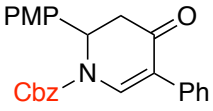

3.11 (Not observed)

[a] Reaction conditions: cyclic enaminone (1 equiv), diphenyliodonium tosylate (1.2 equiv), DTBP (1.2 equiv), DCE (0.1 M) under N_2 at 60 °C for 20 h.

With optimized condition in hand, various cyclic enaminones were reacted with diphenyliodonium tosylate (table 3-6). Monocyclic *N*-benzyl, *N*-phenyl and *N*-

methyl enaminones (table 3-6, **3.1**-**3.4**) were suitable substrates in this transformation and provided moderate yields (51-62%). Bicyclic enaminones with quinolizidine or indolizidine scaffold also proceeded smoothly to give the C5 arylated product in 53% and 45% respectively. *Cis*-bicyclic product **3.7** was obtained from the corresponding *cis*-starting material as expected. Unfortunately, the *trans*-starting material or *trans*-product was susceptible to epimerization to afford only the *cis*-bicyclic product **3.7**. It is worth noting that trisubstituted cyclic enaminones afforded tetrasubstituted alkenes, although the yields were low (table 3-6, **3.8-3.10**). In particular, the C–H arylations of C6-phenyl substituted substrate **3.8** and the external enaminone **3.9** were achieved for the first time. Especially the C6-phenyl substituted substrate **3.8** was only accessible in two-step synthesis via the iodo-enaminone. The product from the *N*-carbamylated cyclic enaminone was not observed, which verifies the proposed mechanistic hypothesis.

3.2.3 Scope of diaryliodonium salts

For a investigation of the scope of the diaryliodonium salts, asymmetric diaryliodonium tosylates were prepared from Koser's-type iodine(III) derivatives.[48] Mesitylphenyliodonium tosylate provided a slightly lower yield compared to the symmetric reagent (table 3-7, **3.1**). Methyl substituted phenyliodonium reagents provided the corresponding products in high yield, however, the *ortho*-substituted reagent did not afford the product, presumably due to steric hindrance (table 3-7, **3.12-3.14**). Halogenated reagents were also suitable for this protocol, providing an

opportunity for further transformations (table 3-7, **3.15-3.16**). On the contrary, the reaction with trifluoromethyl or nitro substituted iodonium salts resulted in poor yields. We believe that these poor conversions are attributable to poor solubility of these reagents.

Table 3-7. Scope of diaryliodonium salts[a]

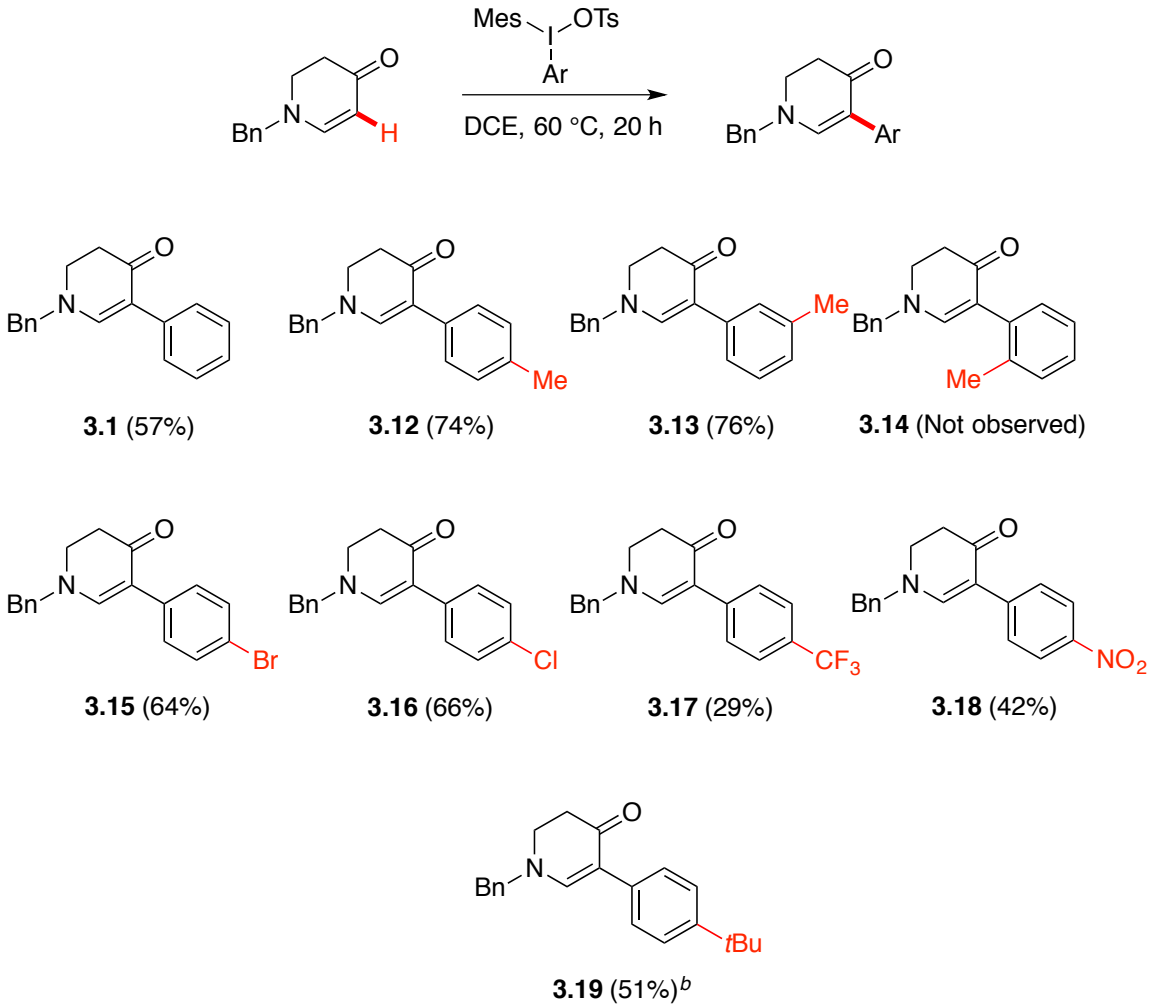

3.1 (57%) **3.12** (74%) **3.13** (76%) **3.14** (Not observed)

3.15 (64%) **3.16** (66%) **3.17** (29%) **3.18** (42%)

3.19 (51%)[b]

[a] Reaction conditions: cyclic enaminone (1 equiv), diaryliodonium tosylate (1.2 equiv), DTBP (1.2 equiv), DCE (0.1 M) under N_2 at 60 °C for 20 h. [b] Bis(4-*tert*-butylphenyl)iodonium tosylate (1.2 equiv) was used.

3.3 Copper-catalyzed C5 arylation of cyclic enaminones

We have successfully demonstrated a metal-free C5 arylation of cyclic enaminones using diaryliodonium salts (chapter 3.2). Nevertheless, relatively low yields obtained for various cyclic enaminones and issues with low solubility of iodonium salts prompted us to find alternative ways to improve this method. Recently, copper(I) reagents have been widely used as a catalyst in combination with diaryliodonium salts in various arylation reactions. The success of these transformations is a result of the formation of a highly electrophilic aryl-Cu(III) species. Accordingly, we aimed for a copper(I)-catalyzed C5 arylation reaction of cyclic enaminones using diaryliodonium salts.

3.3.1 Reaction optimization

3.3.1.1 Optimization for copper catalyzed reaction

We initiated the optimization process by adding copper catalyst to the metal-free condition. With $Cu(OTf)_2$ as the catalyst, the yield was virtually the same as that obtained under the metal-free condition (table 3-8, entry 1), however, a slight increase in yield was observed when DCM was used as solvent (table 3-8, entry 2). At higher temperature (80 °C), the yields were even lower and the starting material was consumed more rapidly through decomposition (table 3-8, entry 3). The absence of DTBP resulted in a more drastic decrease in yield (table 3-8, entry 4), compared to

the metal-free conditions. Other copper sources were found to have no advantageous effect (table 3-8, entries 5-7).

Table 3-8. Optimization for copper catalyzed reaction[a]

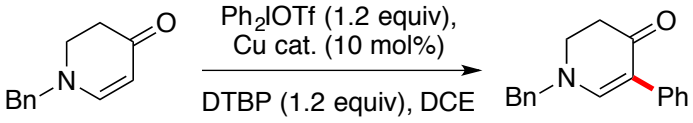

3.1

entry	temp	time	catalyst	yield (%)
1	60 °C	20 h	$Cu(OTf)_2$	40
2[b]	60 °C	20 h	$Cu(OTf)_2$	45
3	80 °C	4 h	$Cu(OTf)_2$	33
4[c]	80 °C	4 h	$Cu(OTf)_2$	< 10
5	80 °C	4 h	CuBr	37
6	80 °C	4 h	$CuCl_2$	21
7	80 °C	4 h	CuI	38

[a] Reaction conditions: cyclic enaminone (1 equiv), diphenyliodonium triflate (1.2 equiv), Cu catalyst (10 mol%), DTBP (1.2 equiv), DCE (0.1 M) under N_2, the yield was determined by ^1H NMR analysis of the crude product using Ph_3SiMe (1 equiv) as the internal standard. [b] DCM. [c] without DTBP.

We then explored the reaction conditions at lower temperatures. We were pleased to find that the yields improved at 40 °C and at room temperature (23 °C) (table 3-9, entries 1-2). The difference we observed under these condition was that the unreacted starting material was fully recovered at room temperature while it was partially decomposed at 40 °C. This observation suggests that there are more opportunities for improving the reaction at room temperature. Switching the solvent to DCM led the reaction to higher efficiency (table 3-9, entry 3). Similar to the metal-free conditions,

the tosylate salt provided a better yield than the triflate and a change to a CuBr catalyst offered the best result (table 3-9, entries 4 and 5).

Table 3-9. Optimization for copper catalyzed reaction[a]

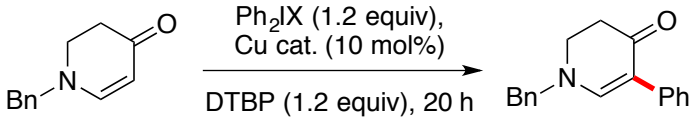

3.1

entry	temp	X	solvent	catalyst	yield (%)
1	40 °C	OTf	DCE	$Cu(OTf)_2$	62
2	23 °C	OTf	DCE	$Cu(OTf)_2$	62
3	23 °C	OTf	DCM	$Cu(OTf)_2$	70
4	23 °C	OTs	DCM	$Cu(OTf)_2$	85
5	23 °C	OTs	DCM	CuBr	92

[a] Reaction conditions: cyclic enaminone (1 equiv), diphenyliodonium salt (1.2 equiv), Cu catalyst (10 mol%), DTBP (1.2 equiv), solvent (0.1 M) under N_2 for 20 h, the yield was determined by ^1H NMR analysis of the crude product using Ph_3SiMe (1 equiv) as the internal standard.

3.3.1.2 Screening of catalyst and time

Next, we screened the amount of CuBr used and the reaction time. Surprisingly the reaction is extremely fast and went to completion within 1 hour with 10 mol % of CuBr at room temperature (table 3-10, entries 1-4). Use of 5 mol % of the catalyst also provided rapid conversion to an arylated product, albeit in slightly lower yield (table 3-10, entries 5-8). The rate of the reaction was much slower with 1 mol % catalyst loading and the yield was lower as well (table 3-10, entries 9-12). Nevertheless, a 1 mol % catalyst loading is still more efficient compared to metal-free

reactions.

Table 3-10. Screening of catalyst and time[a]

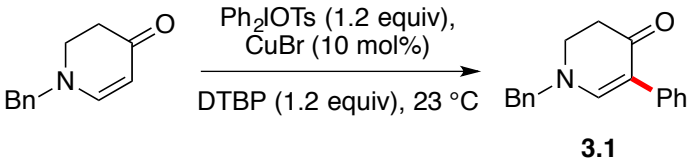

3.1

entry	CuBr	time	yield (%)
1	10 mol%	1 h	92
2	10 mol%	2 h	92
3	10 mol%	3 h	91
4	10 mol%	20 h	92
5	5 mol%	1 h	79
6	5 mol%	2 h	81
7	5 mol%	3 h	81
8	5 mol%	20 h	81
9	1 mol%	1.5 h	18
10	1 mol%	3 h	65
11	1 mol%	6 h	77
12	1 mol%	20 h	77

[a] Reaction conditions: cyclic enaminone (1 equiv), diphenyliodonium tosylate (1.2 equiv), CuBr (10 mol%), DTBP (1.2 equiv), DCM (0.1 M) under N_2 at 23 °C, the yield was determined by ^{1}H NMR analysis of the crude product using Ph_3SiMe (1 equiv) as the internal standard.

3.3.2 Scope of cyclic enaminones

We used this optimized copper-catalyzed conditions in the arylation of various cyclic enaminones. All cyclic enaminones in copper-catalyzed condition provided

higher yields compared to the yields in metal-free condition except **3.9** (table 3-11). It should be noted that α-epimerization was also observed in case of cyclic enaminone **3.7**.

Table 3-11. Scope of cyclic enaminones[a]

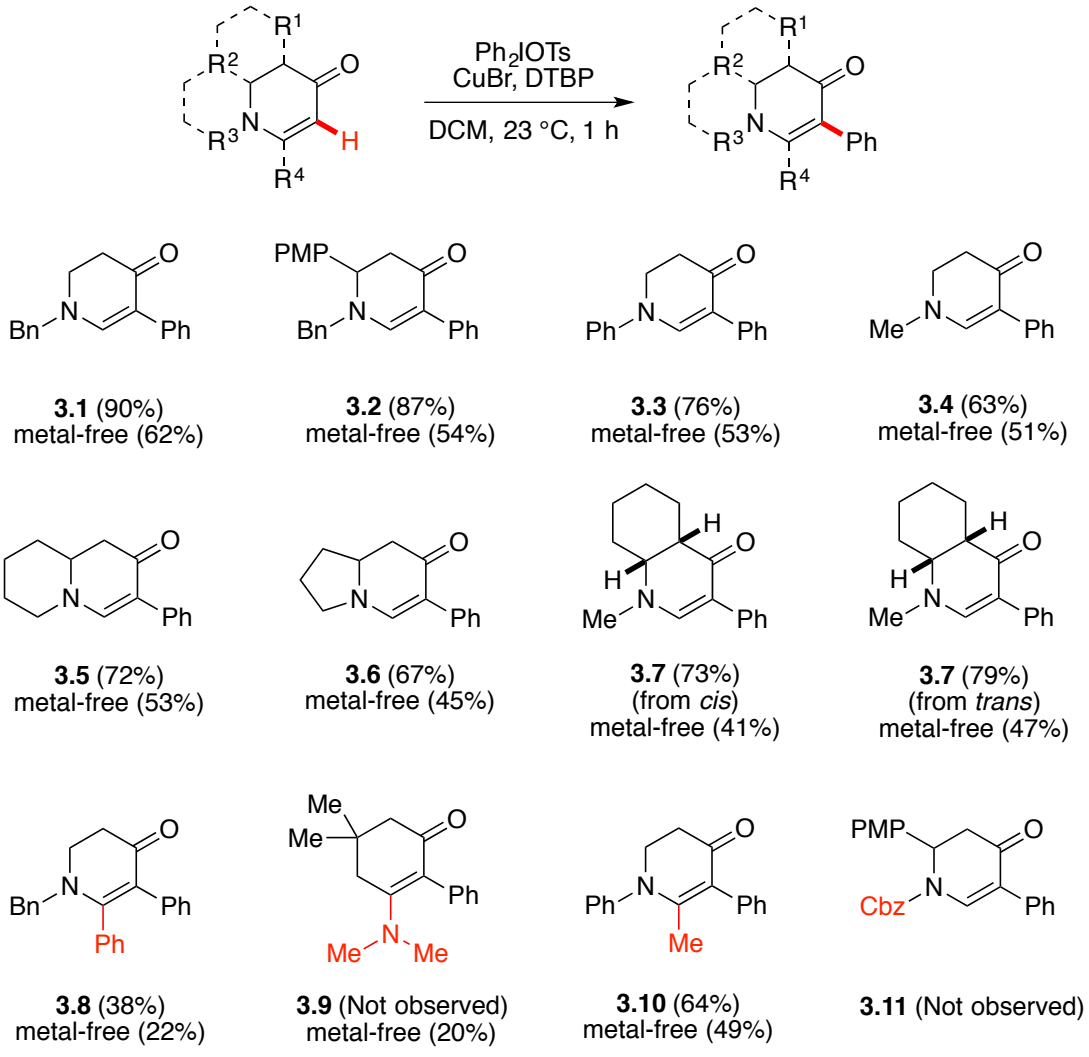

[a] Reaction conditions: cyclic enaminone (1 equiv), diphenyliodonium tosylate (1.2 equiv), CuBr (10 mol%), DTBP (1.2 equiv), DCM (0.1 M) under N_2 at 23 °C for 1 h.

3.3.3 α-Epimerization of bicyclic enaminones

Scheme 3-16. Epimerization of 3.7

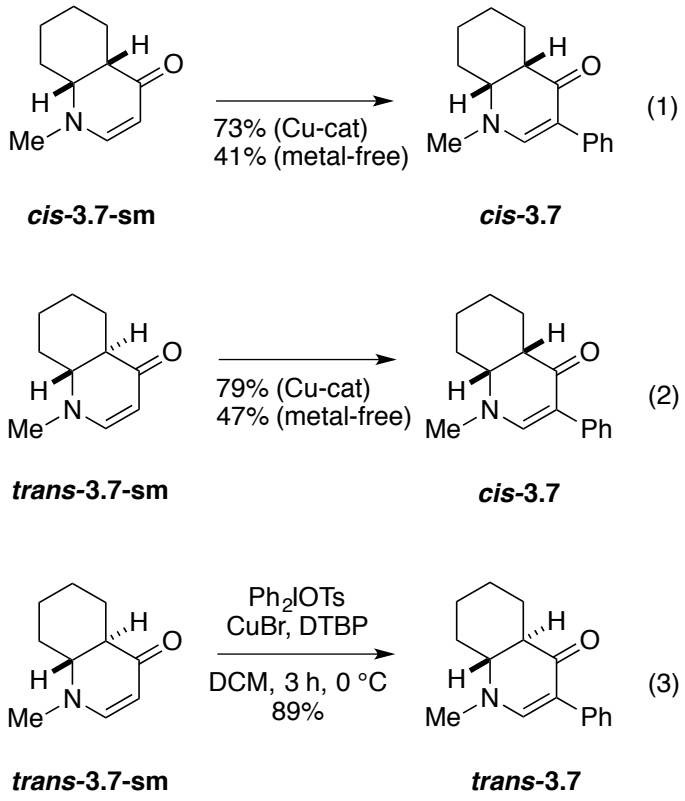

Exploring various cyclic enaminones, we observed epimerization at the α-position of the carbonyl group in bicyclic enaminones. The reaction proceeded without any issues with the *cis* isomer (scheme 3-16, eq 1). However, the complete epimerization of ***trans*-3.7-sm** to ***cis*-3.7** was observed in both copper-catalyzed and metal-free reactions. To address this issue, we conducted a reaction at lower temperature. Under metal-free conditions, there was no opportunity to lower the temperature as 60 °C is the lowest possible temperature for efficient conversion. Thus, we decided to perform

the copper-catalyzed condition at lower temperature. To our delight, we discovered that the reaction at 0 °C for 3 hours provided a single *trans*-isomer without any epimerization. Furthermore, a higher yield (89%) was observed under these reaction conditions (scheme 3-16, eq 3).

3.3.4 Scope of diaryliodonium salts

Table 3-12. Scope of diaryliodonium salts[a]

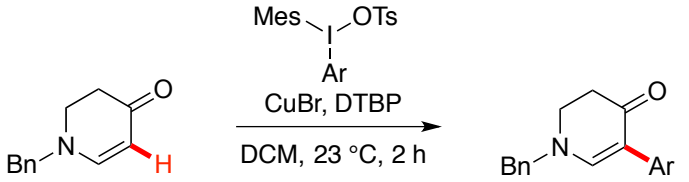

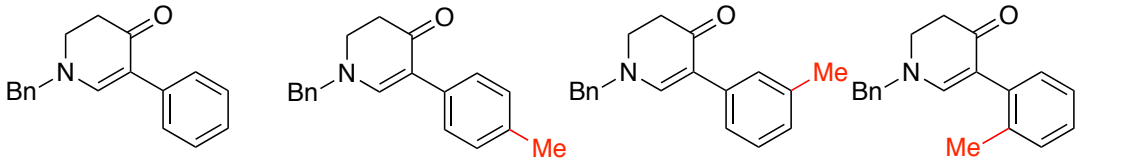

3.1 (79%)
metal-free (57%)

3.12 (86%)
metal-free (74%)

3.13 (91%)
metal-free (76%)

3.14 (Not observed)

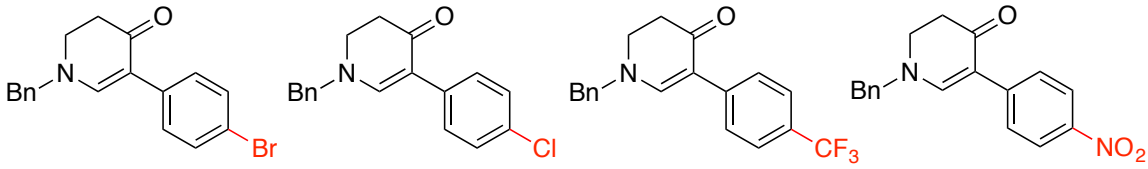

3.15 (75%)
metal-free (64%)

3.16 (78%)
metal-free (66%)

3.17 (69%)
metal-free (29%)

3.18 (70%)
metal-free (42%)

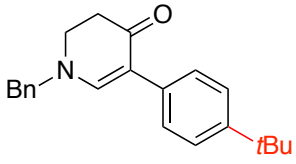

3.19 (82%)[b]
metal-free (51%)

[a] Reaction conditions: cyclic enaminone (1 equiv), diaryliodonium tosylate (1.5 equiv), CuBr (10 mol%), DTBP (1.5 equiv), DCM (0.1 M) under N_2 at 23 °C for 2 h. [b] Bis(4-*tert*-butylphenyl)iodonium tosylate (1.5 equiv) was used.

In the same way, various diaryliodonium salts were reacted under copper-catalyzed condition with the *N*-benzyl cyclic enaminone as the model substrate. Similar to the scope of cyclic enaminones, most diaryliodonium salts yielded the C5 arylated cyclic enaminones more efficiently than observed under metal-free condition. Still, *ortho*-substituted reagent did not furnish the corresponding product. It is noteworthy that the reagents with compromised yields owing to solubility issues were found to be compatible in copper-catalyzed reactions, affording high yields (table 3-12, **3.17** and **3.18**).

3.4 Proposed Mechanism

The proposed mechanism of C5 arylation using diaryliodonium tosylate is shown in figure 3-6. Under metal-free conditions, reaction would occur directly between the nucleophilic carbon and the electrophilic diaryliodonium tosylate, forming a C–Ar bond. A subsequent reductive elimination would provide C5 arylated cyclic enaminone as well as aryl iodide (figure 3-6, eq 1). In copper-catalyzed reaction, an oxidative addition of the copper catalyst into the aryl–iodonium bond would take place initially, generating a highly electrophilic Ar–Cu(III) species. Then the cyclic enaminone and the Cu(III) species would form a C–Cu(III) bond. A reductive elimination would transfer the aryl group to the C5 position, then release the C5

arylated product and the Cu(I) catalyst.

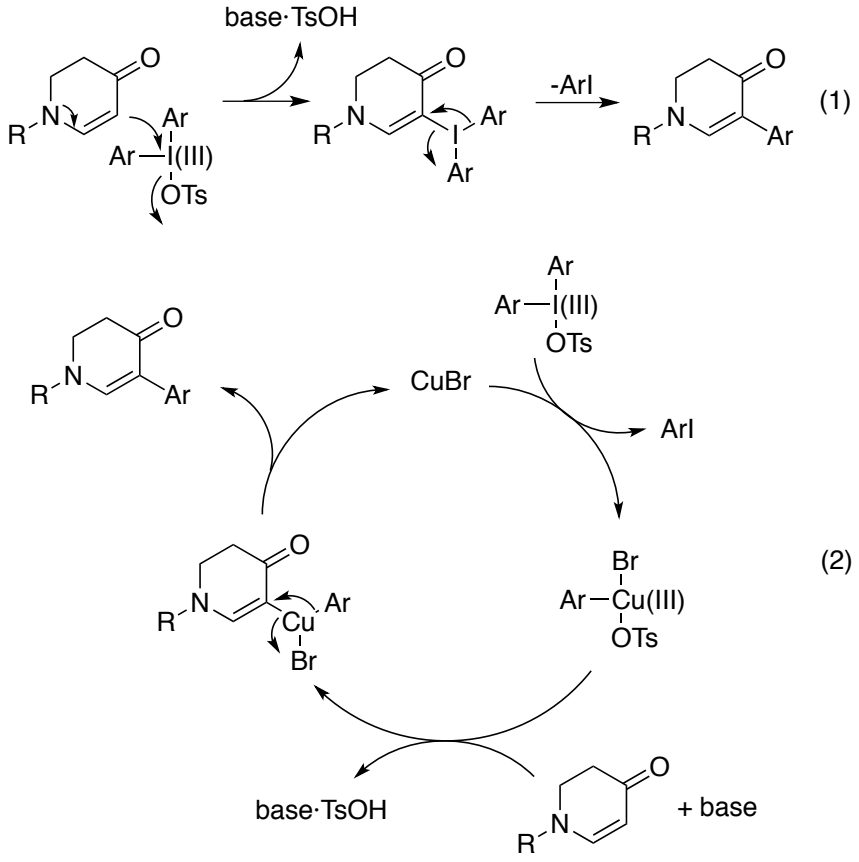

Figure 3-6. **Proposed mechanism of C5 arylation.**

3.5 Conclusion

In conclusion, we have developed efficient methods to provide C5-arylated cyclic enaminones using diaryliodonium tosylates under metal-free or copper-catalyzed conditions. Metal-free reactions offer a green alternative for the C5 arylation of cyclic enaminones, where the use of heavy transition metals has been excluded as a catalyst,

an oxidant or an additive. On the other hand, copper-catalyzed condition provided a highly efficient C5 arylation method under mild reaction conditions within a short period of time.

Chapter 4

C6 arylation of cyclic enaminones

4.1 Introduction

Although direct C5 arylations of cyclic enaminones were extensively studied, the direct C6 arylations are rare and limited. For alkylation/arylation at the C6 position of cyclic enaminones to afford 4-piperidones, conjugate addition reactions can be employed.[4, 48-54] C6 Alkylation with retention of the enaminone system has been achieved by cross-coupling of C6-halo derivatives,[55-57] or organocuprate addition followed by oxidation.[58] A few cases of direct arylation involving a Heck-type reaction have been reported but they are limited to intramolecular reactions.[59-62] Considering the utility of this scaffold, the development of an efficient Pd-mediated intermolecular C6 arylation would be a beneficial process. In this chapter, the development of a method for the direct C6 arylation of cyclic enaminones will be discussed.

4.1.1 C6 Functionalizations of cyclic enaminones

4.1.1.1 Conjugate additions of cyclic enaminones toward 4-piperidones

Scheme 4-1. **Synthesis of a *cis*-2,6-disubstituted 4-piperidone**

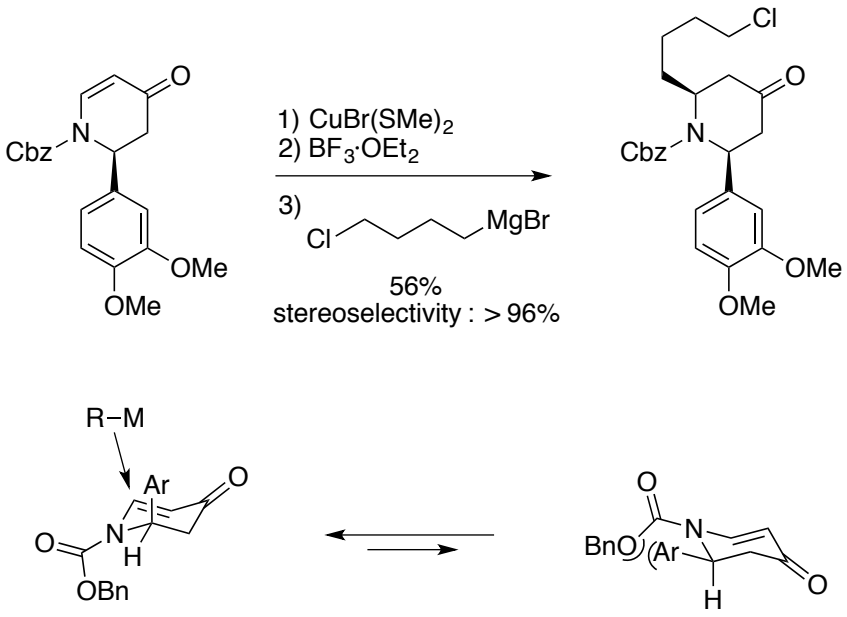

Conjugate addition reaction is often used as a facile C6 functionalization of cyclic enaminones, which converts cyclic enaminones to 4-piperidone systems. In the course of synthetic studies toward (±)-lasubine II, Comins and co-workers developed a copper-mediated conjugate addition of (4-chlorobutyl)magnesium bromide, affording *cis*-2,6-disubstituted piperidone with excellent stereocontrol (scheme 4-1).[48] $A^{1,3}$-strain between the *N*-acyl group and the aryl group at the C2 position places the C2 aryl group into a pseudoaxial position. Then, the *cis*-2,6-disubstituted product is formed by a top-facial approach, where the axial attack is preferred

stereoelectronically.

When the *N*-substituent and C2 group are connected, the cyclic enaminone belongs to a fused ring system. In this case, the stereoelectronically preferred axial addition of the organometal would generate the *trans*-2,6-disubstituted product (scheme 4-2),[51] which was used to construct the core scaffold of the alkaloid, (+)-hyperaspine. This transformation was also exemplified by the generation of a bicyclic *trans*-intermediate in the total synthesis of the tricyclic alkaloid porantheridine,[4] as discussed in chapter **1.2.2** previously.

Scheme 4-2. **Synthesis of *trans*-2,6-disubstituted 4-piperidone**

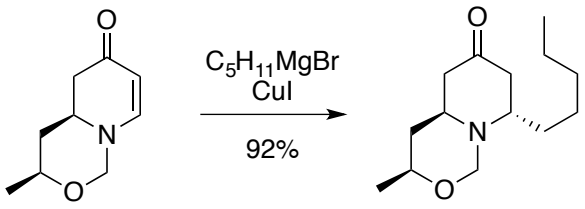

Similarly, an intramolecular anionic conjugate addition was developed using a *N*-tethered aryl iodide (scheme 4-3).[52] The addition of *n*-BuLi to the cyclic enaminone **82** gave the *trans*-indolizidinone **83** via lithium-halogen exchange and subsequent anionic cyclization. This reaction provides a complementary protocol to the intermolecular polar addition, which affords *cis*-2,6-disubstituted product (scheme 4-3).

Scheme 4-3. **Intramolecular synthesis of a *trans*-indolizidinone**

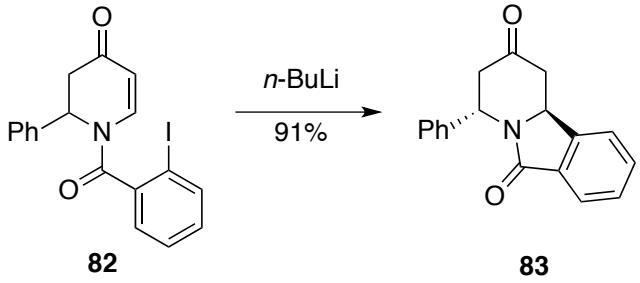

82 **83**

Scheme 4-4. **Intermolecular synthesis of a *trans*-2,6-disubstituted 4-piperidone**

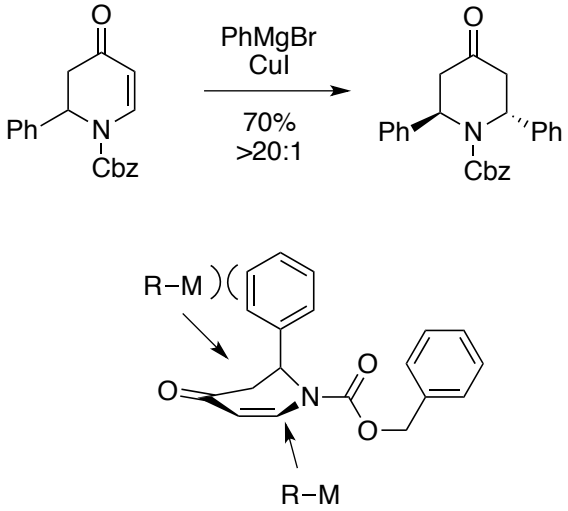

In contrast to the synthesis of *cis*-2,6-disubstituted 4-piperidones by copper promoted conjugate addition of aliphatic Grignard reagents, the use of an aryl Grignard reagent provided the *trans*-isomer exclusively (scheme 4-4).[53] Based on the X-ray structure, it was suggested that the *trans*-product poses a half-boat type conformation to relieve the $A^{1,3}$-strain as well as diaxial interactions observed in a chair conformation. Therefore, the top-face attack of the organocuprate is hindered by the large phenyl substituent at the pseudoaxial position, while the stereoelectronically

preferred axial bond is formed from a pseudo twist boat conformation in the transition state.

Dieter and co-workers performed an extensive study on the stereochemistry of conjugate additions of cyclic enaminones.[54] Conjugate additions with Grignard reagents in the presence of TMSCl produce *trans*-isomer at all times. The reactions with organocuprate reagents without TMSCl resulted in mixtures of *cis* and *trans* isomers. In these cases, the *trans*-isomer is favored with a bulky aryl substituent at C2 while alkyl substituted substrate leads to *cis*-product predominantly (scheme 4-5).

Scheme 4-5. Intermolecular synthesis of *trans*-2,6-disubstituted 4-piperidones

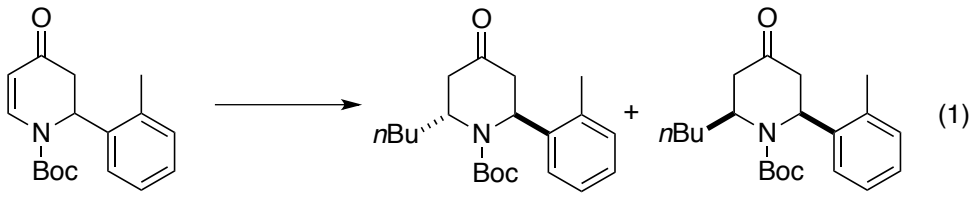

*n*BuMgCl, TMSCl,	88%	–
*n*BuMgCl, CuI, $BF_3{\cdot}OEt_2$	49%	33%
nBu_2CuLi, SMe_2	88%	–

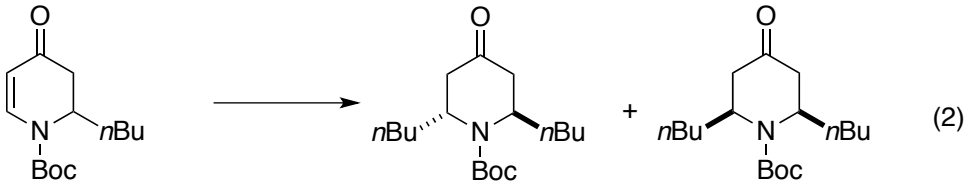

*n*BuMgCl, TMSCl,	89%	–
nBu_2CuLi, SMe_2	–	86%

The *trans*-stereochemistry of the reactions with the combination of Grignard reagent and TMSCl could be rationalized by the formation of an enone-TMSCl complex. The Grignard reagent, which is not associated with the Lewis acid, approaches from the least hindered π-face opposite from the axial R' group (figure 4-1, **A**). On the contrary, conjugate addition of organocuprate reagent often involves metal cation (Li^+) coordinating to the enone carbonyl. Consequently, the cuprate reagent attacks on the same π-face of the axial R' group (figure 4-1, **B**).

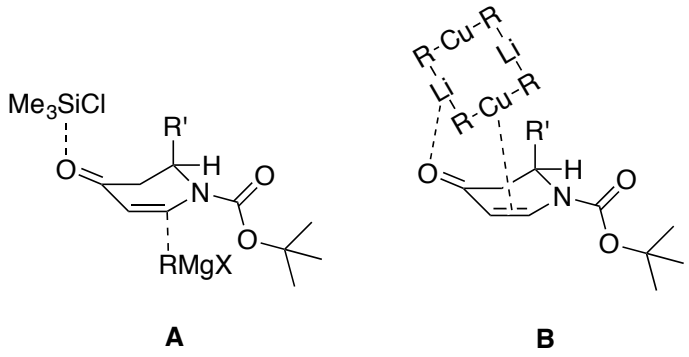

Figure 4-1. **Stereoselectivity in conjugate additions.**

4.1.1.2 C6 alkylation/arylation with retention of the enaminone system

C6 alkylations/arylations with retention of the enaminone system have been achieved by Negishi cross-coupling, however, only a few examples are reported.[55-57] Reaction between a C6-iodo cyclic enaminone **84** and alkylzinc bromide under palladium catalysis afforded C6-alkylation (scheme 4-6, eq 1). Equally, an aryl group was successfully installed at the C6 position by Negishi cross-coupling from C6-

chloro substrate **86** (scheme 4-6, eq 2).

Scheme 4-6. **C6 alkylation/arylation of cyclic enaminones**

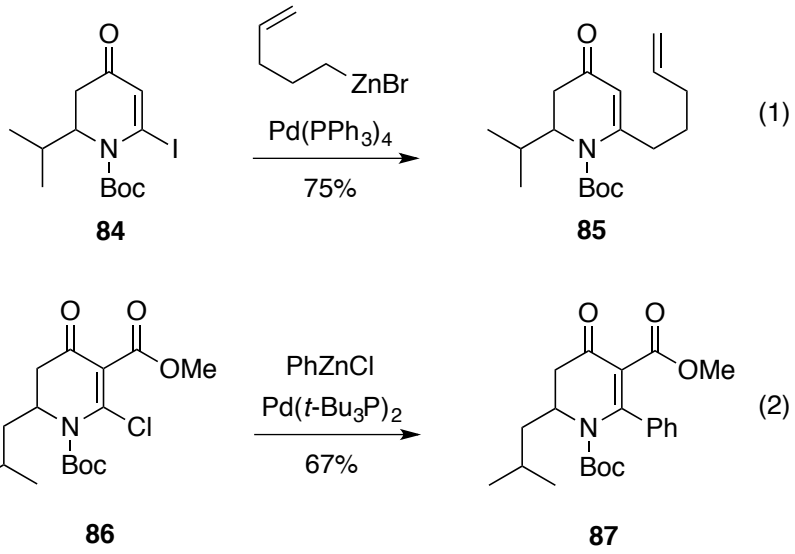

Scheme 4-7. **C6 alkylation by addition and oxidation**

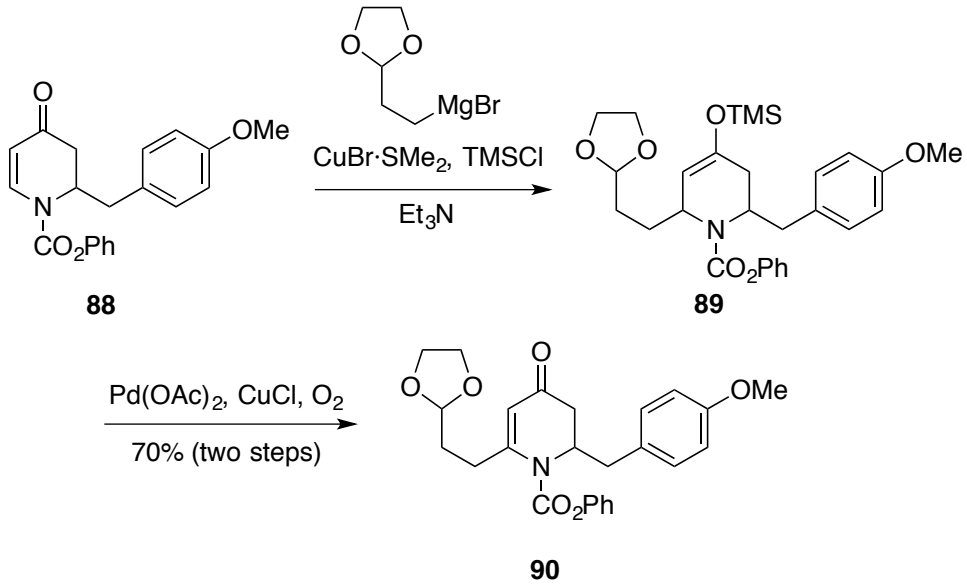

Another strategy to maintain the enaminone system after the conjugate addition is a subsequent oxidation step (scheme 4-7).[58] A conjugate addition of a Grignard reagent derived organocuprate to a cyclic enaminone **88** forms an enolate intermediate, which could be trapped by TMSCl to afford the silyl enol ether **89**. A succeeding oxidative rearrangement of the silyl enol ether by catalytic $Pd(OAc)_2$ provided the C6 alkylation product **90** with the enaminone system.

4.1.1.3 Intramolecular Heck reaction

Scheme 4-8. **Intramolecular Heck reaction**

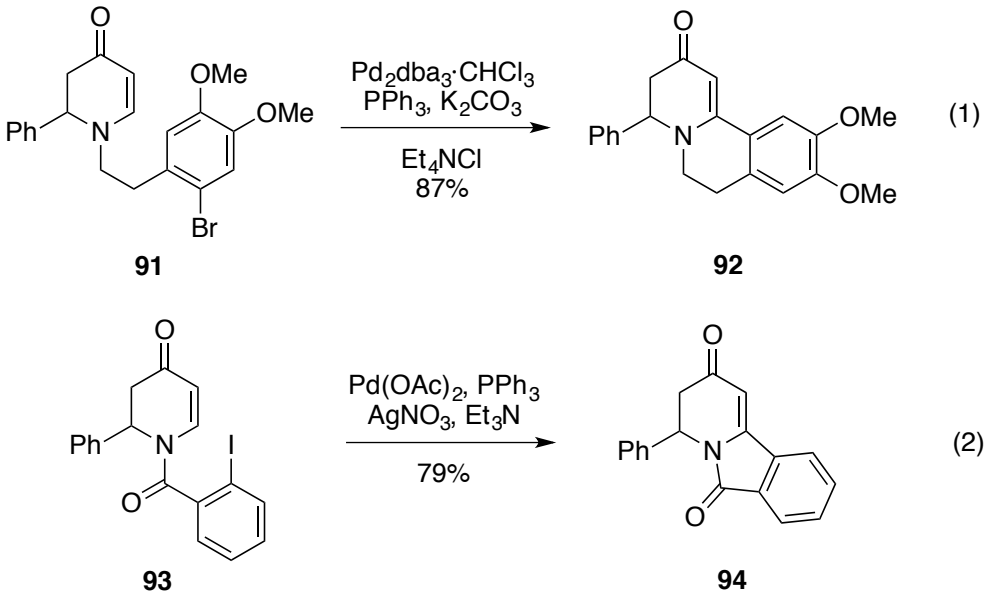

Direct C6 arylations of cyclic enaminones have been reported, but only in intramolecular Heck reactions. Tricyclic benzoquinolizidine and benzoindolizidine could be accessed by intramolecular Heck reaction.[59-62] Heck cyclization of the *ortho*

bromo arylethyl substituted cyclic enaminone **91** produced the benzoquinolizidine scaffold employing Jeffery's conditions (scheme 4-8, eq 1),[63] which is known to accelerate the rate of the reaction with a combination of phase transfer catalyst (tetraalkyl-ammonium salt) and insoluble bases. In addition, benzo-fused indolizidines can also be prepared using an intramolecular Heck-reaction (scheme 4-8, eq 2).

4.1.2 Palladium-catalyzed Heck reaction and conjugate addition in cyclic system

Cyclic enaminones are considered to be challenging substrates for Heck-type reactions, although it has been effective in intramolecular cyclizations (scheme 4-8). Cyclic systems often generate a mixture of the Heck-product and the conjugate addition product because the *syn* β-hydride elimination step needed for a Heck reaction is unfavorable.[64-68] Thus, an alternative mechanistic pathway from the traditional Heck-type process is required such as stereochemical inversion or *anti*-elimination.

Ortho-iodobenzyloxy substituted cyclohexenone **95** was subjected to Heck cyclization, affording a mixture of alkene **96** and alkane **97** (scheme 4-9, eq 1).[64] It was hypothesized that the formation of $XPd(II)L_nH$ is responsible for the reductive cyclization (scheme 4-9, eq 2). The addition of $Et_3N{\cdot}HCl$, which shifts the equilibrium towards a higher concentration of $XPd(II)L_nH$ increased the amount of reduction product. By contrast, addition of $AgNO_3$ to lower the concentration of $XPd(II)L_nH$ by scavenging HX suppressed the reductive cyclization. Both

experiments support the idea that $XPd(II)L_nH$ is the source of the reducing species.

Scheme 4-9. **Heck reaction vs conjugate addition in a cyclic system**

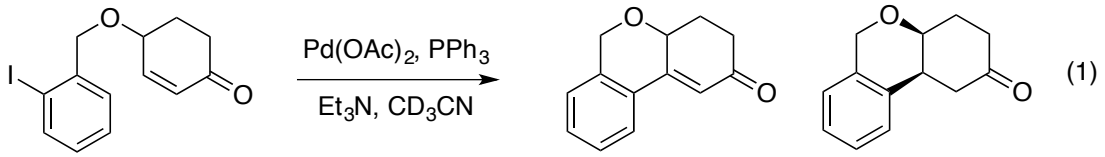

(1)

95 **96** **97**

with no additive	55:45
with $Et_3N{\cdot}HCl$	32:68
with $AgNO_3$	91:9

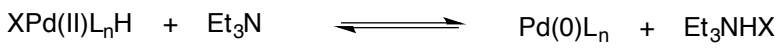

(2)

Scheme 4-10. **Plausible mechanism**

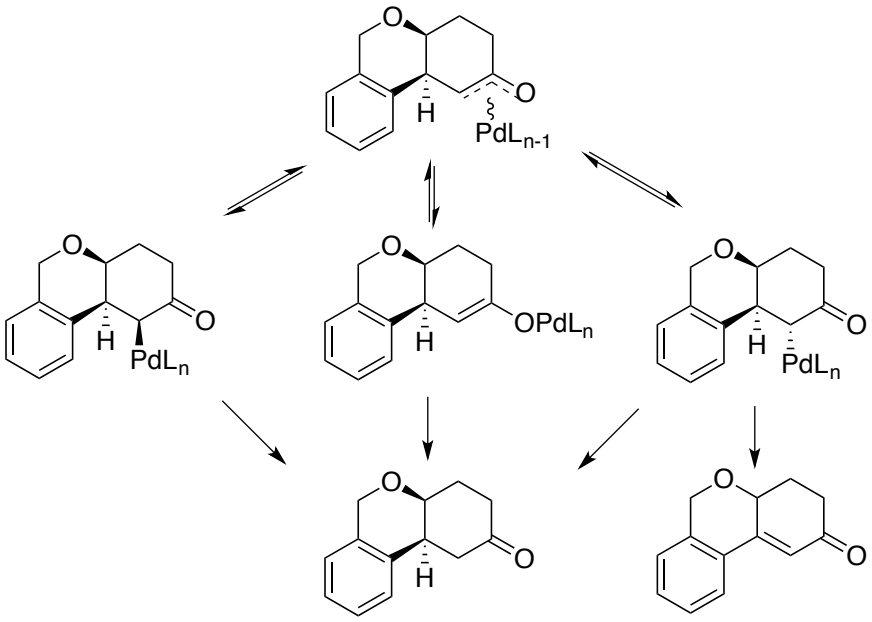

As shown in scheme 4-10, an intermediate without a *syn* β-hydride can be epimerized to an intermediate with a *syn* β-hydride via an oxo-π-allylpalladium intermediate, which can produce the Heck product. In addition, reduction of all intermediates with reductants such as $XPd(II)L_nH$ or $Et_3N{\cdot}HCl$ would yield the conjugate addition product. A *trans*-E2 elimination mechanism is not considered as a major elimination pathway because increasing concentration of Et_3N did not increase the proportion of Heck product.

Scheme 4-11. **Intramolecular Heck reaction with *anti*-H elimination**

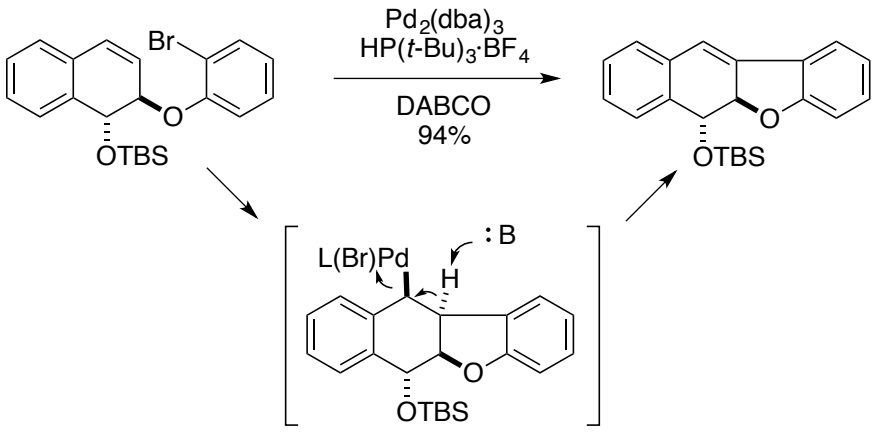

A Heck reaction with *anti*-hydride elimination has been reported in a cyclic system (scheme 4-11).[69] A benzylic palladium intermediate undergoes *anti*-hydride elimination to afford a tetracyclic compound containing the benzofuran scaffold. In this Heck cyclization, *anti*-hydride elimination is accomplished by the removal of a proton using organic base, 1,4-diazabicyclo[2.2.2]octane (DABCO).

Scheme 4-12. **Decarboxylative Heck-type arylation**

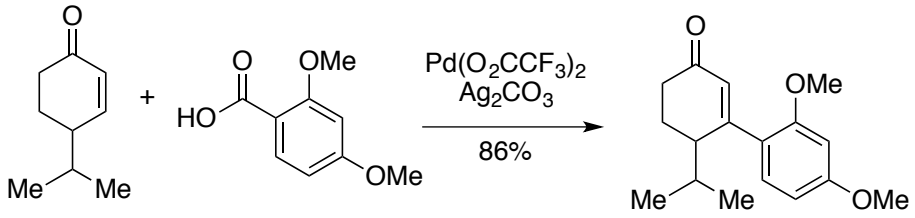

An alternative approach was reported to overcome the production of the conjugate adduct in cyclic systems. In the intermolecular Heck-type reaction of a cyclic system, an arene carboxylic acid was used to replace aryl iodide. A palladium-catalyzed decarboxylative coupling successfully provided the Heck-type arylation product without the formation of the conjugative aryl adduct (scheme 4-12).[68] However, the scope of the arene carboxylic acid is limited since *ortho* palladation or C–H insertion occurs only in substrates with at least one *ortho* substituent.[70]

4.1.3 Boron-Heck reaction in cyclic systems

Recently, boron reagents have emerged as alternative halide surrogates in Heck-type reactions.[71] These oxidative boron-Heck reactions proved to be successful with a few cyclic systems.[72-75] Jung and co-workers reported oxidative palladium(II) catalysis using alkenyl- and arylboron under base free and nitrogenous-ligand conditions.[72] It is worth noting that the reaction proceeded under very mild conditions (12 h at room temperature). In particular, the reaction of cyclohexenone **98** with phenylboronic acid provided the Heck-product **99** (scheme 4-13). As the conjugate

adduct was not observed, the authors proposed that the low possibility for the formation of a palladium enolate is resulting from a palladotropic shift. Consequently, a base-assisted *anti*-elimination was suggested for the Heck reaction of cyclohexenone, where phenanthroline would act as a base in addition to a palladium ligand.

Scheme 4-13. **Boron Heck reaction of cyclohexenone**

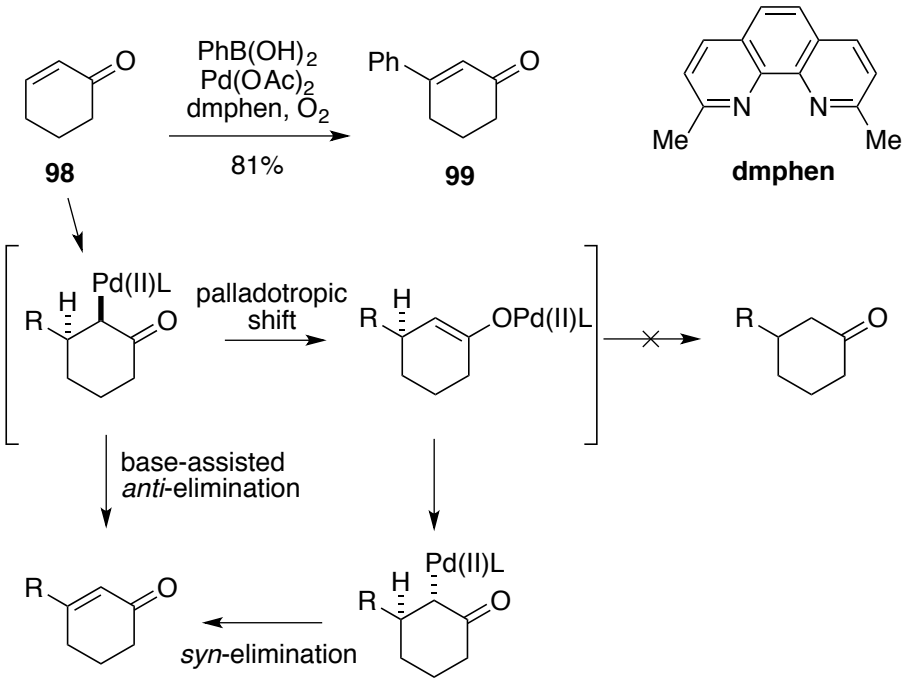

A boron-Heck reaction was also applied to the arylation of benzene-fused cyclic enone systems such as coumarin and chromone derivatives (scheme 4-14).[74] This arylation reaction affords direct and regioselective access to biologically interesting flavone and neoflavone derivatives without prefunctionalization. Compared to the conditions with cyclohexenone (scheme 4-13), this transformation requires

demanding conditions such as high temperature (100 °C) and long reaction times (24 h). Still, the reaction can tolerate various electron-donating/withdrawing substituents, providing diverse compounds.

Scheme 4-14. **Boron Heck reactions of coumarin and chromone**

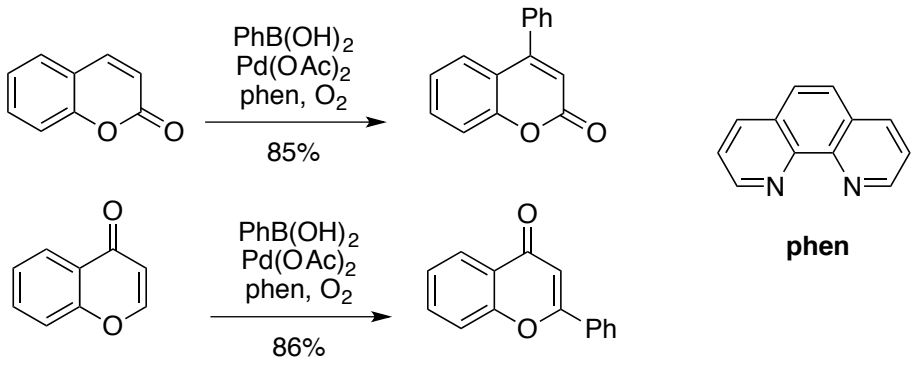

4.1.4 Palladium-catalyzed boron-Heck reaction vs conjugate addition

Shifting the reaction to a Heck-type product in cyclic systems has been successful using the boron-Heck reaction, and strategies for the selective control of the products have been developed. Oxidant-controlled palladium-catalyzed oxidative Heck-type reaction and conjugate addition reaction of glycals was reported (scheme 4-15).[76] Depending on the oxidant, typical boron-Heck conditions provided the ketone **101**, enol ether **102** or enone **103** from a *C*-glycoside **100**.

Scheme 4-15. Oxidant-controlled arylation of a glycal

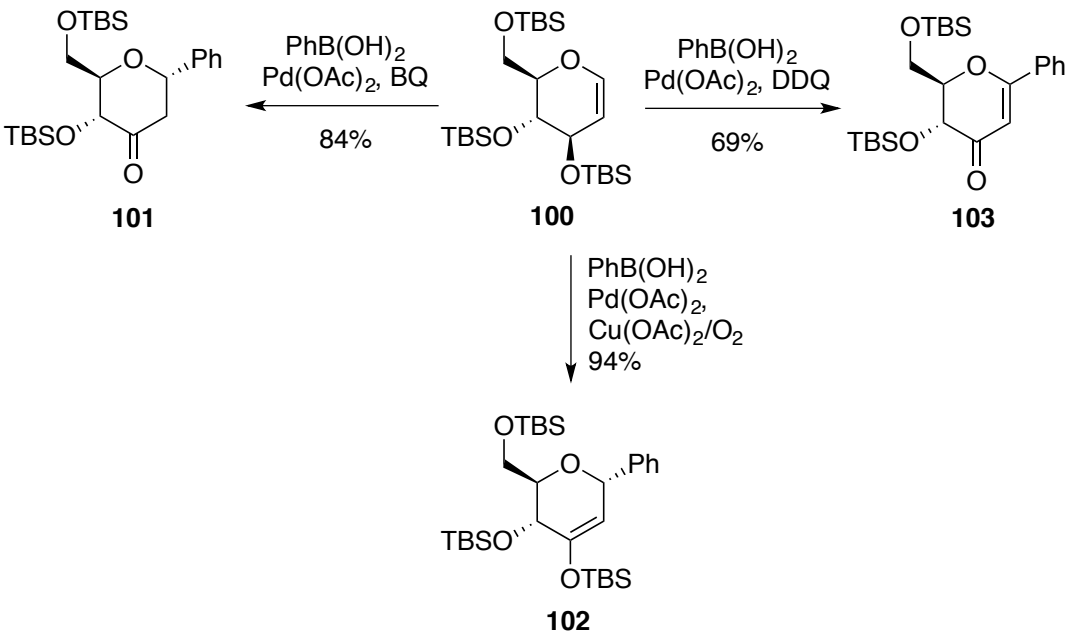

Scheme 4-16. Proposed mechanism of oxidant-controlled arylation

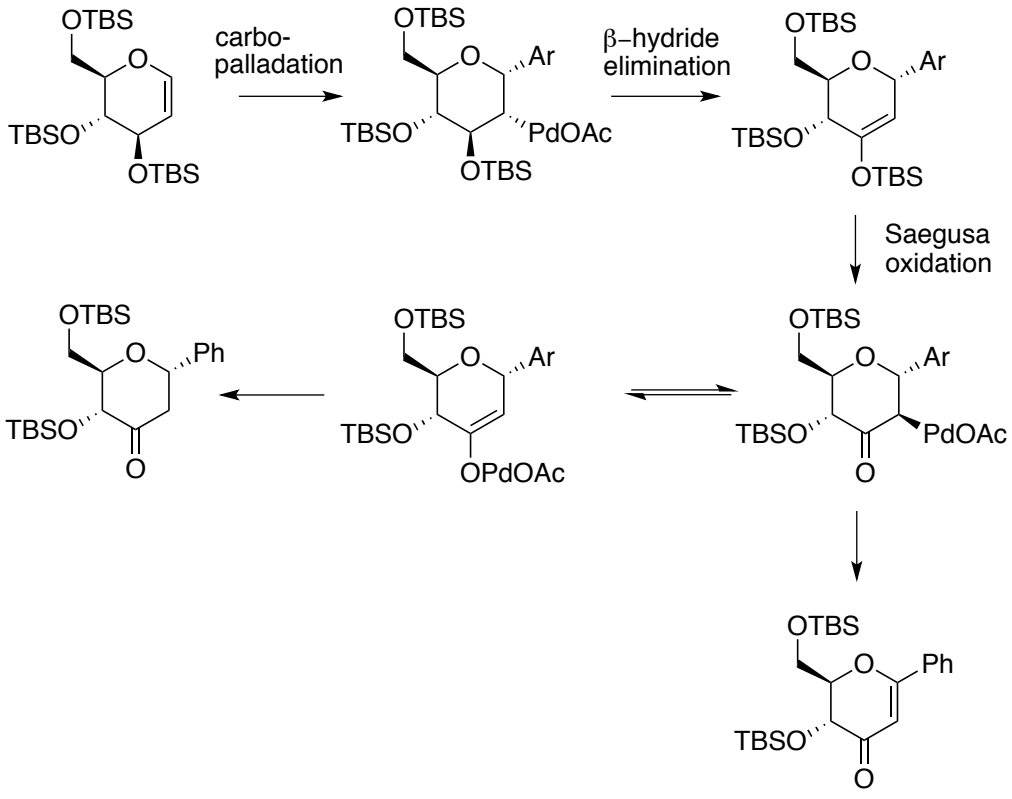

The proposed pathways toward those three products are described as follows (scheme 4-16). Carbopalladation and an immediate elimination of β-hydride adjacent to the silyl ether would provide the enol ether. With the use of BQ (benzoquinone) or DDQ (2,3-dichloro-5,6-dicyano-1,4-benzoquinone) under palladium catalysis, Saegusa oxidation would proceed to form the oxo-π-allyl palladium intermediate. Hydrolysis occurs under BQ condition to form the corresponding ketone, while β-hydride elimination leads to the Heck-type product (enone).

Scheme 4-17. Solvent controlled switching between oxidative Heck and conjugate addition reactions

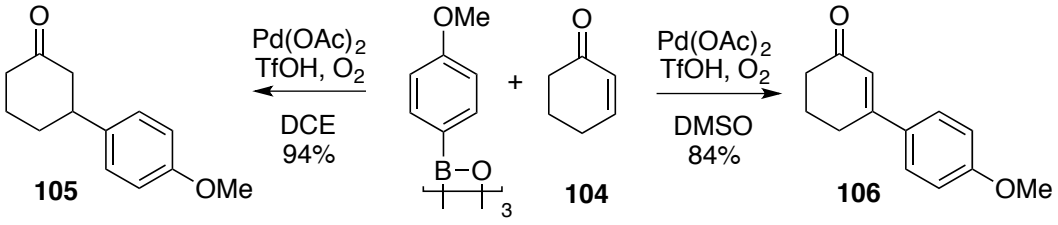

Palladium-catalyzed switching between oxidative Heck and conjugate addition reactions in cyclic enone systems has been reported (scheme 4-17).[77] Cyclohexenone **104** was reacted with 4-methoxyphenylboroxine under palladium(II)-catalysis. The conjugate adduct **105** was formed from the reaction in DCE. A complete switch to an oxidative Heck reaction was observed by simply changing the solvent to DMSO, however, low yields were observed using other types of arylboroxines and cyclic

enones. It was found that arylboroxines in DCE is required in conjugate addition, while arylboronic acids in DMSO are optimal in Heck reactions. Polar and coordinating DMSO is believed to force the reaction to an oxidative Heck reaction by stabilizing the cationic palladium center. In addition, the DMSO solvent is believed to facilitate the epimerization required for *syn*-β-elimination.

4.1.5 Design of C6 arylation

Scheme 4-18. Heck reaction of cyclic enaminones

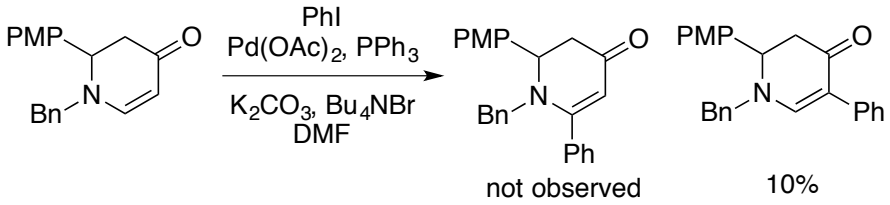

Initially, we explored a conventional intermolecular Heck reaction of a cyclic enaminone using phenyl iodide. In addition to the issues in a cyclic system, another challenge of a Heck reaction with the cyclic enaminone system is the competing electrophilic palladation (C5 functionalization) particularly with an electron donating group at the nitrogen (chapter 2 and 3). In our preliminary results (Scheme 4-18), a preference for C5 arylation was observed under the typical Heck reaction conditions, which was successfully used in intramolecular Heck reactions.[61] On the other hand, the boron-Heck reaction provides successful arylation in a few cyclic systems. In parallel with our previous C5 arylation reaction with arylboronic acids, it was envisioned that an oxidative boron-Heck reaction could be employed to install an aryl

group at the C6 position of cyclic enaminones by a slight modification of the C5 arylation conditions (scheme 4-19). As shown in our previous studies (chapter 2 and 3), it is necessary to increase the electron density of the palladium catalyst to prevent C5 arylation. An electron donating *N,N'*-bidentate ligand[78] was selected with the expectation that this would lead to a switch in the regioselectivity of the reaction. While the palladation is suppressed at the C5 position with an electron-enriched catalytic system, transmetallation will occur with an arylboronic acid to form the arylpalladium(II) complex, then the insertion with the alkene should take place. Therefore, direct arylation at the C6-position could be accomplished. In this chapter, the direct C6 arylation using arylboronic acids under Pd(II)-catalysis is described.

Scheme 4-19. Regioselective arylation of cyclic enaminones

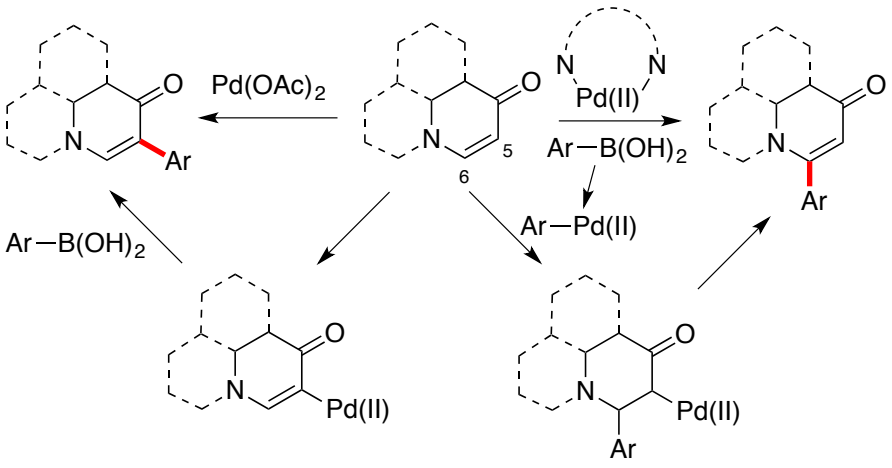

4.2 Reaction optimization

4.2.1 Screening of oxidants

Table 4-1. Screening of oxidants[a]

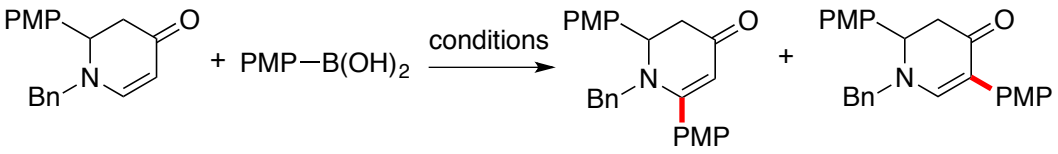

4.1 **4.2** **4.3** **4.4**

entry	reoxidant	yield (%)	ratio (4.3/4.4)
1[b]	$Cu(OAc)_2$+$AgNO_3$	34	1.8
2	$CuCl_2$	–	–
3	$Cu(OTf)_2$	10	1/2.3
4	$Cu(CO_2CF_3)_2$	25	1/11
5	benzoquinone	46	< 1/20
6	Ag_2O	7	> 20/1
7	$PhCO_3t$-Bu	21	> 20/1
8	*t*BuOOH	3	> 20/1
9	dicumyl peroxide	27	> 20/1
10	$Na_2S_2O_8$	–	–
11	**O_2**[c]	**33**	**> 20/1**

[a]Reaction conditions: cyclic enaminone (1 equiv), arylboronic acid (2 equiv), $Pd(OAc)_2$ (10 mol %), 2,2'-bipyridine (11 mol %) and oxidant (2 equiv) in DMF (0.2 M) for 20 h at 60 °C, the yield was determined by ^{1}H NMR analysis of the crude product using Ph_3SiMe (1 equiv) as the internal standard. [b]without 2,2'-bipyridine. [c]balloon pressure.

We initiated the optimization of the reaction using cyclic enaminone **4.1** and 4-methoxyphenylboronic acid **4.2** as model substrates (table 4-1). First, the reaction condition without 2,2'-bipyridine was investigated and a mixture of C6 arylated **4.3** and C5 arylated **4.4** was observed (table 4-1, entry 1). The choice of oxidant was

essential. It should be noted that C5 arylated derivative **4.4** was formed preferentially when a copper salt or benzoquinone was used as an oxidant (table 4-1, entries 3-5). However, the use of $CuCl_2$ as an oxidant did not provide any product (table 4-1, entry 2). The conditions with Ag_2O (table 4-1, entry 6), or peroxy compounds including *tert*-butyl perbenzoate, dicumyl peroxide and *tert*-butyl hydroperoxide (table 4-1, entries 7-9) provided Heck-type product **4.4** exclusively but in low yields. The reaction with oxygen as oxidant provided best the result with complete selectivity, although the yield was moderate (table 4-1, entry 11).

4.2.2 Screening of solvents

Table 4-2. Screening of solvents[a]

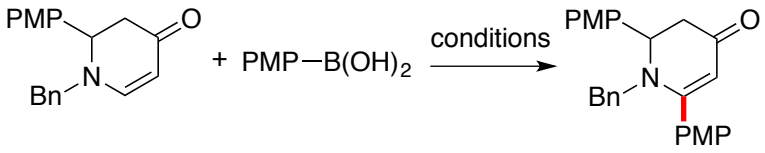

4.1 **4.2** **4.3**

entry	solvent	yield (%)	entry	solvent	yield (%)
1	*t*-BuOH	–	8	THF	7
2	CH_3CN	–	9	DMF	33
3	DCE	–	10	DMA	40
4	DMSO	4	**11**	**NMP**	**49**
5	AcOH	–	12	NMP/DMSO = 10/1	17
6	Toluene	–	13	NMP/ H_2O = 10/1	3
7	1,4-Dioxane	5	14	MeOH/H_2O = 9/1	–

[a]Reaction conditions: cyclic enaminone (1 equiv), arylboronic acid (2 equiv), $Pd(OAc)_2$ (10 mol %), 2,2'-bipyridine (11 mol %), solvent (0.2 M) under O_2 balloon for 20 h at 60 °C, the yield was determined by ^1H NMR analysis of the crude product using Ph_3SiMe (1 equiv) as the internal standard.

The reaction was affected significantly by the solvent selection, where amide solvents such as DMF, DMA and NMP were preferred (table 4-2, entries 9-11). The use of other types of polar and non-polar solvents did not afford a noticeable amount of product (table 4-2 entries 1-6). Furthermore, reactions in ethereal solvents such as 1,4-dioxane and THF failed to provide meaningful yields (table 4-2, entries 7 and 8).

4.2.3 Screening of ligands

Table 4-3. Screening of ligands[a]

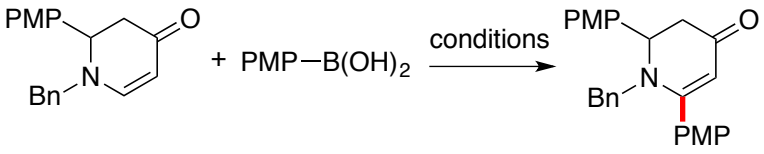

4.1 **4.2** **4.3**

entry	ligand (equiv)	yield (%)
1	ethylenediamine (0.11)	–
2	DMEDA (0.11)	3
3	TMEDA (0.11)	11
4	TMPDA (0.11)	11
5	triethylamine (0.21)	–
6	DABCO (0.21)	< 3
7	pyridine (0.21)	< 3
8	IMesCl (0.21)	4
9	DMAP (0.21)	–

[a]Reaction conditions: cyclic enaminone (1 equiv), arylboronic acid (2 equiv), $Pd(OAc)_2$ (10 mol %), DMP (0.2 M) under O_2 balloon for 20 h at 60 °C, the yield was determined by ^1H NMR analysis of the crude product using Ph_3SiMe (1 equiv) as the internal standard.

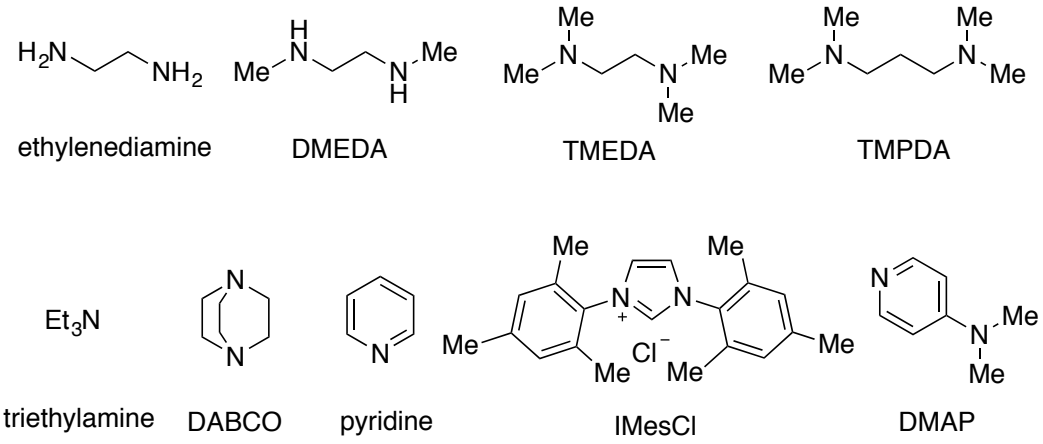

With optimal oxidant and solvent, a variety of ligands were tested in boron-Heck reaction. Reactions with simple aliphatic monodentate and bidentate ligands were not fruitful (table 4-3, entries 1-6), while dimethyl protected amines such as *N,N,N',N*'-tetramethylethylenediamine (TMEDA) and *N,N,N',N*'-tetramethyl-1,3-propane-diamine (TMPDA) gave slightly better yields (table 4-3, entries 3 and 4). More nucleophilic DABCO, aromatic amine and *N*-heterocyclic carbene ligands were not ideal ligands in boron-Heck arylation of cyclic enaminones (table 4-3, entries 6-9).

We turned our attention to bidentate aromatic ligands as they have been used in boron-Heck reactions as described above. Ligands with 1,10-phenanthroline and 2,2'-bipyridine scaffolds were tested in the boron-Heck reaction of the cyclic enaminone. 2,2'-Bipyridine type of ligands were found to be superior to the 1,10-phenanthroline ligand systems. It was found that 2,2'-bipyridine is an optimal ligand with an initial amount (11 mol %), which was used throughout the optimization process (table 4-4, entry 6)

Table 4-4. Screening of ligands[a]

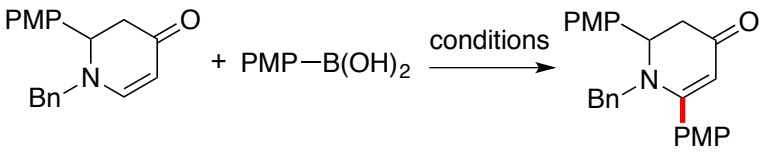

4.1 **4.2** **4.3**

entry	ligand (equiv)	yield (%)
1	1,10-phenanthroline (0.11)	28
2	neocuproine (0.11)	20
3	2,2'-bisquinoline (0.11)	5
4	dmbpy (0.11)	34
5	2,2'-bipyridine (0.05)	30
6	**2,2'-bipyridine (0.11)**	**49**
7	2,2'-bipyridine (0.2)	38
8	2,2'-bipyridine (0.5)	18
9	2,2'-bipyridine (1.0)	8

[a]Reaction conditions: cyclic enaminone (1 equiv), arylboronic acid (2 equiv), $Pd(OAc)_2$ (10 mol %), DMP (0.2 M) under O_2 balloon for 20 h at 60 °C, the yield was determined by ^1H NMR analysis of the crude product using Ph_3SiMe (1 equiv) as the internal standard.

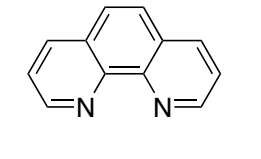

1,10-phenanthroline
(= phen)

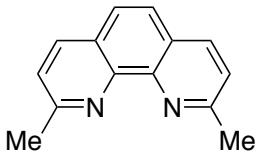

neocuproine
(= dmphen)

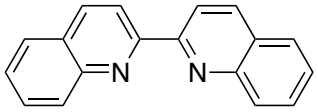

2,2'-biquinoline

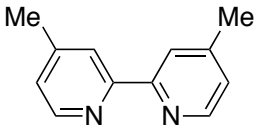

4,4'-dimethyl-2,2'-bipyridine
(= dmbpy)

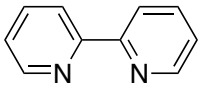

2,2'-bipyridine

4.2.4 Screening of additives

Table 4-5. Screening of additives[a]

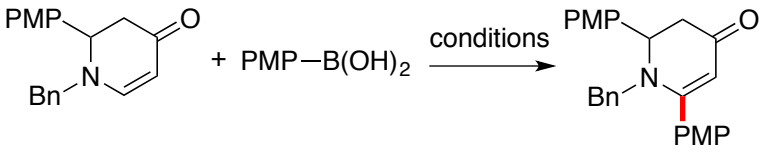

4.1 **4.2** **4.3**

entry	additive (equiv)	yield (%)
1	K_2CO_3	< 3
2	Cs_2CO_3	–
3	CsOAc	–
4	AcOH	27
5	TBABr	–
6	TBACl	–
7	TBAOAc	–
8	LiCl	–
9	CsF	–

[a]Reaction conditions: cyclic enaminone (1 equiv), arylboronic acid (2 equiv), $Pd(OAc)_2$ (10 mol %), additive (1 equiv) in DMP (0.2 M) under O_2 balloon for 20 h at 60 °C, the yield was determined by ^1H NMR analysis of the crude product using Ph_3SiMe (1 equiv) as the internal standard.

After the optimization process for oxidant, solvent and ligand, we sought to improve the efficiency of the reaction in other parameters. By looking into the proposed mechanism of the boron-Heck reaction, it was envisioned that the addition of base would enable the *anti*-β-hydride elimination. Unfortunately, base additives did not enhance the reaction efficiency at all (table 4-5, entries 1-3). Additionally, tetra-alkylammonium salts as well as halide salts were ineffective additives (table 4-5, entries 5-9). Interestingly, Heck product **4.3** was observed with the addition of acetic

acid with lower yield compared to previous conditions (table 4-5, entry 4).

4.2.5 Screening of reaction time

Time-monitoring experiment revealed that the reaction was decelerated after 6 hours, resulting from the depletion of the arylboronic acid by homocoupling (table 4-6). To address this issue, another equivalent of the arylboronic acid was added after 6 hours, yielding improved result of 68% (table 4-6, entry 9).

Table 4-6. Screening of reaction time[a]

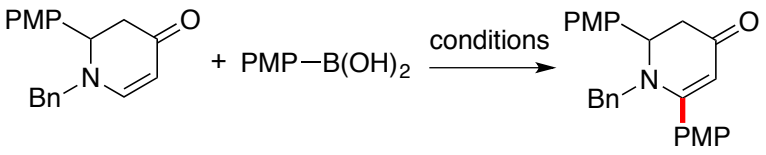

4.1 **4.2** **4.3**

entry	time (h)	yield (%)
1	0.5	< 3
2	1	4
3	2	9
4	4	18
5	6	25
6	9	30
7	12	34
8	20	41
9[b]	**20**	**68**

[a]Reaction conditions: cyclic enaminone (1 equiv), arylboronic acid (2 equiv), $Pd(OAc)_2$ (10 mol %), DMP (0.2 M) under O_2 balloon for 20 h at 60 °C, the yield was determined by ^1H NMR analysis of the crude product using Ph_3SiMe (1 equiv) as the internal standard.

4.3 Scope of boronic acids

Table 4-7. Scope of boronic acids[a]

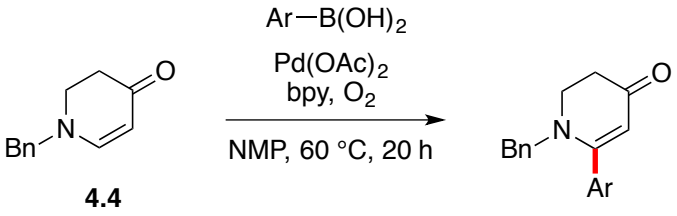

4.4

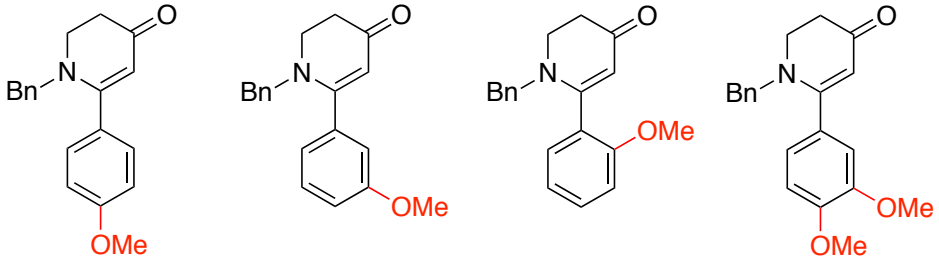

4.5 (74%) **4.6** (77%) **4.7** (Not observed) **4.8** (73%)

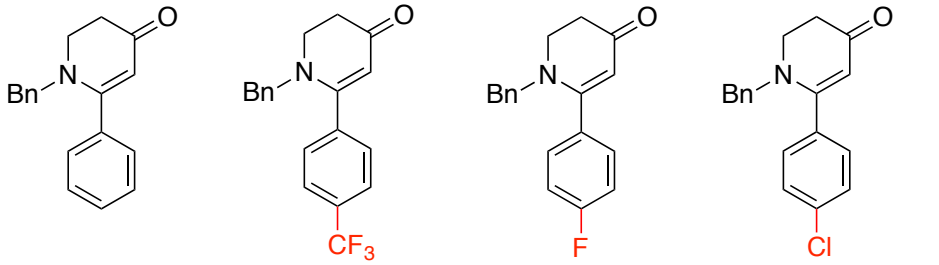

4.9 (71%) **4.10** (61%) **4.11** (58%) **4.12** (53%)

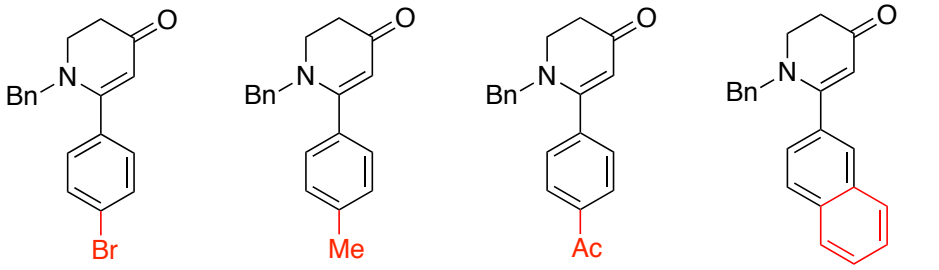

4.13 (47%) **4.14** (67%) **4.15** (77%) **4.16** (74%)

[a]Reaction conditions: cyclic enaminone (0.2 M), arylboronic acid (3 equiv), $Pd(OAc)_2$ (10 mol %), 2,2'-bipyridine (11 mol %), oxygen (balloon pressure).

The scope of arylboronic acids with cyclic enaminone **4.4** was investigated using the optimized reaction conditions (table 4-7). Electron rich as well as electron deficient arylboronic acids provided moderate to good yields (**4.5-4.16**). Generally, electron-rich arylboronic acids provided higher yields than electron-deficient reagents. 2-Methoxyphenyl derivative **4.7** was not observed, presumably due to steric hindrance.

4.4 Scope of cyclic enaminones

Table 4-8. Scope of cyclic enaminones[a]

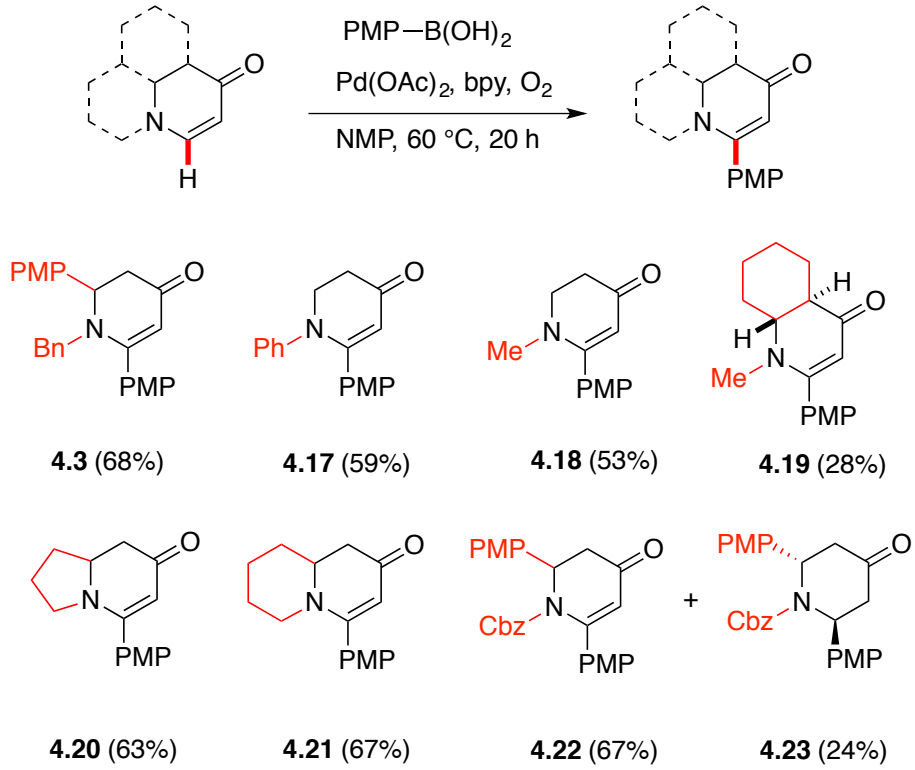

[a]Reaction conditions: cyclic enaminone (0.2 M), arylboronic acid (3 equiv), $Pd(OAc)_2$ (10 mol %), 2,2'-bipyridine (11 mol %), oxygen (balloon pressure).

Other cyclic enaminones bearing *N*-phenyl (**4.17**) or *N*-methyl (**4.18** and **4.19**) groups were suitable substrates for this reaction. Bicyclic enaminones with indolizidine and quinolizidine scaffolds also furnished the C6 arylated products **4.20** and **4.21** in good yields. While the Heck-type products were obtained exclusively with the substrates containing electron-donating groups at the nitrogen, a *N*-carbamylated cyclic enaminone afforded the Heck product **4.22** as well as conjugate addition product **4.23**. The reaction prefers Heck-type product to conjugate adduct with a ratio of 2.8:1. At this point, we sought to shift the reaction to conjugate addition with this substrate.

4.5 Acid-controlled conjugate addition of cyclic enaminones

While we were investigating the factors for the conjugate addition reactions for a *N*-carbamylated cyclic enaminone, it was found that the addition of acid could switch the outcome in favor of the conjugate addition (table 4-9). As the acidity of the acid was increased, more conjugate addition product **4.23** was formed while the yield of the Heck product **4.22** decreased. When acetic acid was used as a co-solvent, **4.23** was formed selectively but in very low yield. As such, the decrease of overall yield was also observed with the use of stronger acid. A complete shift to the conjugate addition product **4.23** was observed with two equivalents of TFA (table 4-8, entry 13) albeit in lower yield than with one equivalent. In addition, it is worth noting that the stereochemistry of **4.24** was confirmed as *trans* by X-ray crystallography. Although only one substrate was shown with this protocol, it provides an alternative method

toward the synthesis of *trans*-2,6-disubstituted piperidones under mild condition, which have been previously prepared via conjugate addition using Grignard reagents.[53, 54]

Table 4-9. Acid-controlled conjugate addition of cyclic enaminone[a]

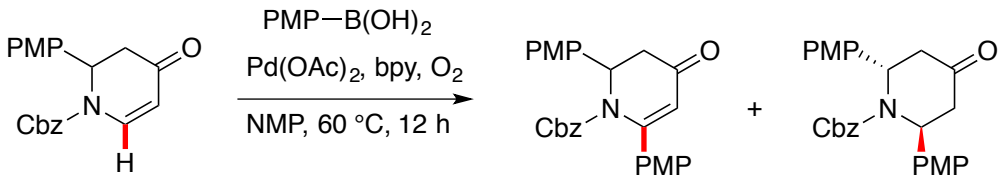

4.24 **4.22** **4.23**

entry	time (hr)	yield (%)	ratio (4.22/4.23)
1[b]	–	91	2.8/1
2	AcOH (1.0)	86	1/1.9
3	AcOH (2.0)	90	1/2.9
4	AcOH (5.0)	87	1/3.8
5	AcOH (10.0)	82	1/6.5
6[c]	–	7	< 1/20
7	TsOH·H_2O (0.1)	87	1/3.4
8	TsOH·H_2O (1.0)	72	1/6.2
9	HCO_2H	87	1/2.8
10	TFA (0.1)	90	1/3.8
11	TFA (0.5)	84	1/11
12	TFA (1.0)	88	1/12
13	TFA (2.0)	60	< 1/20
14	TFA (5.0)	45	< 1/20

[a]Reaction conditions: **4.24** (1 equiv), arylboronic acid (2 equiv), $Pd(OAc)_2$ (10 mol %) and 2,2'-bipyridine (11 mol %) in NMP (0.2 M) under O_2 balloon for 12 h at 60 °C, the yield was determined by ^1H NMR analysis of the crude product using Ph_3SiMe (1 equiv) as the internal standard. [b]20 h, isolated yield. [c]solvent: NMP/AcOH = 1/1.

4.6 Proposed mechanism

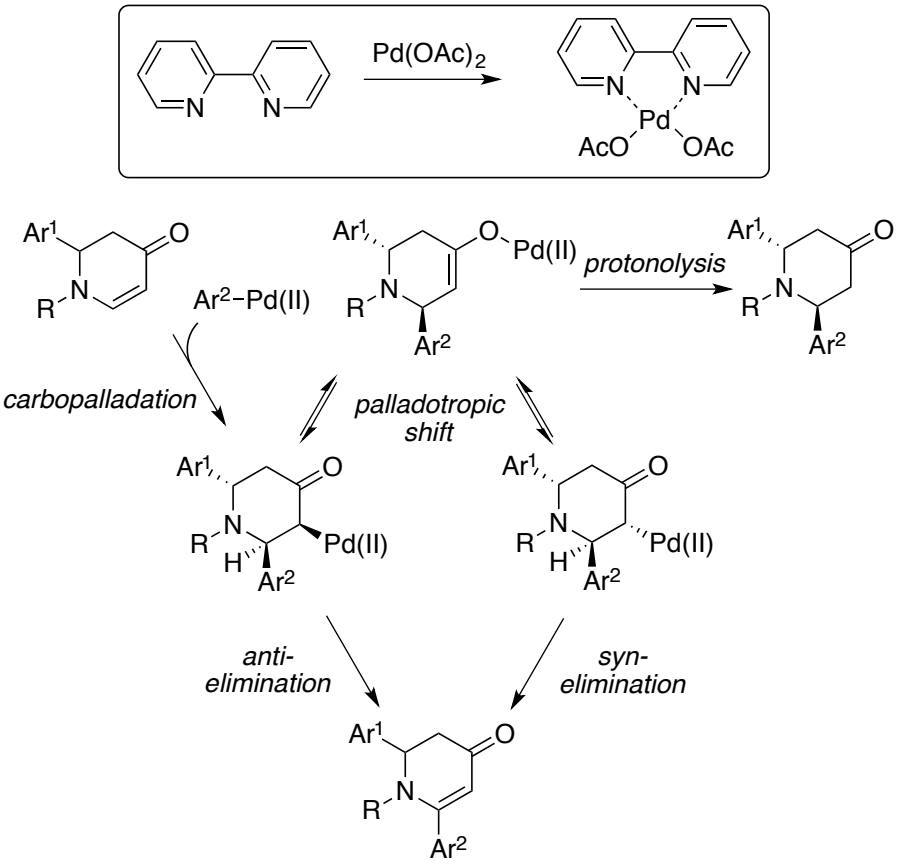

Figure 4-2. Proposed mechanism.

A plausible mechanism is depicted in figure 4-2. The electron-rich palladium ligand complex favors transmetallation with the arylboronic acid rather than C5 palladation of the cyclic enaminone. Carbopalladation generates a palladium complex with *anti*-β-hydride, which can be converted to the palladium enolate as well as an intermediate with *syn*-β-hydride by a palladotropic shift. In the presence of acid, the palladium enolate would undergo protonolysis to furnish the conjugate addition

product. Otherwise the oxidative Heck product could be obtained via elimination reactions.

4.7 Formal synthesis of lasubine II

Scheme 4-20. **Formal synthesis of (±)-lasubine**

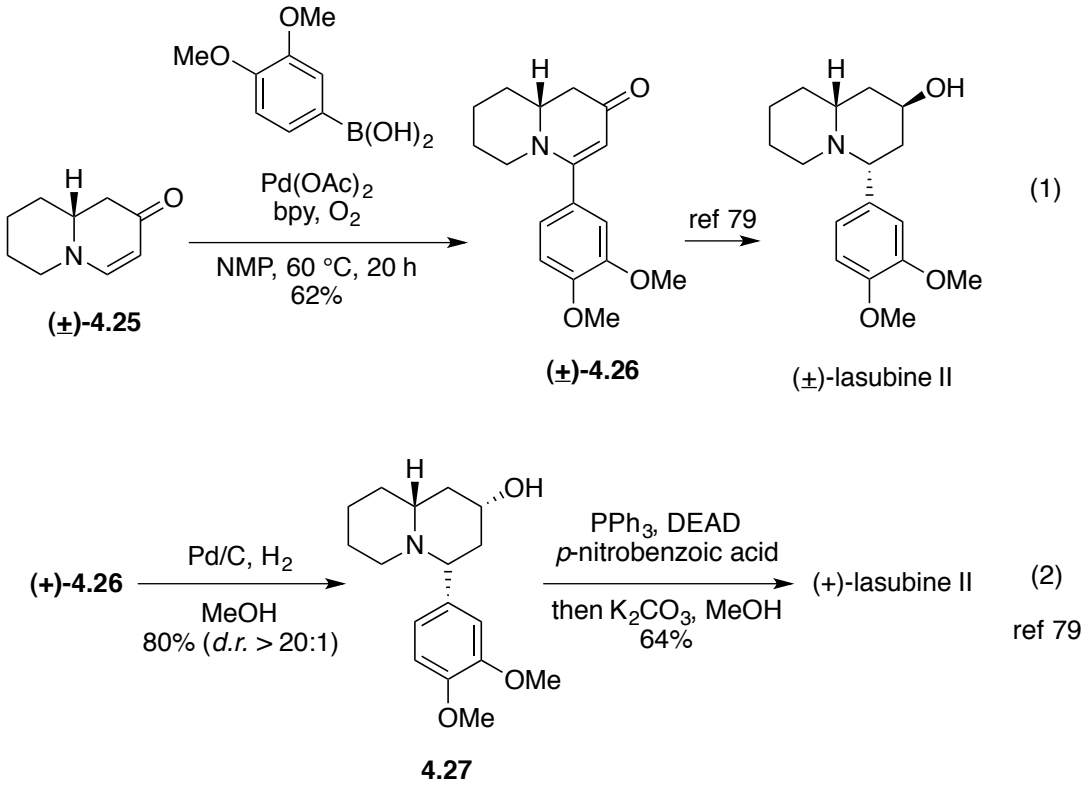

C6 arylated cyclic enaminones can serve as an intermediate in natural product synthesis. For example, lasubine II was obtained from compound **4.26** following the protocol developed by Rovis.[79] Reaction of 3,4-dimethoxyphenylboronic acid with bicyclic enaminone **4.25** gave C6-arylated product **4.26** in 62% yield (scheme 4-20,

eq 1). In the Rovis' synthesis, hydrogenation of enantioenriched **4.26** provided **4.27** diastereoselectively, which can be converted to (+)-lasubine II by a Mitsunobu reaction. The analytical and spectral data of compound **4.26** is consistent with the literature report,[79] which establishes the formal synthesis of lasubine II.

4.8 Conclusion

In summary, we have developed a C6 arylation protocol for cyclic enaminones using the oxidative boron-Heck reaction that proceeds with excellent selectivity over C5 arylation and conjugate addition reactions. This Boron-Heck reaction provides a complementary protocol to previously developed arylation at the C6 position. Furthermore, an acid-controlled reactivity switch to a conjugate addition reaction is viable when the reaction is carried out with *N*-carbamylated enaminones in the presence of an acid.

Chapter 5

Cyclic enaminone derivatives as inhibitors of IKKβ in NF-κB signaling

5.1 Introduction

Nuclear factor kappa B (NF-κB) is a nuclear transcription factor responsible for the transcription of the proinflammatory cytokine genes.[80] The signaling pathways of NF-κB are highly associated with chronic inflammatory diseases and cancer.[81] Inhibitor of kappa B (IκB) kinase β phosphorylates the inhibitory IκB in the canonical NF-κB signaling pathway, thereby controlling the activation of NF-κB.[82] Therefore, IκB kinase β (IKKβ) is an important therapeutic target for chronic inflammation regulation and cancer treatment. In this chapter, the discovery of cyclic enaminone derivatives as IKKβ inhibitors will be discussed.

5.1.1 NF-κB signaling pathway

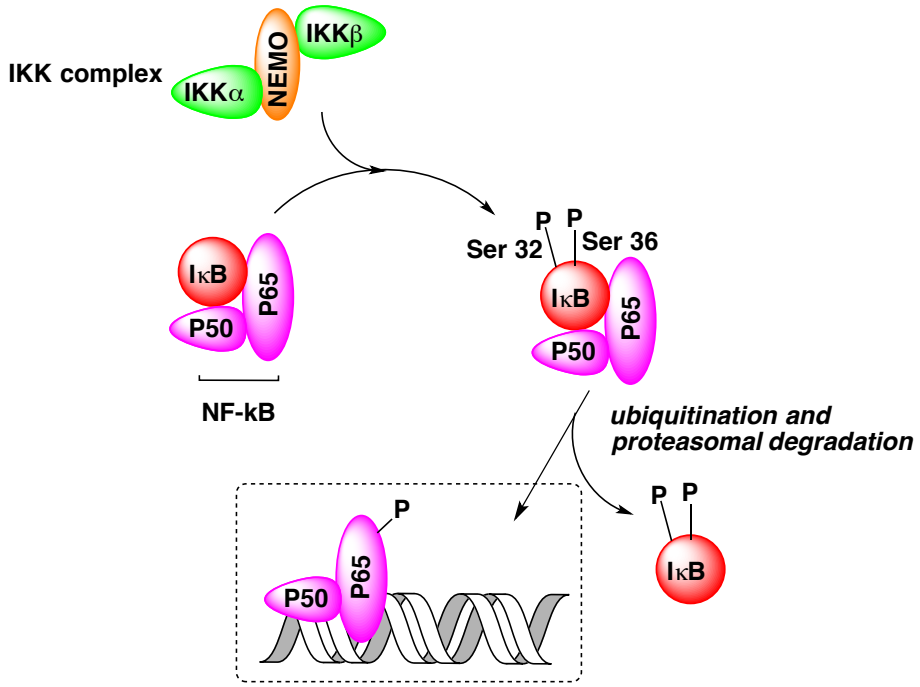

Figure 5-1. NF-κB signaling pathway.

The canonical pathway is one of the NF-κB signaling pathways, which involves signal-induced phosphorylation of IκBα by the IκBα kinase (IKK) complex (figure 5-1).[80, 81] External stimuli such as TNF-α (tumor necrosis factor-α), IL-1b (interlukin-1b) and LPS (lipopolysaccharide) activate the IKK complex in the NF-κB signaling pathway.[83] The activated IKK complex then phosphorylates IκBα at Ser32 and Ser36 in the N-terminus. Phosphorylated IκB is dissociated from the complex of IκB and heterodimeric NF-κB, and then ubiquitinated and finally undergoes proteasomal degradation. On the other hand, released heterodimeric NF-κB (p50/p65) translocates into the nucleus for binding to the response element of nuclear DNA, initiating the

transcription of mRNA for NF-κB gene products.

5.1.2 IKKβ inhibitors

Although many other routes for activating the NF-κB signaling pathway are reported, most signaling pathways are associated with the IKK complex. Inhibition of IKK activity is essential for the inhibition of the NF-κB signaling pathway. Consequently, understanding the IKK complex is a key to understand the NF-κB signaling pathway. The catalytic subunits IKKα and IKKβ as well as the regulatory/scaffold subunit IKKγ (NEMO) comprise a trimeric IKK complex.[84] While both IKKα and IKKβ are known to phosphorylate IκBα at Ser32 and Ser36, IKKβ is responsible for most of the IKK activities.[85a] For example, the IKK activation as well as degradation of IκB by proinflammatory stimuli remained intact in mice lacking the IKKα subunit.[85b] On the other hand, studies with IKKβ–deficient mice have demonstrated that IKKβ is required for the activation of NF-κB signaling pathway by most of the inflammatory stimuli.[85c] As a result, numerous inhibitors of IKKβ have been disclosed recently (figure 5-2),[86] although there is no marketed drug targeting IKKβ so far. Only a few compounds (for example, CHS828 and its prodrug EB-1627) have passed preclinical studies as anticancer agents.[87] The development of novel IKKβ inhibitors is, therefore, a potentially valuable process, considering the essential role of IKKβ in the NF-κB signaling pathway.

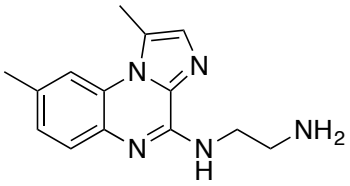

BMS-345541
IC_{50} = 0.3 μM

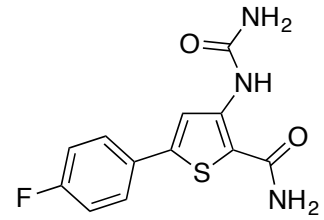

thiopenecarboxamide derivative
IC_{50} = 63 nM

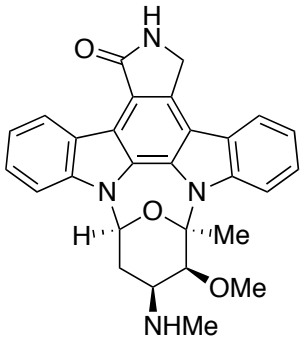

Staurosporine
IC_{50} = 1.6 μM

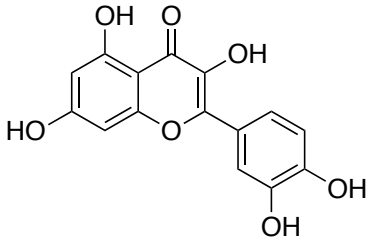

Quercetin
IC_{50} = 4 μM

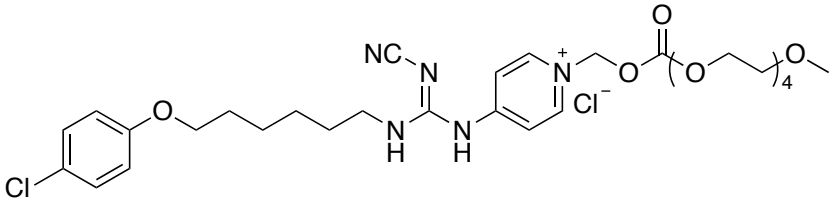

EB-1627

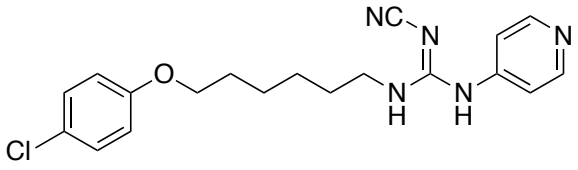

CHS-828
IC_{50} = 8 nM

Figure 5-2. IKKβ inhibitors.

5.2 Synthesis of cyclic enaminone derivatives

Initially, we are seeking to generate diverse scaffolds containing cyclic enaminone for the construction of molecular library. C5 arylated cyclic enaminones are readily accessible using arylboronic acid under palladium (II) catalysis or diaryliodonium salts as discussed in chapter 2 and 3. For the purpose of the molecular library, it was envisioned that bromo- or formyl- derivatives could be beneficial because further derivatization is feasible. For example, a copper catalyzed amidation reaction[88] of C5 arylated cyclic enaminones with bromo substituent could provide arylamides (scheme 5-1, eq 1). On the other hand, a formyl substituted substrate could undergo facile transformation to amines by reductive amination reactions (scheme 5-1, eq 2).

Scheme 5-1. Diversifying the molecular scaffold of cyclic enaminones

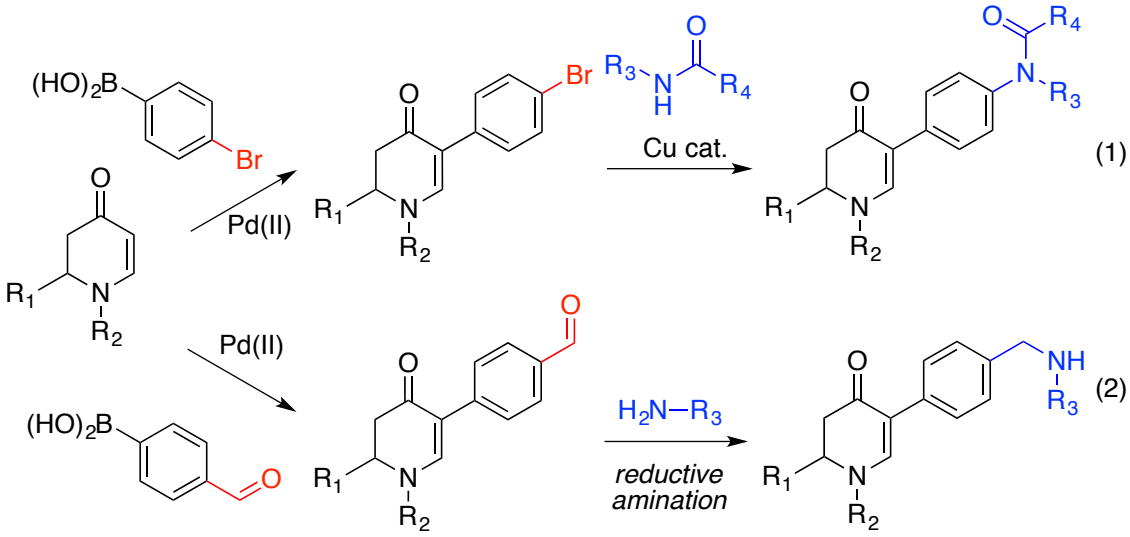

Table 5-1. Preparation of C5 arylated cyclic enaminones

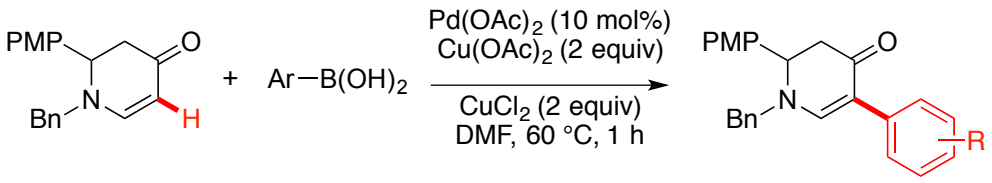

entry	R	yield (%)	entry	R	yield (%)
1	4-OMe (**5.1**)	81	7	4-$CONH_2$ (**5.7**)	74
2	H (**5.2**)	80	8	4-Ac (**5.8**)	82
3	4-Me (**5.3**)	75	9	4-NO_2 (**5.9**)	90
4	4-OH (**5.4**)	62	10	4-CN (**5.10**)	78
5	4-F (**5.5**)	85	11	4-formyl (**5.11**)	83
6	4-Br (**5.6**)	86	12	2-naphthyl (**5.12**)	83

First of all, twelve C5 arylated cyclic enaminones were readily prepared using electronically diverse arylboronic acids under palladium (II) catalysis as discussed in chapter 2 (table 5-1, **5.1**-**5.12**).

A copper catalyzed amidation reaction was utilized for the functionalization of bromo-substituted cyclic enaminone derivative **5.6**. Bromide **5.6** prepared from C5 arylation was reacted with five *N*-phenylacetamide derivatives, providing electron-rich and electron-deficient arylacetamides (table 5-2). The methoxy-substituted substrate gave a slightly lower yield (table 5-2, entry 1) and other coupling partners provided the corresponding products in good yields (table 5-2, entries 2-5). Similarly, reaction with *N*-phenylformamide also provided the corresponding coupled product (table 5-2, **5.18**). One more carbon (carbonyl group) between the nitrogen and the phenyl ring could be introduced using benzamide as a coupling partner, although the yield was low (table 5-2, **5.19**).

Table 5-2. Copper-catalyzed amidation of cyclic enaminone 5.6

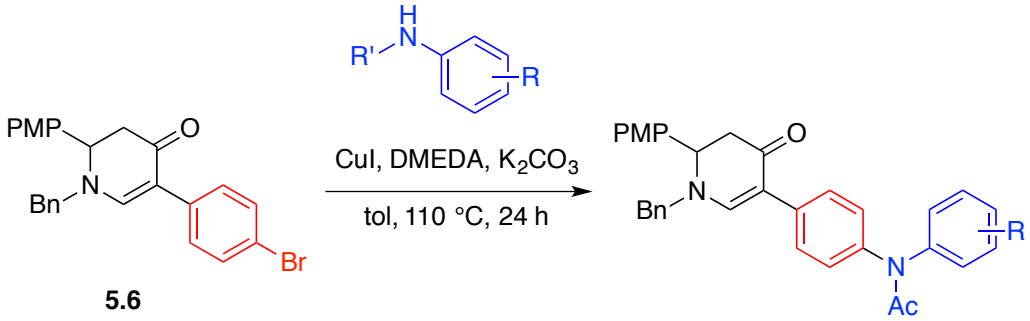

entry	R	yield (%)
1	4-OMe (**5.13**)	49
2	4-Me (**5.14**)	71
3	H (**5.15**)	70
4	4-Cl (**5.16**)	77
5	4-NO_2 (**5.17**)	62

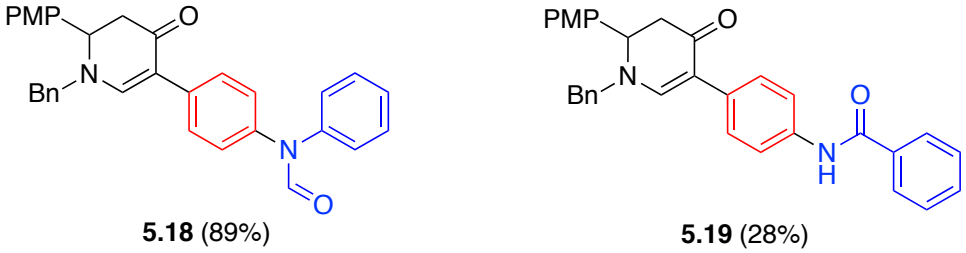

Formyl-substituted cyclic enaminone **5.11** is a suitable substrate for reductive amination reactions. The reactions of five benzylamine derivatives with cyclic enaminone **5.11** produced more complex scaffold, where cyclic enaminone is connected with electronically diversified benzylamine by toluene linker (table 5-3, **5.20**-**5.24**). 3,4-Dihydroxylated benzylamines were also used to prepare these types of compounds (table 5-3, **5.25**-**5.27**).

Table 5-3. Reductive amination of cyclic enaminone 5.11

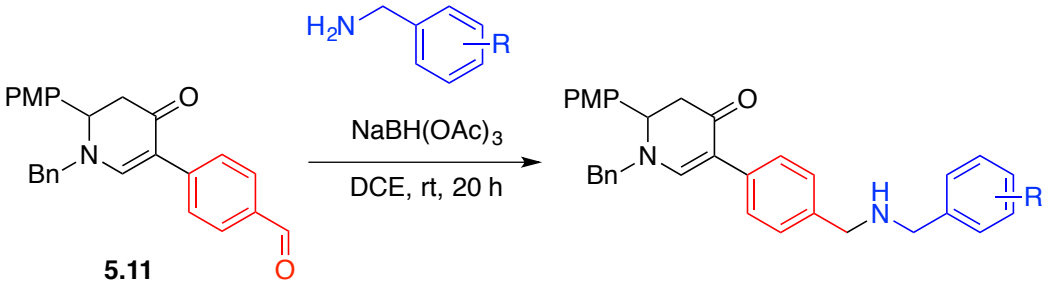

5.11

entry	R	yield (%)
1	4-OMe (**5.20**)	86
2	4-Me (**5.21**)	83
3	H (**5.22**)	90
4	4-Cl (**5.23**)	95
5	4-NO_2 (**5.24**)	51

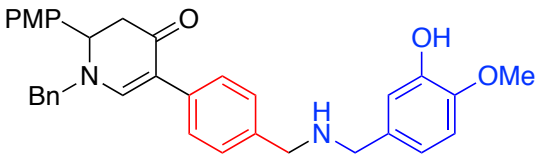

5.25 (37%)

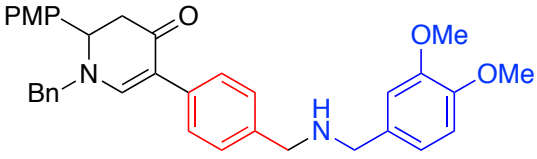

5.26 (66%)

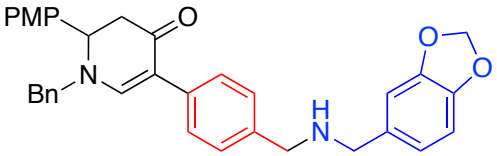

5.27 (78%)

To sum up, a molecular library of cyclic enaminones was constructed involving three types of cyclic enaminones via following reactions (figure 5-3):

1) C5 arylation (**type I**).

2) C5 arylation and copper-catalyzed amidation (**type II**).

3) C5 arylation and reductive amination (**type III**).

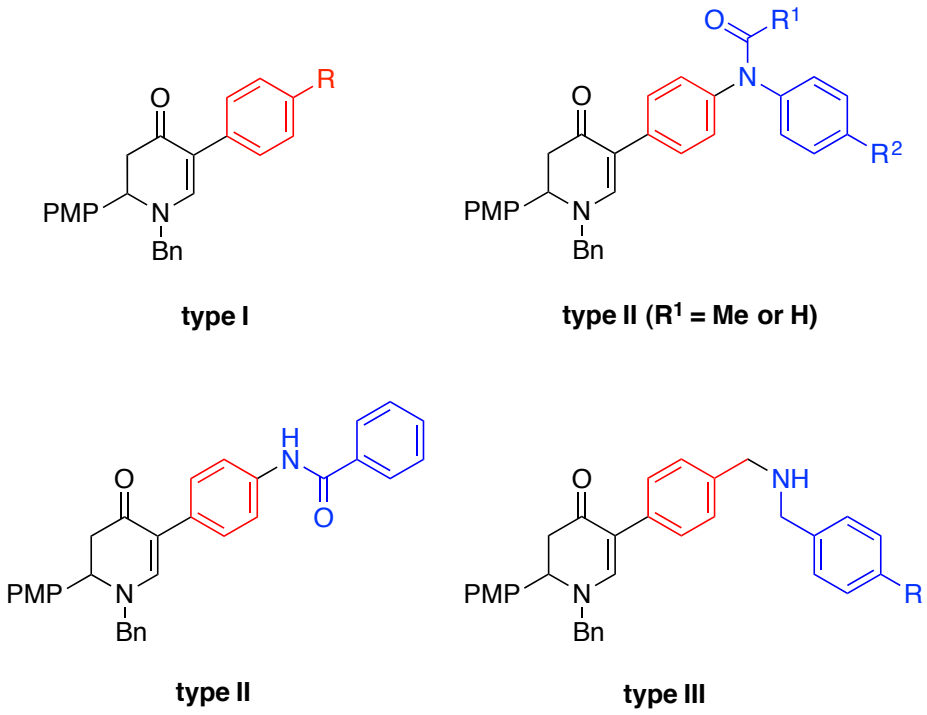

Figure 5-3. Structures of three types of cyclic enaminone derivatives.

5.3 Biological evaluation of cyclic enaminone derivatives

5.3.1 Antiproliferative activity screening

With these three types of cyclic enaminone derivatives in hand, we started various biological studies. We first performed a preliminary screen of antiproliferative activity against A549 (human lung carcinoma cells) at two concentrations (20 μM and 100 μM). Most type I compounds (**5.1**-**5.12**) compounds showed very weak growth inhibition at a concentration of 20 μM and slightly better results at 100 μM, although this series of compounds did not show very good inhibitory activities (graph 5-1).

Graph 5-1. Antiproliferative activity of type I compounds against A549[a]

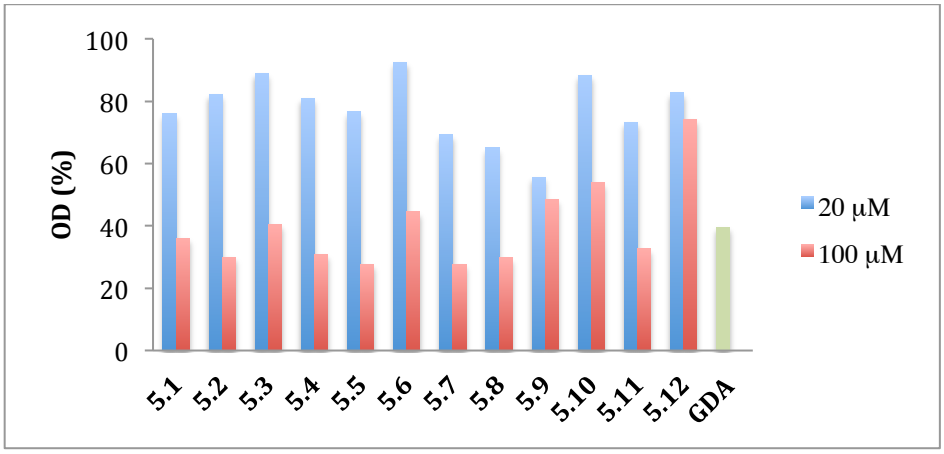

[a]GDA = Geldanamycin, 10 nM.

Graph 5-2. Antiproliferative activity of type II and III compounds against A549[a]

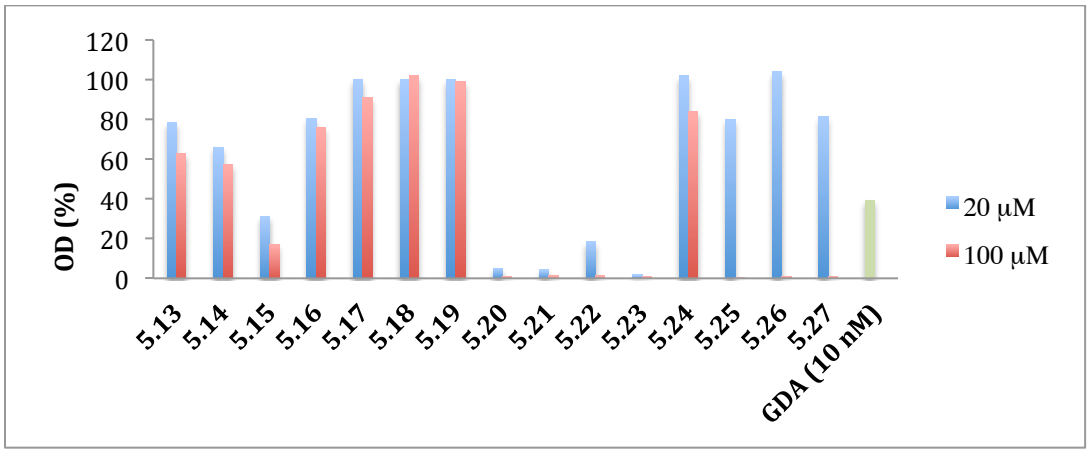

[a]GDA = Geldanamycin, 10 nM.

Then, an antiproliferative screening assay of type II and III compounds (**5.13**-**5.27**) was performed. It was found that **5.15** showed the most growth inhibition among the type II compounds, affording almost 70% growth inhibition at 20 μM and over 80% at 100 μM. However, all the other compounds of type II did not show any noticeable activity against A549 cell lines (graph 5-2). At the same time, the activity of type III compounds was also examined. Gratifyingly, all compounds except compound **5.24** in the type III series demonstrated near complete inhibition at 100 μM treatment. In addition, three compounds (**5.20**, **5.21** and **5.23**) at 20 μM concentration inhibited over 95% of the growth, while compound **5.22** exhibited over 80% inhibition at the same concentration.

5.3.2 Cellular cytotoxicity and NF-κB functional assay

Inspired by these results, we chose four compounds (**5.15**, **5.20**, **5.21** and **5.23**) to

investigate the inhibitory activities against other types of cancer cells and NF-κB. Antiproliferative activities of these compounds were examined to determine the GI_{50} values in A549 and DU-145 (non-hormone sensitive prostate cancer cell line) cell lines. We also investigated the NF-κB inhibitory activity of these compounds using a standard NF-κB luciferase reporter assay in A549 cancer cells (table 5-4). GI_{50} values of these compounds against A549 cells are virtually the same. In DU-145 cells, arylamide derivative **5.15** did not show any activity while benzylamine substrates showed similar GI_{50} values around 20 μM. It was found that all four cyclic enaminone derivatives inhibited the TNF-α induced NF-κB signaling pathway, where the IC_{50} values of these compounds were comparable to their antiproliferative activities in A549 cell lines. In addition, the antiproliferative activities of the cyclic enaminone derivatives are consistent with their inhibitory activities of the NF-κB signaling pathway. This result suggests that the cyclic enaminone derivatives exert the antiproliferative activity via the inhibition of the NF-κB signaling pathway.

Table 5-4. Antiproliferative and NF-κB activity of cyclic enaminone derivatives[a]

	IC_{50} (μM)		
compound	**A549**	**DU-145**	**NF-κB**[b]
parthenolide	2.9	7.9	4.5
5.15	10.1	> 100	10.7
5.20	11.8	20.1	13.7
5.21	13.4	21.5	12.6
5.23	12.6	22.3	12.0

[a]A549/NF-kB-luc = human lung carcinoma; DU-145 = human prostate carcinoma.
[b]NF-kB inhibition was measured by monitoring the luciferase activity from A549/NF-kB-luc cells upon treatment with the indicated compound.

5.3.3 Western blot analysis and IKKβ kinase assay

To gain more insight into the biochemical mechanism of cyclic enaminone derivatives, we conducted a Western blot analysis of proteins involved in the NF-κB signaling pathway with cyclic enaminone derivative **5.23**. As shown in figure 5-3, there was no change in the expression level of IKKβ, which suggests that compound **5.23** does not inhibit any of the proteins affecting the expression level of IKKβ. If cyclic enaminone derivative **5.23** inhibits the p50 or p65 directly, no change would be observed in the level of IκBα. The Western blot analysis of the proteins of interest from A549 cells treated with **5.23** indicated that IκBα was down-regulated in a concentration-dependent manner, which is an indicative of IKKβ inhibition. We compared the effect of compound **5.23** with a known IKKβ inhibitor, BMS-345541, on the IκB expression, finding similar results between these two compounds. Furthermore, the expression level of phosphorylated p65 (p-p65) is also decreased upon the treatment with compound **5.23**. This result is attributable to the inhibition of IKKβ, since IKKβ is known to phosphorylate p65 as well as IκB.[89] On the basis of these results, we believe that compound **5.23** inhibits the kinase activity of IKKβ. It is suggested that cyclic enaminone derivatives would modulate the NF-κB signaling pathway by inhibiting the phosphorylation of IκBα and p65, resulting from the regulation of IKKβ kinase activity.

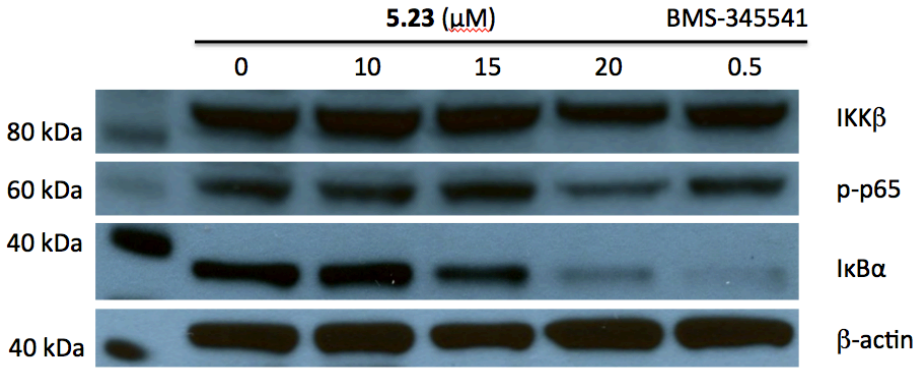

Figure 5-4. Western blot analysis of 5.23 in the NF-κB signaling pathway.

Graph 5-3. Kinase assay

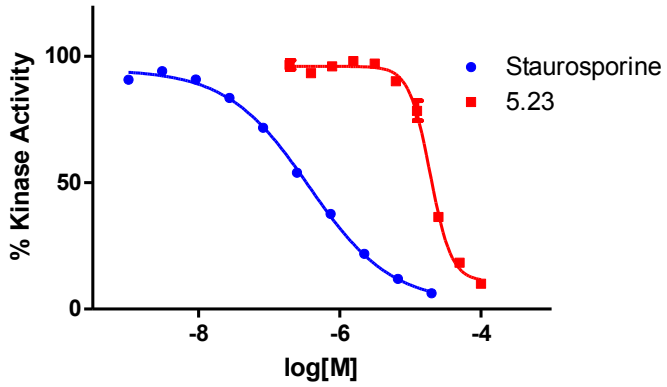

[a] Compound **5.23** was tested in 10-dose IC_{50} mode in duplicate with 2-fold serial dilution starting at 100 μM. Control compound Staurosporine was tested in 10-dose IC_{50} mode with 3-fold serial dilution starting at 20 μM. Reactions were carried out at 10 μM ATP.

To further evaluate the ability of the compound **5.23** as an IKKβ inhibitor, kinase assays of human IKKβ were performed using staurosporine, a known IKKβ inhibitor, as a control compound. The compound **5.23** was shown to have IKKβ inhibitory activity with IC_{50} value of 19.2 ± 0.5 μM (graph 5-3).

5.4 Computational simulation

After validating compound **5.23** as IKKβ inhibitor, we employed computational methods to investigate the possible binding mode of the cyclic enaminone derivatives with IKKβ. Since the crystal structure of human IKKβ is not available, the homology model of human IKKβ was generated based on the reported crystal structure of *Xenopus laevis* (African Clawed Frog)-derived IKKβ (PDB ID: 3RZF, 76% identical to human IKKβ)[90] using PRIME, a structure prediction program in the Schrodinger Suite.[91] Docking simulations of cyclic enaminone derivatives with the human IKKβ homology model were performed using Glide.[92] The docking pose of the ligand **5.23** is shown in figure 5-5, where the benzylamine moiety resides in the hydrophobic pocket (composed of amino acids Gly24, Val29, Ala42, Lys44, Val74, Met96, Ile164 and Asp166) while the *p*-methoxyphenyl and *N*-benzyl groups lie outside of the binding pocket. As shown in figure 5-6, the carbonyl group of the cyclic enaminone participates in H-bonding interaction with Gln100 and Gly101, and the olefin reinforces binding by T-π stacking (yellow dotted lines) with Tyr98.

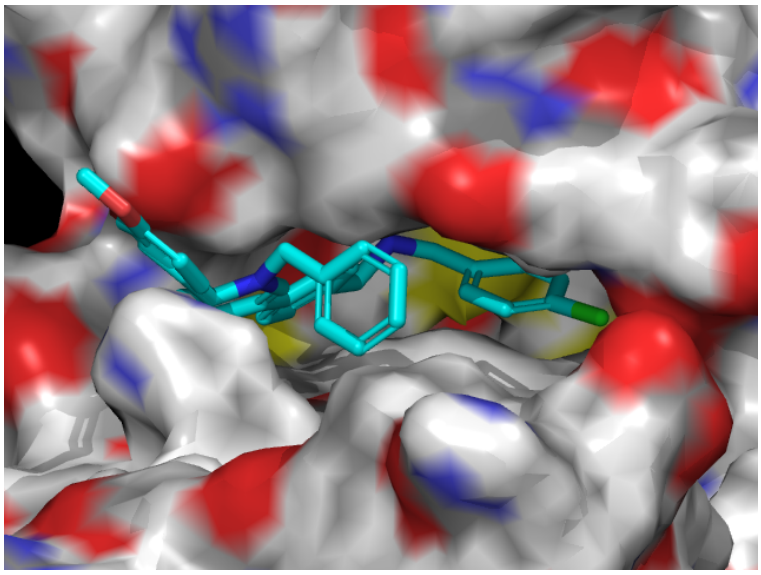

Figure 5-5. Cyclic enaminone derivative 5.23 bound to human IKKβ in the surface model.

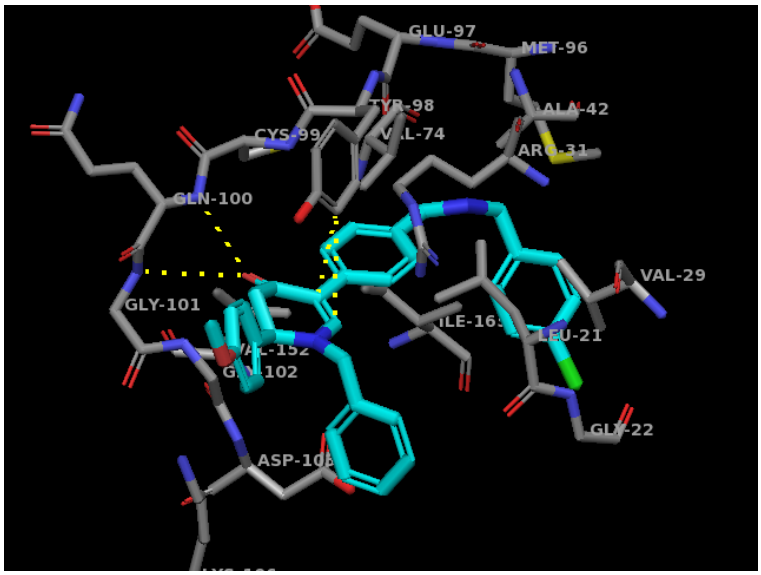

Figure 5-6. Amino acid residues interacting with 5.23 in the crystal structure.

5.5 Conclusion

In summary, novel scaffolds that incorporate cyclic enaminone motifs were designed and synthesized. Biological assays uncovered that some analogues possess IKKβ inhibitory activity. Moreover, the binding mode of these derivatives with the IKKβ was proposed using computational docking simulations following the construction of a homology model of the human IKKβ.

Chapter 6

Experimental Data

6.1 Materials and methods

All commercially available reagents and solvents were directly used without further purification. Flash column chromatography was carried out on silica gel. TLC was conducted on silica gel 250 micron, F_{254} silica gel plates. ^{1}H NMR analyses were performed on a 400 MHz spectrometer and ^{13}C NMR spectra were recorded on a 100 MHz spectrometer with complete proton decoupling. NMR spectra were processed with the MestReNova program. Chemical shifts were reported as ppm relative to chloroform ($CHCl_3$: 7.26 ppm for ^{1}H, 77.0 ppm for ^{13}C). Data are reported as follows: chemical shift, multiplicity (s = singlet, d = doublet, t = triplet, q = quartet, br = broad, m = multiplet), coupling constants (Hz) and integration. IR spectra were obtained by dissolving the sample in CH_2Cl_2 and letting the solvent evaporate on a KBr plate.

6.2 Chapter 2

6.2.1 General Procedure for C5 Arylation

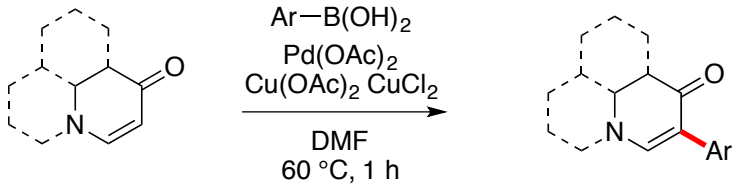

The cyclic enaminone (0.20 mmol), $Pd(OAc)_2$ (4.5 mg, 0.02 mmol), $Cu(OAc)_2$ (73 mg, 0.40 mmol) and $CuCl_2$ (54 mg, 0.40 mmol,) were combined in DMF (1.0 mL) under N_2 and stirred for 5 min (Note: Solvents were used without purification or degassing). The resulting solution was heated to 60 °C and the arylboronic acid (0.40 mmol) was added in one portion. After stirring for 1 h the reaction mixture was cooled to room temperature and diluted with EtOAc (5 mL). The precipitate was filtered through Celite using EtOAc as the eluent. The filtrate was concentrated and purified by flash column chromatography on silica gel using hexanes and an increasing proportion of EtOAc as eluent.

6.2.2 Compounds characterization

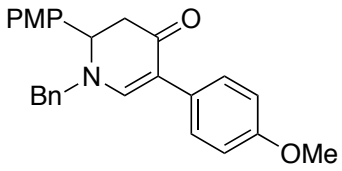

1-Benzyl-2,5-bis(4-methoxyphenyl)-2,3-dihydropyridin-4(1*H*)-one (2.1):

Compound **2.1** was prepared by the general procedure described above and 65 mg (81%) was isolated as light yellow oil. ^{1}H NMR (400 MHz, $CDCl_3$) δ 7.46 (s, 1H), 7.39–7.31 (m, 5H), 7.22–7.14 (m, 4H), 6.92–6.85 (m, 4H), 4.51 (dd, J = 8.6, 6.8 Hz, 1H), 4.38 (d, J = 15.1 Hz, 1H), 4.18 (d, J = 15.1 Hz, 1H), 3.81 (s, 3H), 3.80 (s, 3H),

2.92 (dd, J = 16.2, 6.7 Hz, 1H), 2.82 (dd, J = 16.2, 8.7 Hz, 1H); ^{13}C NMR (100 MHz, $CDCl_3$) δ 188.2, 159.6, 157.9, 152.7, 136.1, 130.6, 129.0, 128.9, 128.6, 128.4, 128.2, 127.7, 114.3, 113.7, 111.1, 60.4, 57.2, 55.3, 44.5; FTIR (KBr, cm^{-1}) 3030, 2932, 2835, 1634, 1594, 1440, 1357, 1302, 1246, 1177, 1124, 1033, 837, 735, 699; HRMS (ESI, TOF) *m/e* calculated for $[M+H]^+$ $C_{26}H_{26}NO_3$: 400.1913, found 400.1902.

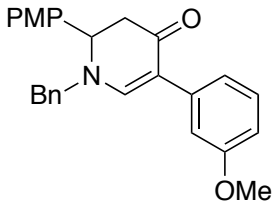

1-Benzyl-5-(3-methoxyphenyl)-2-(4-methoxyphenyl)-2,3-dihydropyridin-4(1H)-one (2.2):

Compound **2.2** was prepared by the general procedure described above and 64 mg (81%) was isolated as light yellow oil. ^{1}H NMR (400 MHz, $CDCl_3$) δ 7.55 (s, 1H), 7.40–7.30 (m, 3H), 7.26–7.13 (m, 5H), 7.09–7.06 (m, 1H), 7.01 (d, J = 7.7 Hz, 1H), 6.90–6.83 (m, 2H), 6.78–6.71 (m, 1H), 4.51 (dd, J = 7.9, 7.1 Hz, 1H), 4.40 (d, J = 15.1 Hz, 1H), 4.20 (d, J = 15.1 Hz, 1H), 3.81 (s, 3H), 3.80 (s, 3H), 2.94 (dd, J = 16.2, 6.8 Hz, 1H), 2.81 (dd, J = 16.2, 8.3 Hz, 1H); ^{13}C NMR (100 MHz, $CDCl_3$) δ 187.7, 159.6, 159.4, 153.2, 137.5, 135.8, 130.3, 129.0, 128.9, 128.3, 128.2, 127.7, 119.8, 114.4, 113.3, 111.3, 110.8, 60.2, 57.4, 55.3, 55.2, 44.5; FTIR (KBr, cm^{-1}) 3030, 2957, 2835, 1635, 1594, 1511, 1453, 1357, 1253, 1178, 1121, 1036, 833, 734, 699; HRMS (ESI, TOF) *m/e* calculated for $[M+H]^+$ $C_{26}H_{26}NO_3$: 400.1913, found 400.1901.

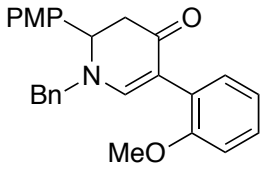

1-Benzyl-5-(2-methoxyphenyl)-2-(4-methoxyphenyl)-2,3-dihydropyridin-4(1*H*)-one (2.3):

Compound **2.3** was prepared by the general procedure described above and 41 mg (51%) was isolated as a light yellow solid (mp 102–105 °C). ^{1}H NMR (400 MHz, $CDCl_3$) δ 7.52 (s, 1H), 7.38–7.30 (m, 4H), 7.26–7.17 (m, 5H), 6.99–6.85 (m, 4H), 4.53 (dd, *J* = 9.0, 6.8 Hz, 1H), 4.34 (d, *J* = 15.1 Hz, 1H), 4.14 (d, *J* = 15.1 Hz, 1H), 3.82 (s, 3H), 3.81 (s, 3H), 2.91 (dd, *J* = 16.2, 6.8 Hz, 1H), 2.84 (dd, *J* = 16.1, 9.1 Hz, 1H); ^{13}C NMR (100 MHz, $CDCl_3$) δ 187.8, 159.6, 157.1, 155.2, 136.1, 132.0, 130.8, 128.8, 128.6, 128.1, 127.8, 127.6, 124.9, 120.6, 114.3, 111.4, 107.4, 60.6, 57.2, 55.7, 55.3, 44.5; FTIR (KBr, cm^{-1}) 3030, 2932, 2835, 1634, 1593, 1512, 1455, 1376, 1306, 1250, 1178, 1129, 1029, 836, 753, 699; HRMS (ESI, TOF) *m/e* calculated for $[M+H]^+$ $C_{26}H_{26}NO_3$: 400.1913, found 400.1898.

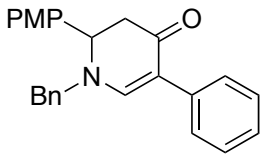

1-Benzyl-2-(4-methoxyphenyl)-5-phenyl-2,3-dihydropyridin-4(1*H*)-one (2.4):

Compound **2.4** was prepared by the general procedure described above and 59 mg (80%) was isolated as light yellow oil. ^{1}H NMR (400 MHz, $CDCl_3$) δ 7.53 (s, 1H), 7.46–7.42 (m, 2H), 7.39–7.29 (m, 5H), 7.23–7.14 (m, 5H), 6.90–6.85 (m, 2H), 4.52 (dd, *J* = 8.2, 6.9 Hz, 1H), 4.40 (d, *J* = 15.1 Hz, 1H), 4.20 (d, *J* = 15.1 Hz, 1H), 3.81 (s,

3H), 2.95 (dd, J = 16.2, 6.8 Hz, 1H), 2.82 (dd, J = 16.2, 8.4 Hz, 1H); ^{13}C NMR (100 MHz, $CDCl_3$) δ 187.9, 159.6, 153.1, 136.1, 135.9, 130.5, 129.0, 128.4, 128.3, 128.2, 127.7, 127.7, 125.8, 114.4, 111.3, 60.4, 57.4, 55.3, 44.5; FTIR (KBr, cm^{-1}) 3030, 2918, 2836, 1635, 1595, 1512, 1452, 1375, 1358, 1304, 1251, 1178, 1124, 1030, 699; HRMS (ESI, TOF) *m/e* calculated for $[M+H]^+$ $C_{25}H_{24}NO_2$: 370.1807, found 370.1810.

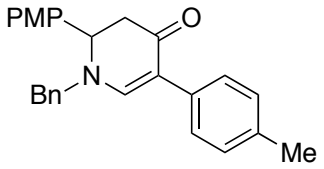

1-Benzyl-2-(4-methoxyphenyl)-5-(*p*-tolyl)-2,3-dihydropyridin-4(1*H*)-one (2.5):

Compound **2.5** was prepared by the general procedure described above and 58 mg (75%) was isolated as a light yellow solid (mp 88–90 °C). ^{1}H NMR (400 MHz, $CDCl_3$) δ 7.49 (s, 1H), 7.38–7.29 (m, 5H), 7.22–7.12 (m, 6H), 6.90–6.84 (m, 2H), 4.51 (dd, J = 8.5, 6.8 Hz, 1H), 4.39 (d, J = 15.1 Hz, 1H), 4.18 (d, J = 15.1 Hz, 1H), 3.81 (s, 3H), 2.93 (dd, J = 16.2, 6.7 Hz, 1H), 2.82 (dd, J = 16.2, 8.6 Hz, 1H), 2.33 (s, 3H); ^{13}C NMR (100 MHz, $CDCl_3$) δ 188.0, 159.6, 152.9, 136.0, 135.4, 133.1, 130.6, 129.0, 128.9, 128.4, 128.2, 127.7, 127.6, 114.4, 111.4, 60.5, 57.3, 55.3, 44.6, 21.1; FTIR (KBr, cm^{-1}) 3028, 2919, 1637, 1595, 1512, 1440, 1357, 1303, 1252, 1178, 1122, 1032, 836, 810, 699; HRMS (ESI, TOF) *m/e* calculated for $[M+H]^+$ $C_{26}H_{26}NO_2$: 384.1964, found 384.1964.

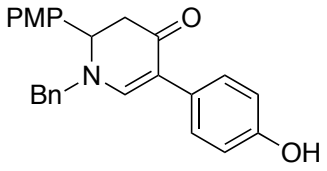

1-Benzyl-5-(4-hydroxyphenyl)-2-(4-methoxyphenyl)-2,3-dihydropyridin-4(1H)-one (2.6):

Compound **2.6** was prepared by the general procedure described above and 48 mg (62%) was isolated as colorless oil. ^{1}H NMR (400 MHz, $CDCl_3$) δ 7.46 (s, 1H), 7.39–7.29 (m, 3H), 7.28–7.26 (m, 1H), 7.25 (d, *J* = 2.9 Hz, 1H), 7.22–7.13 (m, 4H), 6.93–6.85 (m, 2H), 6.80–6.74 (m, 2H), 5.39 (s, 1H), 4.51 (dd, *J* = 8.6, 6.8 Hz, 1H), 4.38 (d, *J* = 15.1 Hz, 1H), 4.18 (d, *J* = 15.1 Hz, 1H), 3.81 (s, 3H), 2.93 (dd, *J* = 16.3, 6.8 Hz, 1H), 2.82 (dd, *J* = 16.3, 8.7 Hz, 1H); ^{13}C NMR (100 MHz, $CDCl_3$) δ 188.4, 159.6, 154.2, 153.1, 136.0, 130.4, 129.2, 129.0, 128.4, 128.3, 128.2, 127.7, 115.3, 114.4, 111.3, 60.4, 57.3, 55.4, 44.4; FTIR (KBr, cm^{-1}) 3326, 1606, 1566, 1511, 1370, 1294, 1248, 1129, 1031, 957, 823, 731, 695, 612, 585; HRMS (ESI, TOF) m/e calculated for $[M+H]^+$ $C_{26}H_{24}NO_3$: 398.1756, found 398.1747.

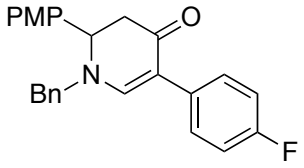

1-Benzyl-5-(4-fluorophenyl)-2-(4-methoxyphenyl)-2,3-dihydropyridin-4(1*H*)-one (2.7):

Compound **2.7** was prepared by the general procedure described above and 66 mg (85%) was isolated as a yellow solid (mp 131–134 °C). ^{1}H NMR (400 MHz, $CDCl_3$)

δ 7.48 (s, 1H), 7.43–7.30 (m, 5H), 7.22–7.13 (m, 4H), 7.06–6.97 (m, 2H), 6.91–6.85 (m, 2H), 4.52 (dd, *J* = 8.2, 6.9 Hz, 1H), 4.40 (d, *J* = 15.1 Hz, 1H), 4.20 (d, *J* = 15.1 Hz, 1H), 3.81 (s, 3H), 2.94 (dd, *J* = 16.3, 6.8 Hz, 1H), 2.81 (dd, *J* = 16.3, 8.4 Hz, 1H); ^{13}C NMR (100 MHz, $CDCl_3$) δ 187.9, 161.2 (d, *J* = 244.3 Hz), 159.7, 152.9, 135.9, 132.0 (d, *J* = 3.2 Hz), 130.3, 129.2 (d, *J* = 7.7 Hz), 128.7 (d, *J* = 63.5 Hz), 128.4, 127.7, 115.1, 114.9, 114.4, 110.4, 60.4, 57.4, 55.3, 44.4; ^{19}F NMR (376 MHz, $CDCl_3$) δ -117.3; FTIR (KBr, cm^{-1}) 3031, 2931, 2837, 1634, 1595, 1509, 1441, 1357, 1295, 1252, 1178, 1123, 1032, 840, 735, 699; HRMS (ESI, TOF) *m/e* calculated for $[M+H]^+$ $C_{25}H_{23}FNO_2$: 388.1713, found 388.1704.

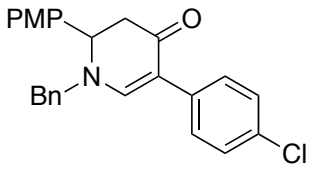

1-Benzyl-5-(4-chlorophenyl)-2-(4-methoxyphenyl)-2,3-dihydropyridin-4(1*H*)-one (2.8):

Compound **2.8** was prepared by the general procedure described above and 63 mg (78%) was isolated as a yellow solid (mp 129–132 °C). ^{1}H NMR (400 MHz, $CDCl_3$) δ 7.51 (s, 1H), 7.41–7.33 (m, 5H), 7.31–7.24 (m, 2H), 7.21–7.13 (m, 4H), 6.93–6.82 (m, 2H), 4.52 (t, *J* = 7.4 Hz 1H), 4.41 (d, *J* = 15.1 Hz, 1H), 4.21 (d, *J* = 15.1 Hz, 1H), 3.81 (s, 3H), 2.94 (dd, *J* = 16.3, 6.8 Hz, 1H), 2.81 (dd, *J* = 16.3, 8.2 Hz, 1H); ^{13}C NMR (100 MHz, $CDCl_3$) δ 187.7, 159.7, 152.9, 135.8, 134.6, 131.3, 130.2, 129.0, 128.8, 128.4, 128.3, 127.7, 114.5, 110.0, 60.3, 57.5, 55.3, 44.3; FTIR (KBr, cm^{-1}) 3030, 2928, 2836, 1634, 1598, 1511, 1440, 1372, 1294, 1251, 1178, 1124, 1032, 837,

735, 698; HRMS (ESI, TOF) *m/e* calculated for $[M+H]^+$ $C_{25}H_{23}ClNO_2$: 404.1417, found 404.1411.

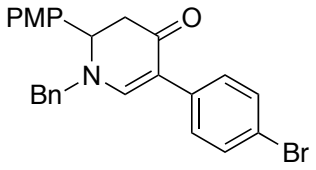

1-Benzyl-5-(4-bromophenyl)-2-(4-methoxyphenyl)-2,3-dihydropyridin-4(1*H*)-one (2.9): Compound **2.9** was prepared by the general procedure described above and 77 mg (86%) was isolated as yellow oil. ^{1}H NMR (400 MHz, $CDCl_3$) δ 7.56–7.47 (m, 1H), 7.45–7.38 (m, 2H), 7.37–7.29 (m, 5H), 7.20–7.11 (m, 4H), 6.89–6.82 (m, 2H), 4.50 (t, *J* = 7.5 Hz, 1H), 4.40 (d, *J* = 15.1 Hz, 1H), 4.20 (d, *J* = 15.1 Hz, 1H), 3.79 (s, 3H), 2.92 (dd, *J* = 16.3, 6.9 Hz, 1H), 2.78 (dd, *J* = 16.3, 8.1 Hz, 1H); ^{13}C NMR (100 MHz, $CDCl_3$) δ 187.6, 159.7, 152.9, 135.7, 135.0, 131.2, 130.2, 129.1, 129.0, 128.3, 127.7, 119.3, 114.5, 110.0, 60.3, 57.5, 55.3, 44.3; FTIR (KBr, cm^{-1}) 3030, 2932, 2835, 1634, 1596, 1511, 1440, 1356, 1294, 1252, 1178, 1123, 1032, 836, 811, 735, 698; HRMS (ESI, TOF) *m/e* calculated for $[M+H]^+$ $C_{25}H_{23}BrNO_2$: 448.0912, found 448.0898.

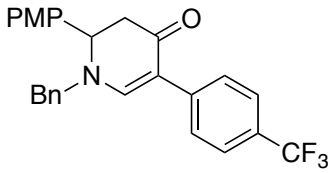

1-Benzyl-2-(4-methoxyphenyl)-5-(4-(trifluoromethyl)phenyl)-2,3-dihydropyridin-4(1*H*)-one (2.10):

Compound **2.10** was prepared by the general procedure described above and 70 mg (80%) was isolated as yellow oil. ^{1}H NMR (400 MHz, $CDCl_3$) δ 7.60 (s, 1H), 7.59–7.53 (m, 4H), 7.43–7.30 (m, 3H), 7.21–7.14 (m, 4H), 6.92–6.85 (m, 2H), 4.55 (t, *J* = 7.4 Hz, 1H), 4.45 (d, *J* = 15.1 Hz, 1H), 4.25 (d, *J* = 15.1 Hz, 1H), 3.81 (s, 3H), 2.97 (dd, *J* = 16.3, 6.9 Hz, 1H), 2.82 (dd, *J* = 16.3, 7.8 Hz, 1H); ^{13}C NMR (100 MHz, $CDCl_3$) δ 187.5, 159.8, 153.3, 139.8, 135.6, 130.1, 129.1, 128.5, 128.3, 127.7, 127.4 (q, *J* = 32.2 Hz), 127.3, 125.1 (q, *J* = 3.8 Hz), 124.5 (q, *J* = 272 Hz), 114.5, 109.6, 60.2, 57.7, 55.3, 44.3; ^{19}F NMR (376 MHz, $CDCl_3$) δ -62.8; FTIR (KBr, cm^{-1}) 3032, 2934, 2838, 1639, 1596, 1512, 1443, 1374, 1325, 1253, 1161, 1112, 1067, 847, 736, 699; HRMS (ESI, TOF) *m/e* calculated for $[M+H]^+$ $C_{26}H_{23}F_3NO_2$: 438.1681, found 438.1692

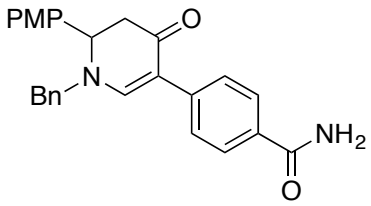

4-(1-Benzyl-6-(4-methoxyphenyl)-4-oxo-1,4,5,6-tetrahydropyridin-3-yl)benzamide (2.11):

Compound **2.11** was prepared by the general procedure described above and 61 mg (74%) was isolated as a light yellow solid (mp 194–197 °C). ^{1}H NMR (400 MHz, DMSO) δ 8.24 (s, 1H), 7.85 (s, 1H), 7.78 (d, *J* = 8.5 Hz, 2H), 7.60 (d, *J* = 8.5 Hz, 2H), 7.42–7.35 (m, 2H), 7.35–7.29 (m, 3H), 7.24 (d, *J* = 8.7 Hz, 2H), 7.21 (s, 1H), 6.92 (d, *J* = 8.7 Hz, 2H), 4.86 (d, *J* = 15.2 Hz, 1H), 4.64 (dd, *J* = 7.0, 4.9 Hz, 1H), 4.23 (d, *J* = 15.2 Hz, 1H), 3.73 (s, 3H), 2.96 (dd, *J* = 16.0, 7.3 Hz, 1H), 2.54 (dd, *J* =

16.0, 4.8 Hz, 1H); ^{13}C NMR (100 MHz, DMSO) δ 186.1, 167.8, 158.8, 154.3, 139.7, 136.9, 130.0, 129.9, 128.7, 127.8, 127.8, 127.6, 127.1, 125.7, 114.2, 107.3, 58.4, 56.8, 55.1, 43.9; FTIR (KBr, cm^{-1}) 3346, 3194, 2925, 1669, 1594, 1511, 1378, 1250, 1027, 820, 774, 734, 699; HRMS (ESI, TOF) *m/e* calculated for $[M+H]^+$ $C_{26}H_{25}N_2O_3$: 413.1865, found 413.1860.

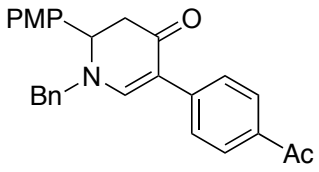

4-(1-Benzyl-6-(4-methoxyphenyl)-4-oxo-1,4,5,6-tetrahydropyridin-3-yl)benzamide (2.12):

Compound **2.12** was prepared by the general procedure described above and 67 mg (82%) was isolated as yellow oil. ^{1}H NMR (400 MHz, $CDCl_3$) δ 7.95–7.87 (m, 2H), 7.68 (s, 1H), 7.61–7.56 (m, 2H), 7.41–7.32 (m, 3H), 7.22–7.12 (m, 4H), 6.91–6.84 (m, 2H), 4.55 (t, *J* = 7.3 Hz, 1H), 4.48 (d, *J* = 15.1 Hz, 1H), 4.26 (d, *J* = 15.1 Hz, 1H), 3.81 (s, 3H), 2.98 (dd, *J* = 16.2, 7.0 Hz, 1H), 2.81 (dd, *J* = 16.2, 7.6 Hz, 1H), 2.57 (s, 3H); ^{13}C NMR (100 MHz, $CDCl_3$) δ 197.7, 187.5, 159.7, 153.5, 141.3, 135.5, 134.1, 130.0, 129.1, 128.5, 128.4, 128.3, 127.7, 126.8, 114.5, 109.6, 60.1, 57.8, 55.3, 44.3, 26.5; FTIR (KBr, cm^{-1}) 3032, 3003, 2961, 2837, 1673, 1634, 1591, 1512, 1442, 1358, 1269, 1180, 1124, 1032, 957, 844, 734, 700; HRMS (ESI, TOF) *m/e* calculated for $[M+H]^+$ $C_{27}H_{26}NO_3$: 412.1913, found 412.1913.

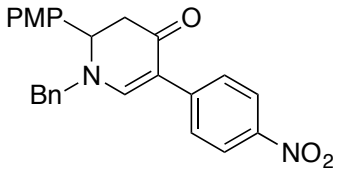

1-Benzyl-2-(4-methoxyphenyl)-5-(4-nitrophenyl)-2,3-dihydropyridin-4(1*H*)-one (2.13):

Compound **2.13** was prepared by the general procedure described above and 75 mg (90%) was isolated as a brown solid (mp 98–101 °C). ^{1}H NMR (400 MHz, $CDCl_3$) δ 8.15–8.11 (m, 2H), 7.75 (s, 1H), 7.67–7.63 (m, 2H), 7.42–7.34 (m, 3H), 7.21–7.15 (m, 4H), 6.90–6.86 (m, 2H), 4.58 (t, *J* = 7.1 Hz, 1H), 4.52 (d, *J* = 15.1 Hz, 1H), 4.30 (d, *J* = 15.1 Hz, 1H), 3.81 (s, 3H), 3.00 (dd, *J* = 16.3, 7.1 Hz, 1H), 2.81 (dd, *J* = 16.3, 7.1 Hz, 1H); ^{13}C NMR (100 MHz, $CDCl_3$) δ 187.3, 159.8, 153.8, 144.9, 143.4, 135.2, 129.7, 129.2, 128.6, 128.2, 127.7, 126.8, 123.6, 114.6, 108.4, 60.0, 58.0, 55.3, 44.1; FTIR (KBr, cm^{-1}) 3031, 2914, 2837, 1638, 1578, 1510, 1443, 1329, 1251, 1179, 1107, 1031, 854, 735, 698; HRMS (ESI, TOF) *m/e* calculated for $[M+H]^+$ $C_{25}H_{23}N_2O_4$: 415.1658, found 415.1651.

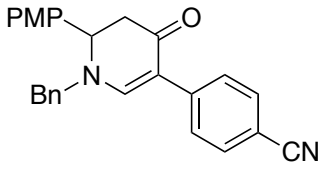

1-Benzyl-2-(4-methoxyphenyl)-5-(4-nitrophenyl)-2,3-dihydropyridin-4(1*H*)-one (2.14):

Compound **2.14** was prepared by the general procedure described above and 62 mg (78%) was isolated as yellow oil. ^{1}H NMR (400 MHz, $CDCl_3$) δ 7.65 (s, 1H), 7.62–

7.54 (m, 4H), 7.42–7.32 (m, 3H), 7.19–7.15 (m, 4H), 6.92–6.85 (m, 2H), 4.56 (t, J = 7.2 Hz, 1H), 4.48 (d, J = 15.1 Hz, 1H), 4.28 (d, J = 15.1 Hz, 1H), 3.81 (s, 3H), 2.98 (dd, J = 16.3, 7.0 Hz, 1H), 2.81 (dd, J = 16.3, 7.4 Hz, 1H); ^{13}C NMR (100 MHz, $CDCl_3$) δ 187.3, 159.8, 153.4, 141.1, 135.3, 132.0, 129.8, 129.2, 128.6, 128.2, 127.7, 127.2, 119.6, 114.6, 108.9, 108.3, 60.1, 57.9, 55.4, 44.2; FTIR (KBr, cm^{-1}) 3032, 2932, 2837, 2221, 1634, 1575, 1512, 1443, 1353, 1253, 1179, 1123, 1032, 962, 844, 735, 700; HRMS (ESI, TOF) *m/e* calculated for $[M+H]^+$ $C_{26}H_{23}N_2O_2$: 395.1760, found 395.1751.

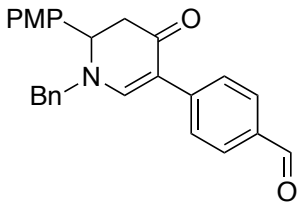

4-(1-Benzyl-6-(4-methoxyphenyl)-4-oxo-1,4,5,6-tetrahydropyridin-3-yl)benzaldehyde (2.15):

Compound **2.15** was prepared by the general procedure described above and 66 mg (83%) was isolated as yellow oil. ^{1}H NMR (400 MHz, $CDCl_3$) δ 9.94 (s, 1H), 7.85–7.76 (m, 2H), 7.71 (s, 1H), 7.68–7.65 (m, 2H), 7.42–7.32 (m, 3H), 7.22–7.13 (m, 4H), 6.92–6.85 (m, 2H), 4.56 (t, J = 7.2 Hz, 1H), 4.49 (d, J = 15.1 Hz, 1H), 4.28 (d, J = 15.1 Hz, 1H), 3.81 (s, 3H), 2.99 (dd, J = 16.2, 7.0 Hz, 1H), 2.82 (dd, J = 16.2, 7.3 Hz, 1H); ^{13}C NMR (100 MHz, $CDCl_3$) δ 191.9, 187.4, 159.8, 153.6, 142.9, 135.4, 133.5, 129.9, 129.1, 128.5, 128.3, 127.7, 127.1, 114.5, 109.4, 60.1, 57.9, 55.3, 44.3; FTIR (KBr, cm^{-1}) 3031, 2933, 2837, 1693, 1590, 1512, 1443, 1353, 1305, 1251, 1176, 1123,

1031, 833, 735, 700; HRMS (ESI, TOF) *m/e* calculated for $[M+H]^+$ $C_{26}H_{24}NO_3$: 398.1756, found 398.1747.

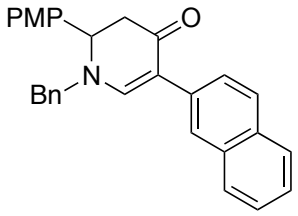

1-Benzyl-2-(4-methoxyphenyl)-5-(naphthalen-2-yl)-2,3-dihydropyridin-4(1*H*)-one (2.16):

Compound **2.16** was prepared by the general procedure described above and 70 mg (83%) was isolated as brown oil. ^{1}H NMR (400 MHz, $CDCl_3$) δ 7.89 (s, 1H), 7.79 (dd, *J* = 8.3, 5.8 Hz, 3H), 7.68–7.59 (m, 2H), 7.46–7.29 (m, 5H), 7.26–7.13 (m, 4H), 6.93–6.85 (m, 2H), 4.53 (t, *J* = 7.5 Hz, 1H), 4.43 (d, *J* = 15.2 Hz, 1H), 4.21 (d, *J* = 15.1 Hz, 1H), 3.80 (s, 3H), 2.98 (dd, *J* = 16.2, 6.8 Hz, 1H), 2.84 (dd, *J* = 16.2, 8.2 Hz, 1H); ^{13}C NMR (100 MHz, $CDCl_3$) δ 188.0, 159.6, 153.4, 135.9, 133.8, 133.7, 131.9, 130.4, 129.0, 128.4, 128.3, 127.7, 127.7, 127.5, 127.5, 126.7, 125.7, 125.3, 125.0, 114.4, 111.0, 60.3, 57.5, 55.3, 44.5; FTIR (KBr, cm^{-1}) 3054, 2960, 2836, 1635, 1592, 1511, 1441, 1360, 1303, 1251, 1178, 1107, 1032, 818, 734, 699; HRMS (ESI, TOF) *m/e* calculated for $[M+H]^+$ $C_{29}H_{26}NO_2$: 420.1964, found 420.1953.

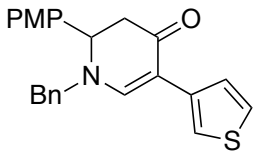

1-Benzyl-2-(4-methoxyphenyl)-5-(thiophen-3-yl)-2,3-dihydropyridin-4(1*H*)-one (2.17):

Compound **2.17** was prepared by the general procedure described above and 18 mg (24%) was isolated as yellow oil. ^{1}H NMR (400 MHz, $CDCl_3$) δ 7.69 (s, 1H), 7.60 (dd, *J* = 3.0, 1.1 Hz, 1H), 7.39–7.31 (m, 3H), 7.27 (dd, *J* = 5.0, 3.0 Hz, 1H), 7.22 (dd, *J* = 5.0, 1.1 Hz, 1H), 7.20–7.14 (m, 4H), 6.90–6.84 (m, 2H), 4.50 (t, *J* = 7.5 Hz, 1H), 4.42 (d, *J* = 15.1 Hz, 1H), 4.21 (d, *J* = 15.1 Hz, 1H), 3.81 (s, 3H), 2.94 (dd, *J* = 16.3, 6.9 Hz, 1H), 2.80 (dd, *J* = 16.3, 8.2 Hz, 1H); ^{13}C NMR (100 MHz, $CDCl_3$) δ 187.8, 159.6, 152.3, 135.9, 130.3, 129.0, 128.4, 128.3, 127.7, 125.6, 124.5, 118.9, 114.4, 106.9, 60.2, 57.5, 55.3, 44.3; FTIR (KBr, cm^{-1}) 3030, 2925, 2853, 1598, 1511, 1440, 1296, 1252, 1178, 1112, 1031, 838, 783, 734, 699; HRMS (ESI, TOF) *m/e* calculated for $[M+H]^+$ $C_{23}H_{22}NO_2S$: 376.1371, found 376.1370.

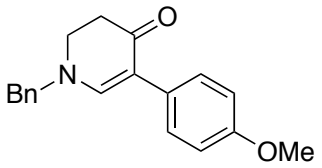

1-Benzyl-5-(4-methoxyphenyl)-2,3-dihydropyridin-4(1*H*)-one (2.19):

Compound **2.19** was prepared by the general procedure described above and 41 mg (70%) was isolated as yellow oil. Spectral data of the title compound was identical to that in our previous report.[13]

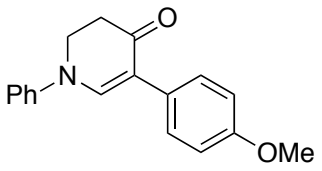

5-(4-Methoxyphenyl)-1-phenyl-2,3-dihydropyridin-4(1H)-one (2.20):

Compound **2.20** was prepared by the general procedure described above and 34 mg (60%) was isolated as a brown solid (mp 129–132 °C). ^{1}H NMR (400 MHz, $CDCl_3$) δ 7.59 (s, 1H), 7.42–7.31 (m, 4H), 7.18–7.10 (m, 3H), 6.91–6.85 (m, 2H), 4.06 (t, *J* = 7.6 Hz, 2H), 3.79 (s, 3H), 2.79 (t, *J* = 7.6 Hz, 2H); ^{13}C NMR (100 MHz, $CDCl_3$) δ 189.7, 158.3, 147.7, 145.2, 129.7, 129.3, 128.2, 124.2, 118.0, 114.4, 113.7, 55.3, 47.6, 36.6; FTIR (KBr, cm^{-1}) 3052, 2952, 2835, 1645, 1583, 1510, 1386, 1302, 1243, 1178, 1130, 1029, 831, 760, 698; HRMS (ESI, TOF) *m/e* calculated for $[M+H]^+$ $C_{18}H_{18}NO_2$: 280.1338, found 280.1339.

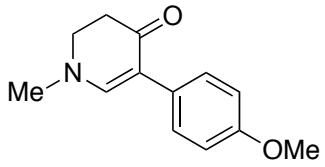

5-(4-Methoxyphenyl)-1-methyl-2,3-dihydropyridin-4(1*H*)-one (2.21):

Compound **2.21** was prepared by the general procedure described above and 28 mg (65%) was isolated as yellow oil. Spectral data of the title compound was identical to that in our previous report.[13]

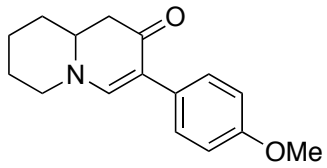

3-(4-Methoxyphenyl)-7,8,9,9a-tetrahydro-1*H*-quinolizin-2(6*H*)-one (2.22):

Compound **2.22** was prepared by the general procedure described above and 42 mg (82%) was isolated as a pale yellow solid. Spectral data of the title compound was identical to that in our previous report.[13]

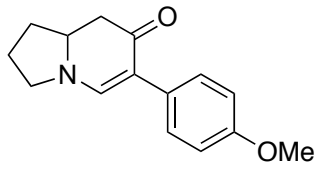

6-(4-Methoxyphenyl)-2,3,8,8a-tetrahydroindolizin-7(1H)-one (2.23): Compound **2.23** was prepared by the general procedure described above and 27 mg (56%) was isolated as a pale yellow solid. Spectral data of the title compound was identical to that in our previous report.[13]

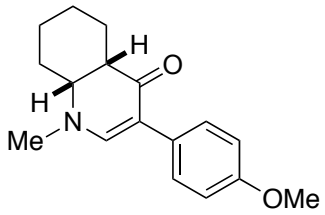

(*cis*)-3-(4-Methoxyphenyl)-1-methyl-4a,5,6,7,8,8a-hexahydroquinolin-4(1*H*)-one (2.24):

Compound **2.24** was prepared by the general procedure described above and 41 mg (76%) was isolated as colorless oil. Spectral data of the title compound was identical to that in our previous report.[13]

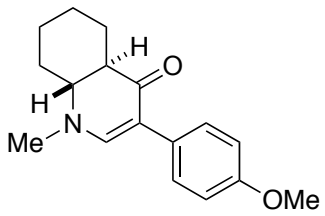

(*trans*)-3-(4-Methoxyphenyl)-1-methyl-4a,5,6,7,8,8a-hexahydroquinolin-4(1*H*)-one (2.25):

Compound **2.25** was prepared by the general procedure described above and 45 mg (83%) was isolated as a pale yellow solid. Spectral data of the title compound was identical to that in our previous report.[13]

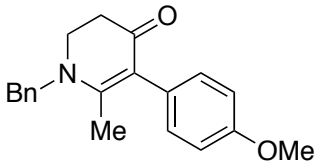

1-Benzyl-5-(4-methoxyphenyl)-6-methyl-2,3-dihydropyridin-4(1H)-one (2.28):

Compound **2.28** was prepared by the general procedure described above and 38 mg (61%) was isolated as a yellow solid (mp 92–95 °C). ^{1}H NMR (400 MHz, $CDCl_3$) δ 7.43–7.36 (m, 2H), δ 7.34–7.30 (m, 1H), 7.27–7.22 (m, 2H), 7.09–7.04 (m, 2H), 6.90–6.85 (m, 2H), 4.58 (s, 2H), 3.79 (s, 3H), 3.56 (t, J = 7.6 Hz, 2H), 2.57 (t, J = 7.6 Hz, 2H), 1.96 (s, 3H); ^{13}C NMR (100 MHz, $CDCl_3$) δ 189.2, 159.9, 158.0, 137.0, 132.7, 129.8, 129.0, 127.8, 126.4, 113.6, 113.4, 55.3, 55.2, 48.8, 36.1, 18.6; FTIR (KBr, cm^{-1}) 3030, 2959, 2834, 1621, 1538, 1469, 1297, 1240, 1160, 1098, 1028, 835, 732, 698; HRMS (ESI, TOF) *m/e* calculated for $[M+H]^+$ $C_{20}H_{22}NO_2$: 308.1610, found 308.1630.

6.3 Chapter 3

6.3.1 General procedures

Method A: Metal-free arylation

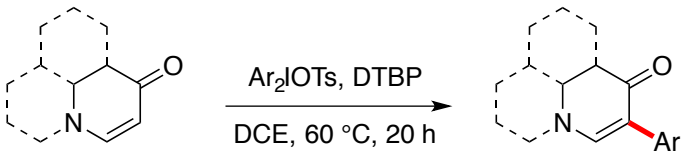

2,6-Di-tert-butylpyridine (1.2 equiv – 1.5 equiv) diaryliodonium salt (1.2 equiv – 1.5 equiv) were added to a solution of the cyclic enaminone (1 equiv) in DCE (0.2M) and the reaction was stirred at 60 °C for 20 h. The reaction mixture was diluted with DCM and washed with satd. $NaHCO_3$. The aqueous layer was further extracted with DCM and the combined organic layer was dried ($MgSO_4$), and evaporated in vacuo. The crude product was purified by flash column chromatography on silica gel using hexanes and an increasing proportion of EtOAc as eluent.

Method B: Copper-catalyzed arylation

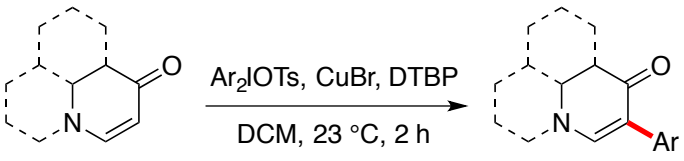

2,6-Di-tert-butylpyridine (1.2 equiv – 1.5 equiv) diaryliodonium salt (1.2 equiv – 1.5 equiv) and CuBr (10 mol %) were added to a solution of the cyclic enaminone (1

equiv) in DCM (0.2M) and the reaction was stirred at 23 °C for 2 h. The reaction mixture was diluted with DCM and washed with satd. $NaHCO_3$. The aqueous layer was further extracted with DCM and the combined organic layer was dried ($MgSO_4$), and evaporated in vacuo. The crude product was purified by flash column chromatography on silica gel using hexanes and an increasing proportion of EtOAc as eluent.

6.3.2 Compounds characterization

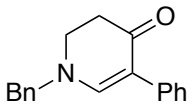

1-Benzyl-5-phenyl-2,3-dihydropyridin-4(1*H*)-one (3.1):

Compound **3.1** was prepared by the general procedure described above and was isolated as colorless oil (Method A: 57%, Method B: 79%). Spectral data of the title compound was identical to that in our previous report.[13]

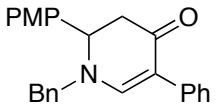

1-Benzyl-2-(4-methoxyphenyl)-5-phenyl-2,3-dihydropyridin-4(1*H*)-one (3.2):

Compound **3.2** was prepared by the general procedure described above and was isolated as yellow oil (Method A: 54%, Method B: 87%). Spectral data of the title compound was identical to that of compound **2.4**.

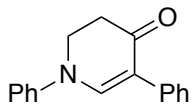

1,5-Diphenyl-2,3-dihydropyridin-4(1*H*)-one (3.3):

Compound **3.3** was prepared by the general procedure described above and was isolated as brown solid (Method A: 53%, Method B: 76%, mp: 113–115 °C). ^{1}H NMR (400 MHz, $CDCl_3$) δ 7.65 (s, 1H), 7.45 – 7.37 (m, 4H), 7.33 (t, *J* = 7.6 Hz, 2H), 7.26 – 7.12 (m, 4H), 4.09 (t, *J* = 7.5 Hz, 2H), 2.81 (t, *J* = 7.5 Hz, 2H); ^{13}C NMR (101 MHz, $CDCl_3$) δ 189.4, 148.3, 145.2, 135.8, 129.7, 128.2, 128.1, 126.3, 124.4, 118.2, 114.6, 47.7, 36.6; FTIR (KBr, cm^{-1}) 3052, 1644, 1582, 1493, 1303, 1129, 755, 696; HRMS (ESI, TOF) *m/e* calculated for $[M+Na]^+$ $C_{17}H_{15}NNaO$: 272.1046, found 272.1042.

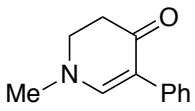

1-Methyl-5-phenyl-2,3-dihydropyridin-4(1*H*)-one (3.4):

Compound **3.4** was prepared by the general procedure described above and was isolated as yellow oil (Method A: 51%, Method B: 63%). ^{1}H NMR (400 MHz, $CDCl_3$) δ 7.40 – 7.35 (m, 2H), 7.32 – 7.25 (m, 2H), 7.20 (s, 1H), 7.18 – 7.13 (m, 1H), 3.49 (t, *J* = 7.9 Hz, 2H), 3.10 (s, 3H), 2.64 (t, *J* = 7.8 Hz, 2H); ^{13}C NMR (101 MHz, $CDCl_3$) δ 188.2, 154.0, 136.4, 128.1, 127.7, 125.6, 110.9, 49.1, 43.4, 36.2; FTIR (KBr, cm^{-1}) 2903, 1628, 1599, 1384, 1298, 1212, 1138, 756, 698; HRMS (ESI, TOF) *m/e* calculated for $[M+Na]^+$ $C_{12}H_{13}NNaO$: 210.0889, found 210.0892.

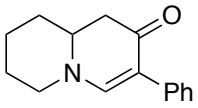

3-Phenyl-1,6,7,8,9,9a-hexahydro-2*H*-quinolizin-2-one (3.5):

Compound **3.5** was prepared by the general procedure described above and was isolated as yellow solid (Method A: 53%, Method B: 72%, mp: 115–118 °C). ^{1}H NMR (400 MHz, $CDCl_3$) δ 7.41 – 7.36 (m, 2H), 7.33 – 7.26 (m, 2H), 7.20 – 7.14 (m, 1H), 7.12 (s, 1H), 3.50 – 3.34 (m, 2H), 3.06 (td, *J* = 12.7, 3.0 Hz, 1H), 2.62 (dd, *J* = 16.2, 5.4 Hz, 1H), 2.51 (dd, *J* = 16.2, 13.2 Hz, 1H), 1.93 – 1.75 (m, 3H), 1.71 – 1.34 (m, 3H); ^{13}C NMR (101 MHz, $CDCl_3$) δ 189.5, 153.9, 136.0, 128.1, 127.7, 125.7, 112.2, 57.2, 53.2, 43.9, 31.7, 25.7, 23.1; FTIR (KBr, cm^{-1}) 2933, 1626, 1592, 1383, 1248, 1130, 978, 756, 700; HRMS (ESI, TOF) *m/e* calculated for $[M+Na]^+$ $C_{15}H_{17}NNaO$: 250.1202, found 250.1200.

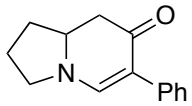

6-Phenyl-2,3,8,8a-tetrahydroindolizin-7(1*H*)-one (3.6):

Compound **3.6** was prepared by the general procedure described above and was isolated as light yellow solid (Method A: 45%, Method B: 67%, mp: 92–95 °C). ^{1}H NMR (400 MHz, $CDCl_3$) δ 7.45 (s, 1H), 7.42 – 7.37 (m, 2H), 7.32 – 7.25 (m, 2H), 7.17 – 7.11 (m, 1H), 3.86 (ddt, *J* = 15.9, 10.7, 5.5 Hz, 1H), 3.69 – 3.51 (m, 2H), 2.60 (dd, *J* = 15.7, 5.1 Hz, 1H), 2.51 (t, *J* = 15.8 Hz, 1H), 2.38 – 2.27 (m, 1H), 2.19 – 2.08 (m, 1H), 2.04 – 1.89 (m, 1H), 1.80 – 1.70 (m, 1H); ^{13}C NMR (101 MHz, $CDCl_3$) δ 188.9, 149.1, 136.8, 128.1, 127.5, 125.3, 109.9, 57.9, 49.9, 42.3, 33.0, 24.4; FTIR

(KBr, cm^{-1}) 2874, 1586, 1408, 1297, 1131, 761, 697; HRMS (ESI, TOF) *m/e* calculated for $[M+Na]^+$ $C_{14}H_{15}NNaO$: 236.1046, found 236.1042.

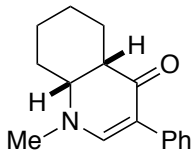

***Cis*-1-methyl-3-phenyl-4a,5,6,7,8,8a-hexahydroquinolin-4(1*H*)-one (*cis*-3.7):**

Compound ***cis*-3.7** was prepared by the general procedure described above and was isolated as yellow oil (Method A: 41%, Method B: 73%). ^1H NMR (400 MHz, $CDCl_3$) δ 7.44 – 7.36 (m, 2H), 7.31 – 7.25 (m, 2H), 7.17 – 7.11 (m, 2H), 3.48 (ddd, *J* = 9.0, 5.7, 3.3 Hz, 1H), 3.11 (s, 3H), 2.78 (d, *J* = 5.1 Hz, 1H), 2.30 (br, 1H), 1.98 – 1.80 (m, 1H), 1.77 – 1.60 (m, 2H), 1.55 – 1.31 (m, 4H); ^{13}C NMR (101 MHz, $CDCl_3$) δ 190.5, 152.3, 136.6, 128.0, 127.6, 125.3, 109.5, 60.2, 45.6, 40.8, 24.4, 23.8, 23.5, 22.8; FTIR (KBr, cm^{-1}) 2932, 1709, 1600, 1447, 1277, 1072, 698; HRMS (ESI, TOF) *m/e* calculated for $[M+Na]^+$ $C_{16}H_{19}NNaO$: 264.1359, found 264.1361.

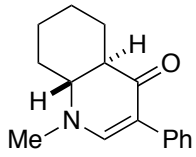

***Trans*-1-methyl-3-phenyl-4a,5,6,7,8,8a-hexahydroquinolin-4(1*H*)-one (*trans*-3.7):**

2,6-Di-tert-butylpyridine (1.2 equiv) diphenyliodonium tosylate (1.2 equiv) and CuBr (10 mol %) were added to a solution of the cyclic enaminone (1 equiv) in DCM (0.2M) at 0 °C, and the reaction was stirred for 3 h. The reaction mixture was diluted

with DCM and washed with satd. $NaHCO_3$. The aqueous layer was further extracted with DCM and the combined organic layer was dried ($MgSO_4$), and evaporated in vacuo. Purification by flash column chromatography on silica gel using hexanes and an increasing proportion of EtOAc as eluent afforded compound ***trans*-3.7** as yellow solid (89%, mp: 118–120 °C). ^{1}H NMR (400 MHz, $CDCl_3$) δ 7.42 – 7.37 (m, 2H), 7.29 (t, *J* = 7.7 Hz, 2H), 7.23 (s, 1H), 7.18 – 7.13 (m, 1H), 3.13 (ddd, *J* = 15.1, 11.4, 4.0 Hz, 1H), 3.03 (s, 3H), 2.49 (dt, *J* = 14.0, 2.7 Hz, 1H), 2.31 – 2.16 (m, 2H), 1.95 – 1.77 (m, 2H), 1.51 – 1.37 (m, 1H), 1.38 – 1.07 (m, 3H); ^{13}C NMR (101 MHz, $CDCl_3$) δ 190.9, 154.2, 136.5, 128.0, 127.7, 125.5, 111.1, 61.9, 48.7, 39.7, 30.4, 24.9, 24.4; FTIR (KBr, cm^{-1}) 2926, 1632, 1598, 1403, 1306, 1154, 1069, 697; HRMS (ESI, TOF) *m/e* calculated for $[M+Na]^+$ $C_{16}H_{19}NNaO$: 264.1359, found 264.1362.

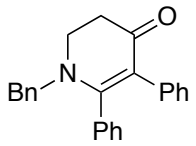

1-Benzyl-5,6-diphenyl-2,3-dihydropyridin-4(1*H*)-one (3.8):

Compound **3.8** was prepared by the general procedure described above and was isolated as yellow oil (Method A: 22%, Method B: 38%). ^{1}H NMR (400 MHz, $CDCl_3$) δ 7.41 – 7.26 (m, 3H), 7.27 – 7.20 (m, 2H), 7.21 – 7.10 (m, 5H), 7.07 – 7.01 (m, 2H), 7.00 – 6.90 (m, 3H), 4.30 (s, 2H), 3.72 (dd, *J* = 8.2, 6.7 Hz, 2H), 2.59 (dd, *J* = 8.2, 6.7 Hz, 2H); ^{13}C NMR (101 MHz, $CDCl_3$) δ 190.0, 162.8, 137.5, 136.4, 134.9, 132.0, 129.3, 128.9, 128.7, 128.2, 127.8, 127.2, 125.4, 114.7, 55.9, 47.4, 35.8; FTIR (KBr, cm^{-1}) 3058, 1626, 1528, 1454, 1233, 1121, 756, 698; HRMS (ESI, TOF) *m/e*

calculated for $[M+Na]^+$ $C_{24}H_{21}NNaO$: 362.1515, found 362.1514.

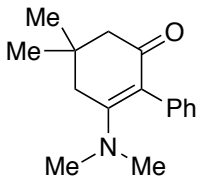

6-(Dimethylamino)-4,4-dimethyl-4,5-dihydro-[1,1'-biphenyl]-2(3*H*)-one (3.9):

Compound **3.9** was prepared by the general procedure described above and was isolated as light yellow solid (Method A: 20%, Method B: 0%, mp: 78–80 °C). ^{1}H NMR (400 MHz, $CDCl_3$) δ 7.31 – 7.25 (m, 2H), 7.17 – 7.10 (m, 3H), 2.67 (s, 6H), 2.47 (s, 2H), 2.31 (s, 2H), 1.13 (s, 6H); ^{13}C NMR (101 MHz, $CDCl_3$) δ 194.5, 162.5, 138.6, 131.5, 127.6, 125.6, 112.8, 50.4, 43.7, 42.9, 31.0, 28.7; FTIR (KBr, cm^{-1}) 3431, 2954, 1559, 1410, 1285, 1152, 803, 615; HRMS (ESI, TOF) *m/e* calculated for $[M+Na]^+$ $C_{16}H_{21}NNaO$: 266.1515, found 266.1511.

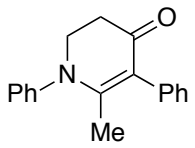

6-Methyl-1,5-diphenyl-2,3-dihydropyridin-4(1*H*)-one (3.10):

Compound **3.10** was prepared by the general procedure described above and was isolated as yellow oil (Method A: 49%, Method B: 64%). ^{1}H NMR (400 MHz, $CDCl_3$) δ 7.46 – 7.40 (m, 2H), 7.38 – 7.29 (m, 3H), 7.27 – 7.15 (m, 5H), 3.94 (dd, J = 8.1, 6.7 Hz, 2H), 2.76 – 2.70 (t, J = 8.2 Hz, 2H), 1.69 (s, 3H); ^{13}C NMR (101 MHz, $CDCl_3$) δ 189.6, 158.8, 145.3, 137.0, 131.5, 129.6, 128.1, 127.2, 126.6, 126.5, 115.7, 52.0, 36.5, 20.2; FTIR (KBr, cm^{-1}) 3054, 1634, 1546, 1493, 1310, 1156, 700; HRMS

(ESI, TOF) *m/e* calculated for $[M+Na]^+$ $C_{18}H_{17}NNaO$: 286.1202, found 286.1200.

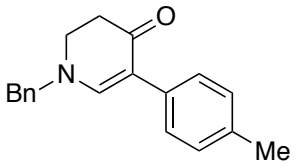

1-Benzyl-5-(*p*-tolyl)-2,3-dihydropyridin-4(1*H*)-one (3.12):

Compound **3.12** was prepared by the general procedure described above and was isolated as yellow oil (Method A: 74%, Method B: 86%). Spectral data of the title compound was identical to that in our previous report.[13]

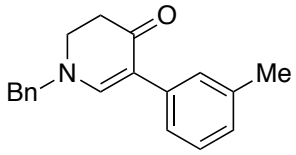

1-Benzyl-5-(*m*-tolyl)-2,3-dihydropyridin-4(1*H*)-one (3.13):

Compound **3.13** was prepared by the general procedure described above and was isolated as yellow oil (Method A: 76%, Method B: 91%). ^{1}H NMR (400 MHz, $CDCl_3$) δ 7.44 – 7.27 (m, 6H), 7.27 – 7.14 (m, 3H), 7.04 – 6.97 (m, 1H), 4.43 (s, 2H), 3.44 (t, *J* = 7.8 Hz, 2H), 2.60 (t, *J* = 7.8 Hz, 2H), 2.34 (s, 3H); ^{13}C NMR (101 MHz, $CDCl_3$) δ 188.6, 153.2, 137.6, 136.2, 135.7, 129.1, 128.6, 128.4, 128.1, 127.6, 126.6, 124.9, 111.3, 60.2, 46.8, 36.4, 21.6; FTIR (KBr, cm^{-1}) 2919, 1598, 1452, 1301, 1190, 1124, 701, 511; HRMS (ESI, TOF) *m/e* calculated for $[M+Na]^+$ $C_{19}H_{19}NNaO$: 300.1359, found 300.1354.

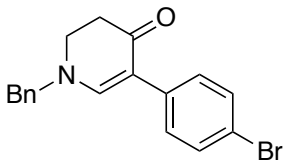

1-Benzyl-5-(4-bromophenyl)-2,3-dihydropyridin-4(1*H*)-one (3.15):

Compound **3.15** was prepared by the general procedure described above and was isolated as light yellow solid (Method A: 64%, Method B: 75%). Spectral data of the title compound was identical to that in our previous report.[13]

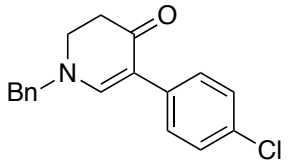

1-Benzyl-5-(4-chlorophenyl)-2,3-dihydropyridin-4(1*H*)-one (3.16):

Compound **3.16** was prepared by the general procedure described above and was isolated as yellow oil (Method A: 66%, Method B: 78%). Spectral data of the title compound was identical to that in our previous report.[13]

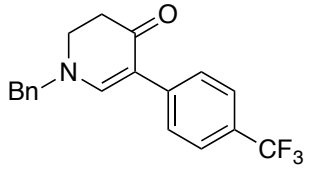

1-Benzyl-5-(4-(trifluoromethyl)phenyl)-2,3-dihydropyridin-4(1*H*)-one (3.17):

Compound **3.17** was prepared by the general procedure described above and was isolated as clear solid (Method A: 29%, Method B: 69%). Spectral data of the title compound was identical to that in our previous report.[13]

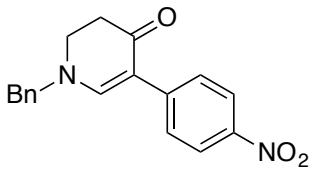

1-Benzyl-5-(4-nitrophenyl)-2,3-dihydropyridin-4(1*H*)-one (3.18):

Compound **3.18** was prepared by the general procedure described above and was isolated as light brown oil (Method A: 42%, Method B: 70%, mp: 92–95 °C). ^{1}H NMR (400 MHz, $CDCl_3$) δ 8.23 – 8.02 (m, 2H), 7.73 – 7.54 (m, 3H), 7.52 – 7.38 (m, 3H), 7.36 – 7.28 (m, 2H), 4.54 (s, 2H), 3.53 (t, *J* = 7.8 Hz, 2H), 2.63 (dd, *J* = 8.3, 7.2 Hz, 2H); ^{13}C NMR (101 MHz, $CDCl_3$) δ 187.9, 153.7, 145.1, 143.5, 134.9, 129.3, 128.8, 127.7, 127.0, 123.6, 108.6, 60.6, 46.5, 36.1; FTIR (KBr, cm^{-1}) 2918, 1635, 1599, 1505, 1331, 1226, 1108, 855, 698; HRMS (ESI, TOF) *m/e* calculated for $[M+Na]^+$ $C_{18}H_{16}N_2NaO_3$: 331.1053, found 331.1056.

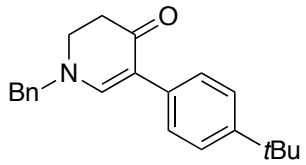

1-Benzyl-5-(4-(*tert*-butyl)phenyl)-2,3-dihydropyridin-4(1*H*)-one (3.19):

Compound **3.19** was prepared by the general procedure described above and was isolated as light yellow solid (Method A: 51%, Method B: 82%, mp: 165–169 °C). ^{1}H NMR (400 MHz, $CDCl_3$) δ 7.43 – 7.26 (m, 10H), 4.42 (s, 2H), 3.45 (t, *J* = 7.8 Hz, 2H), 2.60 (t, *J* = 7.8 Hz, 2H), 1.31 (s, 9H); ^{13}C NMR (101 MHz, $CDCl_3$) δ 188.7, 153.0, 148.5, 135.8, 133.3, 129.1, 128.4, 127.7, 127.4, 125.1, 111.2, 60.2, 46.9, 36.4, 34.4, 31.4; FTIR (KBr, cm^{-1}) 2961, 1600, 1384, 1302, 1223, 1134, 847, 702; HRMS

(ESI, TOF) *m/e* calculated for $[M+Na]^+$ $C_{22}H_{25}NNaO$: 342.1828, found 342.1822.

6.4 Chapter 4

6.4.1 General procedures

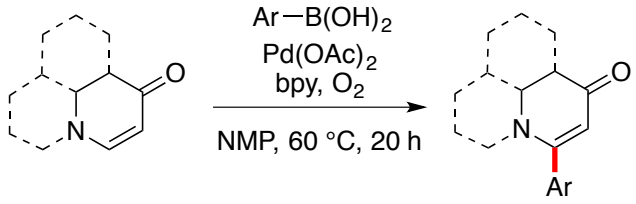

$Pd(OAc)_2$ (4.5 mg, 0.02 mmol) and 2,2'-bipyridine (3.4 mg, 0.022 mmol) in NMP (1.0 mL) were stirred for 30 min. To this solution were added the cyclic enaminone (0.20 mmol), and the arylboronic acid (0.40 mmol,), and the reaction mixture was stirred under O_2 (balloon) at 60 °C. After stirring for 6 h, another equivalent of the arylboronic acid (0.20 mmol) was added and the mixture was stirred for an additional 14 h. The reaction mixture was cooled to room temperature and the solvent was evaporated. The crude mixture was diluted with EtOAc (5 mL) and the precipitate was filtered through Celite using EtOAc as the eluent. The filtrate was concentrated and purified by flash column chromatography on silica gel using hexanes and an increasing proportion of EtOAc as eluent.

6.4.2 Compounds characterization

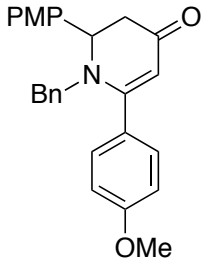

1-Benzyl-2,6-bis(4-methoxyphenyl)-2,3-dihydropyridin-4(1*H*)-one (4.3):

Compound **4.3** was prepared by the general procedure described above and 54.3 mg (68%) was isolated as yellow oil. ^{1}H NMR (400 MHz, $CDCl_3$) δ 7.45 – 7.37 (m, 2H), 7.37 – 7.26 (m, 5H), 7.18 – 7.12 (m, 2H), 7.01 – 6.79 (m, 4H), 5.18 (s, 1H), 4.80 (d, *J* = 15.7 Hz, 1H), 4.61 (dd, *J* = 7.4, 3.8 Hz, 1H), 4.02 (d, *J* = 15.6 Hz, 1H), 3.83 (s, 3H), 3.81 (s, 3H), 2.95 (dd, *J* = 16.5, 7.4 Hz, 1H), 2.60 (dd, *J* = 16.6, 3.9 Hz, 1H); ^{13}C NMR (100 MHz, $CDCl_3$) δ 190.0, 164.3, 160.7, 159.3, 137.8, 131.3, 129.3, 128.9, 128.5, 127.8, 127.8, 127.1, 114.3, 114.2, 102.9, 59.2, 55.4, 55.3, 54.0, 42.4; FTIR (KBr, cm^{-1}) 2959, 2837, 1699, 1633, 1506, 1359, 1252, 1175, 1116, 1032, 836, 733; HRMS (ESI, TOF) *m/e* calculated for $[M+H]^+$ $C_{26}H_{26}NO_3$: 400.1913, found 400.1921.

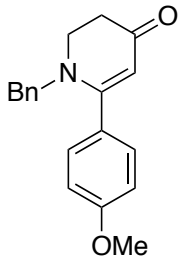

1-Benzyl-6-(4-methoxyphenyl)-2,3-dihydropyridin-4(1*H*)-one (4.5):

Compound **4.5** was prepared by the general procedure described above and 43.4 mg (74%) was isolated as brown oil. ^{1}H NMR (400 MHz, $CDCl_3$) δ 7.39 – 7.26 (m, 5H),

7.23 – 7.18 (m, 2H), 6.95 – 6.88 (m, 2H), 5.17 (s, 1H), 4.41 (s, 2H), 3.82 (s, 3H), 3.61 (t, *J* = 7.5 Hz, 2H), 2.40 (t, *J* = 7.5 Hz, 2H); ^{13}C NMR (100 MHz, $CDCl_3$) δ 192.0, 165.1, 160.8, 137.5, 129.3, 128.9, 128.1, 127.8, 127.0, 114.1, 102.7, 55.5, 55.4, 47.9, 35.5; FTIR (KBr, cm^{-1}) 2960, 2837, 1633, 1514, 1454, 1362, 1252, 1178, 1126, 1029, 839, 734, 699; HRMS (ESI, TOF) *m/e* calculated for $[M+H]^+$ $C_{19}H_{20}NO_2$: 294.1494, found 294.1489.

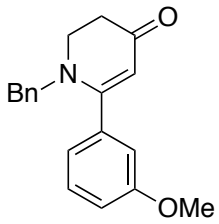

1-Benzyl-6-(3-methoxyphenyl)-2,3-dihydropyridin-4(1*H*)-one (4.6):

Compound **4.6** was prepared by the general procedure described above and 45.2 mg (77%) was isolated as yellow oil. ^{1}H NMR (400 MHz, $CDCl_3$) δ 7.38 – 7.27 (m, 4H), 7.24 – 7.19 (m, 2H), 7.01 – 6.90 (m, 3H), 5.17 (s, 1H), 4.38 (s, 2H), 3.75 (s, 3H), 3.61 (dd, *J* = 8.1, 7.0 Hz, 2H), 2.44 (dd, *J* = 8.2, 6.9 Hz, 2H); ^{13}C NMR (100 MHz, $CDCl_3$) δ 191.8, 165.2, 159.7, 137.3, 137.2, 129.9, 128.9, 127.8, 127.0, 119.9, 115.5, 113.0, 102.5, 55.6, 55.3, 48.0, 35.5; FTIR (KBr, cm^{-1}) 3061, 2836, 1634, 1538, 1475, 1363, 1235, 1174, 1124, 1049, 786, 699; HRMS (ESI, TOF) *m/e* calculated for $[M+H]^+$ $C_{19}H_{20}NO_2$: 294.1494, found 294.1488.

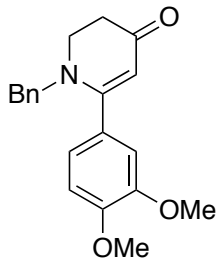

1-Benzyl-6-(3,4-dimethoxyphenyl)-2,3-dihydropyridin-4(1*H*)-one (4.8):

Compound **4.8** was prepared by the general procedure described above and 47.2 mg (73%) was isolated as yellow oil. ^{1}H NMR (400 MHz, $CDCl_3$) δ 7.39 – 7.27 (m, 3H), 7.25 – 7.20 (m, 2H), 7.01 (m, 1H), 6.90 – 6.86 (m, 2H), 5.21 (s, 1H), 4.44 (s, 2H), 3.89 (s, 3H), 3.74 (s, 3H), 3.65 (dd, *J* = 8.1, 6.8 Hz, 2H), 2.44 (dd, *J* = 8.1, 6.8 Hz, 2H); ^{13}C NMR (100 MHz, $CDCl_3$) δ 192.1, 165.2, 150.3, 148.9, 137.6, 128.9, 128.3, 127.8, 126.8, 120.6, 111.0, 110.8, 102.6, 56.0, 55.8, 55.7, 48.2, 35.4; FTIR (KBr, cm^{-1}) 2958, 2835, 1684, 1631, 1517, 1438, 1363, 1247, 1123, 1025, 807, 732, 699; HRMS (ESI, TOF) *m/e* calculated for $[M+H]^+$ $C_{20}H_{22}NO_3$: 324.1600, found 324.1591.

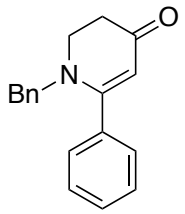

1-Benzyl-6-phenyl-2,3-dihydropyridin-4(1*H*)-one (4.9):

Compound **4.9** was prepared by the general procedure described above and 37.4 mg (71%) was isolated as light yellow solid (mp 83–85 °C). ^{1}H NMR (400 MHz, $CDCl_3$) δ 7.43 – 7.27 (m, 8H), 7.23 – 7.18 (m, 2H), 5.16 (s, 1H), 4.37 (s, 2H), 3.61 (dd, *J* =

8.2, 7.0 Hz, 2H), 2.44 (dd, *J* = 8.2, 6.9 Hz, 2H); ^{13}C NMR (100 MHz, $CDCl_3$) δ 191.8, 165.3, 137.2, 136.0, 129.7, 128.9, 128.8, 127.9, 127.7, 127.1, 102.7, 55.5, 47.9, 35.5; FTIR (KBr, cm^{-1}) 3059, 2899, 1637, 1538, 1433, 1363, 1231, 1126, 1002, 761, 700; HRMS (ESI, TOF) *m/e* calculated for $[M+H]^+$ $C_{18}H_{18}NO$: 264.1388, found 264.1381.

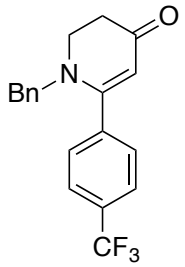

1-Benzyl-6-(4-(trifluoromethyl)phenyl)-2,3-dihydropyridin-4(1*H*)-one (4.10):

Compound **4.10** was prepared by the general procedure described above and 40.4 mg (61%) was isolated as yellow oil. ^{1}H NMR (400 MHz, $CDCl_3$) δ 7.68 (d, *J* = 8.2 Hz, 2H), 7.54 (d, *J* = 8.1 Hz, 2H), 7.40 – 7.29 (m, 3H), 7.22 – 7.17 (m, 2H), 5.13 (s, 1H), 4.33 (s, 2H), 3.64 (t, *J* = 7.6 Hz, 2H), 2.48 (t, *J* = 7.6 Hz, 2H); ^{13}C NMR (100 MHz, $CDCl_3$) δ 191.7, 163.5, 139.5 (d, *J* = 1.1 Hz), 136.8, 131.8 (q, *J* = 32.9 Hz), 129.0, 128.2, 128.1, 126.9, 125.8 (q, *J* = 3.8 Hz), 123.7 (q, *J* = 272.4 Hz), 103.2, 55.6, 48.1, 35.5. ^{19}F NMR (376 MHz, $CDCl_3$) δ -62.9; FTIR (KBr, cm^{-1}) 3031, 2902, 1644, 1543, 1325, 1127, 1067, 1019, 862, 844, 732, 611; HRMS (ESI, TOF) *m/e* calculated for $[M+H]^+$ $C_{19}H_{17}F_3NO$: 332.1287, found 332.1248.

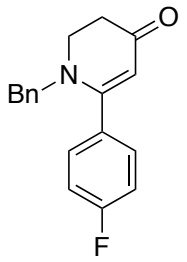

1-Benzyl-6-(4-fluorophenyl)-2,3-dihydropyridin-4(1*H*)-one (4.11):

Compound **4.11** was prepared by the general procedure described above and 32.6 mg (58%) was isolated as light yellow solid (mp 116–117 °C). ^{1}H NMR (400 MHz, $CDCl_3$) δ 7.44 – 7.27 (m, 5H), 7.23 – 7.16 (m, 2H), 7.14 – 7.06 (m, 2H), 5.13 (s, 1H), 4.36 (s, 2H), 3.62 (t, *J* = 7.6 Hz, 2H), 2.43 (t, *J* = 7.6 Hz, 2H); ^{13}C NMR (100 MHz, $CDCl_3$) δ 191.9, 163.4 (d, *J* = 250.3 Hz), 162.2, 137.1, 132.0 (d, *J* = 3.4 Hz), 129.8 (d, *J* = 8.4 Hz), 129.0, 128.0, 127.0, 115.9 (d, *J* = 21.8 Hz), 103.0, 55.5, 48.0, 35.5; ^{19}F NMR (376 MHz, $CDCl_3$) δ -110.5; FTIR (KBr, cm^{-1}) 3061, 2850, 1606, 1515, 13563, 1232, 1157, 999, 844, 733, 699; HRMS (ESI, TOF) *m/e* calculated for $[M+H]^+$ $C_{18}H_{17}FNO$: 282.1243, found 282.1292.

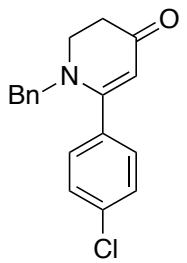

1-Benzyl-6-(4-chlorophenyl)-2,3-dihydropyridin-4(1*H*)-one (4.12):

Compound **4.12** was prepared by the general procedure described above and 31.6 mg (53%) was isolated as yellow oil. ^{1}H NMR (400 MHz, $CDCl_3$) δ 7.42 – 7.28 (m, 7H), 7.22 – 7.16 (m, 2H), 5.13 (s, 1H), 4.35 (s, 2H), 3.62 (dd, *J* = 8.1, 6.9 Hz, 2H), 2.44

(dd, J = 8.2, 6.9 Hz, 2H); ^{13}C NMR (100 MHz, $CDCl_3$) δ 191.8, 163.9, 137.0, 135.9, 134.3, 129.1, 129.1, 129.0, 128.0, 127.0, 103.0, 55.5, 48.0, 35.5. FTIR (KBr, cm^{-1}) 3029, 2901, 1640, 1538, 1473, 1363, 1230, 1126, 1090, 997, 856, 789, 698; HRMS (ESI, TOF) *m/e* calculated for $[M+H]^+$ $C_{18}H_{17}ClNO$: 298.0980, found 298.0987.

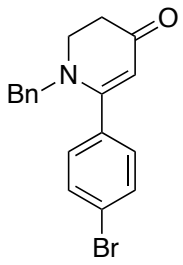

1-Benzyl-6-(4-bromophenyl)-2,3-dihydropyridin-4(1*H*)-one (4.13):

Compound **4.13** was prepared by the general procedure described above and 32.2 mg (47%) was isolated as yellow oil. ^{1}H NMR (400 MHz, $CDCl_3$) δ 7.58 – 7.52 (m, 2H), 7.39 – 7.26 (m, 5H), 7.21 – 7.16 (m, 2H), 5.13 (s, 1H), 4.35 (s, 2H), 3.61 (dd, J = 8.1, 7.0 Hz, 2H), 2.44 (dd, J = 8.2, 6.9 Hz, 2H); ^{13}C NMR (100 MHz, $CDCl_3$) δ 191.8, 163.9, 137.0, 134.8, 132.1, 129.3, 129.0, 128.0, 126.9, 124.1, 102.9, 55.5, 48.0, 35.5; FTIR (KBr, cm^{-1}) 3028, 2851, 1637, 1537, 1471, 1363, 1232, 1184, 1126, 1071, 996, 834, 732, 699; HRMS (ESI, TOF) *m/e* calculated for $[M+H]^+$ $C_{18}H_{17}BrNO$: 342.0494, found 342.0496.

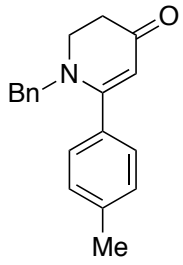

1-Benzyl-6-(*p*-tolyl)-2,3-dihydropyridin-4(1*H*)-one (4.14):

Compound **4.14** was prepared by the general procedure described above and 37.2 mg (67%) was isolated as yellow oil. ^{1}H NMR (400 MHz, $CDCl_3$) δ 7.40 – 7.25 (m, 5H), 7.24 – 7.17 (m, 4H), 5.15 (s, 1H), 4.38 (s, 2H), 3.60 (m, 2H), 2.42 (dd, *J* = 8.2, 6.9 Hz, 2H), 2.37 (s, 3H); ^{13}C NMR (100 MHz, $CDCl_3$) δ 191.9, 165.5, 139.9, 137.4, 133.1, 129.4, 128.9, 127.8, 127.7, 127.1, 102.6, 55.5, 47.9, 35.5, 21.3. FTIR (KBr, cm^{-1}) 3028, 2919, 1634, 1538, 1481, 1362, 1231, 1126, 997, 830, 733, 699; HRMS (ESI, TOF) *m/e* calculated for $[M+H]^+$ $C_{19}H_{20}NO$: 278.1545, found 278.1529.

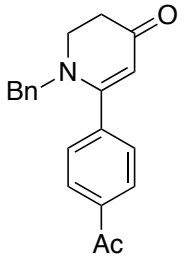

6-(4-Acetylphenyl)-1-benzyl-2,3-dihydropyridin-4(1*H*)-one (4.15):

Compound **4.15** was prepared by the general procedure described above and 47.0 mg (77%) was isolated as yellow oil. ^{1}H NMR (400 MHz, $CDCl_3$) δ 8.02 – 7.96 (m, 2H), 7.55 – 7.49 (m, 2H), 7.40 – 7.28 (m, 3H), 7.21 – 7.17 (m, 2H), 5.15 (s, 1H), 4.34 (s, 2H), 3.63 (dd, *J* = 8.1, 6.9 Hz, 2H), 2.62 (s, 3H), 2.47 (dd, *J* = 8.2, 6.9 Hz, 2H); ^{13}C NMR (100 MHz, $CDCl_3$) δ 197.2, 191.7, 163.9, 140.4, 137.9, 136.8, 129.0, 128.7, 128.0, 127.0, 103.0, 55.6, 48.1, 35.5, 26.7; FTIR (KBr, cm^{-1}) 3030, 2851, 1684, 1538, 1361, 1265, 1232, 1127, 959, 861, 789, 699, 599; HRMS (ESI, TOF) *m/e* calculated for $[M+H]^+$ $C_{20}H_{20}NO_2$: 306.1494, found 306.1496.

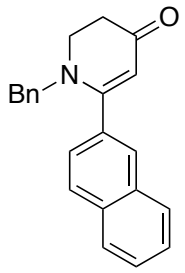

1-Benzyl-6-(naphthalen-2-yl)-2,3-dihydropyridin-4(1*H*)-one (4.16):

Compound **4.16** was prepared by the general procedure described above and 46.4 mg (74%) was isolated as yellow solid (mp 148–150 °C). ^{1}H NMR (400 MHz, $CDCl_3$) δ 8.01 – 7.78 (m, 4H), 7.62 – 7.41 (m, 3H), 7.39 – 7.25 (m, 3H), 7.23 7.21 (m, 2H), 5.27 (s, 1H), 4.41 (s, 2H), 3.66 (t, *J* = 7.5 Hz, 2H), 2.47 (t, *J* = 7.5 Hz, 2H); ^{13}C NMR (100 MHz, $CDCl_3$) δ 191.9, 165.3, 137.2, 133.6, 133.3, 132.9, 128.9, 128.5, 128.4, 127.9, 127.8, 127.6, 127.2, 127.1, 126.9, 124.8, 103.1, 55.6, 48.0, 35.6; FTIR (KBr, cm^{-1}) 3054, 2900, 1633, 1538, 1495, 1363, 1235, 1118, 947, 812, 731, 698; HRMS (ESI, TOF) *m/e* calculated for $[M+H]^+$ $C_{22}H_{20}NO$: 314.1545, found 314.1533.

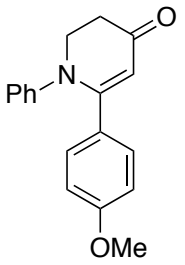

6-(4-Methoxyphenyl)-1-phenyl-2,3-dihydropyridin-4(1*H*)-one (4.17):

Compound **4.17** was prepared by the general procedure described above and 33.0 mg (59%) was isolated as yellow solid (mp 114–116 °C). ^{1}H NMR (400 MHz, $CDCl_3$) δ 7.22 – 7.14 (m, 4H), 7.05 – 6.99 (m, 1H), 6.94 – 6.88 (m, 2H), 6.74 – 6.69 (m, 2H), 5.52 (s, 1H), 4.20 (dd, *J* = 7.6, 6.5 Hz, 2H), 3.75 (s, 3H), 2.64 – 2.59 (m, 2H); ^{13}C

NMR (100 MHz, $CDCl_3$) δ 193.3, 161.4, 160.7, 145.9, 130.4, 129.0, 128.1, 125.1, 124.7, 113.6, 105.9, 55.2, 53.0, 36.0; FTIR (KBr, cm^{-1}) 3052, 2931, 1643, 1605, 1506, 1463, 1361, 1255, 1213, 1130, 1032, 836, 763, 698; HRMS (ESI, TOF) *m/e* calculated for $[M+H]^+$ $C_{18}H_{18}NO_2$: 280.1338, found 280.1322.

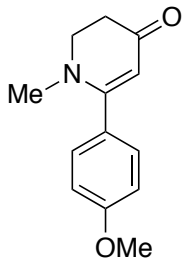

6-(4-Methoxyphenyl)-1-methyl-2,3-dihydropyridin-4(1*H*)-one (4.18):

Compound **4.18** was prepared by the general procedure described above and 23.0 mg (53%) was isolated as yellow oil. ^1H NMR (400 MHz, $CDCl_3$) δ 7.29 – 7.22 (m, 2H), 6.96 – 6.89 (m, 2H), 5.07 (s, 1H), 3.84 (s, 3H), 3.63 (dd, *J* = 8.2, 7.1 Hz, 2H), 2.93 (s, 3H), 2.54 (dd, *J* = 8.2, 7.0 Hz, 2H); ^{13}C NMR (100 MHz, $CDCl_3$) δ 191.7, 165.5, 160.6, 129.3, 128.4, 113.9, 101.8, 55.4, 51.0, 40.4, 35.4; FTIR (KBr, cm^{-1}) 2957, 1627, 1578, 1538, 1487, 1364, 1251, 1171, 1027, 970, 838, 807; HRMS (ESI, TOF) *m/e* calculated for $[M+H]^+$ $C_{13}H_{16}NO_2$: 218.1141, found 218.1176.

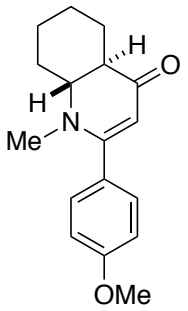

***Trans*-2-(4-methoxyphenyl)-1-methyl-4a,5,6,7,8,8a-hexahydroquinolin-4(1*H*)-one (4.19):**

Compound **4.19** was prepared by the general procedure described above and 15.2 mg (28%) was isolated as colorless oil. ^{1}H NMR (400 MHz, $CDCl_3$) δ 7.23 – 7.18 (m, 2H), 6.95 – 6.88 (m, 2H), 4.96 (s, 1H), 3.84 (s, 3H), 3.48 (ddd, *J* = 11.4, 6.1, 4.1 Hz, 1H), 2.91 (s, 4H), 2.51 (d, *J* = 12.1 Hz, 1H), 2.14 – 1.96 (m, 1H), 1.87 – 1.77 (m, 1H), 1.77 – 1.67 (m, 1H), 1.50 (m, 1H), 1.43 – 1.28 (m, 3H); ^{13}C NMR (100 MHz, $CDCl_3$) δ 192.5, 162.6, 160.3, 129.2, 128.9, 113.8, 100.2, 63.0, 55.3, 44.1, 38.5, 25.0, 24.2, 22.4, 22.2; FTIR (KBr, cm^{-1}) 2931, 2856, 1623, 1579, 1540, 1489, 1298, 1252, 1175, 1031, 839, 791; HRMS (ESI, TOF) *m/e* calculated for $[M+H]^+$ $C_{17}H_{22}NO_2$: 272.1651, found 272.1632.

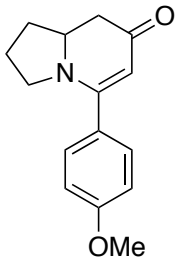

5-(4-Methoxyphenyl)-2,3,8,8a-tetrahydroindolizin-7(1*H*)-one (4.20):

Compound **4.20** was prepared by the general procedure described above and 30.7 mg (63%) was isolated as light yellow oil. ^{1}H NMR (400 MHz, $CDCl_3$) δ 7.38 – 7.32 (m, 2H), 6.95 – 6.90 (m, 2H), 5.09 (s, 1H), 4.12 – 3.99 (m, 1H), 3.84 (s, 3H), 3.60 – 3.51 (m, 1H), 3.28 (dt, *J* = 11.0, 7.2 Hz, 1H), 2.54 – 2.37 (m, 2H), 2.37 – 2.22 (m, 1H), 2.09 – 1.72 (m, 3H); ^{13}C NMR (100 MHz, $CDCl_3$) δ 192.0, 162.7, 160.9, 129.3, 128.6, 113.9, 99.9, 58.7, 55.4, 49.6, 41.6, 31.8, 24.6; FTIR (KBr, cm^{-1}) 2963, 2876,

1606, 1511, 1338, 1296, 1245, 1176, 1133, 1031, 837, 773; HRMS (ESI, TOF) *m/e* calculated for $[M+H]^+$ $C_{15}H_{18}NO_2$: 244.1297, found 244.1329.

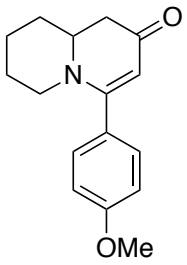

4-(4-Methoxyphenyl)-1,6,7,8,9,9a-hexahydro-2*H*-quinolizin-2-one (4.21):

Compound **4.21** was prepared by the general procedure described above and 34.5 mg (67%) was isolated as yellow oil. ^{1}H NMR (400 MHz, $CDCl_3$) δ 7.26 – 7.17 (m, 2H), 6.96 – 6.88 (m, 2H), 5.07 (s, 1H), 3.83 (s, 3H), 3.68 – 3.58 (m, 1H), 3.47 (ddt, *J* = 11.5, 7.7, 6.0 Hz, 1H), 2.66 – 2.53 (m, 2H), 2.43 (dd, *J* = 16.3, 11.2 Hz, 1H), 1.91 – 1.83 (m, 1H), 1.81 – 1.70 (m, 2H), 1.62 – 1.50 (m, 1H), 1.52 – 1.39 (m, 2H); ^{13}C NMR (100 MHz, $CDCl_3$) δ 191.6, 165.9, 160.1, 129.0, 128.5, 114.0, 103.5, 58.7, 55.3, 50.4, 42.6, 31.4, 26.0, 23.9; FTIR (KBr, cm^{-1}) 2935, 2838, 1635, 1509, 1440, 1350, 1250, 1176, 1101, 1027, 836, 779, 728; HRMS (ESI, TOF) *m/e* calculated for $[M+H]^+$ $C_{16}H_{20}NO_2$: 258.1494, found 258.1494.

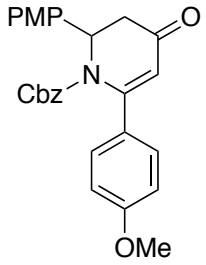

Benzyl 2,6-bis(4-methoxyphenyl)-4-oxo-3,4-dihydropyridine-1(2*H*)-carboxylate

(4.22):

Compound **4.22** was prepared by the general procedure described above and 59.4 mg (67%) was isolated as yellow solid (mp 89–90 °C). ^{1}H NMR (400 MHz, $CDCl_3$) δ 7.41 – 7.33 (m, 2H), 7.30 – 7.17 (m, 3H), 7.18 – 7.10 (m, 2H), 6.91 – 6.84 (m, 4H), 6.79 – 6.71 (m, 2H), 6.11 – 6.03 (m, 1H), 5.63 (s, 1H), 5.03 (q, *J* = 12.1 Hz, 2H), 3.78 (s, 3H), 3.76 (s, 3H), 3.14 (dd, *J* = 17.5, 5.8 Hz, 1H), 3.03 (dt, *J* = 17.6, 1.5 Hz, 1H); ^{13}C NMR (100 MHz, $CDCl_3$) δ 194.0, 161.3, 159.2, 154.8, 154.0, 134.6, 130.1, 129.7, 128.4, 128.3, 128.3, 128.2, 127.5, 113.9, 113.9, 113.7, 68.8, 57.4, 55.3, 55.2, 41.1; FTIR (KBr, cm^{-1}) 3004, 2837, 1710, 1659, 1606, 1590, 1512, 1387, 1253, 1179, 1119, 1032, 991, 836, 735, 698; HRMS (ESI, TOF) *m/e* calculated for $[M+H]^+$ $C_{27}H_{26}NO_5$: 444.1811, found 444.1797.

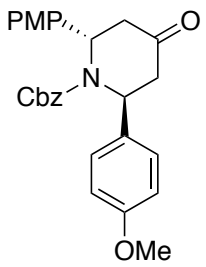

Benzyl *trans*-2,6-bis(4-methoxyphenyl)-4-oxopiperidine-1-carboxylate (4.23):

Compound **4.23** was prepared by the general procedure described above and 21.4 mg (24%) was isolated as yellow solid (mp 149–150 °C). ^{1}H NMR (400 MHz, $CDCl_3$) δ 7.27 – 7.17 (m, 3H), 7.13 (d, *J* = 8.3 Hz, 4H), 7.05 – 6.97 (m, 2H), 6.88 – 6.83 (m, 4H), 5.75 (s, 2H), 5.11 (q, *J* = 12.4 Hz, 2H), 3.80 (s, 6H), 3.00 (dd, *J* = 17.6, 6.4 Hz, 2H), 2.84 (d, *J* = 17.7 Hz, 2H); ^{13}C NMR (100 MHz, $CDCl_3$) δ 205.7, 158.7, 156.2, 136.1, 133.8, 128.3, 127.9, 127.8, 126.5, 114.3, 67.6, 55.3, 54.0, 45.2; FTIR (KBr,

cm^{-1}) 3002, 2934, 1725, 1698, 1611, 1512, 1399, 1293, 1253, 1180, 1033, 817, 737, 699; HRMS (ESI, TOF) *m/e* calculated for $[M+Na]^+$ $C_{27}H_{27}NO_5Na$: 468.1787, found 468.1797.

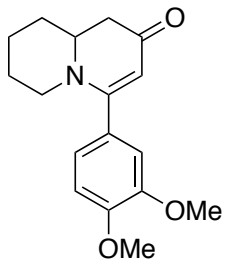

4-(3,4-Dimethoxyphenyl)-1,6,7,8,9,9a-hexahydro-2*H*-quinolizin-2-one (4.26):

Compound **4.26** was prepared by the general procedure described above and 35.6 mg (62%) was isolated as yellow oil. ^1H NMR (400 MHz, $CDCl_3$) δ 6.92 – 6.82 (m, 2H), 6.79 (d, *J* = 1.7 Hz, 1H), 5.10 (s, 1H), 3.91 (s, 3H), 3.89 (s, 3H), 3.70 – 3.61 (m, 1H), 3.48 (ddt, *J* = 11.5, 8.0, 6.0 Hz, 1H), 2.61 (dt, *J* = 16.0, 5.8 Hz, 2H), 2.44 (dd, *J* = 16.3, 11.1 Hz, 1H), 1.92 – 1.83 (m, 1H), 1.80 – 1.74 (m, 2H), 1.63 – 1.58 (m, 1H), 1.53 – 1.38 (m, 2H); ^{13}C NMR (100 MHz, $CDCl_3$) δ 191.6, 165.8, 149.6, 148.9, 129.3, 119.7, 111.0, 110.3, 103.4, 58.7, 56.0, 56.0, 50.5, 42.6, 31.4, 26.0, 23.9; FTIR (KBr, cm^{-1}) 2935, 2836, 1685, 1634, 1513, 1439, 1248, 1139, 1024, 879, 730, 703; HRMS (ESI, TOF) *m/e* calculated for $[M+H]^+$ $C_{17}H_{22}NO_3$: 288.1600, found 288.1599.

6.5 Chapter 5

6.5.1 General procedures for the preparation of compounds

Method A: Copper-catalyzed amidation

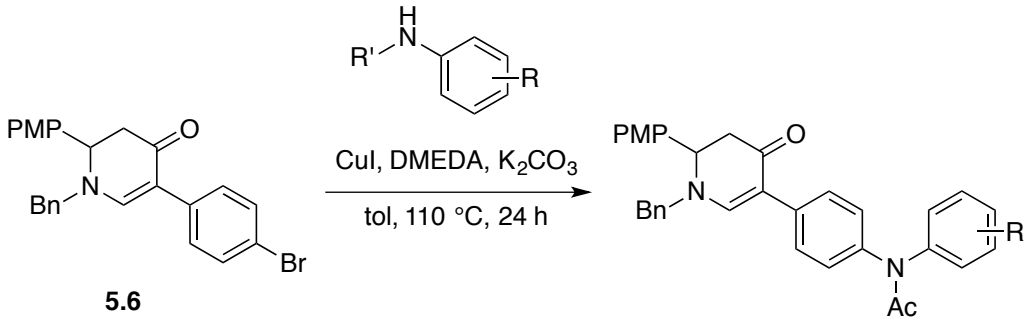

An oven-dried vial was charged with CuI (2.8 mg, 0.0147 mmol, 10 mol%), amide (0.177 mmol) and K_2CO_3 (40.6 mg, 0.294 mmol) evacuated and backfilled with argon. *N, N*'-dimethylethylenediamine (3.16 μL, 0.0294 mmol, 20 mol%), compound **5.6** (66mg, 0.147 mmol) in toluene (0.15 mL) were added under argon. The reaction mixture was stirred at 110 °C for 24 h and then cooled to room temperature. The crude product was filtered through a pad of silica gel eluting with ethyl acetate. The filtrate was concentrated in vacuo and purified by flash chromatography to afford the product.

Method B: Reductive amination

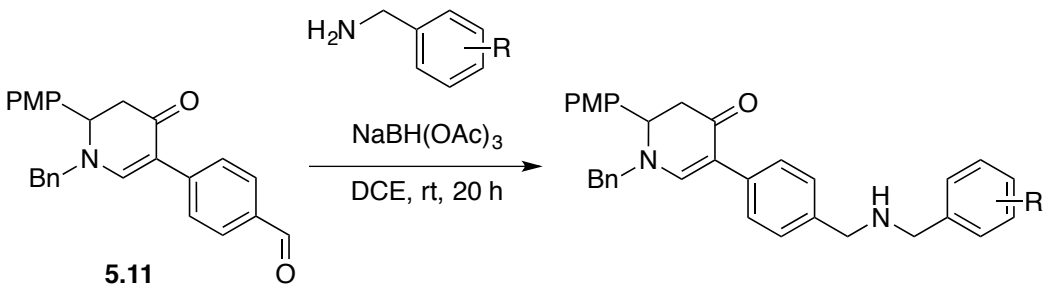

Sodium triacetoxyborohydride (42.4 mg, 0.200 mmol) was added to a solution of benzylamine (0.133 mmol) and compound **5.11** (53 mg, 0.133 mmol) in DCE (1.3 ml, 0.1 M) at room temperature and the reaction was stirred for 20 h. The reaction mixture was diluted with DCM and washed with water. The aqueous layer was further extracted with DCM and the combined organic layer was dried ($MgSO_4$), and evaporated in vacuo. The crude product was purified by flash column chromatography on silica gel using hexanes and an increasing proportion of EtOAc as eluent.

6.5.2 Compounds characterization

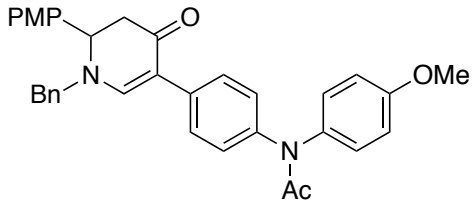

***N*-(4-(1-benzyl-6-(4-methoxyphenyl)-4-oxo-1,4,5,6-tetrahydropyridin-3-yl)phenyl)-*N*-(4-methoxyphenyl)acetamide (5.13):**

Compound **5.13** was prepared by **Method A** described above and 38.4 mg (49%) was isolated as yellow oil. ^{1}H NMR (400 MHz, $CDCl_3$) δ 7.59 – 7.32 (m, 6H), 7.24 – 7.13 (m, 8H), 6.97 – 6.81 (m, 4H), 4.52 (s, 1H), 4.41 (d, J = 15.1 Hz, 1H), 4.22 (br, 1H), 3.81 (s, 6H), 2.94 (br, 1H), 2.80 (dd, J = 16.2, 8.0 Hz, 1H), 2.07 (s, 3H); ^{13}C NMR (101 MHz, $CDCl_3$) δ 187.8, 170.8, 159.7, 153.1, 135.8, 129.0, 128.3, 127.7, 126.0, 114.4, 64.4, 60.3, 57.5, 55.5, 55.3, 44.4, 30.6, 29.7, 23.7, 21.1, 19.1, 14.2, 13.7; FTIR

(KBr, cm^{-1}) 2932, 1666, 1509, 1371, 1248, 1032, 832, 734; HRMS (ESI, TOF) *m/e* calculated for $[M+Na]^+$ $C_{34}H_{32}N_2NaO_4$: 555.2254, found 555.2282.

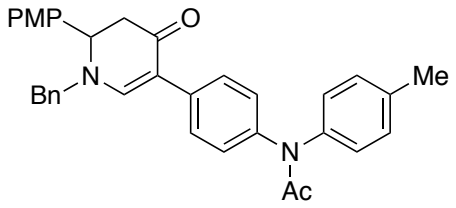

***N*-(4-(1-benzyl-6-(4-methoxyphenyl)-4-oxo-1,4,5,6-tetrahydropyridin-3-yl)phenyl)-*N*-(*p*-tolyl)acetamide (5.14):**

Compound **5.14** was prepared by **Method A** described above and 53.9 mg (71%) was isolated as yellow oil. ^1H NMR (400 MHz, $CDCl_3$) δ 7.61 – 7.29 (m, 6H), 7.23 – 7.08 (m, 10H), 6.92 – 6.79 (m, 2H), 4.53 (d, *J* = 7.7 Hz, 1H), 4.41 (d, *J* = 15.0 Hz, 1H), 4.21 (d, *J* = 15.1 Hz, 1H), 2.93 (br, 1H), 2.80 (dd, *J* = 16.2, 8.0 Hz, 1H), 2.33 (s, 3H), 2.07 (s, 3H); ^{13}C NMR (101 MHz, $CDCl_3$) δ 187.8, 170.7, 159.7, 153.1, 135.8, 130.2, 129.0, 128.3, 128.1, 127.7, 126.3, 114.4, 64.4, 60.3, 57.5, 55.3, 44.4, 30.6, 23.8, 21.0, 19.1, 14.2, 13.7; FTIR (KBr, cm^{-1}) 2925, 1668, 1596, 1510, 1370, 1252, 1030, 817, 734; HRMS (ESI, TOF) *m/e* calculated for $[M+Na]^+$ $C_{34}H_{32}N_2NaO_3$: 539.2305, found 539.2304.

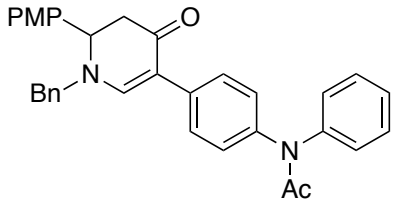

***N*-(4-(1-benzyl-6-(4-methoxyphenyl)-4-oxo-1,4,5,6-tetrahydropyridin-3-yl)phenyl)-*N*-phenylacetamide (5.15):**

Compound **5.15** was prepared by **Method A** described above and 51.7 mg (70%) was isolated as yellow oil. ^{1}H NMR (400 MHz, $CDCl_3$) δ 7.58 – 7.26 (m, 10H), 7.25 – 7.13 (m, 7H), 6.92 – 6.84 (m, 2H), 4.52 (t, *J* = 7.5 Hz, 1H), 4.42 (d, *J* = 15.0 Hz, 1H), 4.22 (d, *J* = 15.4 Hz, 1H), 3.81 (s, 3H), 2.95 (dd, *J* = 16.1, 6.9 Hz, 1H), 2.81 (dd, *J* = 16.2, 8.0 Hz, 1H), 2.08 (s, 1H); ^{13}C NMR (101 MHz, $CDCl_3$) δ 187.7, 170.6, 159.7, 153.1, 135.7, 129.0, 128.4, 128.3, 127.7, 114.5, 60.3, 57.6, 55.3, 53.8, 44.3, 29.7, 29.3, 23.9; FTIR (KBr, cm^{-1}) 2978, 1668, 1594, 1510, 371, 1251, 1030, 733; HRMS (ESI, TOF) *m/e* calculated for $[M+Na]^+$ $C_{33}H_{30}N_2NaO_3$: 525.2149, found 525.2159.

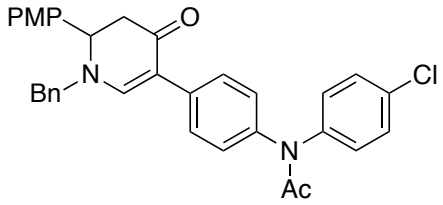

***N*-(4-(1-benzyl-6-(4-methoxyphenyl)-4-oxo-1,4,5,6-tetrahydropyridin-3-yl)phenyl)-*N*-(4-chlorophenyl)acetamide (5.16):**

Compound **5.16** was prepared by **Method A** described above and 60.8 mg (77%) was isolated as yellow oil. ^{1}H NMR (400 MHz, $CDCl_3$) δ 7.62 – 7.42 (m, 3H), 7.42 – 7.27 (m, 8H), 7.24 – 7.13 (m, 8H), 6.92 – 6.85 (m, 2H), 4.54 (t, *J* = 7.4 Hz, 1H), 4.43 (d, *J* = 15.0 Hz, 1H), 4.24 (d, *J* = 15.1 Hz, 1H), 3.81 (s, 3H), 2.97 (dd, *J* = 16.4, 6.9 Hz, 1H), 2.81 (dd, *J* = 16.3, 7.9 Hz, 1H), 2.08 (s, 3H); ^{13}C NMR (101 MHz, $CDCl_3$) δ 187.7, 159.7, 153.2, 140.1, 135.7, 130.1, 129.1, 128.8, 128.4, 128.3, 127.7, 114.5, 64.4, 60.4, 60.2, 57.6, 55.3, 44.3, 30.6, 23.9, 21.0, 19.1, 14.2, 13.7; FTIR (KBr, cm^{-1})

2930, 1671, 1596, 1511, 1370, 1252, 1124, 829, 734; HRMS (ESI, TOF) *m/e* calculated for $[M+Na]^+$ $C_{33}H_{29}ClN_2NaO_3$: 559.1759, found 559.1779.

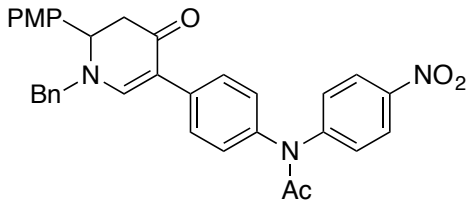

***N*-(4-(1-benzyl-6-(4-methoxyphenyl)-4-oxo-1,4,5,6-tetrahydropyridin-3-yl)phenyl)-*N*-(4-nitrophenyl)acetamide (5.17):**

Compound **5.17** was prepared by **Method A** described above and 49.9 mg (62%) was isolated as brown solid (mp 135–139 °C). ^{1}H NMR (400 MHz, $CDCl_3$) δ 8.19 – 8.10 (m, 2H), 7.63 (s, 1H), 7.62 – 7.54 (m, 2H), 7.50 – 7.41 (m, 2H), 7.44 – 7.33 (m, 3H), 7.22 – 7.16 (m, 6H), 6.92 – 6.86 (m, 2H), 4.57 (t, *J* = 7.3 Hz, 1H), 4.47 (d, *J* = 15.2 Hz, 1H), 4.27 (d, *J* = 15.1 Hz, 1H), 3.82 (s, 3H), 3.01 (dd, *J* = 16.3, 7.0 Hz, 1H), 2.83 (dd, *J* = 16.3, 7.6 Hz, 1H), 2.10 (s, 3H); ^{13}C NMR (101 MHz, $CDCl_3$) δ 187.7, 170.9, 159.8, 153.3, 148.4, 144.4, 139.1, 136.8, 135.6, 130.0, 129.1, 128.9, 128.5, 128.4, 128.3, 127.7, 125.5, 125.0, 124.2, 114.5, 109.4, 60.2, 57.7, 55.4, 44.2, 24.6; FTIR (KBr, cm^{-1}) 2926, 1682, 1595, 1511, 1343, 1300, 1255, 1111, 852, 735; HRMS (ESI, TOF) *m/e* calculated for $[M+Na]^+$ $C_{33}H_{29}N_3NaO_5$: 570.1999, found 570.1993.

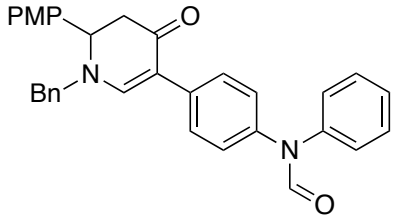

***N*-(4-(1-benzyl-6-(4-methoxyphenyl)-4-oxo-1,4,5,6-tetrahydropyridin-3-**

yl)phenyl)-*N*-phenylformamide (5.18):

Compound **5.18** was prepared by **Method A** described above and 63.9 mg (89%) was isolated as yellow oil. ^{1}H NMR (400 MHz, $CDCl_3$) δ 8.66 (d, *J* = 11.6 Hz, 1H), 7.55 (d, *J* = 3.0 Hz, 1H), 7.52 – 7.44 (m, 2H), 7.44 – 7.27 (m, 6H), 7.29 – 7.20 (m, 2H), 7.24 – 7.09 (m, 6H), 6.93 – 6.85 (m, 2H), 4.54 (q, *J* = 7.2 Hz, 1H), 4.42 (dd, *J* = 15.1, 6.7 Hz, 1H), 4.23 (dd, *J* = 15.1, 8.7 Hz, 1H), 3.82 (s, 3H), 2.96 (ddd, *J* = 15.8, 8.8, 6.8 Hz, 1H), 2.82 (ddd, *J* = 16.2, 8.1, 4.8 Hz, 1H); ^{13}C NMR (101 MHz, $CDCl_3$) δ 187.75, 187.72, 161.78, 161.77, 159.71, 159.66, 153.2, 153.0, 141.9, 139.8, 139.1, 137.0, 135.73, 135.70, 135.3, 135.0, 130.3, 130.2, 129.6, 129.06, 129.04, 129.03, 128.6, 128.38, 128.34, 128.32, 128.2, 127.76, 127.71, 126.8, 126.6, 126.0, 125.9, 125.2, 124.9, 114.48, 114.46, 110.4, 109.9, 60.38, 60.34, 57.55, 57.51, 55.3, 44.4, 44.3.; FTIR (KBr, cm^{-1}) 2929, 1684, 1595, 1511, 1305, 1253, 1122, 734; HRMS (ESI, TOF) *m/e* calculated for $[M+Na]^+$ $C_{32}H_{28}N_2NaO_3$: 511.1992, found 511.1980.

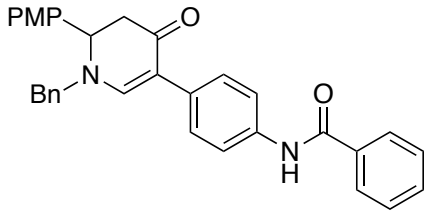

***N*-(4-(1-benzyl-6-(4-methoxyphenyl)-4-oxo-1,4,5,6-tetrahydropyridin-3-yl)phenyl)benzamide (5.19):**

Compound **5.19** was prepared by **Method A** described above and 20.1 mg (28%) was isolated as light yellow solid (mp 196–199 °C). ^{1}H NMR (400 MHz, $CDCl_3$) δ 7.99 (s, 1H), 7.92 – 7.85 (m, 2H), 7.66 – 7.58 (m, 2H), 7.57 – 7.48 (m, 2H), 7.51 – 7.41 (m, 4H), 7.42 – 7.31 (m, 3H), 7.24 – 7.13 (m, 4H), 6.93 – 6.84 (m, 2H), 4.51 (dd, *J* =

8.3, 6.8 Hz, 1H), 4.42 (d, *J* = 15.1 Hz, 1H), 4.21 (d, *J* = 15.1 Hz, 1H), 3.82 (s, 3H), 2.93 (dd, *J* = 16.2, 6.8 Hz, 1H), 2.81 (dd, *J* = 16.2, 8.4 Hz, 1H); ^{13}C NMR (101 MHz, $CDCl_3$) δ 188.0, 165.6, 159.6, 153.0, 135.9, 135.7, 135.1, 132.5, 131.7, 130.4, 129.0, 128.7, 128.4, 128.3, 128.1, 127.8, 127.1, 120.2, 114.4, 110.7, 60.3, 57.5, 55.3, 44.5; FTIR (KBr, cm^{-1}) 3299, 2923, 1592, 1513, 1251, 1029, 698; HRMS (ESI, TOF) *m/e* calculated for $[M+Na]^+$ $C_{32}H_{28}N_2NaO_3$: 511.1992, found 511.2007.

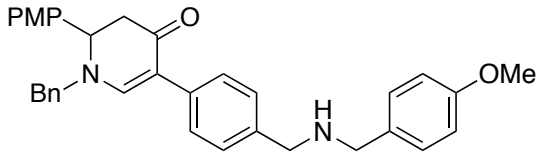

1-Benzyl-5-(4-(((4-methoxybenzyl)amino)methyl)phenyl)-2-(4-methoxyphenyl)-2,3-dihydropyridin-4(1*H*)-one (5.20):

Compound **5.20** was prepared by **Method B** described above and 59.3 mg (86%) was isolated as yellow oil. ^{1}H NMR (400 MHz, $CDCl_3$) δ 7.53 (s, 1H), 7.44 (d, *J* = 8.1 Hz, 2H), 7.41 – 7.23 (m, 7H), 7.22 – 7.12 (m, 4H), 6.92 – 6.83 (m, 4H), 6.53 (br, 1H), 4.51 (t, *J* = 7.5 Hz, 1H), 4.41 (d, *J* = 15.1 Hz, 1H), 4.20 (d, *J* = 15.1 Hz, 1H), 3.84 (s, 2H), 3.82 (s, 2H), 3.81 (s, 3H), 3.79 (s, 3H), 2.94 (dd, *J* = 16.2, 6.8 Hz, 1H), 2.80 (dd, *J* = 16.3, 8.2 Hz, 1H); ^{13}C NMR (101 MHz, $CDCl_3$) δ 187.8, 176.6, 159.6, 159.4, 153.2, 136.0, 135.8, 130.4, 130.3, 129.02, 128.99, 128.4, 128.3, 127.8, 127.7, 114.4, 114.1, 110.5, 60.2, 57.5, 55.3, 50.5, 50.2, 44.4, 29.3, 22.6; FTIR (KBr, cm^{-1}) 2932, 2602, 1595, 1513, 1251, 1031, 833, 733, 700; HRMS (ESI, TOF) *m/e* calculated for $[M+H]^+$ $C_{34}H_{35}N_2O_3$: 519.2642, found 519.2637.

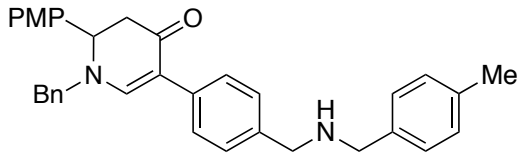

1-Benzyl-2-(4-methoxyphenyl)-5-(4-(((4-methylbenzyl)amino)methyl)phenyl)-2,3-dihydropyridin-4(1*H*)-one (5.21):

Compound **5.21** was prepared by **Method B** described above and 55.5 mg (83%) was isolated as light brown oil. ^{1}H NMR (400 MHz, $CDCl_3$) δ 7.52 (s, 1H), 7.47 – 7.40 (m, 2H), 7.41 – 7.26 (m, 5H), 7.24 (d, *J* = 8.0 Hz, 2H), 7.20 – 7.12 (m, 6H), 6.90 – 6.83 (m, 2H), 6.72 (br, 1H), 4.51 (dd, *J* = 8.2, 6.7 Hz, 1H), 4.40 (d, *J* = 15.1 Hz, 1H), 4.20 (d, *J* = 15.1 Hz, 1H), 3.84 (s, 2H), 3.83 (s, 2H), 3.81 (s, 3H), 2.94 (dd, *J* = 16.2, 6.8 Hz, 1H), 2.80 (dd, *J* = 16.2, 8.2 Hz, 1H); ^{13}C NMR (101 MHz, $CDCl_3$) δ 187.9, 176.6, 159.6, 153.2, 137.6, 135.8, 133.2, 133.0, 130.3, 129.4, 128.99, 128.96, 128.4, 128.3, 127.8, 127.7, 114.4, 110.5, 60.2, 57.5, 55.3, 50.8, 50.7, 44.4, 22.6, 21.2; FTIR (KBr, cm^{-1}) 2923, 1633, 1595, 1512, 1252, 1123, 809, 723; HRMS (ESI, TOF) *m/e* calculated for $[M+H]^+$ $C_{34}H_{35}N_2O_2$: 503.2693, found 503.2705.

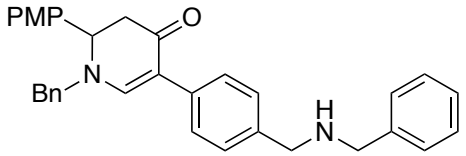

1-Benzyl-5-(4-((benzylamino)methyl)phenyl)-2-(4-methoxyphenyl)-2,3-dihydropyridin-4(1*H*)-one (5.22):

Compound **5.22** was prepared by **Method B** described above and 58.5 mg (90%) was isolated as yellow solid (mp 109–113 °C). ^{1}H NMR (400 MHz, $CDCl_3$) δ 7.53 (s,

1H), 7.44 – 7.39 (m, 2H), 7.39 – 7.28 (m, 9H), 7.25 (d, *J* = 3.3 Hz, 1H), 7.22 – 7.14 (m, 4H), 6.91 – 6.85 (m, 2H), 4.52 (dd, *J* = 8.4, 6.8 Hz, 1H), 4.41 (d, *J* = 15.1 Hz, 1H), 4.20 (d, *J* = 15.1 Hz, 1H), 3.81 (s, 3H), 3.80 (s, 4H), 2.95 (dd, *J* = 16.2, 6.8 Hz, 1H), 2.82 (dd, *J* = 16.2, 8.4 Hz, 1H); ^{13}C NMR (101 MHz, $CDCl_3$) δ 188.0, 159.6, 153.0, 140.3, 137.6, 135.9, 134.8, 130.4, 129.0, 128.39, 128.37, 128.24, 128.17, 128.10, 127.72, 127.65, 126.9, 114.4, 111.1, 60.4, 57.4, 55.3, 53.0, 52.9, 44.5; FTIR (KBr, cm^{-1}) 2924, 1594, 1511, 1251, 1122, 698; HRMS (ESI, TOF) *m/e* calculated for $[M+H]^+$ $C_{33}H_{33}N_2O_2$: 489.2537, found 489.2525.

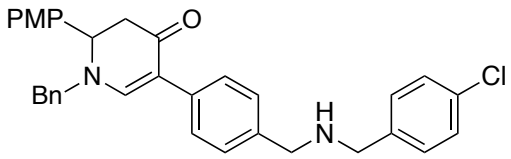

1-Benzyl-5-(4-(((4-chlorobenzyl)amino)methyl)phenyl)-2-(4-methoxyphenyl)-2,3-dihydropyridin-4(1*H*)-one (5.23):

Compound **5.20** was prepared by **Method B** described above and 66.1 mg (95%) was isolated as yellow oil. ^{1}H NMR (400 MHz, $CDCl_3$) δ 7.53 (s, 1H), 7.47 – 7.39 (m, 2H), 7.40 – 7.30 (m, 3H), 7.32 – 7.23 (m, 6H), 7.22 – 7.11 (m, 4H), 6.92 – 6.82 (m, 2H), 6.34 (br, 1H), 4.51 (dd, *J* = 8.2, 6.8 Hz, 1H), 4.41 (d, *J* = 15.1 Hz, 1H), 4.20 (d, *J* = 15.1 Hz, 1H), 3.82 (s, 4H), 3.81 (s, 3H), 2.94 (dd, *J* = 16.3, 6.8 Hz, 1H), 2.81 (dd, *J* = 16.3, 8.2 Hz, 1H); ^{13}C NMR (101 MHz, $CDCl_3$) δ 187.9, 176.3, 159.6, 153.2, 135.8, 135.7, 135.5, 133.9, 133.5, 130.2, 129.0, 128.8, 128.7, 128.4, 128.3, 127.8, 127.7, 114.4, 110.6, 60.3, 57.5, 55.3, 51.4, 50.7, 44.3; FTIR (KBr, cm^{-1}) 2927, 1634, 1595, 1512, 1357, 1252, 1123, 835, 734, 699; HRMS (ESI, TOF) *m/e* calculated for

$[M+H]^+$ $C_{33}H_{32}ClN_2O_2$: 523.2147, found 523.2160.

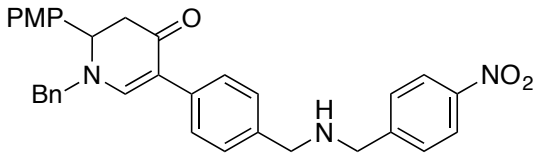

1-Benzyl-2-(4-methoxyphenyl)-5-(4-(((4-nitrobenzyl)amino)methyl)phenyl)-2,3-dihydropyridin-4(1*H*)-one (5.24):

Compound **5.24** was prepared by **Method B** described above and 36.2 mg (51%) was isolated as brown oil. ^{1}H NMR (400 MHz, $CDCl_3$) δ 8.22 – 8.13 (m, 2H), 7.57 – 7.49 (m, 3H), 7.47 – 7.39 (m, 2H), 7.42 – 7.31 (m, 3H), 7.33 – 7.25 (m, 2H), 7.24 – 7.13 (m, 4H), 6.92 – 6.84 (m, 2H), 4.53 (dd, *J* = 8.3, 6.8 Hz, 1H), 4.42 (d, *J* = 15.1 Hz, 1H), 4.22 (d, *J* = 15.1 Hz, 1H), 3.92 (s, 2H), 3.81 (s, 4H), 3.56 (s, 2H), 2.96 (dd, *J* = 16.3, 6.8 Hz, 1H), 2.83 (dd, *J* = 16.2, 8.3 Hz, 1H); ^{13}C NMR (101 MHz, $CDCl_3$) δ 188.0, 159.6, 153.2, 147.3, 147.1, 136.2, 135.8, 135.3, 130.3, 129.0, 128.9, 128.4, 128.30, 128.25, 127.8, 127.7, 123.6, 114.4, 110.8, 60.4, 57.5, 55.3, 52.6, 51.7, 44.4; FTIR (KBr, cm^{-1}) 2925, 1633, 1595, 1513, 1375, 1345, 1251, 835, 735; HRMS (ESI, TOF) *m/e* calculated for $[M+H]^+$ $C_{33}H_{32}N_3O_4$: 534.2387, found 534.2397.

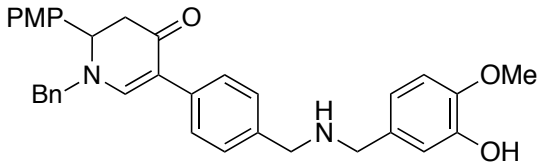

1-Benzyl-5-(4-(((3-hydroxy-4-methoxybenzyl)amino)methyl)phenyl)-2-(4-methoxyphenyl)-2,3-dihydropyridin-4(1*H*)-one (5.25):

Compound **5.25** was prepared by **Method B** described above and 26.3 mg (37%) was isolated as yellow oil. ^{1}H NMR (400 MHz, $CDCl_3$) δ 7.52 (s, 1H), 7.39 (d, *J* = 7.9 Hz, 2H), 7.37 – 7.31 (m, 3H), 7.29 (d, *J* = 8.1 Hz, 2H), 7.17 (ddd, *J* = 12.3, 6.9, 1.9 Hz, 4H), 6.94 (s, 1H), 6.87 (d, *J* = 8.6 Hz, 2H), 6.79 (s, 2H), 6.19 (br, 1H), 4.51 (t, *J* = 7.5 Hz, 1H), 4.41 (d, *J* = 15.1 Hz, 1H), 4.20 (d, *J* = 15.1 Hz, 1H), 3.85 (s, 3H), 3.81 (s, 5H), 3.75 (s, 2H), 2.94 (dd, *J* = 16.2, 6.8 Hz, 1H), 2.80 (dd, *J* = 16.3, 8.2 Hz, 1H); ^{13}C NMR (101 MHz, $CDCl_3$) δ 187.9, 159.6, 153.3, 146.8, 146.3, 135.9, 135.6, 130.3, 129.0, 128.9, 128.4, 128.3, 127.74, 127.72, 120.4, 115.5, 114.4, 110.8, 110.6, 60.2, 57.5, 55.9, 55.3, 51.02, 50.99, 44.4, 29.7, 29.3; FTIR (KBr, cm^{-1}) 2923, 1593, 1511, 1439, 1250, 1130, 732; HRMS (ESI, TOF) *m/e* calculated for $[M+H]^+$ $C_{34}H_{35}N_2O_4$: 535.2591, found 535.2584.

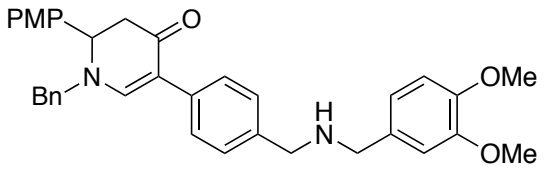

1-Benzyl-5-(4-(((3,4-dimethoxybenzyl)amino)methyl)phenyl)-2-(4-methoxyphenyl)-2,3-dihydropyridin-4(1*H*)-one (5.26):

Compound **5.26** was prepared by **Method B** described above and 48.2 mg (66%) was isolated as yellow oil. ^{1}H NMR (400 MHz, $CDCl_3$) δ 7.53 (s, 1H), 7.47 – 7.40 (m, 2H), 7.40 – 7.27 (m, 5H), 7.23 – 7.12 (m, 4H), 6.94 (d, *J* = 1.9 Hz, 1H), 6.92 – 6.83 (m, 3H), 6.82 (d, *J* = 8.1 Hz, 1H), 5.20 (br, 1H), 4.52 (dd, *J* = 8.2, 6.8 Hz, 1H), 4.41 (d, *J* = 15.1 Hz, 1H), 4.20 (d, *J* = 15.2 Hz, 1H), 3.88 (s, 3H), 3.86 (s, 3H), 3.82 (s, 2H), 3.81 (s, 3H), 3.78 (s, 2H), 2.95 (dd, *J* = 16.2, 6.8 Hz, 1H), 2.81 (dd, *J* = 16.2, 8.3

Hz, 1H); ^{13}C NMR (101 MHz, $CDCl_3$) δ 187.9, 159.6, 153.1, 149.0, 148.4, 135.9, 135.4, 130.3, 129.0, 128.6, 128.4, 128.32, 128.27, 127.7, 127.7, 120.8, 114.4, 111.8, 111.0, 110.7, 60.3, 57.5, 55.9, 55.3, 53.8, 51.6, 44.4, 29.3; FTIR (KBr, cm^{-1}) 2932, 2600, 1636, 1595, 1513, 1253, 1028, 810, 734; HRMS (ESI, TOF) *m/e* calculated for $[M+H]^+$ $C_{35}H_{37}N_2O_4$: 549.2748, found 549.2765.

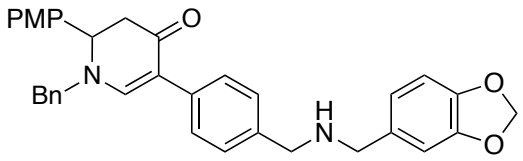

5-(4-(((Benzo[*d*][1,3]dioxol-5-ylmethyl)amino)methyl)phenyl)-1-benzyl-2-(4-methoxyphenyl)-2,3-dihydropyridin-4(1*H*)-one (5.27):

Compound **5.27** was prepared by **Method B** described above and 55.3 mg (78%) was isolated as yellow oil. ^{1}H NMR (400 MHz, $CDCl_3$) δ 7.53 (s, 1H), 7.46 – 7.40 (m, 2H), 7.39 – 7.32 (m, 3H), 7.32 – 7.27 (m, 2H), 7.22 – 7.12 (m, 4H), 6.93 – 6.84 (m, 3H), 6.83 – 6.69 (m, 2H), 5.93 (s, 2H), 5.24 (br, 1H), 4.51 (dd, *J* = 8.2, 6.8 Hz, 1H), 4.41 (d, *J* = 15.1 Hz, 1H), 4.20 (d, *J* = 15.1 Hz, 1H), 3.81 (s, 3H), 3.80 (s, 2H), 3.74 (s, 2H), 2.94 (dd, *J* = 16.2, 6.8 Hz, 1H), 2.81 (dd, *J* = 16.2, 8.3 Hz, 1H); ^{13}C NMR (101 MHz, $CDCl_3$) δ 188.0, 159.6, 153.1, 147.8, 146.8, 135.9, 135.5, 135.3, 132.2, 130.4, 129.0, 128.5, 128.4, 128.3, 127.7, 121.9, 114.4, 110.8, 109.1, 108.2, 101.0, 60.3, 57.4, 55.3, 51.72, 51.67, 44.4, 29.3,; FTIR (KBr, cm^{-1}) 2923, 1633, 1595, 1511, 1444, 1251, 1036, 734; HRMS (ESI, TOF) *m/e* calculated for $[M+H]^+$ $C_{34}H_{33}N_2O_4$: 533.2435, found 533.2436.

6.5.3 Biological evaluation

6.5.3.1 Antiproliferation assay with alamarBlue

A549/NF-κB-luc cancer cells were cultured with DMEM (ATCC P/N 30-2002) with 10% FBS, penicillin, streptomycin and hygromycin and DU-145 cancer cells were cultured with ENEM (30-2003) with 10% FBS in T-75 culture flasks. Cancer cells were incubated at 5% CO_2 and 37 °C, and subcultured with 90% confluency. The cancer cells were harvested from an exponential-phase maintenance culture with 125 G centrifuge for 5 min. Then the cells were re-suspended in new culture media as used above (DMEM (ATCC P/N 30-2002) with 10% FBS, penicillin, streptomycin and hygromycin) (A549/NF-κB-luc), and ENEM (30-2003) with 10% FBS (DU-145)). The cells were adjusted to 10^5 cells/mL and dispensed in 96-well culture plates with a density of 5000 cells per well (50 μL), then the cells were incubated overnight. Assay concentrations of the test compounds were prepared via serial dilution with fresh culture medium from 20 mM stock solutions of compounds in DMSO. The culture medium (50 μL) containing varying concentrations of the test and control compounds was added to each well. AlamarBlue (10 μL) was added to each well after 72 h. After 1.5 h, the fluorescence excitation (530 nm) and emission (590 nm) of each well were measured for the optical density. Each compound was tested in triplicate with less than 5% variation.

6.5.3.2 Cell-based NF-κB Functional Assay

A549/NF-κB-luc cells were cultured with growth medium (ATCC P/N 30-2002, 10% FBS, penicillin and streptomycin) containing hygromycin at 37 °C with 5% CO_2. After trypsinizing and centrifuging the cells (150 × G for 5 min), The cells were adjusted to 10^5 cells/mL and dispensed in 96-well culture plates with a density of 5000 cells per well (50 μL), then the cells were incubated for 24 h. The test compound with varying concentration in the complete growth medium (50 μL) was added to each well. After 30 min, TNF-α (5 μL of TNF-α solution in 1X PBS (1:667 dilution of TNF-α in 1X PBS)) was added to each well Luciferin reagent (100 μL; Bright-Glo™ from Promega) was added to each well after another 7 h. After 2 min, luciferase activity was measured. Each compound was tested in triplicate with less than 5% variation.

6.5.3.3 Western Blot Analysis

For the preparation of cell lysates from cell lines, A549 cells (1×10^6) treated with different concentration of compound **5.23** were harvested and incubated in RIPA buffer with protease inhibitor and phophatase inhibitor (Pierce, Rockford, IL) for 10 min on ice. The preparations were centrifuged (14,000 *g* for 10 min at 4°C), the supernatants collected, the protein concentration measured using a BCA protein assay kit (Pierce, Rockford, IL), samples aliquoted and stored at −80°C.

For western immunoblotting, 50 μg for cell culture sample were electrophoresed on a 4-12 % Novex Tris–glycine gel (Invitrogen, Carlsbad, CA), and transferred to a polyvinylidene difluoride (PVDF) membrane (Bio-Rad). After blocking with tris-buffered saline (TBS) containing 0.05% Tween20 (TBST) and 5% non-fat powdered milk, the membrane was incubated with the primary antibody solution at 4^{o}C overnight. Subsequently, the membrane was washed with TBST and incubated with the appropriate horseradish peroxidase-conjugated secondary antibody for 1 h at room temperature. The protein-antibody complexes were detected by enhanced chemiluminescence (ECL kit) in accordance with the manufacturer's directions (Pierce, Rockford, IL). All membranes were stripped and reprobed with anti-β-actin (1:1000) to check for differences in the amount of protein loaded in each lane. For each protein, at least three western assays were carried out. For quantitative determination of protein levels, densitometric measurements of Western blot bands were performed using digitalized scientific software program UN-SCAN-IT software (Silk Scientific, Orem, Utah). Anti-phospho-p65, anti-Iκbα, anti-β-actin and were from Cell Signaling Technology (Beverly, MA).

6.5.3.4 Kinase assay

Reaction Biology Corp. (Malvern, PA) performed the kinase assay of IKKβ with compound **5.23** as follows: IKKtide was prepared in fresh base reaction buffer (20 mM Hepes (pH 7.5), 10 mM $MgCl_2$, 1 mM EGTA, 0.02% Brij35, 0.02 mg/ml BSA, 0.1 mM Na_3VO_4, 2 mM DTT, 1% DMSO). IKKβ was delivered into the solution,

which was gently mixed. Compound **5.23** in DMSO was delivered to the reaction mixture, and then ^{33}P-ATP (specific activity 0.01 μCi/μl final) was added to initiate the reaction. After the incubation for 120 min at room temperature, reactions are spotted onto P81 ion exchange paper (Whatman # 3698-915). Filters were washed extensively in 0.75% Phosphoric acid. Compound **5.23** was tested in 10-dose IC_{50} mode in duplicate with 2-fold serial dilution starting at 100 μM. Control compound Staurosporine was tested in 10-dose IC_{50} mode with 3-fold serial dilution starting at 20 μM.

6.5.4 Computational simulation

6.5.4.1 Homology modeling

The crystal structure of *Xenopus laevis* (African Clawed Frog)-derived IKKβ (PDB ID: 3RZF, 76% identical to human IKKβ) was imported from the RSCB Protein Data Bank (www.pdb.org) and used as a template for the homology model. The sequence file of human human IKKβ was imported from www.uniprot.org (O14920). The sequence alignment and homology modeling were performed in Prime.[91] The initially constructed model underwent energy minimization in MacroModel[93] with OPLS2005 in water. The minimization was set to stop either at the maximum iteration of 5,000 or at the convergence threshold of 0.05. Selecting Leu21, Lys44, Ala42, Met96, Glu97, Tyr98, Cys99, Gln100, Gly102, Asp103 and Lys106 in Glide[92] generated a grid of the homology model.

6.5.4.2 Molecular docking

Compound **5.23** used for this study was prepared in LigPrep.[94] Docking simulations of compound **5.23** in human IKKβ homology model were performed in the XP flexible docking mode with input ring conformation and post docking minimization. Docked compounds were merged with the protein and the complex underwent energy minimization. Energy minimizations of the model structures were performed in MacroModel. OPLS2005 force field was used and the minimization was set up to stop either at maximum iteration of 5,000 or at the threshold gradient of 0.05.

6.6 X-Ray crystallographic structure of 4.23

REFERENCE NUMBER: 12195a

CRYSTAL STRUCTURE REPORT

$C_{27}H_{27}NO_5$

Report prepared for:

Yong Wook Kim / Prof. G. Georg

September 21, 2012

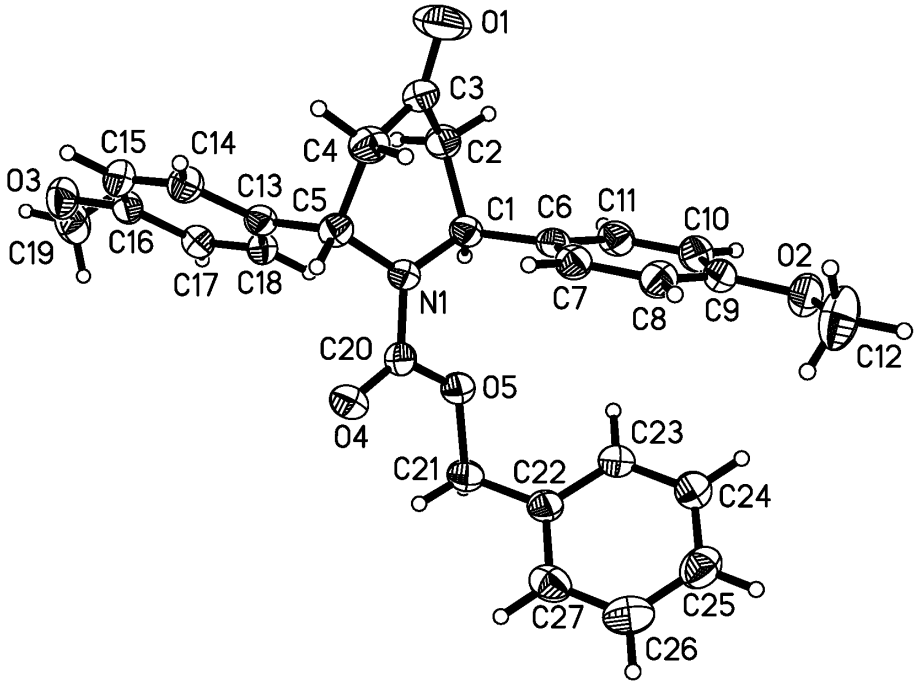

Victor G. Young, Jr.
X-Ray Crystallographic Laboratory
Department of Chemistry
University of Minnesota
207 Pleasant St. S.E.

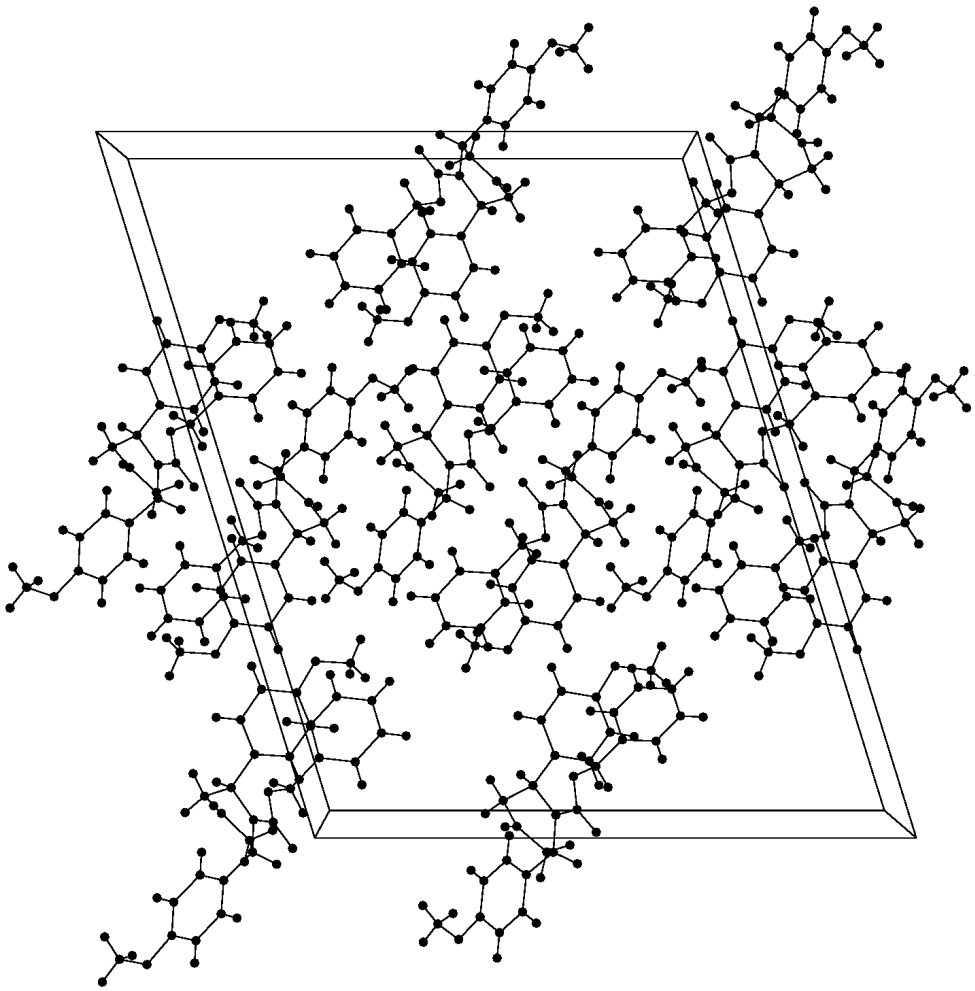

Data collection

A crystal (approximate dimensions 0.40 x 0.26 x 0.08 mm^3) was placed onto the tip of a 0.1 mm diameter glass capillary and mounted on a Bruker APEX-II CCD diffractometer for a data collection at 173(2) K.[1] A preliminary set of cell constants was calculated from reflections harvested from three sets of 12 frames. These initial sets of frames were oriented such that orthogonal wedges of reciprocal space were surveyed. This produced initial orientation matrices determined from 45 reflections.

The data collection was carried out using MoKa radiation (graphite monochromator) with a frame time of 60 seconds and a detector distance of 6.0 cm. A randomly oriented region of reciprocal space was surveyed to the extent of one sphere and to a resolution of 0.80 Å. Four major sections of frames were collected with 0.50º steps in w at four different f settings and a detector position of -28º in 2q. The intensity data were corrected for absorption and decay (SADABS).[2] Final cell constants were calculated from 2786 strong reflections from the actual data collection after integration (SAINT).[3] Please refer to Table 1 for additional crystal and refinement information.

Structure solution and refinement

The structure was solved using SHELXS-2008 (Sheldrick, 2008/1)[4] and refined using SHELXL-2008 (Sheldrick, 2008/1).[4] The space group C2/c was determined based on systematic absences and intensity statistics. A direct-methods solution was calculated which provided most non-hydrogen atoms from the E-map. Full-matrix least squares / difference Fourier cycles were performed which located the remaining non-hydrogen atoms. All non-hydrogen atoms were refined with anisotropic displacement parameters. All hydrogen atoms were placed in ideal positions and refined as riding atoms with relative isotropic displacement parameters. The final full matrix least squares refinement converged to $R1 = 0.0417$ and $wR2 = 0.1070$ (F^2, obs. data).

Structure description

The structure is the one suggested. The molecules are positioned on general sites. The 4-methoxyphenyl groups are *trans* with respect to C1 and C5.

Data collection and structure solution were conducted at the X-Ray Crystallographic Laboratory, 193 Kolthoff Hall, Department of Chemistry, University of Minnesota. All calculations were performed using Pentium computers using the current SHELXTL suite of programs. All publications arising from this report MUST either 1) include Victor G. Young, Jr. as a coauthor or 2) acknowledge Victor G. Young, Jr. and the X-Ray Crystallographic Laboratory.

[1] APEX-2, Bruker Analytical X-ray Systems, Madison, WI (2010).

[2] An empirical correction for absorption anisotropy, R. Blessing, *Acta Cryst.* **A51**, 33-38 (1995).

[3] SAINT+ V7.68, Bruker Analytical X-Ray Systems, Madison, WI (2010).

[4] SHELX-2008/1, Bruker Analytical X-Ray Systems, Madison, WI (2008).

Some equations of interest:

$$R_{int} = \Sigma\ |F_o^2 - < F_o^2 >| \ / \ \Sigma|F_o^2|$$

$$R_1 = \Sigma||F_o|-|F_c|| \ / \ \Sigma|F_o|$$

$$wR2 = [\Sigma[w(F_o^2-F_c^2)^2] \ / \ \Sigma\ [w(F_o^2)^2]]^{1/2}$$

where $w = q \ / \ [\sigma^2\ (F_o^2) + (a*P)^2 + b*P + d + e*\sin(\theta)]$

$$\text{GooF} = S = [\Sigma[w(F_o^2-F_c^2)^2] \ / \ (n-p)]^{1/2}$$

Table 1. Crystal data and structure refinement for 12195a.

Identification code	12195a	
Empirical formula	$C_{27}\ H_{27}\ N\ O_5$	
Formula weight	445.50	
Temperature	173(2) K	
Wavelength	0.71073 Å	
Crystal system	Monoclinic	
Space group	C2/c	
Unit cell dimensions	a = 27.410(3) Å	α = 90°
	b = 7.7863(8) Å	β = 107.210(1)°
	c = 22.292(2) Å	γ = 90°
Volume	4544.6(8) Å^3	
Z	8	
Density (calculated)	1.302 Mg/m^3	
Absorption coefficient	0.090 mm^{-1}	
F(000)	1888	
Crystal color, morphology	colorless, plate	
Crystal size	0.40 x 0.26 x 0.08 mm^3	
Theta range for data collection	2.08 to 26.41°	
Index ranges	$-34 \le h \le 32$, $0 \le k \le 9$, $0 \le l \le 27$	
Reflections collected	20393	
Independent reflections	4658 [R(int) = 0.0384]	
Observed reflections	3326	
Completeness to theta = 26.41°	99.8%	
Absorption correction	multi-scan	
Max. and min. transmission	0.9929 and 0.9650	
Refinement method	Full-matrix least-squares on F^2	
Data / restraints / parameters	4658 / 0 / 300	
Goodness-of-fit on F^2	1.029	
Final R indices [I>2sigma(I)]	R1 = 0.0417, wR2 = 0.0941	
R indices (all data)	R1 = 0.0670, wR2 = 0.1070	
Largest diff. peak and hole	0.153 and -0.192 e.Å^{-3}	

Table 2. Atomic coordinates (x 10^4) and equivalent isotropic displacement parameters ($Å^2$x 10^3) for 12195a. U_{eq} is defined as one third of the trace of the orthogonalized U_{ij} tensor.

	x	y	z	U_{eq}
O1	310(1)	13753(2)	3278(1)	74(1)
O2	2467(1)	11596(2)	5868(1)	43(1)
O3	-1611(1)	6817(2)	1785(1)	46(1)
O4	-32(1)	7292(2)	4701(1)	39(1)
O5	764(1)	6932(1)	4609(1)	37(1)
N1	290(1)	9128(2)	4120(1)	28(1)
C1	727(1)	9578(2)	3893(1)	30(1)
C2	559(1)	10820(2)	3336(1)	35(1)
C3	257(1)	12314(2)	3450(1)	39(1)
C4	-116(1)	11927(2)	3804(1)	36(1)
C5	-202(1)	10010(2)	3892(1)	30(1)
C6	1175(1)	10254(2)	4418(1)	29(1)
C7	1120(1)	10994(2)	4959(1)	32(1)
C8	1540(1)	11485(2)	5450(1)	34(1)
C9	2025(1)	11234(2)	5402(1)	34(1)
C10	2089(1)	10533(2)	4857(1)	38(1)
C11	1670(1)	10049(2)	4375(1)	35(1)
C12	2422(1)	12352(3)	6425(1)	64(1)
C13	-560(1)	9137(2)	3316(1)	28(1)
C14	-1061(1)	9731(2)	3070(1)	36(1)
C15	-1398(1)	8940(2)	2562(1)	39(1)
C16	-1247(1)	7513(2)	2287(1)	34(1)
C17	-755(1)	6886(2)	2526(1)	32(1)
C18	-420(1)	7702(2)	3039(1)	30(1)
C19	-1458(1)	5403(3)	1472(1)	52(1)
C20	313(1)	7743(2)	4497(1)	30(1)
C21	862(1)	5495(2)	5045(1)	42(1)
C22	1265(1)	5960(2)	5643(1)	35(1)
C23	1690(1)	6915(2)	5633(1)	43(1)

C24	2068(1)	7300(2)	6180(1)	49(1)
C25	2027(1)	6733(2)	6748(1)	47(1)
C26	1609(1)	5779(2)	6768(1)	49(1)
C27	1228(1)	5389(2)	6217(1)	40(1)

Table 3. Bond lengths [Å] and angles [°] for 12195a.

O(1)-C(3)	1.208(2)	C(11)-H(11A)	0.9500
O(2)-C(9)	1.373(2)	C(12)-H(12A)	0.9800
O(2)-C(12)	1.412(2)	C(12)-H(12B)	0.9800
O(3)-C(16)	1.3713(19)	C(12)-H(12C)	0.9800
O(3)-C(19)	1.431(2)	C(13)-C(18)	1.385(2)
O(4)-C(20)	1.2173(18)	C(13)-C(14)	1.397(2)
O(5)-C(20)	1.3441(19)	C(14)-C(15)	1.377(2)
O(5)-C(21)	1.4548(19)	C(14)-H(14A)	0.9500
N(1)-C(20)	1.357(2)	C(15)-C(16)	1.391(2)
N(1)-C(5)	1.4635(19)	C(15)-H(15A)	0.9500
N(1)-C(1)	1.4743(19)	C(16)-C(17)	1.384(2)
C(1)-C(6)	1.518(2)	C(17)-C(18)	1.390(2)
C(1)-C(2)	1.534(2)	C(17)-H(17A)	0.9500
C(1)-H(1A)	1.0000	C(18)-H(18A)	0.9500
C(2)-C(3)	1.493(2)	C(19)-H(19A)	0.9800
C(2)-H(2A)	0.9900	C(19)-H(19B)	0.9800
C(2)-H(2B)	0.9900	C(19)-H(19C)	0.9800
C(3)-C(4)	1.495(2)	C(21)-C(22)	1.502(2)
C(4)-C(5)	1.533(2)	C(21)-H(21A)	0.9900
C(4)-H(4A)	0.9900	C(21)-H(21B)	0.9900
C(4)-H(4B)	0.9900	C(22)-C(27)	1.388(2)
C(5)-C(13)	1.526(2)	C(22)-C(23)	1.388(2)
C(5)-H(5A)	1.0000	C(23)-C(24)	1.378(3)
C(6)-C(7)	1.384(2)	C(23)-H(23A)	0.9500
C(6)-C(11)	1.398(2)	C(24)-C(25)	1.375(3)
C(7)-C(8)	1.387(2)	C(24)-H(24A)	0.9500
C(7)-H(7A)	0.9500	C(25)-C(26)	1.376(3)
C(8)-C(9)	1.379(2)	C(25)-H(25A)	0.9500
C(8)-H(8A)	0.9500	C(26)-C(27)	1.390(3)
C(9)-C(10)	1.389(2)	C(26)-H(26A)	0.9500
C(10)-C(11)	1.374(2)	C(27)-H(27A)	0.9500
C(10)-H(10A)	0.9500		

C(9)-O(2)-C(12)	117.61(14)	C(7)-C(6)-C(11)	117.83(15)
C(16)-O(3)-C(19)	117.12(14)	C(7)-C(6)-C(1)	122.91(14)
C(20)-O(5)-C(21)	117.57(13)	C(11)-C(6)-C(1)	119.17(14)
C(20)-N(1)-C(5)	117.17(12)	C(6)-C(7)-C(8)	121.51(15)
C(20)-N(1)-C(1)	120.47(13)	C(6)-C(7)-H(7A)	119.2
C(5)-N(1)-C(1)	121.98(12)	C(8)-C(7)-H(7A)	119.2
N(1)-C(1)-C(6)	111.93(12)	C(9)-C(8)-C(7)	119.59(15)
N(1)-C(1)-C(2)	110.29(13)	C(9)-C(8)-H(8A)	120.2
C(6)-C(1)-C(2)	112.75(13)	C(7)-C(8)-H(8A)	120.2
N(1)-C(1)-H(1A)	107.2	O(2)-C(9)-C(8)	124.65(15)
C(6)-C(1)-H(1A)	107.2	O(2)-C(9)-C(10)	115.41(15)
C(2)-C(1)-H(1A)	107.2	C(8)-C(9)-C(10)	119.93(16)
C(3)-C(2)-C(1)	113.71(13)	C(11)-C(10)-C(9)	119.90(16)
C(3)-C(2)-H(2A)	108.8	C(11)-C(10)-H(10A)	120.0
C(1)-C(2)-H(2A)	108.8	C(9)-C(10)-H(10A)	120.0
C(3)-C(2)-H(2B)	108.8	C(10)-C(11)-C(6)	121.20(15)
C(1)-C(2)-H(2B)	108.8	C(10)-C(11)-H(11A)	119.4
H(2A)-C(2)-H(2B)	107.7	C(6)-C(11)-H(11A)	119.4
O(1)-C(3)-C(2)	122.90(17)	O(2)-C(12)-H(12A)	109.5
O(1)-C(3)-C(4)	121.44(17)	O(2)-C(12)-H(12B)	109.5
C(2)-C(3)-C(4)	115.66(14)	H(12A)-C(12)-H(12B)	109.5
C(3)-C(4)-C(5)	114.82(14)	O(2)-C(12)-H(12C)	109.5
C(3)-C(4)-H(4A)	108.6	H(12A)-C(12)-H(12C)	109.5
C(5)-C(4)-H(4A)	108.6	H(12B)-C(12)-H(12C)	109.5
C(3)-C(4)-H(4B)	108.6	C(18)-C(13)-C(14)	117.54(15)
C(5)-C(4)-H(4B)	108.6	C(18)-C(13)-C(5)	122.67(14)
H(4A)-C(4)-H(4B)	107.5	C(14)-C(13)-C(5)	119.71(14)
N(1)-C(5)-C(13)	112.29(13)	C(15)-C(14)-C(13)	121.14(16)
N(1)-C(5)-C(4)	109.92(13)	C(15)-C(14)-H(14A)	119.4
C(13)-C(5)-C(4)	114.20(13)	C(13)-C(14)-H(14A)	119.4
N(1)-C(5)-H(5A)	106.6	C(14)-C(15)-C(16)	120.33(15)
C(13)-C(5)-H(5A)	106.6	C(14)-C(15)-H(15A)	119.8
C(4)-C(5)-H(5A)	106.6	C(16)-C(15)-H(15A)	119.8

O(3)-C(16)-C(17)	124.49(16)
O(3)-C(16)-C(15)	115.84(15)
C(17)-C(16)-C(15)	119.68(15)
C(16)-C(17)-C(18)	119.17(15)
C(16)-C(17)-H(17A)	120.4
C(18)-C(17)-H(17A)	120.4
C(13)-C(18)-C(17)	122.13(15)
C(13)-C(18)-H(18A)	118.9
C(17)-C(18)-H(18A)	118.9
O(3)-C(19)-H(19A)	109.5
O(3)-C(19)-H(19B)	109.5
H(19A)-C(19)-H(19B)	109.5
O(3)-C(19)-H(19C)	109.5
H(19A)-C(19)-H(19C)	109.5
H(19B)-C(19)-H(19C)	109.5
O(4)-C(20)-O(5)	124.67(15)
O(4)-C(20)-N(1)	124.21(15)
O(5)-C(20)-N(1)	111.12(13)
O(5)-C(21)-C(22)	110.45(13)
O(5)-C(21)-H(21A)	109.6
C(22)-C(21)-H(21A)	109.6
O(5)-C(21)-H(21B)	109.6
C(22)-C(21)-H(21B)	109.6
H(21A)-C(21)-H(21B)	108.1
C(27)-C(22)-C(23)	118.50(17)
C(27)-C(22)-C(21)	120.32(16)
C(23)-C(22)-C(21)	121.14(16)
C(24)-C(23)-C(22)	121.06(17)
C(24)-C(23)-H(23A)	119.5
C(22)-C(23)-H(23A)	119.5
C(25)-C(24)-C(23)	120.04(18)
C(25)-C(24)-H(24A)	120.0
C(23)-C(24)-H(24A)	120.0
C(24)-C(25)-C(26)	119.86(19)
C(24)-C(25)-H(25A)	120.1
C(26)-C(25)-H(25A)	120.1
C(25)-C(26)-C(27)	120.27(17)
C(25)-C(26)-H(26A)	119.9
C(27)-C(26)-H(26A)	119.9
C(22)-C(27)-C(26)	120.26(17)
C(22)-C(27)-H(27A)	119.9
C(26)-C(27)-H(27A)	119.9

Symmetry transformations used to generate equivalent atoms:

Table 4. Anisotropic displacement parameters ($Å^2 x\ 10^3$) for 12195a. The anisotropic displacement factor exponent takes the form: $-2\pi^2[\ h^2\ a^{*2}U_{11} + ...\ + 2\ h\ k\ a^*\ b^*\ U_{12}\ ]$

	U_{11}	U_{22}	U_{33}	U_{23}	U_{13}	U_{12}
O1	71(1)	46(1)	113(1)	38(1)	40(1)	10(1)
O2	35(1)	47(1)	41(1)	-2(1)	1(1)	-2(1)
O3	35(1)	54(1)	43(1)	-3(1)	2(1)	-8(1)
O4	39(1)	38(1)	41(1)	8(1)	15(1)	-4(1)
O5	32(1)	31(1)	45(1)	10(1)	7(1)	1(1)
N1	28(1)	29(1)	28(1)	4(1)	9(1)	-1(1)
C1	32(1)	29(1)	28(1)	1(1)	11(1)	-2(1)
C2	38(1)	40(1)	27(1)	3(1)	9(1)	-5(1)
C3	39(1)	34(1)	37(1)	10(1)	1(1)	-2(1)
C4	43(1)	30(1)	35(1)	-2(1)	9(1)	3(1)
C5	31(1)	32(1)	28(1)	1(1)	10(1)	3(1)
C6	32(1)	25(1)	31(1)	5(1)	10(1)	0(1)
C7	32(1)	27(1)	37(1)	2(1)	11(1)	4(1)
C8	38(1)	30(1)	34(1)	-2(1)	8(1)	2(1)
C9	33(1)	28(1)	37(1)	4(1)	3(1)	-3(1)
C10	30(1)	42(1)	42(1)	6(1)	12(1)	-2(1)
C11	36(1)	38(1)	34(1)	1(1)	15(1)	-2(1)
C12	49(1)	78(2)	54(1)	-26(1)	-2(1)	2(1)
C13	28(1)	29(1)	29(1)	4(1)	10(1)	0(1)
C14	32(1)	34(1)	41(1)	3(1)	13(1)	5(1)
C15	26(1)	44(1)	44(1)	8(1)	8(1)	3(1)
C16	29(1)	42(1)	30(1)	4(1)	6(1)	-7(1)
C17	33(1)	31(1)	35(1)	0(1)	12(1)	-2(1)
C18	26(1)	32(1)	32(1)	3(1)	8(1)	0(1)
C19	48(1)	61(1)	45(1)	-13(1)	10(1)	-19(1)
C20	29(1)	30(1)	29(1)	0(1)	6(1)	-2(1)
C21	40(1)	27(1)	55(1)	13(1)	6(1)	-1(1)
C22	32(1)	26(1)	44(1)	9(1)	9(1)	4(1)

C23	38(1)	43(1)	44(1)	15(1)	7(1)	-4(1)
C24	38(1)	44(1)	56(1)	14(1)	3(1)	-4(1)
C25	50(1)	40(1)	44(1)	1(1)	2(1)	6(1)
C26	65(1)	45(1)	41(1)	6(1)	23(1)	9(1)
C27	40(1)	31(1)	55(1)	6(1)	22(1)	5(1)

Table 5. Hydrogen coordinates (x 10^4) and isotropic displacement parameters ($Å^2$ x 10^3) for 12195a.

	x	y	z	U(eq)
H1A	843	8497	3735	35
H2A	866	11254	3238	42
H2B	351	10182	2964	42
H4A	-448	12457	3578	44
H4B	5	12473	4223	44
H5A	-369	9923	4234	36
H7A	786	11170	4994	38
H8A	1493	11992	5817	41
H10A	2423	10389	4819	45
H11A	1718	9566	4005	42
H12A	2763	12548	6716	96
H12B	2230	11583	6620	96
H12C	2242	13450	6325	96
H14A	-1170	10699	3256	43
H15A	-1736	9370	2399	46
H17A	-647	5911	2343	39
H18A	-84	7261	3205	36
H19A	-1746	5048	1114	78
H19B	-1354	4440	1765	78
H19C	-1172	5751	1321	78
H21A	975	4489	4851	51
H21B	543	5181	5141	51
H23A	1722	7309	5243	51
H24A	2356	7956	6165	58
H25A	2286	7001	7125	57
H26A	1582	5385	7160	59
H27A	941	4728	6234	48

Table 6. Torsion angles [°] for 12195a.

C20-N1-C1-C6	-70.23(18)	N1-C5-C13-C18	-1.7(2)
C5-N1-C1-C6	117.11(15)	C4-C5-C13-C18	124.32(16)
C20-N1-C1-C2	163.38(14)	N1-C5-C13-C14	174.84(13)
C5-N1-C1-C2	-9.29(19)	C4-C5-C13-C14	-59.15(19)
N1-C1-C2-C3	49.24(18)	C18-C13-C14-C15	-1.3(2)
C6-C1-C2-C3	-76.69(17)	C5-C13-C14-C15	-178.01(14)
C1-C2-C3-O1	140.00(19)	C13-C14-C15-C16	0.6(3)
C1-C2-C3-C4	-39.2(2)	C19-O3-C16-C17	-3.4(2)
O1-C3-C4-C5	170.32(17)	C19-O3-C16-C15	176.89(15)
C2-C3-C4-C5	-10.4(2)	C14-C15-C16-O3	179.92(14)
C20-N1-C5-C13	-82.67(16)	C14-C15-C16-C17	0.2(2)
C1-N1-C5-C13	90.23(16)	O3-C16-C17-C18	-179.86(14)
C20-N1-C5-C4	149.03(14)	C15-C16-C17-C18	-0.2(2)
C1-N1-C5-C4	-38.07(19)	C14-C13-C18-C17	1.4(2)
C3-C4-C5-N1	48.06(19)	C5-C13-C18-C17	177.96(14)
C3-C4-C5-C13	-79.18(18)	C16-C17-C18-C13	-0.6(2)
N1-C1-C6-C7	-24.0(2)	C21-O5-C20-O4	-5.1(2)
C2-C1-C6-C7	101.02(17)	C21-O5-C20-N1	175.42(13)
N1-C1-C6-C11	152.63(14)	C5-N1-C20-O4	-7.0(2)
C2-C1-C6-C11	-82.33(18)	C1-N1-C20-O4	179.99(14)
C11-C6-C7-C8	-1.5(2)	C5-N1-C20-O5	172.49(13)
C1-C6-C7-C8	175.23(14)	C1-N1-C20-O5	-0.5(2)
C6-C7-C8-C9	0.0(2)	C20-O5-C21-C22	-110.14(16)
C12-O2-C9-C8	-3.1(2)	O5-C21-C22-C27	142.12(15)
C12-O2-C9-C10	178.41(17)	O5-C21-C22-C23	-40.1(2)
C7-C8-C9-O2	-176.85(15)	C27-C22-C23-C24	-0.4(3)
C7-C8-C9-C10	1.6(2)	C21-C22-C23-C24	-178.20(17)
O2-C9-C10-C11	176.85(15)	C22-C23-C24-C25	0.1(3)
C8-C9-C10-C11	-1.7(2)	C23-C24-C25-C26	0.2(3)
C9-C10-C11-C6	0.3(3)	C24-C25-C26-C27	-0.2(3)
C7-C6-C11-C10	1.3(2)	C23-C22-C27-C26	0.3(3)
C1-C6-C11-C10	-175.50(15)	C21-C22-C27-C26	178.19(16)

C25-C26-C27-C22 -0.1(3)

Symmetry transformations used to generate equivalent atoms:

Chapter 7

Bibliography

(1) Michael, J. P. *Nat. Prod. Rep.* **2008**, *25*, 139–165.

(2) Joseph, S.; Comins, D. L. *Curr. Opin. Drug Discovery Dev.* **2002**, *5*, 870–880.

(3) Comins, D. L.; Hong, H. *J. Am. Chem. Soc.* **1991**, *113*, 6672–6673.

(4) Comins, D. L.; Hong, H. *J. Am. Chem. Soc.* **1993**, *115*, 8851–8852.

(5) Brimioulle, R.; Bach, T. *Science* **2013**, *342*, 840–843.

(6) McCall, W. S.; Grillo, T. A.; Comins, D. L. *J. Org. Chem.* **2008**, *73*, 9744–9751.

(7) Comins, D. L.; Kuethe, J. T.; Miller, T. M.; Février, F. C.; Brooks, C. a. *J. Org. Chem.* **2005**, *70*, 5221–5234.

(8) Comins, D.; Joseph, S.; Chen, X. *Tetrahedron Lett.* **1995**, *36*, 9141–9144.

(9) (a) Comins, D. L.; Chen, X.; Morgan, L. a. *J. Org. Chem.* **1997**, *62*, 7435–7438. (b) Sharma, V. M.; Adi Seshu, K. V.; Vamsee Krishna, C.; Prasanna, P.; Chandra Sekhar, V.; Venkateswarlu, a.; Rajagopal, S.; Ajaykumar, R.; Deevi, D. S.; Rao Mamidi, N. V. S.; Rajagopalan, R. *Bioorg. Med. Chem. Lett.* **2003**, *13*, 1679–1682.

(10) Comins, D.; Ollinger, C. *Tetrahedron Lett.* **2001**, *42*, 4115–4118.

(11) Comins, D. L.; Hiebel, a C.; Huang, S. *Org. Lett.* **2001**, *3*, 769–771.

(12) Wang, X.; Turunen, B. J.; Leighty, M. W.; Georg, G. I. *Tetrahedron Lett.* **2007**, *48*, 8811–8814.

(13) Ge, H.; Niphakis, M. J.; Georg, G. I. *J. Am. Chem. Soc.* **2008**, *130*, 3708–3709.

(14) Bi, L.; Georg, G. I. *Org. Lett.* **2011**, *13*, 5413–5415.

(15) (a) Yu, Y.-Y.; Niphakis, M. J.; Georg, G. I. *Org. Lett.* **2011**, *13*, 5932–5935. (b) DOI: 10.1002/adsc.201300904

(16) (a) Niphakis, M. J.; Georg, G. I. *J. Org. Chem.* **2010**, *75*, 6019–6022. (b) Chen, X.; Chu, Y.; Han, G. *Zhongguo Yaolixue Tongbao* **1998**, *14*,167–169. (c) Chen, X.; Chu, Y. *Zhongguo Yaolixue Tongbao* **1998**, *14*, 243–244. (d) Wang, L.; Chu, Y. *Yaoxue Xuebao* **1996**, *31*, 806–811. (e) Lee, S. K.; Nam, K.-A.; Heo, Y.-H. *Planta Med.*, **2003**, *69*, 21–25.

(17) (a) Leighty, M. W.; Georg, G. I. *ACS Med. Chem. Lett.* **2011**, *2*, 313-315. (b) Yan, J.; Luo, D.; Luo, Y.; Gao, X.; Zhang, G. *Int. J. Gynecol. Cancer* **2006**, *16*, 165 – 170.

(18) Niphakis, M. J.; Georg, G. I. *Org. Lett.* **2011**, *13*, 196–199.

(19) (a) Farina, V.; Kapadia, S.; Krishnan, B.; Wang, C.; Liebeskind, L. S. *J. Org. Chem.* **1994**, *59*, 5905–5911. (b) Mee, S. P. H.; Lee, V.; Baldwin, J. E. *Angew. Chem., Int. Ed.* **2004**, *43*, 1132–1136. (c) Han, X.; Stoltz, B. M.; Corey, E. J. *J. Am. Chem. Soc.* **1999**, *121*, 7600–7605.

(20) (a) Li, J.-H.; Li, J.-L.; Wang, D.-P.; Pi, S.-F.; Xie, Y.-X.; Zhang, M.-B.; Hu, X.-C. *J. Org. Chem.* **2007**, *72*, 2053–2057. (b) Savarin, C.; Liebeskind, L. S. *Org. Lett.* **2001**, *3*, 2149–2152. (c) Thathagar, M. B.; Beckers, J.; Rothenberg, G. *J. Am. Chem. Soc.* **2002**, *124*, 11858–11859.

(21) Chinchilla, R.; Najera, C. *Chem. Soc. Rev*. **2011**, *50*, 5084–5121.

(22) (a) Deng, J. Z.; Paone, D. V.; Ginnetti, A. T.; Kurihara, H.; Dreher, S. D.; Weissman, S. A.; Stauffer, S. R.; Burgey, C. S. *Org. Lett.* **2009**, *11*, 345–347. (b) Gooßen, L. J.; Deng, G.; Levy, L. M. *Science* **2006**, *313* 662–664.

(23) (a) D. M. T. Chan, K. L. Monaco, R.-P. Wang, M. P. Winters, *Tetrahedron Lett*. **1998**, *39*, 2933 – 2936. (b) D. A. Evans, J. L. Katz, T. R. West, Tetrahedron Lett. 1998, 39, 2937 – 2940. (c) P. Y. S. Lam, C. G. Clark, S. Saubern, J. Adams, M. P. Winters, D. M. T. Chan, A. Combs, Tetrahedron Lett. 1998, 39, 2941 –2944. For reviews: (d) Qiao, J.; Lam, P. *Synthesis* **2010**, 829–856. (e) Ley, S. V; Thomas, A. W. *Angew. Chem. Int. Ed. Engl.* **2003**, *42*, 5400–5449.

(24) (a) Peterson, K. P.; Larock, R. C. *J. Org. Chem.* **1998**, *63*, 3185–3189. (b) Steinhoff, B. A.; Fix, S. R.; Stahl, S. S. *J. Am. Chem. Soc.* **2002**, *124*, 766–767. (c) Zhou, C.; Larock, R. C. *J. Am. Chem. Soc.* **2004**, *126*, 2302–2303.

(25) Jia, C.; Lu, W.; Oyamada, J.; Kitamura, T.; Matsuda, K.; Irie, M.; Fujiwara, Y. *J. Am. Chem. Soc.* **2000**, *122*, 7252–7263.

(26) For copper mediated homocoupling of arylboronic acids: (a) Koza, D. J.; Carita, E. *Synthesis* **2002**, 2183–2186. (b) Demir, A. S.; Reis, O.; Emrullahoglu, M. *J. Org. Chem.* **2003**, *68*, 10130–10134. (c) Cheng, G.; Luo, M. *Eur. J. Org. Chem.* **2011**, *13*, 2519–2523.

(27) Stang, P. J. *J. Org. Chem.* **2003**, *68*, 2997–3008.

(28) Ochiai, M. *Top. Curr. Chem.* **2003**, *224*, 5 – 68.

(29) Merritt, E. a; Olofsson, B. *Angew. Chem. Int. Ed. Engl.* **2009**, *48*, 9052–9070.

(30) Iwama, T.; Birman, V. B.; Kozmin, S. a; Rawal, V. H. *Org. Lett.* **1999**, *1*, 673–676.

(31) Beringer, F. M.; Forgione, P. S.; Yudis, M. D. *Tetrahedron* **1960**, *8*, 49-63

(32) Oh, C. H.; Kim, J. S.; Jung, H. H. *J. Org. Chem.* **1999**, *64*, 1338–1340.

(33) Ochiai, M.; Kitagawa, Y.; Takayama, N.; Takaoka, Y.; Shiro, M. *J. Am. Chem. Soc.* **1999**, *121*, 9233–9234.

(34) Aggarwal,V. K.; Olofsson, B. *Angew. Chem. Int. Ed. Engl.* **2005**, *44*, 5516-5519.

(35) Allen, A. E.; MacMillan, D. W. C. *J. Am. Chem. Soc.* **2011**, *133*, 4260–4263.

(36) Bigot, A.; Williamson, A. E.; Gaunt, M. J. *J. Am. Chem. Soc.* **2011**, *133*, 13778–13781.

(37) Daugulis, O.; Zaitsev, V. G. *Angew. Chem. Int. Ed. Engl.* **2005**, *44*, 4046–4048.

(38) Kalyani, D.; Deprez, N. R.; Desai, L. V; Sanford, M. S. *J. Am. Chem. Soc.* **2005**, *127*, 7330–7331.

(39) Phipps, R. J.; Gaunt, M. J. *Science* **2009**, *323*, 1593–1597.

(40) Deprez, N. R.; Kalyani, D.; Krause, A.; Sanford, M. S. *J. Am. Chem. Soc.* **2006**, *128*, 4972–4973.

(41) Phipps, R. J.; Grimster, N. P.; Gaunt, M. J. *J. Am. Chem. Soc.* **2008**, *130*, 8172–8174.

(42) Kita, Y.; Morimoto, K.; Ito, M.; Ogawa, C.; Goto, A.; Dohi, T. *J. Am. Chem. Soc.* **2009**, *131*, 1668–1669.

(43) Ackermann, L.; Dell'Acqua, M.; Fenner, S.; Vicente, R.; Sandmann, R. *Org. Lett.* **2011**, *13*, 2358–2360.

(44) Eastman, K.; Baran, P. S. *Tetrahedron* **2009**, *65*, 3149–3154.

(45) Toh, Q. Y.; McNally, A.; Vera, S.; Erdmann, N.; Gaunt, M. J. *J. Am. Chem. Soc.* **2013**, *135*, 3772–3775.

(46) Suero, M. G.; Bayle, E. D.; Collins, B. S. L.; Gaunt, M. J. *J. Am. Chem. Soc.* **2013**, *135*, 5332–5335.

(47) Walkinshaw, A. J.; Xu, W.; Suero, M. G.; Gaunt, M. J. *J. Am. Chem. Soc.* **2013**, *135*, 12532–12535.

(48) Brown, J. D.; Foley, M. A.; Comins, D. L. *J. Am. Chem. Soc.* **1988**, *110*, 7445-7447.

(49) Comins, D. L.; LaMunyon, D. H.; Chen, X. *J. Org. Chem.* **1997**, *62*, 8182-8187.

(50) Kuethe, J. T.; Comins, D. L. *Org. Lett.* **1999**, *1*, 1031-1033.

(51) Comins, D. L.; Sahn, J. J. *Org. Lett.* **2005**, *7*, 5227-5228.

(52) Comins, D. L.; Zhang, Y. *J. Am. Chem. Soc.* **1996**, *118*, 12248-12249.

(53) Hamblett, C. L.; Sloman, D. L.; Kliman, L. T.; Adams, B.; Ball, R. G.; Stanton, M. G. *Tetrahedron Lett.* **2007**, *48*, 2079-2082.

(54) Guo, F.; Dhakal, R. C.; Dieter, R. K. *J. Org. Chem.* **2013**, *78*, 8451-8464.

(55) Sahn, J. J.; Comins, D. L. *J. Org. Chem.* **2010**, *75*, 6728-6731.

(56) Sahn, J. J.; Bharathi, P.; Comins, D. L. *Tetrahedron Lett.* **2012**, *53*, 1347-1350.

(57) Young, D. W.; Comins, D. L. *Org. Lett.* **2005**, *7*, 5661-5664.

(58) Gotchev, D. B.; Comins, D. L. *J. Org. Chem.* **2006**, *71*, 9393-9402.

(59) Comins, D. L.; Joseph, S. P.; Zhang, Y. *Tetrahedron Lett.* **1996**, *37*, 793-796.

(60) Kirschbaum, S.; Waldmann, H. *Tetrahedron Lett.* **1997**, *38*, 2829-2832.

(61) Comins, D. L.; Higuchi, K. *Beilstein J. Org. Chem.* **2007**, *3*, 42.

(62) Kirschbaum, S.; Waldmann, H. *J. Org. Chem.* **1998**, *63*, 4936-4946.

(63) Jeffery, T. *Tetrahedron* **1996**, *52*, 10113-10130.

(64) Friestad, G. K.; Branchaud, B. P. *Tetrahedron Lett.* **1995**, *36*, 7047-7050.

(65) Sollewijn Gelpke, A. E.; Veerman, J. J. N.; Schreuder Goedheijt, M.; Kamer, P. C. J.; van Leeuwen, P. W. N. M.; Hiemstra, H. *Tetrahedron* **1999**, *55*, 6657-6670.

(66) Costa, A.; Nájera, C.; Sansano, J. M. *J. Org. Chem.* **2002**, *67*, 5216-5225.

(67) Genet, J. P.; Blart, E.; Savignac, M. *Synlett* **1992**, *1992*, 715-717.

(68) Tanaka, D.; Myers, A. G. *Org. Lett.* **2004**, *6*, 433-436.

(69) Lautens, M.; Fang, Y.-Q. *Org. Lett.* **2003**, *5*, 3679-3682.

(70) Myers, A. G.; Tanaka, D.; Mannion, M. R. *J. Am. Chem. Soc.* **2002**, *124*, 11250-12151.

(71) (a) Cho, C. S.; Uemura, S. *J. Organomet. Chem.* **1994**, *465*, 85-92. (b) He, Z.; Kirchberg, S.; Fröhlich, R.; Studer, A. *Angew. Chem. Int. Ed. Engl.* **2012**, *51*, 3699-3702. (c) Sun, P.; Zhu, Y.; Yang, H.; Yan, H.; Lu, L.; Zhang, X.; Mao, J. *Org. Biomol. Chem.* **2012**, *10*, 4512-4515. (d) Zheng, C.; Wang, D.; Stahl, S. S. *J. Am. Chem. Soc.* **2012**, *134*, 16496-16499. (e) Ruan, J.; Li, X.; Saidi, O.; Xiao, J. *J. Am. Chem. Soc.* **2008**, *130*, 2424-2425. (f) Werner, E. W.; Sigman, M. S. *J. Am. Chem. Soc.* **2010**, *132*, 13981-13983. (g) Lindh, J.; Enquist, P.-A.; Pilotti, A.; Nilsson, P.; Larhed, M. *J. Org. Chem.* **2007**, *72*, 7957-7962. (h) Delcamp, J. H.; Brucks, A. P.; White, M. C. *J. Am. Chem. Soc.* **2008**, *130*, 11270-11271. (i) Andappan, M. M. S.; Nilsson, P.; von Schenck, H.; Larhed, M. *J. Org. Chem.* **2004**, *69*, 5212-5218.

(72) Yoo, K. S.; Yoon, C. H.; Mishra, R. K.; Jung, Y. C.; Yi, S. W.; Jung, K. W. *J. Am. Chem. Soc.* **2006**, *128*, 16384-16393.

(73) Gottumukkala, A. L.; Teichert, J. F.; Heijnen, D.; Eisink, N.; van Dijk, S.; Ferrer, C.; van den Hoogenband, A.; Minnaard, A. J. *J. Org. Chem.* **2011**, *76*, 3498-3501.

(74) Khoobi, M.; Alipour, M.; Zarei, S.; Jafarpour, F.; Shafiee, A. *Chem. Commun.* **2012**, *48*, 2985-2987.

(75) Li, Y.; Qi, Z.; Wang, H.; Fu, X.; Duan, C. *J. Org. Chem.* **2012**, *77*, 2053-2057.

(76) Xiong, D.; Zhang, L.; Ye, X. *Org. Lett.* **2009**, *11*, 1709-1712.

(77) Walker, S. E.; Boehnke, J.; Glen, P. E.; Levey, S.; Patrick, L.; Jordan-Hore, J. a; Lee, A.-L. *Org. Lett.* **2013**, *15*, 1886-1889.

(78) Andappan, M. M. S.; Nilsson, P.; Larhed, M. *Chem. Commun.* **2004**, *2*, 218-219.

(79) Yu, R. T.; Rovis, T. *J. Am. Chem. Soc.* **2006**, *128*, 12370-12371.

(80) Hayden, M. S.; Ghosh, S. *Cell* **2008**, *132*, 344–362.

(81) Vallabhapurapu, S.; Karin, M. *Annu. Rev. Immunol.* **2009**, *27*, 693–733.

(82) (a) DiDonato, J. a; Hayakawa, M.; Rothwarf, D. M.; Zandi, E.; Karin, M. *Nature* **1997**, *388*, 548–554. (b) Mercurio, F.; Zhu, H.; Murray, B. W.; Shevchenko, A.; Bennett, B. L.; Li, J. W.; Young, D.; B.; Bardosa, M.; Mann, M.; Manning, A.; Rao, A. *Science* **1997**, *278*, 860-866. (c) Woronicz, J. D.; Gao, X.; Cao, Z.; Rothe, M.; Goeddel, D. V.; *Science* **1997**, *278*, 866-870.

(83) (a) Bonizzi, G.; Karin, M. *Trends Immunol.* **2004**, *25*, 280–288. (b) Karin, M.; Greten, F. R. *Nat. Rev. Immunol.* **2005**, *5*, 749–759.

(84) (a) Krappmann, D.; Hatada, E. N.; Tegethoff, S.; Li, J.; Klippel, a; Giese, K.; Baeuerle, P. a; Scheidereit, C. *J. Biol. Chem.* **2000**, *275*, 29779–29787. (b) Miller, B. S.; Zandi, E. *J. Biol. Chem.* **2001**, *276*, 36320–36326. (c) Karin, M.; Ben-Neriah, Y. *Annu. Rev. Immunol.* **2000**, *18*, 621–663.

(85) (a) Ghosh, S.; Karin, M. *Cell* **2002**, *109*, S81–S96. (b) Hu, Y.; Baud, V.; Delhase, M.; Zhang, P.; Deerinck, T.; Ellisman, M.; Johnson, R.; Karin, M. *Science* **1999**, *284*, 316–320. (c) Li, Q.; Antwerp, D. V.; Mercurio, F.; Lee, K.-F.; Verma, I. M. *Science* **1999**, *284*, 321–325.

(86) (a) Nagarajan, S.; Choo, H.; Cho, Y. S.; Oh, K.-S.; Lee, B. H.; Shin, K. J.; Pae, A. N. *Bioorg. Med. Chem.* **2010**, *18*, 3951–3960. (b) Baxter, A.; Brough, S.; Cooper, A.; Floettmann, E.; Foster, S.; Harding, C.; Kettle, J.; McInally, T.; Martin, C.; Mobbs, M.; Needham, M.; Newham, P.; Paine, S.; St-Gallay, S.; Salter, S.; Unitt, J.; Xue, Y. *Bioorg. Med. Chem. Lett.* **2004**, *14*, 2817–2822. (c) Peet, G. W. *J. Biol. Chem.* **1999**, *274*, 32655–32661. (d) Nagashima, K.; Sasseville, V. G.; Wen, D.; Bielecki, A.; Yang, H.; Simpson, C.; Grant, E.; Hepperle, M.; Harriman, G.; Jaffee, B.; Ocain, T.; Xu, Y.; Fraser, C. C. *Blood* **2006**, *107*, 4266–4273. (e) Schön, M.; Wienrich, B. G.; Kneitz, S.; Sennefelder, H.; Amschler, K.; Vöhringer, V.; Weber, O.; Stiewe, T.; Ziegelbauer, K.; Schön, M. P. *J. Natl. Cancer Inst.* **2008**, *100*, 862–875. (f) Burke, J. R.; Pattoli, M. a; Gregor, K. R.; Brassil, P. J.; MacMaster, J. F.; McIntyre, K. W.; Yang, X.; Iotzova, V. S.; Clarke, W.; Strnad, J.; Qiu, Y.; Zusi, F. C. *J. Biol. Chem.* **2003**, *278*, 1450–1456. (g) Yang, J.; Amiri, K. I.; Burke, J. R.; Schmid, J. a; Richmond, A. *Clin. Cancer Res.* **2006**, *12*, 950–960.

(87) (a) Olsen, L. S.; Hjarnaa, P.-J. V.; Latini, S.; Holm, P. K.; Larsson, R.; Bramm, E.; Binderup, L.; Madsen, M. W. *Int. J. Cancer* **2004**, *111*, 198–205. (b) Binderup, E.; Björkling, F.; Hjarnaa, P. V.; Latini, S.; Baltzer, B.; Carlsen, M.; Binderup, L. *Bioorg. Med. Chem. Lett.* **2005**, *15*, 2491–2494. (c) Olsen, L. S.; Hjarnaa, P.-J. V.; Latini, S.; Holm, P. K.; Larsson, R.; Bramm, E.; Binderup, L.; Madsen, M. W. *Int. J. Cancer* **2004**, *111*, 198–205. (d) Lövborg, H.; Wojciechowski, J.; Larsson, R.; Wesierska-Gadek, J. *Cancer Res.* **2002**, *62*, 4206–4211.

(88) (a) Sakurai, H.; Chiba, H.; Miyoshi, H.; Sugita, T.; Toriumi, W. *J. Biol. Chem.* **1999**, *274*, 30353–30356. (b) Sakurai, H.; Suzuki, S.; Kawasaki, N.; Nakano, H.; Okazaki, T.; Chino, A.; Doi, T.; Saiki, I. *J. Biol. Chem.* **2003**, *278*, 36916–36923. (c) Yang, F.; Tang, E.; Guan, K.; Wang, C.-Y. *J. Immunol.* **2003**, *170*, 5630–5635.

(89) Klapars, A.; Antilla, J. C.; Huang, X.; Buchwald, S. L. *J. Am. Chem. Soc.* **2001**, *123*, 7727–7729.

(90) Xu, G.; Lo, Y.-C.; Li, Q.; Napolitano, G.; Wu, X.; Jiang, X.; Dreano, M.; Karin, M.; Wu, H. *Nature* **2011**, *472*, 325–330.

(91) Prime, version 3.0, Schrodinger, LLC, New York, NY, 2011.

(92) Glide, version 5.7, Schrodinger, LLC, New York, NY, 2011.

(93) Macromodel, version 9.9, Schrodinger, LLC, New York, NY, 2011.

(94) Ligprep, version 2.5, Schrodinger, LLC, New York, NY, 2011.